Mitochondrial Localisation of hTERT Protects Against Nuclear DNA Damage and Mitochondrial ROS Production After Endogenous and Exogenous Stress

Chatchawan Singhapol

A thesis submitted in accordance with the requirements for the degree of Doctor of Philosophy

Institute for Ageing and Health
Newcastle University

September 2012

Abstract

Under oxidative stress condition, telomerase catalytic subunit can shuttle from the nucleus and localises within mitochondria. hTERT can improve mitochondrial functions and contribute to a decreased oxidative stress suggesting an entirely new function of telomerase in protecting mitochondria and cells under stress. However, there are still many questions about the mechanism and what factors influence the protective function of telomerase.

In this study we investigated the kinetic exclusion of hTERT, the catalytic subunit of telomerase, in various cell lines under different oxidative stress conditions. We also used organelle specific hTERT localisation vectors to model hTERT localisation and investigated a correlation between hTERT location, nuclear DNA damage and ROS production. We found that cells excluded endogenous hTERT from the nucleus in a heterogeneous fashion independently of the cell types. Importantly, nuclear DNA damage showed a significant correlation with the localisation of hTERT. Cells where hTERT remained in the nucleus displayed high DNA damage while cells which excluded hTERT from the nucleus displayed no or very low DNA damage. Our results from specific hTERT localisation vectors specified that mitochondrial localisation of hTERT protects the nucleus from DNA damage and did not showed any sign of apoptosis induction while nuclear localisation of hTERT correlated with higher amounts of DNA damage and apoptosis. Moreover, mitochondrial localisation of hTERT decreased mitochondrial ROS generation levels directly after both endogenous and exogenous stress which we interpret as the reason for the prevention of nuclear DNA damage.

Additionally, we analysed whether p53 status might influence the protective function of telomerase. Our results in an isogenic cell pair of glioblastoma cells showed that p53 status does not prominently influence the protective function of mitochondrial hTERT under low stress condition. However, nuclear hTERT of cells which contained inactive p53 displayed a significantly higher nuclear DNA damage than cells which contained an active p53 and this became more pronounced when stress levels were increased. We hypothesise that telomerase localisation might possibly interact with p53 when a cancer cell is under stress condition. However, the molecular mechanism for that is unknown.

Our results demonstrate a novel link between mitochondrial localisation of hTERT, decrease of mitochondrial ROS generation and the protective capacity of hTERT to nuclear DNA from damage after stress treatments.

Acknowledgements

I would like to thank warmly all those who helped me during my Ph.D study. Most importantly my supervisor Dr. Gabriele Saretzki for her guidance, advice, continuous patience and support for me throughout this study.

I would like to thank Prof. Dr. Ioakim Spyridopoulos, Prof. Dr. Thomas Von Zglinicki, Dr. Joao Passos, Dr. Satomi Miwa and Dr. Glyn Nelson for their advice and useful guidance throughout my PhD.

I would also like to thank Rafal Czapiewski, Dean Hallam, Deepali Pal and everybody at the Crucible lab, International centre for life for great working atmosphere, social environment and sharing their experiences.

I would like to thank everybody at the Office of Education Affair-London and everybody in Thai Society-Newcastle University for their support and also special thanks to King Mongkut's University of Technology North Bangkok and Ministry of Science and Technology scholarship, Thailand, for funding this PhD project.

Finally I would like to thank my family: Dad, Mom, brother and sister and my close friend in London for their love and ongoing support over the last few years and especially during the last few months of my writing.

List of Figures and Tables

Abbreviations used in this thesis

Ab	Antibody
APS	Ammonium persulfate
ATCC	American Type Culture Collection
BSA	Bovine Serum Albumin
D	Day
DAPI	4',6-diamidino-2-phenylindole
DDR	DNA Damage Response
DMEM	Dulbecco's Modified Eagle Medium
DMSO	Dimethyl Sulphoxide
DNA	Desoxyribonucleic acid
DTT	Dithiothreitol
ECACC	The European Collection of Cell Cultures
EDTA	Ethylene diamine tetra acetate
FBS	Fetal Bovine Serum
GAPDH	Glycerinaldehyde 3-phosphate dehydrogenase
hTERT	human Telomerase Reverse Transcriptase
hTR	human Telomerase RNA
hrs	Hours
kb	kilo base paires
Mito	Mitochondria
mM	Millimilar
μM	Micromolar
nM	Nanomolar
Nuc	Nucleus
PBS	Phosphate Buffered Saline
PBG	PBS-BSA-fishskin Gelatin
PFA	Paraformaldehyde
ROS	Reactive Oxygen Species
RNA	Ribonucleic acid
SDS	sodium dodecylsulfate
T	Temperature
TAF	Telomere associated foci
TBS	Tris buffered saline

TEMED	N, N, N', N' - Tetramethylethylenediamide
TERT	Telomerase Reverse Transcriptase
TIM	Translocase of Inner Membrane
TOM	Translocase of Outer Membrane
TR	Telomerase RNA

Chapter 1

Introduction

1.1 Telomerase

Telomerase, a ribonucleoprotein complex, is a unique reverse transcriptase which has a canonical function to maintain telomere length by adding specific nucleotide repeat sequence onto the telomeres. However, evidence suggests that telomerase has additional physiological functions. Telomerase has been related to DNA damage response and repair, apoptosis resistance and changes in chromatin structure and gene expression (Smith et al., 2002, Sharma et al., 2003, Masutomi et al, 2005, Choi et al., 2008, Park et al., 2009a). Ectopic expression of telomerase in normal human cells leads to the extension of lifespan (Bodnar et al., 1998). Inhibition of telomerase in telomerase positive cancer cells can lead cell to death (Saretzki et al., 2001, Wong et al., 2002; Zhang et al., 2003; Rubio et al., 2004; Cong and Shay, 2008). Moreover, hTERT, the catalytic subunit of telomerase, can shuttle from the nucleus to the mitochondria upon oxidative stress and drug treatment (Santos et al., 2004, 2006; Ahmed et al., 2008; Haendeler et al., 2003, 2004, 2009; Indran et al., 2010). hTERT has been demonstrated to bind and protect mitochondrial DNA against UV-induced depletion and increase the respiratory chain activity specially complex I (Haendeler et al., 2009). Previous experiments of our group have shown that mitochondrial DNA (mtDNA) in hTERT over-expressing fibroblasts is better protected against the oxidative DNA damage. hTERT is excluded from the nucleus and protects mitochondria under oxidative stress condition. hTERT over-expressing fibroblasts show a lower mitochondrial superoxide generation, less mitochondrial DNA damage, less mitochondrial mass/mtDNA copy number and higher mitochondrial membrane potential under stress conditions (Ahmed et al., 2008). Thus, localisation of hTERT in mitochondria seems to correlate to mitochondrial protection. However, a disadvantage of the general over-expression of hTERT in those cells is that the protein shuttles dynamically.

1.2 The history of telomerase discovery

Telomerase was first discovered in an *in vitro* study by Carol Greider and Elizabeth Blackburn in 1985. They were using a biochemical assays in *Tetrahymena thermophila* cell-free extracts and discovered a telomere-specific terminal transferase activity that was subsequently named telomerase (Greider and Blackburn, 1985). In their

experiments, Greider and Blackburn showed that the terminal transferase was sensitive to proteinase K, micrococcal nuclease, and Rnase A and that a 159 nucleotides RNA subunit co-purified with telomerase activity over five fractionation steps (Greider and Blackburn, 1985, Greider and Blackburn, 1987). This experiment provided strong biochemical evidence that the terminal transferase was a cellular ribonucleoprotein reverse transcriptase.

In human cells, telomerase activity was first identified by Gregg Morin in 1989 (Morin, 1989). He analysed nucleus and cytoplasm extracted from Hela and found a repeating pattern of 6 nucleotides which sequenced as TTAGGG as found at human telomeres. His experiments also showed that human telomerase can synthesise only 65-70 repeating nucleotide sequences under optimal assay conditions while Tetrahymena enzyme could synthesise up to 8000 nucleotides as reported by Blackburn and colleagues in 1989 (Morin, 1989). In 1995, Feng and co-workers identified the RNA component of human telomerase (hTR) in normal somatic cells, germline tissues and tumor cell lines (Feng et al., 1995). The template region of 11 nucleotides (5'-CUAACCCUAAC) that they found is complementary with human telomere sequence (TTAGGG)n. They confirmed their findings by transfecting Hela cells with an antisense of hTR sequence. The results showed loss of telomeric DNA in Hela and cells began to die after 23 to 26 doublings.

The telomerase catalytic protein subunit was first identified in 1996 through genetic screens in yeast (Lendvay et al., 1996) and biochemical purification of *Euplotes aediculatus* telomerase (Lingner and Cech, 1996). The E. aediculatus protein was found to be a homolog of the yeast protein and sequence comparison with prototypical RTs revealed an evolutionarily-conserved reverse transcriptase domain in both proteins. Substitution of residues within the reverse transcriptase motifs of the yeast protein caused telomere shortening and cellular senescence, indicating that the RT domain was required for telomere synthesis in vivo (Lingner et al., 1997).

Human telomerase catalytic subunit gene was independently identified by two research groups (Kilian et al., 1997; Nakamura et al., 1997). Nakamura and co-workers reported a conserved telomerase catalytic subunit gene in human cells. Blast search information (GeneBank AA281296) and cDNA cloned from adenovirus transfected-human embryonic kidney cells were used to construct the hTERT motif. The expression of the hTERT gene was identified in 6 telomerase-positive immortal cell lines (Nakamura et al., 1997). In the same year, Kilian and co-workers identified a 4 kb long human catalytic subunit gene in colon cancer cell line. By using this sequence, RT-PCR of

mRNA confirmed the expression of this discovered catalytic subunit gene corresponding with high telomerase activity in several telomerase-positive and tumor cell lines.

1.3 Telomerase activity and its' biological function

Telomerase activity is varying in different human cells and tissues. Telomerase is active during early embryonic development but it is switched off in the majority of cells starting at 20 weeks of gestation in the human embryo (Ulaner et al., 1998; Geserick and Blasco, 2006). In embryonic stem cell, decrease of the expression of telomerase activity during differentiation is because of the deacetylation of histone H3 and H4 in the promoter region of hTERT and H3 at the hTR promoter resulting in downregulation of telomerase gene expression (Saretzki et al., 2008). Telomerase has been progressively repressed through differentiation in the majority of human adult tissues while some cell types such as lymphocytes, endothelial cells and adult stem cells retain a certain level of telomerase activity. Rare events of telomerase expression in human fibroblasts have been reported. Masutomi and co-workers found a small quantity of telomerase activity in two primary presenescent human fibroblasts (BJ-fibroblast and WI-38 fibroblasts) that exhibited hTERT activity in S-phase and noted that telomere shortening on its own cannot trigger senescence and cells need the bimodal action of hTERT depletion and telomere shortening (Masutomi et al., 2003). However, telomerase activity remains inactive in most other somatic cells.

Telomerase activity and telomere maintenance are prerequisites for cellular immortality. Telomerase activity has been detected in 90% of all human malignancies (Shay and Bacchetti, 1997). Over-expression of hTERT is sufficient to counteract telomere shortening and extend cellular lifespan in human diploid fibroblasts (Bodnar et al., 1998; McSharry et al., 2001). Over expression of hTERT in two human embryonic stem cell lines resulted in enhancement of cellular pluripotency and suppression of cellular *in vitro* differentiation while downregulation counteracted pluripotency and proliferation (Yang et al., 2008). All of these results indicate an important function of telomerase activity in telomerase positive cells.

1.4 The hTERT gene and its transcription

Regulation of telomerase occurs at several different levels (Cong et al., 2002; and Vega et al., 2003). The correlation between the expression of hTERT mRNA and telomerase activity indicates the transcriptional regulation of the hTERT gene. As shown in figure

1.1, the hTERT gene is located on chromosome band 5p15.33 in human diploid cells and it is approximately 2Mb away from the telomeres (Leem et al., 2002). The hTERT gene is composed of 16 exons and 15 introns extending over 35kb and all the splice junctions at exon/intron boundaries conform to GT/AG sequence except for the last intron (Cong et al.,1999). The sequence of the hTERT promoter contains a core region extending from 330 bp upstream of the hTERT ATG to 37 bp of the gene. The core region does not contain TATA or CAAT boxes but contains binding sites for several transcription factors (Cong et al., 1999). hTERT transcriptional activity is regulated by transcription factors like SP1 (Kyo et al., 2000), c-Myc (Greenberg et al., 1999), and also by the papillomavirus E6 protein (Klingelhutz et al., 1996). Hoffmeyer and colleagues reported recently that Wnt/β-catenin binds to the transcription start site (TSS) and regulates TERT expression in embryonic and adult mouse stem cells as well as human carcinoma cells (Hoffmeyer et al., 2012).

There are many factors that have been shown to repress the expression of TERT including E2F, histone deacetylases, and Rb family of proteins (Cong et al., 2002; and Takakura et al., 2001). Mad1 and p53 were identified as negative regulators of hTERT transcription (Xu et al., 2001; Kanaya et al., 2000).

Only the full length hTERT transcript is associated with telomerase activity (Cong et al., 2002). However, The hTERT gene is also differentially spliced. Several hTERT transcripts have been detected in human cells including α variant, β variant and alternative combination of α and β variants. All of the various transcripts are expressed during fetal development in a tissue-dependent and gestational age-dependent manner (Ulaner et al., 1998). Also this alternative splicing of hTERT mRNA takes place and seems to be related to some diseases such as skin cancer (melanoma) (Lincz et al., 2008) and kidney cancer (malignant renal tumour) (Fan et al., 2005). Changes of hTERT alternative splicing patterns were found in gastric carcinogenesis and can be used for the diagnosis of gastric cancer or percancerous lesions (Xu et al., 2009).

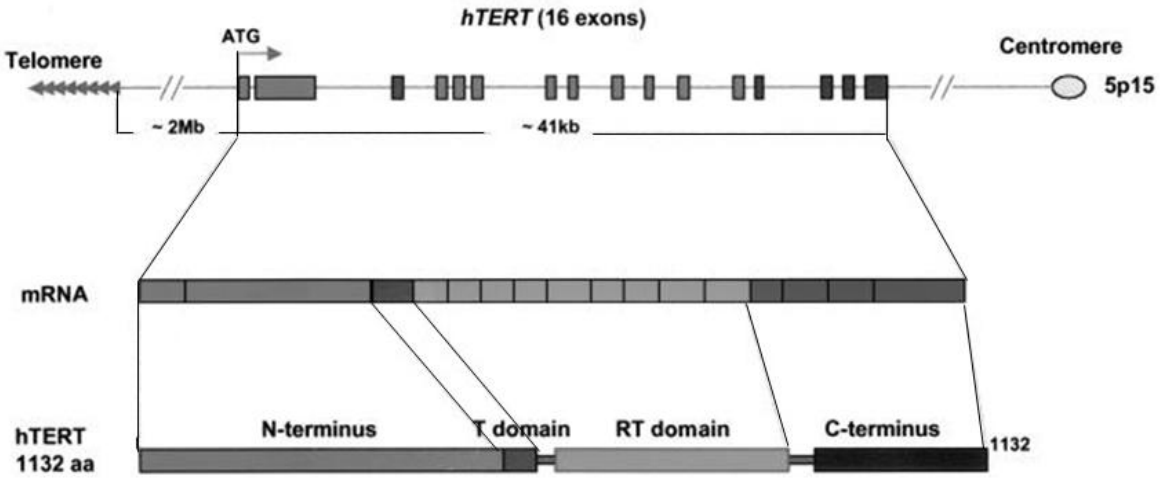

Figure 1.1 Gene organisation of the hTERT gene. hTERT consists of 16 exons and 15 introns located on the short arm of chromosome 5 (5p15.33) (Cong et al., 2002).

1.5 Post-translational modification of hTERT

hTERT is found throughout the nucleoplasm in S phase, but is concentrated in nucleoli in the remaining phases of the cell cycle (Wong et al., 2002; and Yang et al., 2002). PinX1p, an inhibitor of telomerase, regulates telomerase by sequestering TERT into the nucleolus, thus preventing the association of TERT with the RNA subunit (Lin and Blackburn, 2004). ADP-ribosylation of hTERT by PARPs (Poly (ADP-ribose) polymerases) regulates telomerase activity (Ghosh and Bhattacharya, 2005). Akt kinase and protein kinase C enhance human telomerase activity through phosphorylation of the hTERT subunit (Li et al., 1998; Kharbanda et al., 2000, Kang et al., 2006). Moreover, phosphorylation of TERT by Akt and/or PKCα is necessary for nuclear translocation (Jagadeesh and Banerjee, 2006). Under H_2O_2 stress condition (Haendeler et al., 2003) and possibly others stresses such as hyperoxia (Ahmed et al., 2008), Src kinase phosphorylates hTERT at tyrosine 707 and stimulates hTERT to translocate from the nucleus into cytoplasm via nuclear pores in a CRM1/Ran-GTPase dependent manner. Moreover, hTERT can be translocated into mitochondria under stress condition (Ahmed et al., 2008; Haendeler et al., 2009; Indran et al., 2011; Sharma et al., 2012). Therefore, intracellular shuttling is an important mechanism to regulate telomerase since the absence of telomerase in the nucleus can lead to telomere shortening (Ahmed et al., 2008). The oxidative stress can induce dramatic changes in hTERT localisation which are related to telomere independent functions of telomerase in mitochondria as described in 1.15.

1.6 Canonical function of telomerase

Telomerase is a unique reverse transcriptase which has a canonical function to maintain telomere length by adding specific nucleotide repeat sequence onto the telomeres.

Telomeres are special structures which are found at the end of eukaryote chromosomes. In mammals, telomeres are composed of 5-15 kb of a TTAGGG specific repetitive DNA sequences (Moyzis et al., 1988) with a multi protein complex. In humans, the protein complex is known as "shelterin" which is composed of six important proteins: TRF1, TRF2, hRap1, TIN2, TPP1 and POT1 (de Lange, 2005; Deng et al., 2008). These proteins help to form special complex structures to protect the end of a chromosome (Griffith et al., 1999). TRF1 and TRF2 bind to the double stranded telomeric sequence and fold telomere DNA back onto itself to form a large telomere loop (T-loop). POT1 binds to the 3' end overhang on the telomere and folds the DNA to bind to the double stranded telomeric sequence of the 5'end to form a displacement loop (D-loop) (Smogorzewska et al., 2000; Baumann and Cech, 2001). The structure of a telomere is described in figure 1.2. This three-dimensional structure can protect telomeres and prevent them from an inappropriate DNA repair such as exonucleolytic degradation and ligation of one chromosome end to another (Smogorzewska and De Lange, 2004; Wright and Shay, 2005; de Lange, 2006). However, during each cell division, telomere DNA is gradually shortening due to the oxidative stress (Von Zglinicki et al., 1995, Richter and Von Zglinicki, 2007) and the failure of the replication mechanism to replicate the last bases of the chromosome end what is called ''end replication problem'' (Olovnikov, 1973).

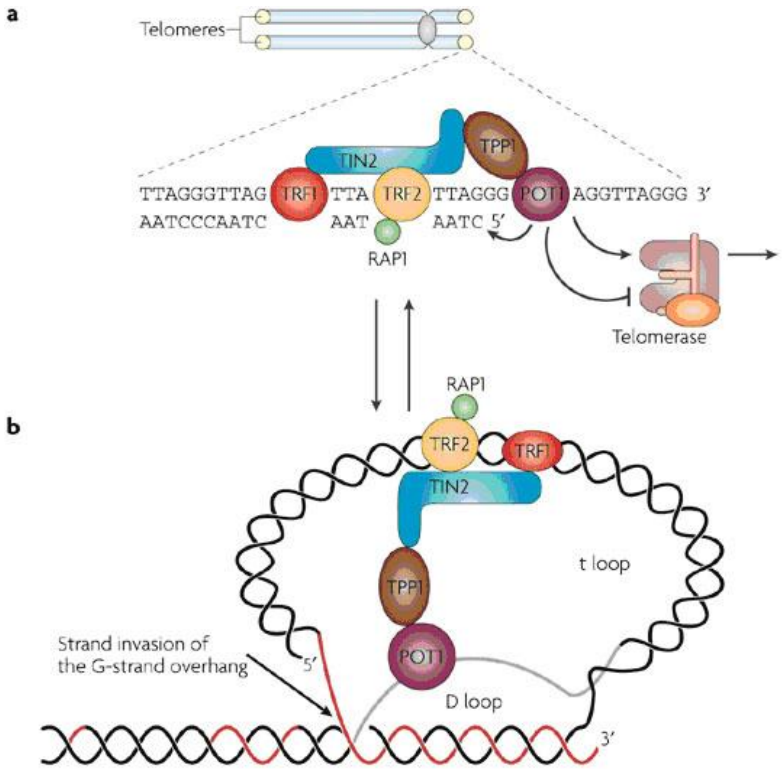

Figure 1.2. Telomere structure A: Telomeres cap mammalian chromosomes and are composed of TTAGGG repetitive sequences that terminate in a 3' single-stranded (ss) overhang. Telomeric DNA is complexed by the six-protein shelterin complex, composed of telomeric-repeat binding factor 1 (TRF1), TRF2, RAP1, TRF1-interacting nuclear factor 2 (TIN2), TPP1 and POT1. The TPP1–POT1 heterodimer regulates telomerase access to the telomeric substrate. **B:** The single stand overhang can invade the double-stranded region of the telomere to form a protective telomere (t) loop with a ss displacement (D) loop at the invasion site. Mammalian telomeres also transiently interact with a host of other factors, many of which are involved in the DNA damage response (from Blasco, 2005).

This shortening of telomeres limits cells from indefinite cell division. Somatic cells without telomerase activity lose about 50-100 nucleotides of telomere sequence each time the cell divides which depends on the oxidative stress and intracellular anti-oxidant capacity. During cell division, on the lagging strand, DNA polymerase α cannot continue replication all the way through the end of chromosomes because the semiconservative replication of DNA which processes only in the 5' to 3' direction. DNA polymerase α has to use a 3‘ hydroxyl group from RNA primer to start replication of short DNA sequences as called Okazaki fragment. After removal of RNA primers, DNA ligase will continue to fill up the gap between Okazaki fragments. However at the very end of the lagging strand in telomere region, after removed of RNA primer, DNA ligase can not fill up the last gap because of lagging of 3‘ hydroxyl group resulting in

the shortening of telomere in every time of cellular division. Once the length of the telomeric DNA reaches a critical level the cells will undergo replicative senescence and withdraw from cell cycle (Reddel, 2003). This phenomenon of normal somatic cells could limit cells to a fixed number of divisions which might be responsible for ageing on the cellular level and hence acting as a potent tumour suppressor mechanism. However, germ line cells, immortal cells and unicellular organisms express high levels of telomerase activity and thereby overcome the telomere shortening that leads to senescence (Shippen-Lentz and Blackburn, 1989).

As shown in figure 1.3. telomerase synthesises telomeric sequences by recognising the tip of the telomeric G-rich strand with the 3'overhang of an existing telomere DNA repeat sequence and elongates it in the 5'-to-3' direction. Telomerase synthesises telomeric sequence using the 11 nucleotode long template region of hTR and extends the ssDNA 3'-end (telomerase-mediated extension step) to a length that is sufficient for another priming event. The telomere is subsequently extended by the semi-conservative replication machinery (C-strand fill-in reaction) and then removed. A 5'-3' nuclease has been proposed to generate the ssDNA overhang at the 3'-end of the leading strand, as well as catalyse the resection of the lagging strand 5'-end (5'-end resection step).

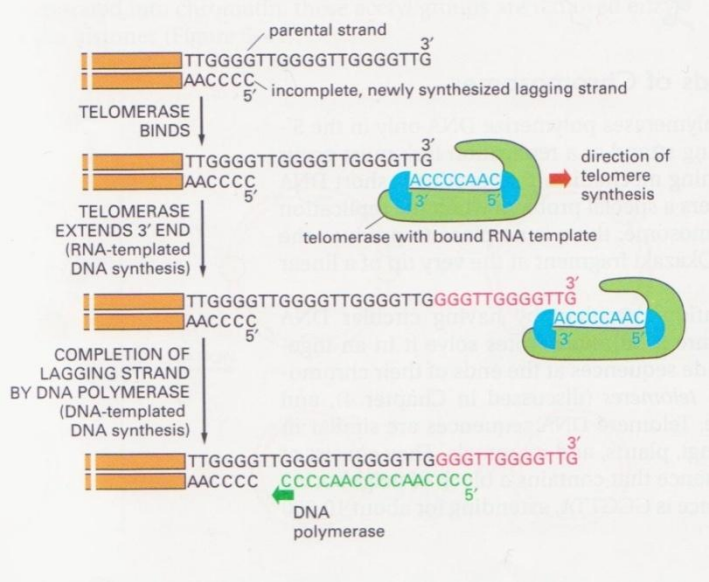

Figure 1.3 Telomere elongation by telomerase. The 3' end of the parental DNA stand is extended by the RNA-dependent DNA polymerase function of telomerase. This allows the incomplete daughter DNA strand that is paired with it to be extended in the 5' direction. The incomplete lagging strand is presumed to be completed by DNA polymerase α.

1.7 Telomere-independent functions of telomerase in cancer cells

Telomerase activity and telomere maintenance have been considered as a pre-requisit for the immortality of cancer cells. However, despite the absence of net telomere elongation, telomerase might play an important role in cancer development. The first evidence which suggested a telomere independent function of telomerase and related to tumourigenesis was obtained in mice. Gonzales-Suarez and co-workers (Gonzales-Suarez et al., 2001) generated a transgenic mTERT overexpressing mouse and found that without any significant extension of telomeres compared with the aged-matched wild-type mice, mTERT overexpressing mice displayed more sensitive to a chemical carcinogen and mitogenic effects of phorbol esters than wild-type mice. mTERT overexpressing mice were more susceptible to the development of neoplasias. Moreover, mTERT overexpressing mice expressed a significant faster wound-healing rate than the corresponding wild type which could reflect a proliferative advantage of telomerase overexpressing cells. These observations indicated a role of telomerase in signalling proliferation under mitogenic condition (Gonzales-Suarez et al., 2001).

In humans, the increased of telomerase activity in already-formed tumours is viewed as a negative prognostic marker for cancer formation (Wesbuer et al., 2010). However, telomerase does not only promote tumour cell immortalisation but also expresses an additional function through the apoptotic pathway. Rahman and co-workers reported a link between p53 and telomerase activity. Constitutive over-expression of hTERT antagonised p53-induced apoptosis independently of its canonical function in Burkitt lymphoma and colon carcinoma cells (Rahman et al., 2005). Massard and co workers reported a pro-neoplastic function of telomerase as an endogenous inhibitor of the mitochondrial pathway of apoptosis. Inhibition of hTERT by siRNA could induce Bax, a pro apoptotic Bcl-2 family protein. This expression occurred in a p53-independent fashion (Massard et al., 2006). Moreover, Terrien and colleagues reported that in primary B lymphocytes, ectopic expression of telomerase down regulated the expression of BZLF1 which is the main activator for the Epstein-Barr virus (EBV) lytic cycle. Interestingly, hTERT positive EBV infected B cells grow significantly faster than hTERT negative EBV infected B cells. This ectopic expression of hTERT increased cellular resistance to lytic cycle induction, and also enhanced in vitro growth properties and proliferation of B lymphocytes. Thus hTERT might confer a cellular growth advantage in this circumstance (Terrin et al., 2007). Since this establishment of viral infection is a crucial prerequisite for Epstein-driven B cell transformation, telomerase may directly contribute to various EBV-related lymphoid malignancies (Maeda et al.,

2009). Thus, telomerase enables cells with altered and unstable genomes to survive and induce the risk of many diseases.

All together, telomerase does not express only its canonical function but also relates to other independent roles such as inhibition of apoptosis and interaction with cellular signalling in cancer cells which indicates the existence of independent function of telomerase from telomere maintenance. The mitochondrial function of telomerase is explained in 1.15.

1.8 Telomere-independent functions of telomerase in non-cancer cells

Beyond the clear role of telomerase in maintaining telomere length, ectopic expression of telomerase in normal human cells leads to the extension of cellular lifespan (Bodnar et al., 1998) or can promote increases the immortalisation (Kondo et al., 1998). Ectopic expression of hTERT can immortalise human foreskin fibroblasts compared with their parental primary cells (Kampinga et al., 2004). Telomerase is also necessary for the long-term proliferation potential of stem cells. Sarin et al. (2005) showed an effect of TERT over-expression in an mTR knockout background on the proliferation of hair follicle stem cells. Transfection of the hTERT gene into rhesus monkey bone marrow stem cells can increase the population doubling up to 50 PD without any effect on cellular phenotypes (Gao et al., 2008). Moreover, expression of exogenous hTERT can bypass the Rb and p53 pathway-dependent barriers to proliferation and immortalised normal human urothelial cells (Chapman et al., 2006).

Telomerase also promotes cell growth. Telomerase modulates the expression of growth-controlling genes and enhances cell proliferation. TERT can induce growth-related proteins such as epidermal growth factor receptor (EGFR) in mammary epithelial cells (Smith et al., 2003) and interferes with the TGF-beta network of growth factors in primary murine cell lines (Geserick et al., 2006). Telomerase also associates with multiple regulatory proteins which might be involved in various intracellular pathways. It has also been shown that ectopic expression of hTERT leads to increased expression of genes involved in DNA damage repair and changes in the interaction of the telomeres with the nuclear matrix inside the cell nucleus (Sharma et al., 2003). Over-expression of telomerase in human oral fibroblasts resulted in enhanced nucleotide excision repair and DNA end joining capacity of UV damaged DNA (Shin et al., 2004). Transfection of hTERT gene into normal human embryonic lung cells can up-regulate the expression of vascular endothelial growth factor (VEGF) which is a key regulator of angiogenesis (Zhou et al., 2009). Telomerase modulates Wnt/β-catenin signalling which is sufficient

to activate quiescent epidermal stem cells (Park et al., 2009a; Hoffmeyer et al., 2012). Moreover, TERT has shown properties of an RNA-dependent RNA polymerase when in a complex with the RNA component of the mitochondrial endoribonuclease RMRP and synthesises double stranded RNA which can be further processed into siRNAs (Maida et al., 2009).

1.9 Telomerase and apoptosis

Inhibition of telomerase is widely investigated in order to induce apoptosis in cancer cells. The link between apoptosis and telomerase has been considered to be cause by the role of telomerase in telomere maintanence (Zhang et al., 1999; Herbert et al, 1999). However, evidence suggests that telomerase has an additional role in apoptosis regulation independently from telomere maintenance. The first evidence of independent function of telomerase in apoptosis has been reported in 2002. Fu and co-workers reported a novel role of telomerase in mediating the cell survival-promoting actions of two neurotrophic factors in developing hippocampal neurons. Telomerase activity and hTERT mRNA were increased by brain-derived neurotrophic factor (BDNF) and a secreted form of β-amyloid precursor protein (sAPP) in embryonic hippocampal neuron. However, the increase in telomerase activity happened only during the early stages of cultured embryonic neurons (Fu et al., 2002). Results from the same group in mouse hippocampus suggested a decrease in mTERT levels during adulthood. Telomerase activity in mouse brain declines until it is undetectable by day 10 postnatal which is the period that cell death occurs. This finding indicates an important role of telomerase in early neuronal development stage (Klapper et al., 2001).

Inhibition of telomerase can probably also induce telomere-independent apoptosis in cancer cells. Inhibition of telomerase with an antisense telomerase expression vector increased the susceptability to cisplatin-induced apoptotic cell death in human malignant glioblastomas cell lines (Kondo et al., 1998). Inhibition of telomerase in mass cultures of ovarian cancer cells induced cell death independent of telomere shortening (Saretzki et al., 2001).

Telomerase is also related to apoptosis via a mitochondrial mechanism. Massard and colleagues reported a function of telomerase as an endogenous inhibitor of the mitochondrial pathway of apoptosis (Massard et al., 2006). Del Bufalo and colleagues reported an apoptosis induction by inhibiting Bcl-2 which is a regulator of telomerase with specific oligonucleotide in human breast carcinoma (Del Bufalo et al., 2005). Inhibition of Bcl-2 could repress telomerase expression which indicates a strong

correlation between telomerase and Bcl-2. Moreover, hTERT protects cells from chemical-induced apoptosis independently of its enzymatic and telomere-maintaining activity. Interestingly, inducing ROS generation in these cancer cells induces nuclear export of hTERT. Telomerase was excluded from the nucleus to the cytosol and attenuate mitochondrial apoptosis induced by interfering with the Bcl-2-dependent mitochondrial apoptosis (Del Bufalo et al., 2005).

Taking together, telomerase may be involved in various cellular pathways which affect apoptosis.

1.10 Telomerase and nuclear DNA damage response

TERT has been shown to play a role in chromatin remodelling and DNA damage response as one of the non-canonical function (Sharma et al., 2003, Masutomi et al, 2005, Park et al., 2009a). In mammals, cellular responses to DNA damage are mediated by many protein kinases including ATM (ataxia telangiectasia mutated) and ATR (ATM and Rad3-related) (Ljungman, 2010). ATM regulates a number of DNA damage response factors to response to the damage such as DNA double strand breaks by phosphorylate H2A.X at serine 139 and facilitates the assembly of checkpoint and DNA repair factors including 53BP1, MDC1⁄ NFBD1 and NBS1 to form a DNA damage response complex at the site of DNA double stand breaks. MDC1, which binds to the phosphorylated H2A.X will allow ubiquitin ligase RNF8 to bind. As shown in figure 1.4, RNF8 ubiquitylates histones in the chromatin surrounding the damage, thereby recruiting BRCA1 via the RAP80 protein and 53BP1 via chromatin structure alterations in the vicinity of DNA damage (Huyen et. al., 2004). When assembled, this complex enhanced DNA double strand break repair and increased resistance to radiation (Yan and Jetten, 2008).

Masutomi and co-workers reported that transient expression of hTERT in normal fibroblasts modulated DNA damage response (DDR). Fibroblasts with stably suppressed hTERT function by RNA interference exhibited a lack of induction of ATM and H2A.X phosphorylation after radiation, irionotecan and etoposide (Masutomi et al, 2005). Nitta and colleagues reported that mice with double deficient ATM and TERT demonstrated increased progression of ageing and had shorter lifespan compared to mice lacking only ATM which indicates a correlation between TERT and ATM (Nitta et al., 2011).

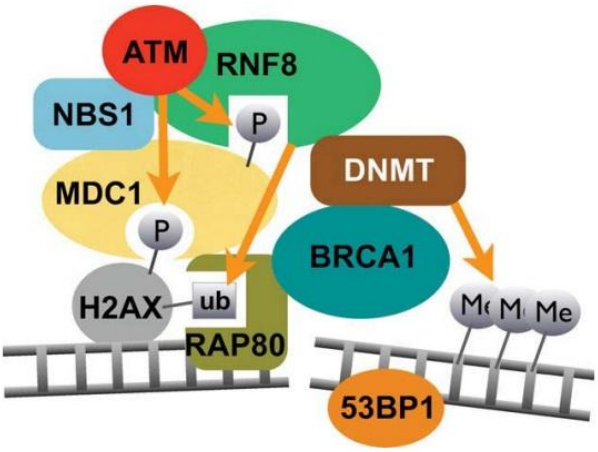

Figure 1.4. Formation of a DDR complex at site of DNA DSB. A DSB induces a topological alteration in the DNA/chromatin that leads to the activation of ATM and the C-terminal tail of H2A.X becomes available for phosphorylation by ATM. Phosphorylation of H2A.X then triggers the assembly of a large DDR complex consiting of MDC1, RNF8 BRCA1, 53BP1, and DNMT (Ljungman, 2010).

1.11 Mitochondria

Mitochondria are the main energy generating organelles in the cell and are in addition considered the major source of intracellular ROS generation. As shown in fugure 1.5, mitochondria are double membrane organelles located in the cytoplasm of eukaryotic cells (Kakkar et al., 2007). The basic structure of a mitochondrion consists of outer membrane, intermembrane space, inner membrane, cristae, and matrix in size of about 1 μm. The outer membrane of mitochondria is very similar to that of a eukaryotic cell membrane in both structure and composition (Voet et al., 2004).

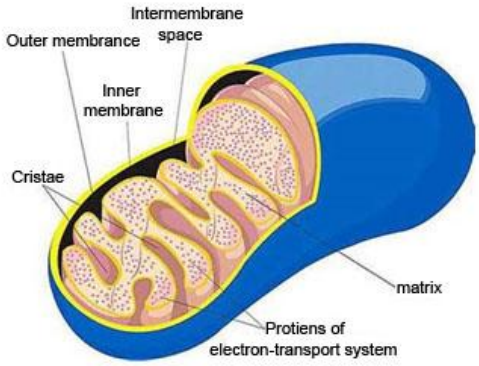

Figure 1.5. The general organization of a mitochondrion. Mitochondria are a double membranous organelle found in the cytoplasm of all eukaryotic cells. They contain the outer membrane and the inner membrane which is made up of proteins and phospholipids. The space between the two membranes is called the inter-membrane space. (Image taken from http:// amrita.vlab.co.in/)

The outer membrane contains large amounts of the protein ‘porin‘ which creates transport pores for the diffusion of the molecules (Ryan 2005). Any large proteins that enter the mitochondrion must be labelled at the N-terminus and actively transported by the protein translocase of the outer membrane (Ryan 2005).

The mitochondrion contains several copies of mtDNA as well as ribosomes and associated proteins required for mtDNA transcription and translation (Voet et al., 2004). The mitochondrion is the energy producing factory of the cell (Wallace 2006). The mechanism that converses the metabolic energy into adenosine triphosphate (ATP) takes place inside mitochondria. The mechanism is known as oxidative phosphorylation which electron transport through the oxidative phosphorylation enables the pumping of protons from mitochondrial matrix into the intermembrane space, generating a proton motive gradient (Schultz et al., 2001). Mitochondrial dysfunction has an effect to cell signalling, programmed cell death (apoptosis), control of the cell cycle and senescence (Wallace 2006; Kakkar et al., 2007, Passos et al., 2010).

1.12 Oxidative phosphorylation

Mitochondria are the energy producing factory of the cell that converses the metabolic energy into adenosine triphosphate (ATP). The process that uses energy released from the oxidation of glucose to produce ATP is known as oxidative phosphorylation (OXPHOS). This process requires the passing of electrons (via electron transport chain, ETC) through specific protein complexes, the OXPHOS proteins (Hansford 2002) and

enables the pumping of protons (H+) from the mitochondrial matrix into the intermembrane space which drives the production of ATP (Voet et al., 2004).

In the process, a glycolysis step breaks down glucose to produce pyruvate, which is an essential component of aerobic respiration. Pyruvate will be transported into the mitochondria via pyruvate dehydrogenase (PDH), and converted via a series of reactions to acetyl CoA. This acetyl CoA is substrate for citric acid cycle (Krebs cycle) which provide several electron donors for electron transport chain (ETC).

There is a series of 5 enzymes (Complex I-V) related to ETC. As shown in fugure 1.6, these 5 complexes are located within the mitochondrial inner membrane. The first enzyme in the ETC is NADH dehydrogenase (complex I). Complex I will receive electrons from NADH from Krebs cycle and transfer to ubiquinone (coenzyme Q10). During this process 4 protons (H+) are pumped across the membrane (Hansford 2002).

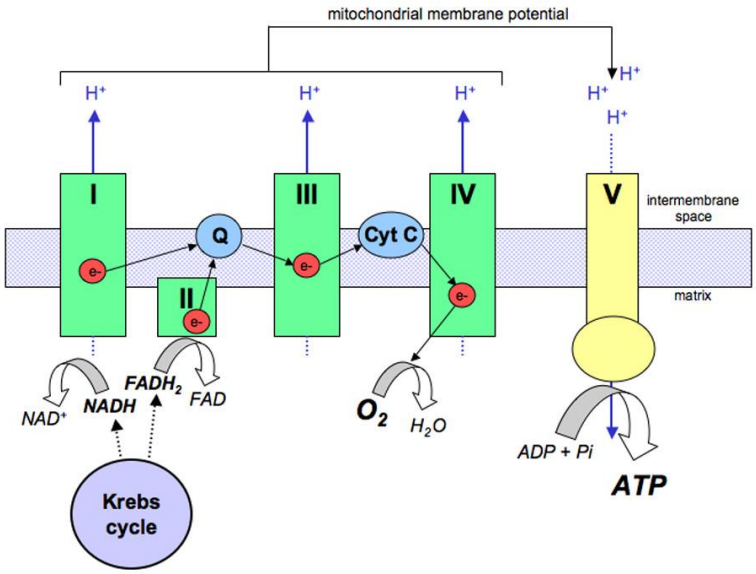

Figure 1.6. Oxidative phosphorylation in mitochondria Electrons donated from NADH and $FADH_2$ from Krebs cycle pass down the electron transport chain with oxygen being the terminal acceptor at complex IV. This movement of electrons results in a shift of protons across the inner mitochondrial membrane and generating the energy for ATP synthase to produce ATP from ADP. (Protti and Singer *Critical care* 2006 10:228 doi:10.1186/cc5014)

The second enzyme, succinate dehydrogenase (complex II) will transfer electrons to Q10. This complex also has a role in the Krebs cycle (Horsefield et al., 2004). Complex II oxidises succinate to fumarate and transfers these electrons to Q10. Coenzyme Q10 will be reduced and becomes ubiquinol.

Ubiquinol is oxidised by mitochondrial cytochrome bc1 complex (complex III), resulting in the transfer of electrons and pumping of more protons.

Complex III contains several cytochrome subunits, proteins that contain hemegroups and transfer electrons (Kakkar et al., 2007). Oxidation of ubiquinol allows complex III to transfer electrons to a mitochondrial associated protein or cytochrome c, which will transfer electrons to the final ETC complex, cytochrome c oxidase (complex IV). A series of hemegroups and metal co-factors in complex IV will utilise and transfer electrons to oxygen and reduce it to H_2O.

Finally the potential energy created from this step allows the pumping of protons (Hansford 2002). The net pumping of protons by ETC will create a chemi-osmotic gradient, which allow protons through the enzyme ATP synthase (Schultz et al., 2001). As these protons pass back down into the matrix, a conformational change in the 'head' of ATP synthase forces ADP and Pi (in-organic phosphate) to bind, resulting in the production of ATP (Dimroth et al., 2000). This ATP will transport out from mitochondria and be used as energy for the cell.

However, during this process each O_2 molecule must accept two electrons to become fully reduced to H_2O. However, the process is imperfect and often only one electron is donated, leading to the formation of the superoxide anions. The mistake happens mostly at two discrete steps, complex I (NADH dehydrogenase) and Complex III (ubiquinone-cytochrome c reductase).

Under normal conditions complex III is the main site of ROS formation (Turrens 1997). Studies have shown that the rate of flow of electrons during oxidative phosphorylation can influence the amount of ROS produced and many treatments that affect electron flow produce (complex activity inhibitors) increases in ROS production (Lenaz 2001). The frequency of this mistake has been reported to be about 0.1% of all oxygen molecules (Imlay and Fridovich 1991). Thus the formation of this ROS is enough to qualify the mitochondria as the main source of cellular ROS.

1.13 Reactive Oxygen Species (ROS)

ROS, also called free radicals or oxygen radicals are highly reactive small molecules containing unpaired electrons. These molecules can react with several organic molecules (nucleotides, proteins or lipids) and, in doing so, can cause considerable damage, impairing normal cellular function (Finkel and Holbrook 2000; Kirkinezos and Moraes 2001). The term Reactive oxygen species (ROS) is used to describe a variety of molecules including the superoxide anion ($O_2^{\bullet -}$), hydroxyl ($HO^{\bullet}$), peroxyl ($RO_2^{\bullet}$) and alkoxyl ($RO^{\bullet}$) radicals, as well as non-radical species including hydrogen peroxide (H_2O_2) (Halliwell and Cross, 1994).

ROS can damage three kinds of organic molecules which are lipids, proteins and nucleotides. When reactive oxygen species react with cellular lipids, they can decrease membrane fluidity, influence endoperoxide generation and interact with the unsaturated aldehydes which are highly reactive and may act as mutagens, inactivate enzymes or operate as endogenous cross-linking agents (Beckman and Ames 1998). Oxidation of proteins by oxygen radicals leads to formation of carbonyls, protein-protein cross-linking, peptide fragmentation and inactivation of proteins with iron-sulfur clusters (Beckman and Ames 1998). Overall, any of these interactions between ROS and biomolecules promote cellular dysfunction.

DNA is susceptible to the damage by ROS, especially the highly damaging hydroxyl radical. When ROS damage nucleotides, adduct base and sugar groups may form single- and double-strand breaks in the nucleotide backbone or cross-linking to other molecules can occur. These altered nucleotides can eventually lead to mutation, DNA rearrangements or problems during transcription (Beckman and Ames 1998). The main products of oxidative DNA base damage are thymine glycol (Wang, Kreutzer and Essigmann, 1998) and 7,8-dihydro-8-oxo-2'-deoxyguanosine (8-oxodG) (De Bont and van Larebeke, 2004).

Thymine gycol has a low mutagenicity, while 8-oxodG has the ability, albeit with low frequency to cause G-T transversions upon replication (Alexeyev, 2009).

It is also important to point out that telomere dependent replicative senescence is also influenced by cellular stress, in that telomere attrition is affected by the level of oxidative stress in the cell (von Zglinicki et al., 1995).

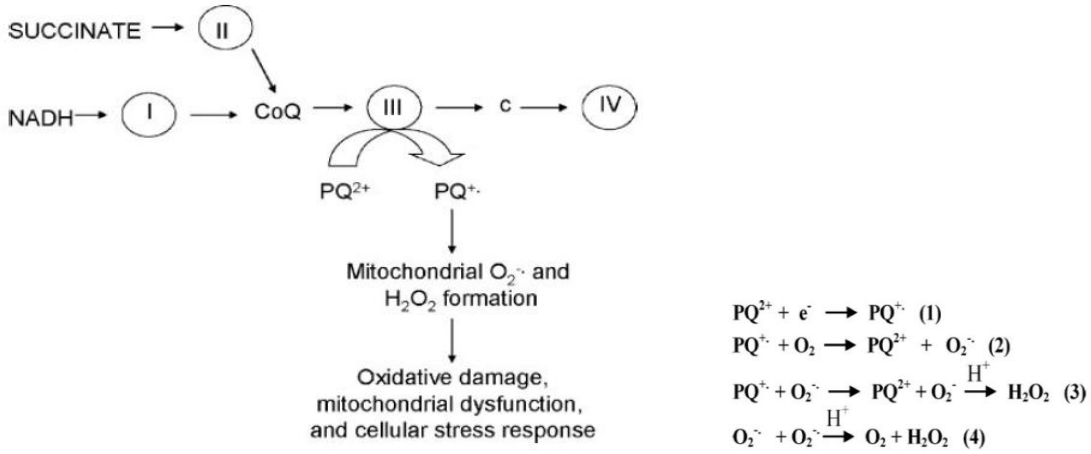

Figure 1.7. Involvement of ETC in PQ^{2+} -dependent H2O2 generation in brain mitochondria Complex III on ETC has the ability to transfer electrons to participate in mechanisms of H_2O_2 production by PQ^{2+} (Castello et al., 2007)

In addition to the naturally occuring ROS generated by OXPHOS, mitochondrial ROS production can be modulated by the use of reagents, specific conditions and irradiation. The example of a chemical which can activate mitochondrial ROS production is paraquat (Ali et al., 1996; Castello et. Al., 2007; Shibata et. Al., 2010).

As shown in figure 1.7, paraquat (PQ^{2+}) is a bipyridyl group (1,1‘ –dimethyl-4,4‘ – bipyridylium) herbicide, the prototype toxin known to exert injurious effect through oxidative stress and bears a structural similarity to parkinson disease toxicant, 1-methyl-4-pheynlpyridinium (Mohammadi-Bardbori and Ghazi-Khansari, 2008). It is widely accepted that PQ^{2+} -induced generation of ROS arises from a number of cellular sources. However, mitochondria are a principle cellular site of PQ^{2+} -induced H_2O_2 production. Electron from Complex II and complex III in the electron transport chain can be transfered to a PQ^{2+} molecule and is proposed to participate in mechanisms of H_2O_2 production by PQ^{2+}(Castello et. al., 2007).

1.14 p53

One important gene which is affected by ROS is p53. Among the tumour suppressor genes, p53, a guardian of the genome, is a DNA-binding protein which acts as a transcription factor to control the expression of proteins involved in the cell cycle. p53 was first identified in 1979 in association with simian virus 40 (SV40) large T-antigen. Wei et al reported in 2006 that a combination of bio-informatic and ChIP based

informationsuggested that the number of genes containing p53 binding sites may vary between 500 and 1600 (Wei et al., 2006). Genes involved in the responses of cell-cycle arrest and apoptosis are largely attributed to p53. Once cells are undergoing stress, p53 mediates a series of cellular outcomes that vary from cell cycle arrest to DNA-repair and senescence or apoptosis. The up regulation of p53 occurs at the post-translational level (phosphorylation, tetramerisation), and is achieved through stabilisation of the protein (Choisy-Rossi et al., 1999). The key role played by p53 in tumour suppression is underscored by the frequent inactivation of this gene by various mutations as found in many in human cancer types (Martins et al., 2006). This p53 inactivation occurs in around 50% all tumours and might contribute to better cancer cell survival because the cells do not arrest even with a high load of DNA damage (Hollstein et al., 1994). How p53 shows its anticancer function seems to differ according to the tumour type. For example, restoring p53 function in p53-deficient lymphomas could induce apoptosis (Ventura et al., 2007). In contrast, p53 reactivation in hepatocarcinoma cells induces growth arrest and cellular senescence (Xue et al., 2007). It is not clear which features of cancer cells determine whether its response to p53 activation is apoptosis or senescence but both outcomes are associated with tumour regression.

1.15 Activation of p53

A variety of stress signals lead to p53 activation. DNA damage is the first type of stress found to activate p53 (Lane, 1992). DNA damage signalling is triggered by a variety of exogenous and endogenous events that might compromise the genome integrity by altering the structure of DNA which generates mutations, and/or by causing double strand breaks (DSB). The exogenous damage might be caused by UV radiation, ionizing radiations or chemical mutagenic compounds. However, endogenous DNA damage derives from normal cellular processes such as metabolism. DNA damage signals can activate p53 through Ser/Thr kinases which mediate p53 phosphorylations (Lambert et al., 1998). ATM and ATR, the two DNA damage sensor kinases and their respective downstream kinases Chk1 and Chk2, can phosphorylate p53 at different sites. ATM and Chk2 act in response to ionizing radiation and DSBs leading to phosphorylation of p53 at Ser15, Thr 18, and Ser20. However, ATR and Chk1 which seems to response to UV damage and hypoxia can phosphorylate p53 at Ser15 and Ser37 while Chk1 itself can phosphorylates p53 at Ser6, Ser9 and Ser20 (Banin et al., 1998; Chehab et al., 1999; Hammond et al., 2002). In response to stress, p53 may also contribute to a constitutive chronic stress such as the generation of cellular ROS. Persistent activation of p53

enhances ROS production via pathways involving p38MAPK and transforming growth-factor-β (TGFb), which in turn contributes to DNA damage formation and further activation of p53, forming a positive feedback loop that stabilizes p53-mediated cellular reactions (Chen et al. 2003; Bragado et al. 2007; Passos et al. 2010, see also chapter 1.19).

1.16 p53 and cellular senescence

Several lines of evidence support the idea of p53 mediate the induction of senescence, a program leading to irreversible arrest of cell growth accompanied by a characteristic set of phenotypic changes in the cell. Senescence can be triggered by shortening of telomeres due to proliferation (replicative senescence) or by other exogenous or endogenous acute and chronic stress signals (telomere-independent or premature senescence). Many reports have revealed the importance of DNA-damage response (DDR) in initiating both replicative and premature senescence. A common signal is the occurrence of double strand breaks caused by telomere erosion, replication stresses or by oncogene activation (Bartkova et al., 2006; Di Micco et al., 2006; Hemann and Narita, 2007). In models of cellular senescence induced by DNA damaging agents causing double strand breaks, ATR/ATM mediates the activation of cell-cycle checkpoints via CHK1/CHK2 and p53 with the participation of p21, p16 and Rb (Itahana et al., 2004). p21 is a crucial transcription target in mediating p53-induced senescence (Brown et al., 1997). pRb activation via the CDK inhibitor p21 could represent a p53-mediated senescence since disruption of p21 by homologous recombination is able to bypass senescence in human diploid fibroblasts (Brown et al., 1997). However, disruption of p21 fails to bypass senescence in mouse cells (Pantoja and Serrano, 1999). Furthermore, human cells can undergo senescence without activity of pRb or its family members which points to alternative, pRb-independent routes of p53-mediated senescence (Smogorzewska and de Lange, 2002).

1.17 p53 and apoptosis

The main role of p53 is to prevent the outgrowth of damaged or stressed cells that may develop into tumor cells. This can be achieved by eliminating cells through apoptosis. The best known transcriptional targets of p53 include a large number of pro-apoptotic genes that can be divided into categories depending on their specific functions (Wei et al., 2006). Genes related to apoptosis are generally classified into the extrinsic and intrinsic apoptotic pathways. Only intrinsic pathway relates to p53. The extrinsic

apoptotic pathway engages death-receptors belonging to the TNF-receptor family and leads to the induction of a cascade of caspases which induce apoptosis (Attardi et al., 2000). The intrinsic pathway is activated in response to different signals such as DNA damage, oncogenic signalling or hypoxia and is associated with mitochondrial depolarization and release of cytochrome C from the mitochondrial as well as caspase activation (Cory and Adams, 2002).

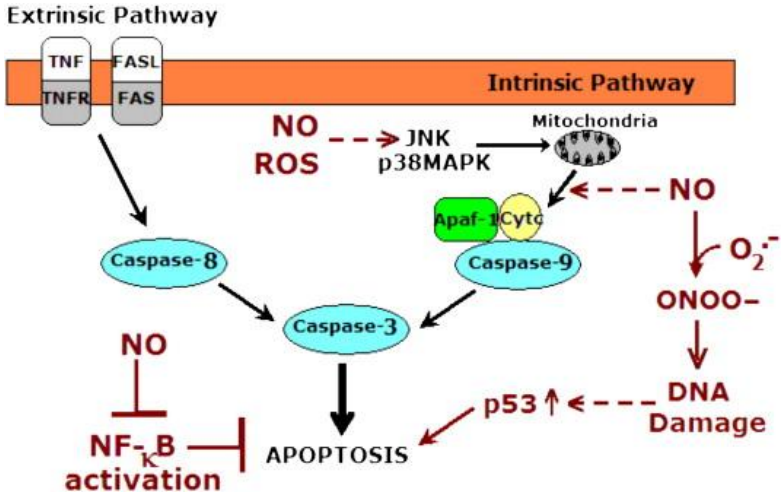

Figure 1.8 Extrinsic and intrinsic pathways for apoptosis. (Aslan et al., 2008)

For this intrinsic pathway, p53 can contribute to several p53-regulated genes such as Bax, Noxa and PUMA (Miyashita and Reed, 1995). Bax was the first identified p53-regulated pro-apoptotic Bcl-2 family member (Miyashita and Reed, 1995). Loss of Bax accounts for nearly half of the accelerated tumour growth which resulted from the loss of p53 in brain tumour (Schmitt et al., 2002). Bax is also responsible for nearly half of p53-dependent apoptosis induced by 5-FU in colorectal cancer cells (Zhang et al., 2000). In contrast, Bax is dispensable for the apoptosis induced by γ-irradiation in thymocytes and intestinal epithelial cells (Bouvard et al., 2000). PUMA and Noxa are activated in a p53-dependent manner following DNA damage (Nakano and Vousden, 2001; Yu et al., 2001). PUMA mediates apoptosis induced by p53 in response to hypoxia, DNA damaging agents, and endoplasmic reticulum stress in human colorectal cancer cells (Yu et al., 2003). The absence of Noxa resulted in resistance to X-ray-induced apoptosis in the small intestinal crypts *in vivo* (Shibue et al., 2003; Villunger et al., 2003). Moreover, under genotoxic, hypoxic, and oxidative stresses, the p53 protein can translocate to mitochondria (Marchenko et al., 2000). This translocation is dependent on Mdm2 (Marchenko et al., 2007; Pei et al., 2012). At the mitochondria,

p53 has been found to interact with the Bcl-xL and Bcl-2 protective proteins (Mihara et al., 2003).

There is a crosstalk among p53 functions at the mitochondria and its transcriptional activity, in fact upon stress-induced-stabilisation and activation within the nucleus, p53 induces the transcription of Puma and this one is able to release cytoplasmic p53 from the inhibitory interaction with Bcl-xL, thus allowing it to directly activate Bax (Chipuk et al., 2005). p53 interacts also with Bad and the mitochondrial p53/Bad complex promotes apoptosis via activation and oligomerization of Bak (Jiang et al., 2006). Moreover, p53 acts directly on the pro-apoptotic Bak promoting its dissociation from the anti-apoptotic protein MCL1 (Leu et al., 2004). Once the inhibitory interactions upon Bax and Bak are relieved, they oligomerise to form a transmembrane pore for the release of cytochrome C from mitochondria.

1.18 p53 mutations

Various mutations at hot spots have been described to inactivate p53 in many cancer types (Liu et al., 2010; Ye et al., 2009; Campitelli et al., 2012). The physiological expression of point-mutated p53 can strongly limit the overall cellular p53 function (de Vries et al., 2002). The most common p53 mutations are missense mutations on the DNA binding domain which affect the full length protein so that it is incapable to bind DNA. There are two types of p53 DNA binding domain mutations, conformational mutants and contact site mutants (Willis et al., 2004). p53 is active in tetramer form (Friedmann et al.,1993). Since most of the mutations found in cancers are not located within its tetramerisation domain, most of the p53 mutants are functional for tetramerisation (Chene, 1998). Mutant p53 can tetramerise with wild-type p53 to form hetero-tetramers and drive the wild-type subunits into a mutant conformation (Milner et al., 1991; Brachmann et al., 1996; Ko and Prives, 1996). This dominant negative activity is important for inactivating the wild-type p53 allele in heterozygous tumours (Chene, 1998). Moreover, p53 mutants can actually alter patterns of gene expression. Mutant p53 can upregulate promoters of genes such as MRD-1 (Atema and Chene, 2002) and c-myc (Frazier et al., 1998). The presence of mutated p53 reduces the ability of wild-type p53 in inducing p21, MDM2 and PIG3 (Willis et al., 2004). Thus mutant p53 exerts its dominant negative activity by abrogating functional wile-type p53.

1.19 Cellular senescence

Since there is a correlation between p53 and cellular senescence as explained in 1.16, cellular senescence can acts as a barrier to prevent cancerous phenotypes, averting the accumulation of mutations and therefore plays an important role in tumour suppression (Ohtani et al., 2009). Most somatic cells cannot divide indefinitely. They permanently stop dividing after a finite number of cell divisions and enter a state known as cellular or replicative senescence. This limit of replication was first described by Hayflick, and is often termed the 'Hayflick limit' (Hayflick and Moorhead, 1961). Replicative senescence is induced by critically short telomeres, counting the number of cell divisions as they progressively shorten with each division (d'Adda di Fagagna et al., 2003). Importantly, telomere shortening can be exacerbated by oxidative stress (von Zglinicki et al., 1995; Lu and Finkel, 2008). The telomere dependence of replicative senescence gained support from evidence showing that addition of hTERT (telomerase catalytic subunit) can immortalise human somatic cells (Bodnar et al., 1998). In addition to telomere shortening, cellular senescence can be induced by other multiple extrinsic factors such as DNA damaging agents, oxidising agents, over expression of certain oncogenes or lack of nutrients or growth factors as shown in figure 1.18 (Ben-Porath and Weinberg, 2005). This 'extrinsic form' of induction of senescence occurs much more rapidly than that induced by telomere attrition. This led to a distinction between 'replicative senescence' which refers to senescence due to population doublings which most likely is induced by telomere erosion and 'stress-induced premature senescence' (SIPS), where senescence is induced more rapidly by exogenous factors other than loss of telomere segments (Dierick et al., 2002).

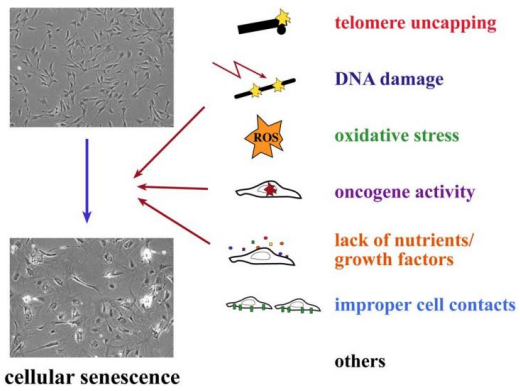

Figure 1.9 The signals activating senescence. Multiple types of stress can induce cellular senescence (Ben-Porath and Weinberg, 2005).

1.20 Stress-Induced Premature Senescence (SIPS)

These are several exogenous factors which can activate SIPS including external DNA damage using chemotherapeutic agents, irradiation, oxidative stress, damage to chromatin structure and oncogene activity which can cause cells to enter an immediate growth arrest without any measurable telomere shortening (Saretzki, 2010). Oxidative stress and the accumulation of intracellular reactive oxygen species (ROS) is one of the signals playing an important role in this premature senescence (von Zglinicki et al., 1995; Lu and Finkel, 2008). Internal ROS can damage cellular components through the oxidation of DNA, proteins and lipids (Chen et al., 1998; Sitte et al., 2000). Increase of intracellular ROS levels through hydrogen peroxide treatment or through the inhibition of ROS scavenging enzymes, such as superoxide dismutase can cause premature senescence (Blander et al., 2003). Oxidative stress can cause DNA damage and accelerate telomere shortening rates (von Zglinicki et al., 1995, Chen et al., 1998). Oxidative stress induces single stranded breaks in telomeric DNA (von Zglinicki et al., 2000) and causes an impaired cellular redox state, irreparable DNA damage and oxidatively damaged proteins (von Zglinicki et a., 2005). Moreover, ROS can act directly as a second messenger to regulate specific signalling pathways (Saitoh et al., 1998). It has been shown that the reduction of ambient oxygen levels does not reduce the fraction of p16-expressing cells in a pre-senescent population of normal fibroblasts. However, it is the proportion of p21-expresssing cells that is reduced (Itahana et al., 2003). Thus this data suggests that oxidative stress might acts through DNA damage response and p53→p21→Rb to induce senescence (Chen et al., 1998; Ben-Porath and Weinberg, 2005).

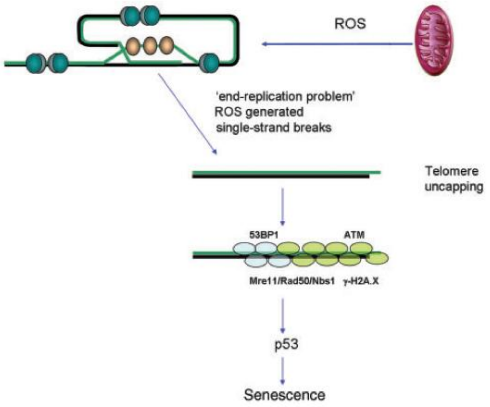

Figure 1.10 Telomere shortening and DNA damaged by ROS, which are generated by mitochondrial respiration, induce a DNA damage response including the formation of telomeric DNA damage foci. This process could activate p53 which triggers cellular senescence (Passos et al., 2007).

Moreover, a long-term activation of p21 (CDKN1A) could induce mitochondrial dysfunction and the production of mitochondrial ROS through a serial signalling GADD45-MAPK14(p38MAPK)-GRB2-TGFBR2-TGF (Passos et al., 2010). In this study, MRC5 fibroblast were treated with ionizing radiation (20Gy). After irradiation, the number of DNA damage foci permanently increased which indicated the development of cells into stress-induced premature senescence. At 24 hours after irradiation, the level of mitochondrial superoxide (measured as mitoSOX by flow cytometry) and cellular peroxides (measured as DHR by flow cytometry) increased and remained elevated during the observation. Not only was ROS production increased, but mitochondria in stress-induced senescent cells also showed an increase in mitochondrial mass (measured by NAO fluorescence), mitochondrial uncoupling (increase transcription of *UCP-2* and decrease of mitochondrial membrane potential (measure by JC-1 fluorescence) (Passos et al., 2010). This feedback loop persists in both *in vivo* and *in vitro* cellular senescence.

Oxidative stress can cause DNA damage and accelerated telomere shortening (Chen et al., 1998) triggers a DNA damage response and cellular senescence (Wang et al., 2009). This DNA damage response is characterised by the activation of ATM and ATR (Ljungman, 2010). The proteins are recruited to the site of damage and lead to phosphorylation of Ser-139 of the histone H2A.X molecules (c-H2A.X) close to the site of DNA damage as described previously in 1.10. The phosphorylation of histone H2A.X facilitates the assembly of checkpoints and DNA repair factors including 53BP1, MDC1 and NBS1, and also promotes the activation by phosphorylation of Chk1 and Chk2 that ultimately result in cell cycle arrest (Smogorzewska & de Lange, 2002). The focus size increases rapidly after formation, and remains present until damage is repaired. Since the signalling pathway activated by DNA damage has to be maintained to keep cells in a senescent state, cellular senescence can be observed as a permanently maintained DNA damage response state (Saretzki, 2010). Therefore, γH2A.X foci can be used as a marker for stress induced senescence. Thus antibodies against DNA damage foci components, such as γH2A.X or 53BP1 can be used as a marker for senescent cells.

1.21 Telomerase shuttling

Extra-nuclear localisation of telomerase has been described by various groups (Santos et al., 2006; Ahmed et al., 2008; Haendeler et al., 2009, Indran et al., 2010). The hTERT

protein contains a nuclear and nucleolar localisation signal as well as a nuclear export signal (Santos et al., 2004, 2006). Telomerase can be found in the nucleolus (and there are clear functions described) and can be associated with the signalling protein 14-3-3 and nuclear exportin CRM1 that are involved in the sub-cellular shuttling of several proteins (Seimiya et al., 2000; Wong et al., 2002; Zhang et al., 2003). Endogenous TERT can be found in the nucleus and cytoplasm of mouse hippocampal neurons, human cells and mouse tissues (Fu et al., 2000, Haendeler et al., 2009). This data suggests that sub-cellular shuttling is not an artefact of forced hTERT expression. It occurs naturally within cells and is dynamically regulated. This shuttling process depends on various factors such as cell cycle phase, DNA damage and oxidative stress (Saretzki, 2009).

1.22 Mitochondrial localisation of hTERT

Since many proteins show a capacity to shuttle between the nucleus and mitochondria, different models have been used to determine telomerase function in different subcellular fractions including over-expression of a GFP/hTERT fusion protein in cancer cells or hTERT over-expression in normal and tumour cells. Recent studies from four different groups have shown that hTERT can shuttle from the nucleus to the mitochondria upon oxidative stress and drug treatment (Santos et al., 2004, 2006; Ahmed et al., 2008; Haendeler et al., 2003, 2004, 2009; Indran et al., 2011). Haendeler and colleagues found that hTERT is phosphorylated at tyrosine 707 in a Src kinase-dependent manner and excluded from the nucleus after oxidative stress (Haendeler et al., 2003). They also showed that nuclear export of endogenous hTERT occurs in endothelial cells approaching senescence due to increased oxidative stress, whereas treatment with antioxidants was able to reverse this process (Haendeler et al., 2004). Santos and co-workers have described a specific mitochondrial targeting signal (MTS) at the N-terminus of hTERT (Santos et al., 2004). The transportation of hTERT to the mitochondria seems to be an induced, directed and naturally occurring process.. Santos and colleagues reported that mitochondrially localised hTERT increased mitochondrial DNA damage and apoptosis after H_2O_2 treatment and suggested a potential role of iron metabolism (Santos et al., 2004). This result is different from the report of Ahmed and co-workers in 2008 that fibroblasts over-expressing hTERT do not maintain telomere length under oxidative stress but exclude hTERT from nucleus and protect mitochondria. The accumulation of TERT in mitochondria diminishes mitochondrial superoxide production and intracellular ROS under increased chronic oxidative stress

condition compared to parental fibroblasts under the same conditions. They also showed that hTERT over-expression in human fibroblasts protected mtDNA from DNA damage upon acute (H_2O_2 treatment) and chronic (hyperoxia) oxidative stress. The frequency of apoptosis after treatment with H_2O_2 and etoposide also was substantially lower in hTERT over-expressing cells compared to parental or vector-transfected fibroblasts. (Ahmed et al., 2008).

In 2009, Haendeler and coworkers reported that TERT is transported into the mitochondrial matrix by using translocase of outer membrane (TOM) and translocase of inner membrane (TIM), binds to mitochondrial DNA coding regions for ND1 and ND2 and increases complex I respiratory efficiency. They also showed that binding of TERT to the mitochondrial DNA can protect the mitochondria against ethidium bromide damage induction and increases overall respiratory chain activity which increases mitochondrial respiratory efficiency. Moreover, inhibition of hTERT expression using siRNA in endothelial cells (Ahmed et al., 2008) and shRNA in HEK293 (Haendeler et al., 2009) also shows increase of oxidative stress. They also demonstrated that heart mitochondria from TERT knockout mice had a less efficient respiration in comparison to wild type mice. However, the same effect could not be shown in liver cells. At the same time they have demonstrated a positive correlation between mitochondrially localised hTERT and apoptosis resistance as well as an increase in mitochondrial ROS generation after hTERT ablation (Haendeler et al., 2009). In 2010, Indran and coworkers reported that hTERT is localised at the inner as well as outer mitochondrial membrane fraction in transient hTERT transfection of Hela cells. Hela cells transfected with a vector containing hTERT display a significant lower basal and mitochondrial ROS levels compare to wildtype Hela cells and Hela cells transfected with the control vector after H_2O_2 treatment. siRNA-mediated gene silencing in transiently hTERT overexpressing Hela cells increased the level of ROS generation (Indran et al., 2010). Moreover, they also reported an enhancement of glutathione antioxidant defence capacity in Hela and hTERT overexpressing MRC5. hTERT overexpressing Hela showed inhibition of cytosolic acidification, blocking of mitochondrial translocation of Bax, the drop in transmembrane protential and the release of cytochrome C to the cytosol (Indran et al., 2011). Thus, from independent model systems, three independent groups have demonstrated a protective effect of hTERT to the mitochondria.

Previously, Santos and colleagues had described a specific mitochondrial import sequence and reported that mitochondrially localised hTERT increased mitochondrial DNA damage and apoptosis after H_2O_2 treatment (Santos et al., 2004, 2006). However,

new results from her group demonstrate a protective function of hTERT to mitochondria. Kovalenko and colleagues reported that cell with mutated hTERT protein blocking the translocation of hTERT to mitochondria produce high levels of mitochondrial reactive oxygen species (Kovalenko et al., 2010b). Sharma and co-workers reported in 2011 that absence of hTERT from mitochondria resulted in increased ROS production, mtDNA damage, mitochondria distension and autophagosomes complex (Sharma et al., 2012). The new data from J. Santos's group confirm the protective properties of telomerase in mitochondria found by others.

Ahmed and co-workers reported that oxidative stress causes 80–90% of all hTERT to enter the mitochondria (Ahmed et al., 2008), with the remaining telomerase in the nucleus being unable to maintain telomere length under conditions of chronic hyperoxia (40% oxygen) (Ahmed et al., 2008). Furthermore, Haendeler and colleagues have analysed the distribution of telomerase activity in three cellular subfractions of HEK 293 cells. They found that cells show around 60% of telomerase activity within the nucleus, 20% in the mitochondria and 20% in the remaining cytoplasm before oxidative stress (Haendeler et. al., 2009). Thus, localisation of hTERT in mitochondria is increased under cellular stress condition.

G Saretzki's group also showed that shifting of hTERT over-expressing cells back from hyperoxia to normoxia can reverse the nuclear exclusion of telomerase (Ahmed et al., 2008). Interestingly, Santos' group constructed a mutant hTERT with a disrupted nuclear export signal (NES) of hTERT which renders it nuclear and unable to shuttle to mitochondria. Transfected into primary human foreskin fibroblasts (NHF) these NES-hTERT showed premature senescence and where refractory to immortalisation and that overexpression of this NES-hTERT protein in primary fibroblast was associated with telomere-based cellular senescence, multinucleated cells and the activation of DDR genes ATM, Chk2 and p53 (Kovalenko et al., 2010a). This localisation of a mutated hTERT protein in the nucleus increased DNA damage in both telomeric and extra-telomeric sites. The mutated hTERT also impaired the mitochondria. Cells expressing this mutant protein produce high levels of mitochondrial reactive oxygen species (Kovalenko et al., 2010b). This observation corresponds well with the beneficial role of shuttling TERT to mitochondria as described by Ahmed (Ahmed et al., 2008) and Haendeler (Haendeler et al., 2009).

Thus, the nuclear exclusion and shuttling capacity of hTERT to mitochondria could present an important physiological mechanism in human cells that are positive for telomerase such as lymphocytes, endothelial cells and stem cells. It could mean that

telomerase that protects telomeres under normal growth conditions shifts its protective function towards mitochondria under conditions of increased oxidative stress (Saretzki, 2009).

Nuclear exclusion might be a novel regulatory mechanism for mitochondrial protection of the telomerase catalytic subunit. There is data suggesting that the mitochondrial function might co-exist with the telomeric function and 20–30% of telomerase has been found outside the nucleus and partially within mitochondria already under normal basal conditions in various cell types (Ahmed et al., 2008; Haendeler et al., 2009; Indran et al., 2010).

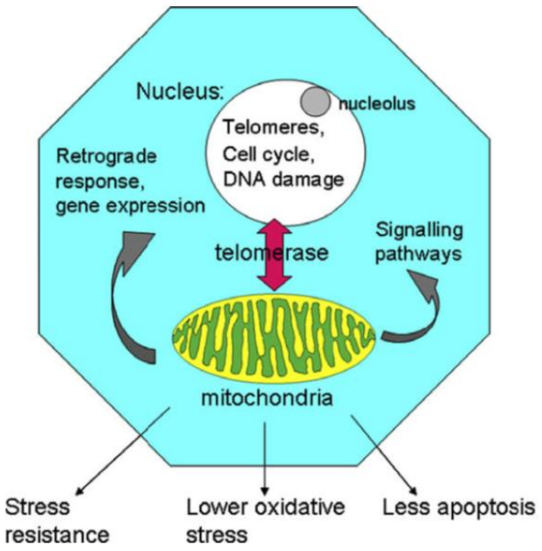

Figure 1.11 Schematic representation of known telomerase localisations and respective functions (Saretzki, 2009).

Although telomerase requires both catalytic subunit and RNA component in telomere elongation, hTR is not present in mitochondria and mitochondrial hTERT can work independently from hTR (Maida et al., 2009, Sharma et al., 2011). This data might suggest the hypothesis of a protective effect of hTERT to the mitochondria independently of its RNA component. Whereas hTERT can bind to mitochondrial nucleic acid and mitochondrial tRNA (Sharma et al., 2011), it is not entirely clear via what mechanisms hTERT protects mitochondrial DNA. One possible mechanism could be the decrease of mitochondrial ROS generation by improved coupling or more effective respiration, direct binding to and protection of mtDNA, improved DNA repair

or an accelerated degradation of mitochondria harbouring damaged DNA (Saretzki, 2009).

The functions of telomerase in different subcellular location is summarised in Figure 1.8. The demonstration of telomere-independent function of telomerase in protection of mitochondria under stress condition describes a new function of telomerase independent of the canonical function on telomere maintenance. However, there are still many questions about what factors influence this telomere-independent function of telomerase.

Aims

The aims of this project were:

Aim 1: Has mitochondrial localisation of telomerase effect on nuclear DNA damage?

Previous experiments of our group have shown that mitochondria in hTERT over-expressing fibroblasts seem to be better protected. hTERT is excluded from the nucleus and protects mitochondria under oxidative stress conditions (Ahmed et al., 2008). hTERT over-expressing fibroblasts showed lower production of oxidative stress, less mitochondrial DNA damage, less mitochondrial mass/mtDNA copy number and high mitochondrial membrane potential (Ahmed et al., 2008). Moreover, mitochondrial ROS are also known to be responsible for nuclear DNA damage (Passos et al., 2010). Therefore the aim was to analyse whether ROS reduction due to mitochondrial hTERT localisation might also help to reduce DNA damage in the nucleus.

However, general hTERT overexpression made it difficult to analyse where the protein is localised under specific conditions. To analyse whether there exists a direct correlation between physical location of hTERT in the mitochondria and its protective function, we used specific shooter vectors (Invitrogen) that deliver proteins specifically to various cellular locations. Various cell lines were transfected with hTERT-containing shooter vectors which include localisation signals specific for the mitochondria or the nucleus (further on called mitoTERT and nuclTERT). Cells were double stained with γH2A.X and myc-tag. γH2A.X was used because it is a sensitive marker for detecting DNA double-strand breaks (DSBs) in cells. DNA damage foci were compared under normal and stress condition between mitochondrial and nuclear TERT containing shooter vector. These experiments should uncover whether localisation of telomerase affects nuclear DNA damage after stress treatment. As stressors hydrogen peroxide and

x-irradiation were used. This experiment should also demonstrate whether mitochondrial localisation of hTERT alone is sufficient and necessary to protect nuclear DNA under normal and stress condition compared to the situation when only nuclear hTERT is present.

Aim 2: Is physical localisation of telomerase in mitochondria necessary and sufficient for decrease of mitochondrial superoxide after exogenous stress?

The aim was to analyse whether the reason for the protection of nuclear DNA after exogenous stress is the localisation of telomerase in mitochondria. The same transfection of hTERT-expressing shooter vectors to the mitochondria and nucleus were performed in various cell types. Hydrogen peroxide and irradiation were used as an exogenous stress in this experiment. Cells transfected with mitoTERT and nuclTERT vectors were compared regarding their mitochondrial superoxide level under normal and exogenous stress conditions induced by hydrogen peroxide and x-irradiation. This experiment should show whether the reduction of mitochondrial superoxide by hTERT localisation in mitochondria would has a direct effect on the nuclear DNA protection by reducing the number of damage foci.

Aim 3: Does p53 status influence the protective function of hTERT?

For this aim we analysed whether there is an effect of p53 function on the protective function of the telomerase catalytic subunit. We hypothesised that function of p53 protein might influence the protection of hTERT and might influence the level of nuclear hTERT exclusion. In order to achieve that an isogenic cell pair of glioblastoma cells were used to analyse whether the p53 status might play any role for the correlation between mitochondrial protection of hTERT and DNA damage. The glioblastoma cell line U87 which contains active wild type p53 was compared with a U87 clone (further called UP96) transfected with a mutated p53 allele (Saretzki et al., 1999). Again, the isogenic cell pair was transfected with mito-hTERT and nucl-hTERT vectors and treated with irradiation. Cells were double stained with γH2A.X and myc-tag and their DNA damage foci under normal and exogenous stress condition will be compared for both cell lines. The mitochondrial superoxide levels were correlated to nuclear DNA damage. This experiment will show whether p53 status might have an effect to the protective function of hTERT. In addition, we analysed the co-localisation between hTERT and DNA damage for nucl-hTERT transfected U87 and UP96 cells using Telo-

Fish. This experiment should clarify whether the sites of nuclear damage are different for cells with active or inactive p53.

Aim 4: Is physical localisation of telomerase in mitochondria necessary and sufficient for decrease of mitochondrial superoxide and nuclear DNA damage after endogenously induced stress?

The aim was to demonstrate whether the protective capacity of telomerase occurs not only after exogenous stress but also after endogenously generated oxidative stress. We used paraquat as an endogenous stress inducer to investigate the protective function of telomerase when it localises in the mitochondria. Paraquat is a chemical which can activate mitochondrial ROS production by influencing oxidative phosphorylation of mitochondria by an impairment of mitochondrial complexes resulting in inhibition of electron transport with subsequent increased production of superoxide anions (Boelsterli and Lim, 2007). An isogenic cell pair (MRC-5 and MRC-5/hTERT) was used and cells transfected with mitoTERT and nuclTERT shooter vectors. Cells were double stained with γH2A.X and myc-tag and their DNA damage foci correlated to mitochondrial superoxide level untreated and after paraquat treatment. This experiment should clarify whether the protective capacity of telomerase works not only after exogenous stress but also protects a cell from endogenous stress via reduction of mitochondrial superoxide level.

Chapter 2
Materials and Methods

2.1 Materials

2.1.1 Cell lines

MRC5 (Human embryonic lung fibroblast); ECACC (Salisbury,UK)

hTERT overexpressing MRC5 (MRC5-hTERT); retroviral transfection of MRC-5 fibroblasts with pLCP-hTERT (Clontech) (Ahmed et al., 2008)

SV40-transformed MRC-5 (SV40-MRC5) American Type Culture Collection (ATCC), Rockville, MD

Hela (human cervix adenocarcinoma); American Type Culture Collection (ATCC), Rockville, MD

MCF7 (human breast adenocarcinoma); American Type Culture Collection (ATCC), Rockville, MD

U87 (glioblastoma astrocytoma); American Type Culture Collection (ATCC), Rockville, MD

UP96 (mutated p53-glioblastoma astrocytoma); Wtp53 U87 cells were transfected by electroporation with the vector pC53-SCX3 which expresses a p53 cDNA point-mutated at codon 143 (resulting in alanine-valine substitution) under the control of the CMV promoter/enhancer (Saretzki et al., 1999). Transfected cells were selected using G-418 sulfate (Calbiochem) in a concentration of 500 μg/ml.

2.1.2 Antibody, restriction enzymes and molecular probes

Primary antibodies	manufacturer/distributor
Anti-Telomerase catalytic subunit (hTERT) (Rabbit)	Rockland
Anti-Myc-Tag antibody (Mouse)	ABCAM
Anti-Myc-Tag (Rabbit)	Cell Signaling
Anti-Phospho-Histone H2A.X (mouse monoclonal IgG)	Invitrogen
Anti-Histone H2A.X Antibody (Rabbit)	Cell Signaling
Anti-COX II (Goat polyclonal)	Santa Cruz
Anti-p53	Cell Signaling
Anti-Phospho-p53 (Ser 15)	Cell Signaling
Anti-β Tubulin	ABCAM

Secondary antibodies

Alexa Fluor® 594 goat anti-mouse IgG (H+L)	A-11005	Molecular probes/Invitrogen
Alexa Fluor® 594 goat anti-rabbit IgG (H+L)	A-11012	Molecular probes/Invitrogen
Alexa Fluor® 488 goat anti-mouse IgG (H+L)	A-11029	Molecular probes/Invitrogen
Alexa Fluor® 488 goat anti-rabbit IgG (H+L)	A-11008	Molecular probes/Invitrogen
Alexa Fluor® 405 goat anti-mouse IgG (H+L)	A-31553	Molecular probes/Invitrogen
Alexa Fluor® 405 goat anti-rabbit IgG (H+L)	A-31556	Molecular probes/Invitrogen
Alexa Fluor® 488 donkey anti-goat IgG (H+L)	A-11055	Molecular probes/Invitrogen
Restriction enzymes for digest (HindIII and EcoRI)		Sigma-Aldrich

Molecular probes

MitoSOX™ Red mitochondrial superoxide indicator	Invitrogen
Dihydrorhodamine 123 (DHR)	Invitrogen
Cy-3-labelled telomere specific (C3TA3) 3 peptide nucleic acid (PNA) probe	Panagene, Korea

2.1.3 Buffers, Solution, Media

30% Acrylamide/ Bis-Acrylamide 37.5:1	Severn Biotech LTD, UK
BioRad Protein Assay	Bio-Rad, Germany
Blue/Orange Loading Dye (6x)	Promega, UK
Bovine serum albumin	Sigma-Aldrich, Germany
Crystal UV ploidy (DAPI solution)	Partec GmbH, Germany
DMEM (Dulbecco's modified Eagle's medium)	PAA Laboratories GmbH, Austria
DMEM with supplements	DMEM supplemented with 10 % FCS (Sigma), 1 % L-Glutamine, 1 % Penicillin/ Streptomycin
DMSO	Sigma-Aldrich, Germany
ECL solution	Amersham, UK
FBS, F9665, HYBI-MAX®	Sigma-Aldrich, Germany
Fish skin gelatin (G7765)	Sigma-Aldrich, Germany
G-418 sulfate	Sigma-Aldrich, Germany
Hybridisation buffer	PAA Laboratories GmbH, Austria

Hybridisation mix for Telomere-FISH	2.5µl 1M Tris pH 7.2 (1mM), 21.4µl Magnesium chloride buffer, 175µl Formamide deionized, 5µl PNA probe (25µg/ml from Panagene, Korea), 12.5µl Blocking reagent (from Roche), 33.6µl Water
Hydrogen Peroxide (H_2O_2)	Sigma-Aldrich, Germany
L-Glytamine	PAA Laboratories GmbH, Austria
Laemmli sample buffer (2x),	Sigma-Aldrich, Germany
Lysis Reagent (CHAPS buffer)	Telo TAGGG Telomerase PCR Elisa Kit Roche, USA
Magnesiumchloride buffer pH7.0 for Telomere-FISH	25mM Magnesiumchloride, 9mM Citric acid,82mM Sodium hydrogen phosphate
MEM (Eagle's minimal essential medium)	Gibco, Invitrogen, UK
Non-essential amino acid 100X	Gibco, Invitrogen, UK
Penicillin-Streptomycin 100X	Calbiochem
Paraformaldehyde (PFA)	Sigma-Aldrich, Germany
PBS 10x	Gibco, Invitrogen, UK
PBG	0.5 % BSA, 0.2 % fish skin gelatin(Sigma) in PBS
PBG-triton	0.5%BSA, 0.5% Triton X100, 0.2% Fish skin gelatin in PBS
PFA (4%)	0.4g PFA, 10 ml 1x PBS
Resolving buffer (4x)	0.4% SDS, 1.5 M Tris-HCl, pH 8.8
Restriction enzymes Hind III and EcoR1	Sigma-Aldrich, Germany
Running buffer (10x)	25 mM Tris, 192 mM glycine, 0.1 % SDS, pH 8.3
SSC	0.015 M Sodium Chloride, 0.15 M Sodium Citrate
TAE buffer (1x) for agarose gel running	0.04 M Tris acetate, 0.001 M EDTA, pH 8
TBST (10x)	10 mM Tris, pH 7.5, 50 mM NaCl, 0.1% Tween 20
TE buffer	10 mM Tris-Cl, 50 mM Tris, 2.7 mM

	KCl, pH7
Transfer buffer for Western-blotting (1x)	39 mM glycine, 20% methanol, 0.04% SDS, 480mM Tris base
Trypsin	Sigma-Aldrich, Germany
Trypsin-EDTA	0.05% Trypsin, 0.02% EDTA (w/v) in water
Wash buffer for telomere-FISH	70ml Formamide (70%), 1ml 1M Tris pH7.2 (10mM Tris), 1ml BSA 10% (0,1% BSA), 28ml water
Western blot stripping Buffer	Pierce, USA

2.1.4 Ready-to-use kits, standards

100 bp DNA Ladder,	Invitrogen
1 KDa DNA Ladder,	Invitrogen
Rainbow molecular protein marker	Amersham
EndoFree Plasmid Maxi Kit	Qiagen

2.1.5 Plasmids

Nuclear and mitochondrial shooter vectors were used in this experiment. pShooter vectors containing hTERT were a kind gift from Dr. J Haendeler (University Düsseldorf Germany) and were constructed using pCDNA 3.1 (figure 2.2). Invitrogen pShooter™ vectors containing GFP were used to verify the transfection conditions. These vectors are a family of vectors designed to express and target the recombinant protein to the desired intracellular location in mammalian cells. pShooter™ vectors are 5.5 kb expression vectors that express the recombinant protein as a fusion to a targeting sequence for the respective subcellular localisation and the *c-myc* epitope (Evan et al., 1985). Fluorescence was used for GFP shooter vector. The plasmid carries protein sequences into a specific location of a cell upon 'targeting sequences' encoded within the sequence of a protein. The presence of a nuclear localisation sequence from SV40 T antigen (Fisher-Fantuzzi and Vesco,1988) directs the protein to the nucleus, while the mitochondrial leader sequence isolated from subunitVIII of human cytochrome c oxidase (Rizzuto et al., 1992) which is removed upon translocation, directs proteins to the mitochondria. The mitochondrial targeting sequence (MTS) is localised at the N-

terminus of hTERT sequence while the nuclear localisation sequence (NLS) is localised at the C-terminus of hTERT sequence.

Table 2.1 Mitochondria and nucleus targeting signal of pShooter plasmid**.**

Vector design	**Location**	**Targeting Signal**
pCMV/*myc*/nuc (V82120 invitrogen)	Nucleus	DPKKKRKV
pCMV/*myc*/mito (V82220 invitrogen)	Mitochondria	MSVLTPLLLRGLTGSARRLPVPRAKIHSL

(Invitrogen, publish 09 May 2001, http://tools.invitrogen.com/content/sfs/manuals/ pshooter_pcmv_man.pdf)

The Invitrogen pShooter™ vectors containing GFP (figure 2.2) were also used as controls to exclude the effect of shooter vector transfection itself and prove the effect hTERT localisation in mitochondria to ROS level and nuclear DNA damage.

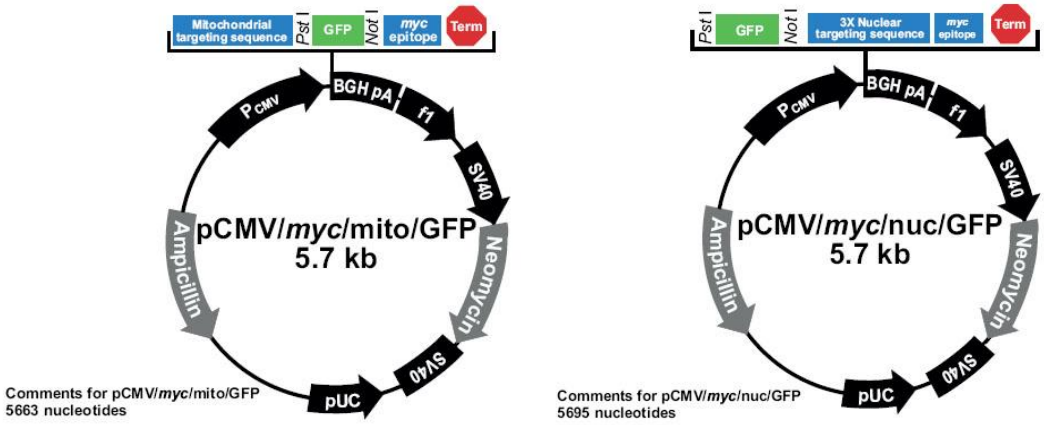

Figure 2.1 pCMV/myc/mito/GFP and pCMV/myc/nuc/GFP maps (Invitrogen)
(http://tools.invitrogen.com/content/sfs/manuals/ pshooter_pcmv_man.pdf)

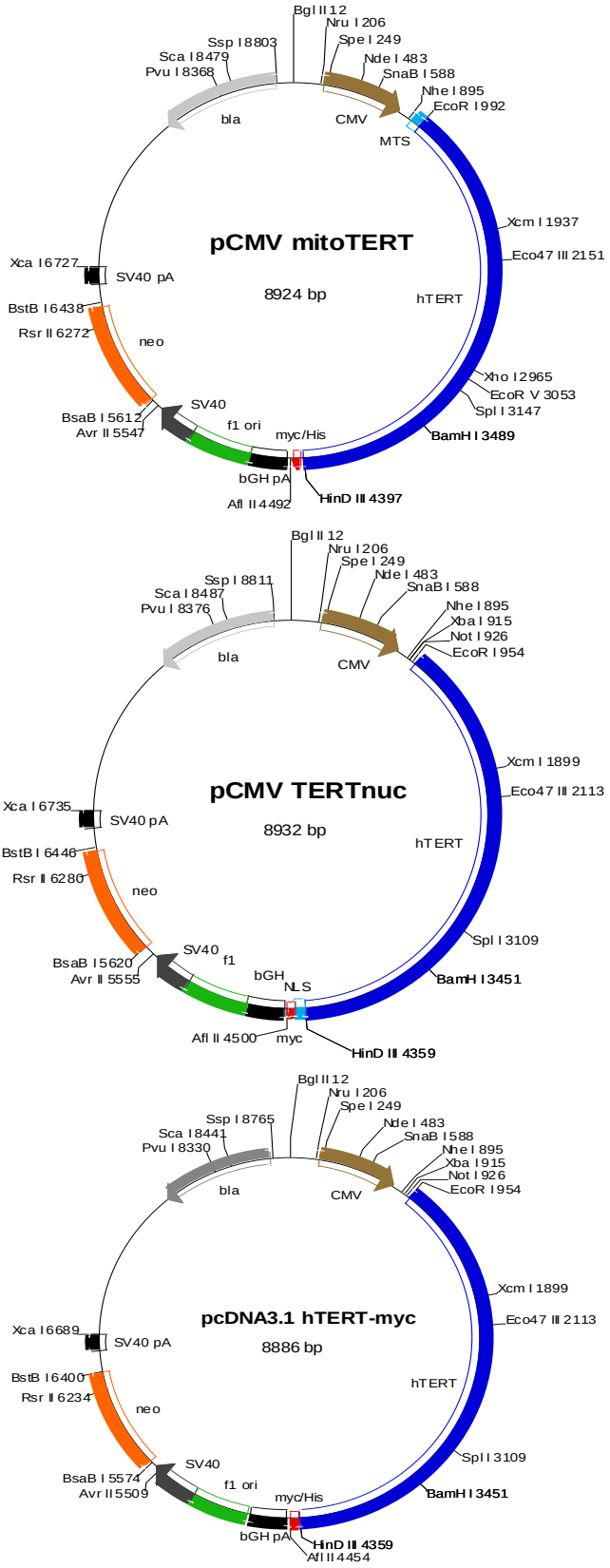

Figure 2.2 Structure of pCMV/mito/TERT and pCMV/nuc/TERT vectors (gift from Dr. J Haendeler, University Düsseldorf, Germany)

2.1.6 Consumable items

19 mm coverslips	VWR international, LLC, USA
Cell culture flasks (75, 150 cm^2)	IWAKI, Japan
ECL™ Hybond™ membrane (PVDF membrane)	Amersham, Pharmacia Biotech

2.1.7 Equipments

BioRad Gel Doc2000	Bio Rad, Germany
Fluoroskan Ascent FL	Thermo Labsystem, USA Ascent software
Chemiluminescence detector system	Raytek Scientific Limited, UK
Fluoroskan Ascent FL	Thermo Scientific
LAS-3000	Intelligent dark box, Fujifilm ImageReader LAS-3000, Lite Aida Image Reader Analyser 4.13, Japan
ND-1000 V3.2.1NanoDrop® ND-1000 UV-Vis Spectrophotometer	ThermoFisher Scientific, USA
Flow Cytometer	Partec GmbH, Germany
Faxitron for X-irradiation	Faxitron MP1 (Qados, UK).,
HEPA filtered steri-cycle carbon dioxide incubator	Thermo Forma, OH, USA
Western Blot chambers and gel tanks	Bio-Rad, Germany
Microscope	Carl Zeiss Microscopy GmbH, Germany
Zeiss Microscope AxioCam	Zeiss HRc, Carl Zeiss Micro Microscope GmbH, Germany
Zeiss Microscope Axioplan	Zeiss Image Browser Carl Zeiss Microscopy GmbH, Germany
Zeiss Microscope AxioImager Z1	Zeiss LSM, Axio Vision, Carl Zeiss Microscopy GmbH, Germany

2.1.8 Software

ImageJ 1.46	ImageJ (version 1.41, freeware) Toronto Western Research Institute, Canada
AxioVision V4.8.0.0	Zeiss LSM Image Browser, Carl Zeiss Microscopy GmbH, Germany
FlowMax instrument software for FACS	Partec GmbH, PAS, Muenster, Germany
SIGMAPlot11	Systat Software Inc, USA

2.2 Methods

2.2.1 Cell culture

All cells were stored frozen in FBS with 7% DMSO in liquid N_2 and thawed prior to culture. Cells were cultured on 75 cm^2 polystyrene tissue culture flasks with double sealed caps. Hela, MCF7, MRC5 and MRC5-hTERT were maintained in DMEM with high glucose and 1% L-glutamine further supplemented with 10 % FBS, 1% penicillin-streptomycin. U87 and it' isogenic clone UP96 were grown under MEM supplemented with 1% non-essential amino acid, 10% fetal calf serum, 1% glutamine, and 1% penicillin/streptomycin. Transfected UP96 cells were selected using G-418 sulfate in a concentration of 500 μg/ml. MRC5/ SV40 cells were maintained in DMEM with high glucose supplemented with 1% non-essential amino acid, 1% L-Glutamine, 10 % FBS and 1% penicillin-streptomycin. Tissue culture conditions were used as follows: at 37^oC, 5% CO2 in a HEPA filtered steri-cycle carbon dioxide incubator (Thermo Forma, OH, USA). Cells were subcultured at 85-90 % confluency and were frequently monitored for adherence, and signs of bacterial. All cells were tested for mycoplasma contamination regularly.

To check the mycoplama contamination, cells were trypsinised and sub-cultured in a 12 well plate overnight. Culture medium was discarded then cells were washed with PBS twice and fixed with 70% Ethanol, then incubated with DAPI for 5 minutes in the dark. DAPI solution was discarded and cells were washed with PBS and then analysed using an inverse fluorescent microscope (Zeiss Microscope AxioCam, Germany).

To subculture, cells were washed with 1X PBS and detached by adding 1X Trypsin–EDTA (0.05% trypsin, 0.02%EDTA), 2ml for a 75 cm^2 flask. Cells were incubated in

trypsin/EDTA at 37^{o}C for one minute or less. Trypsinised cells were added to the regular medium to stop the action of trypsin. Cells were used for further experiments (seeding 1x10^{6} cells in 75 ml^{2} flask then sub-culture at 90% confluency) or stored in FBS with 7% DMSO, frozen down slowly in a Nalgene cryo-box in -80 overnight and then transferred to and kept under liquid N_2.

2.2.2 Cellular transfection: Lipofectamine ™ 2000

Preparation for lipofectamine transfection: one day before transfection 0.5-2 x 10^{5} cells were plated to a well of a 12-well plate (with or without a coverslip) in 1 ml of regular DMEM medium. Cells were cultured to be 90-95% confluent at the time of transfection. For a 6-well plate, 0.5-2 x 10^{5} cells were plated in 2 ml of regular DMEM medium.

On the day of transfection plasmid-Lipofectamine 2000 complexes were freshly prepared. For a 12-well plate, 1.6 μg of plasmid was diluted in 100 μl of Opti-MEM® I reduced serum medium, mixed gently and incubated for 5 minutes at room temperature.

After the 5 minute incubation, diluted plasmids were combined with the diluted lipofectamine 2000 (total volume was 200 μl for 12-well plate and 500 μl for 6-well plate). All solutions were mixed gently and incubated for 20 minutes at room temperature to allow the DNA-lipofectamine 2000 complexes to form.

DNA-lipofectamine complexes were added of to each well containing cells and medium. They were mixed gently by rocking the plate back and forth.

Transfected cells were incubated at 37°C in a CO_2 incubator for 48 hours before assayed for transgene expression as shown in 2.2.7-2.2.10.

2.2.3 Restriction of pCMV-TERT shooter vectors

Both mito-hTERT and nucl-hTERT were amplified in E. Coli, extracted and restricted as showed in figure 2.3. 1 μg from each vector was mixed with 1 unit HindIII and incubated at 37°C for 30 minutes. Then 2 units EcoRI were added to the mixture and continued to be incubated at 37°C for 30 minutes. The restriction reaction was stopped by adding 0.5 M EDTA pH8 for the final concentration of 10 mM. All restricted shooter vectors were analysed by agarose gel electrophoresis to confirm the right size of the hTERT insert on the shooter vector in our plasmid preparation as shown in figure 2.3. The expected size of mito-hTERT is 8.92 Kb, nucl-hTERT is 8.93 Kb and pCDNA 3.1 is 5.44 Kb. Bands in the first and third lane showed 3 forms of DNA conformation which is expected as linear, circular and supercoiled plasmid DNA forms. The

restriction with HindIII and EcoRI restriction enzymes is shown in lanes 2 and 4 (fig. 2.3) which showed the expected hTERT fragment size (3.405 Kb) and pCDNA 3.1 size (5.44 Kb). Results from HindIII and EcoRI restriction were compared with the restrictions of controls (original plasmid stock from Dr. J Haendeler (University Düsseldorf Germany)

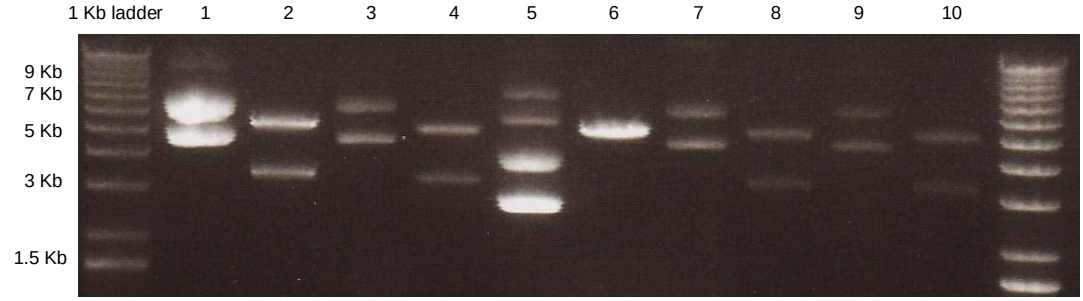

Figure 2.3 Restriction of pCMV-TERT shooter by HindIII and EcoRI pCMV MitoTERT (8.92 Kb) and pCMV NuclTERT (8.93 Kb) were cut by HindIII and EcoRI restriction enzyme compared with pCDNA 3.1 (5.44 Kb). Expected hTERT sized is 3.405 Kb. 1 is pmito-hTERT shooter, 2 is pmito-hTERT shooter restricted by HindIII and EcoRI, 3 is pNUC-TERT shooter, 4 is pNUC-TERT shooter restricted by HindIII and EcoRI, 5 is pCDNA3.1, 6 is p CDNA 3.1 restricted by HindIII, 7 is pmito-hTERT shooter original stock, 8 is a original stock pmito-hTERT shooter restricted by HindIII and EcoRI, 9 is pNUC-TERT shooter original stock and 10 is original stock pNUC-TERT shooter restricted by HindIII and EcoRI.

2.2.4 Oxidative treatment: hydrogen peroxide treatment (H_2O_2)

Cells which were incubated at 37°C in a CO_2 incubator were washed with serum-free culture medium, then treated as required (1 or 3 hours) at 37°C with the required concentration of H_2O_2 (100, 200, 400 or 500 μM) prepared in serum free medium freshly from a stock solution (8.4M). After the treatment cells were washed with regular (FCS containing) culture medium and continued to culture for 24 hours. The reason for this incubation period was to avoid the direct effect of hydrogen peroxide treatment to influence the endogenous ROS measurement. After 24 hours, cells were washed twice with PBS and fixed with paraformaldehyde (4% PFA in PBS) for 10 minutes at room temperature. Paraformaldehyde was removed and cells were dried 3 min and then frozen at -80°C or immediately used for further experiments.

2.2.5 X-Irradiation treatment

X-irradiation was chosen as a second, independent damage treatment and to avoid the delay between H_2O_2 treatment and analysis of ROS using mitoSox staining and microscopy. Cells were incubated at 37°C in a CO_2 incubator on cover slips in 12 well

plates and exposed to the x-ray at the required doses (1,2,5 10 or 20 Gy). Immediately after the treatment, cells were washed with regular culture medium and rewashed with PBS. Cells were fixed with paraformaldehyde (4% PFA in PBS) for 10 minutes at room temperature. Paraformaldehyde was removed, cells were dried for 3 min and frozen at -80°C or continued with for immune-fluorescence (IF) staining.

2.2.6 Paraquat (PQ^{2+}) treatment

Two days after transfection cells which were incubated at 37°C in a CO_2 incubator were washed with serum-free culture medium and treated with 400 μM paraquat. Cells were kept with paraquat for different time periods (1-24h). After the end of the treatment (1-24h), cells were washed with 1X PBS and fixed with paraformaldehyde (4% PFA in PBS) for 10 minutes at room temperature. Paraformaldehyde was removed and cells were frozen at -80°C or used immediately for IF staining.

2.2.7 Staining of mitochondrial superoxide with mitoSOX™

For staining of mitochondrial superoxide in non-fixed cells: cells were grown on 19 mm circular cover slips in 12-well plates. After aspirating the medium, cells were washed twice with serum free medium and incubated with 5 μM mitoSox diluted in serum free medium. Cells were kept under 37°C and protected from light for 15 min. After aspiration, cells were washed twice with PBS then fixed with 1 ml 4 % PFA in PBS for 10 min. During this step, cells were protected from light by covering with aluminium foil. Cells were either immediately stained or frozen at -80 ºC until required.

2.2.8 Quantification of mitochondrial superoxide

Fluorescence images were obtained using a fluorescence microscope and digital imaging software (AxioVision 4.8.0.0). Filters used were DAPI (emission filter wavelength: 345nm, excitation filter wavelength: 458nm), Texas Red (emission filter wavelength: 620 nm, excitation filter wavelength: 595 nm) and FITC (emission filter wavelength: 520 nm, excitation filter wavelength: 495) at 40X and 63X magnifications. For each individual experiment, at least twenty random fields were chosen. Experiments were repeated 3 times. The levels of mitoSox were manually quantified.

For cytoplasmic ROS, the mitoSox signal was quantified by JAVA-based image processing software (Image J version 1.46, Wright Cell Imaging Facility, Toronto Western Research Institute, Toronto, ON, Canada, http://rsbweb.nih.gov/ij/). Digital images were set into 8 bit black and white type and adjust for the clear expression of

ROS level. This thresholds setting was constant for the whole analysis. The cytoplasmic area was determined using the freehand selection function. Expression signals in the selected areas were evaluated using the area calculation function. ROS levels based on mitoSox measurement were calculated as:

$$\%\ \text{ROS level per cytoplasmic area} = \left[\frac{\text{mitosox signal in cytoplasmic area}}{\text{Total cytoplasmic area}}\right] \text{x}100$$

The percentage of the red pixel (ROS signal) in the cytoplasmic area per total pixel (total cytoplasmic area) was used to discard the variation of cell size. ROS signal was calculated in each individual cell. Then the average percentage of at least 30 individual cells was taken to determine the average percentage of one experiment. ROS level of the population was an average from three independent experiments.

2.2.9 Immunofluorescence – single staining

Cells were grown on 19 mm circular cover slips in 12-well plates. After aspirating the medium, all cover slips were washed twice with PBS and fixed with 4 % PFA.

After fixation or thawing, the washing step was repeated. Permeablising of the cells was carried out with 1 ml PBG-Triton for 45 minutes with slight shaking at room temperature. Then, 400 µl of the diluted primary antibody in PBG was applied to the cells. The plate was slightly shaken for one hour at room temperature. After washing three times with PBG for five minutes, cells were incubated with the second antibody (Alexa Fluor® 594 or 488, 1:2000 in PBG) for one hour at room temperature. After aspiration of the second antibody, cells were washed three times with PBS and nuclear staining was carried out with 400 µl of DAPI solution for 10 minutes. Afterwards, the washing step was repeated three times before mounting cells on slides using an anti-fade mounting medium. Slides were sealed with nail polish and examined using a fluorescence microscope.

2.2.10 Immunofluorescence - double staining

After fixation or thawing, cells were washed twice with PBS and then permeablised in 1 ml PBG-triton as for the single staining. Cells were slightly shaken at room temperature for 45 minutes. Then, 400 µl of the diluted first primary antibody in PBG was applied to the cells. The plate was slightly shaken for one hour at room temperature. After washing two times with PBG for five minutes, cells were incubated with the first secondary antibody (Alexa Fluor® 594 or 488, 1:2000 in PBG) for one hour at room temperature. After this step, cover slips were protected from light by

covering with aluminium foil. After aspiration of the first secondary antibody, cells were washed twice in PBG and then incubated with the second primary antibody for one hour under room temperature or overnight under 4°C. The plate was slightly shaken to circulate the antibody around the cover slip. Cells were washed again two times with 1 ml PBG before incubation with the second secondary antibody (Alexa Fluor®, 1:2000 in PBG) for one hour. Cells were washed three times with PBS before staining the nuclei with 400 µl of DAPI solution for 10 minutes. Afterwards, the washing step was repeated three times before mounting cells on slides using an anti-fade mounting medium. Slides were sealed with nail polish and examined using a fluorescence microscope

Table 2.2 Antibody concentration used for single and double staining

Antibody	Used Concentration
Anti-Telomerase catalytic subunit (hTERT)	1:2000
Anti-Myc-Tag antibody (ab9106) (Mouse)(ABCAM®)	1:2000
Anti-Myc-Tag (71D10) Rabbit mAb #2278 (Cell Signaling)	1:2000
Anti-Phospho-Histone H2A.X	1:1000
Anti-Histone H2A.X Antibody	1:500
anti- COX II	1:100
Alexa Fluor® 594 goat anti-mouse IgG	1:4000 (Single staining) 1:2000 (double staining)
Alexa Fluor® 594 goat anti-rabbit IgG	1:4000 (Single staining) 1:2000 (double staining)
Alexa Fluor® 488 goat anti-mouse IgG	1:4000 (Single staining) 1:2000 (double staining)
Alexa Fluor® 488 goat anti-rabbit IgG	1:4000 (Single staining) 1:2000 (double staining)
Alexa Fluor® 405 goat anti-mouse IgG	1:4000 (Single staining) 1:2000 (double staining)
Alexa Fluor® 405 goat anti-rabbit IgG	1:4000 (Single staining) 1:2000 (double staining)

2.2.11 Measurement of TERT exclusion rate

For each individual cell, hTERT localisation was manually quantified by determining the hTERT signals inside and outside the nucleus using Image J (version 1.46, http://rsbweb.nih.gov/ij/). Subcellular areas were determined for nuclear and cytosolic regions by using freehand selection. Expression signals in the selected area were evaluated using area calculation function after thresholding to remove noise. Total hTERT signal in each individual cell means hTERT signal in nucleus area plus hTERT signal in cytoplasmic area of that cell. The result of each individual cell indicated a percentage of hTERT signal expressed in the subcellular compartment:

$$\%\ \text{nuclear hTERT signal} = \left[\frac{\text{hTERT signal in nucleus area}}{\text{total hTERT signal}}\right] \times 100$$

$$\%\ \text{cytoplasmic hTERT signal} = \left[\frac{\text{hTERT signal in cytosolic area}}{\text{total hTERT signal}}\right] \times 100$$

The average percentage of nuclear and cytoplasmic localisation of hTERT from at least 30 individual cells was taken to determine the average percentage of the subcellular distribution of TERT per condition (treatment and transfection). Average values from 3 independent experiments were used to determine the distribution of hTERT in subcellular compartment of the whole population.

2.2.12 Analysis of DNA damage

Analysis of DNA damage response was performed using immuno-fluorescence either as a single staining with γ-H2A.X antibody or double staining of γ-H2A.X antibody with hTERT antibody. Cells were fixed, permeabilised and stained with a γ-H2A.X antibody as described before. Slides were examined using a Fluorescence microscope (Axio-Plan HRc and Axio-Imager Z1) and digital imaging software (AxioVision 4.8.0.0) as before. The number of DNA damage foci for each individual cells was counted. The result from 20-40 cells per group was taken to determine the average percentage of the whole population.

2.2.13 Determination of protein content: Bradford Assay

A Bradford assay was performed to determine the protein concentration of the Western blot samples. First, cell pellets that had to be analysed were lysed with lysis buffer containing a mild detergent (3-[(3-Cholamidopropyl) dimethylammonio]-1-propanesulfonate, CHAPS) on ice for 30 min. A standard curve was created with 0 to

5 µl of 1.4 mg/ml protein (BSA) in 800 µl of sterile water and 200 µl protein assay solution. Absorbance was measured at 595 nm using a fluorescence imager (Fluoroskan Ascent FL).

2.2.14 Westernblot analysis

30-50 µg of protein were loaded for each sample. Samples were prepared for Western blotting by adding equal volume of 2x Laemmli (1x final concentration). After heating samples to 95°C for 5 min, they were shocked on ice. Protein samples and rainbow molecular marker were separated on 8% SDS-polyacrylamide gels and transferred to PVDF membranes at 300 mV for 90 min at 4 °C. Membranes were washed in 1x TBST and blocked in 1x TBST plus 5% skimmed milk for 1 h at room temperature. Membranes were incubated overnight on a shaker at 4 °C with one of the primary antibodies (see table 2.3). Membranes were washed with 1x TBST and incubated with the specific peroxidise labelled secondary antibody (see table 2.4) for 1 hour at room temperature. After washing with 1x TBST, membranes were developed with ECL solution. The blots were exposed using the chemiluminescence software LAS 3000 of a chemiluminescence detector. Western Blot Stripping buffer (Thermo Scientific, USA) was used for stripping the membranes at 37 °C for 1 h. Membrane was re-probing with tubulin as a loading control. Membranes were washed in 1x TBST and blocked in 1x TBST plus 5% skimmed milk for 30 minutes at room temperature. Membranes were incubated 1 hour on a shaker at room temperature with tubulin antibody. Membranes were washed with 1x TBST and incubated with the secondary antibody for 1 hour at room temperature. After washing with 1x TBST, membranes were developed with ECL solution. The blots were exposed using the chemiluminescence software LAS 3000 of a chemiluminescence detector.

Table 2.3 Primary antibodies for western blot analysis

Primary Antibodies	Used Concentration
Anti-p53 (Cell Signalling Tech®,USA)	1:1000
Anti-Phospho p53 (Cell Signalling Tech®,USA)	1:1000
hTERT (Rockland, USA)	1:500
Anti-β-tubulin (ABCam, UK)	1:2000

Table 2.4 Secondary Antibodies for western blot analysis

Secondary antibodies	Used Concentration
hRP labelled goat anti rabbit (ABCam,UK)	1:5000
hRP labelled donkey anti rabbit (ABCam,UK)	1:5000

2.2.15 Antibody specificity

The hTERT antibody (Rockland, USA) was tested for its specificity using Western blotting. Hela, MCF7, A549 as well as MRC5 (negative control) and TERT-overexpressing MRC5 (positive control) were used in this experiment. Results in figure 3.5 show that the hTERT antibody detects a specific band at the right molecular weight (127 kD) which is not present in MRC5 fibroblast which don't have any endogenous telomerase/TERT expression. These results correspond to those from Wu et al, (2006).

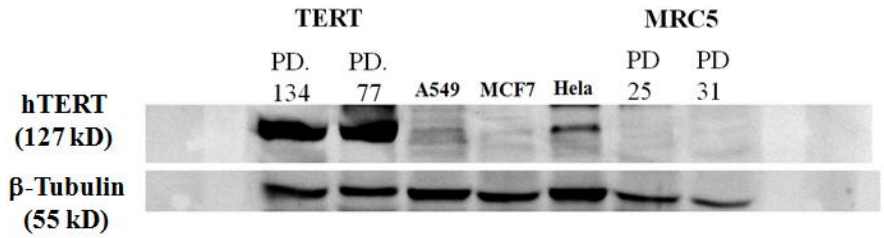

Figure 2.4 Western blot analysis of cells using hTERT antibody and β-tubulin. TERT are hTERT-overexpressing fibroblast (Positive control), A549 is a lung adenocarcinoma cell line, MCF7 is a human breast adenocarcinoma cell line, Hela are human cervical cancer cells, MRC5 are human embryonic lung fibroblasts (Negative control)

2.2.16 Cellular peroxide measuring: dihydrorhodamine123 (DHR)

Cellular peroxide level were evaluated using dihydrorhodamine123 (DHR). Cells were washed with 1xPBS, trypsinised and the reaction stopped with serum containing DMEM. Cells were counted and centrifuged at 1800 rpm for 3 minutes at room temperature. Typically, $2x10^5$ cells were used per reaction. The supernatant was removed by aspiration. 15µl of 10mM DHR stock solution was added to 5 ml serum

containing DMEM, then the cell pellet was re-suspended with this 30μM solution. Cells were incubated at 37^0C for 30 minutes in the absence of light and centrifuged at 1800 rpm for 3 minutes. After removing the supernatant the pellet was re-suspended in 3 ml of serum containing DMEM and analysed by flow cytometry.

2.2.17 ROS measurement with mitoSOX

Mitochondrial ROS levels were evaluated using mitoSOX staining. After trypsinisation, cells were counted and centrifuged at 1800 rpm for 3 minutes at room temperature. The supernatant was removed by aspiration. Typically, $2x10^5$ cells were used per reaction. Cells were stained with 200 μl of 5μM of mitoSox for 15 min at 37 C in the absence of light. After incubation, cells were centrifuged at 1800 rpm for 3 min and the supernatant was discarded. Cells were then resuspended in 3 ml of DMEM without serum and analysed by flow cytometry.

2.2.18 Flow cytometry

To evaluate the oxidative stress, free radical generation was monitored using dihydrorhodamine 123 (DHR) and mitoSOX staining. Cells were stained as described in 2.2.16 and 2.2.17. Before each analysis, the flow cytometry (Partec GmbH, Germany) was calibrated in order to ensure accuracy and reliability by using Partec 3 μM calibration beads (Partec). These beads are fluorescence stained and allow the calibration of laser, optics and stream flow. The gains for FL1 were set to 100 and those for FL3 to 180 in order to make different measurements comparable to each other.

Cell populations were defined using forward and sideway scatter. Fluorescence channels were FL1 (green) and FL3 (red). Cells were gated in FSC/SSC, and the median of the gated FL1 and FL3 fluorescence peak for DHR analysis or FL3 peak for mitoSox analysis was used as estimates of the peroxide or mitochondrial superoxide concentration, respectively. All analyses were repeated at least three times. Unstained cells were used in order to subtract the background in the FL3 channel. At the end of each use the flow cytometer was cleaned with 2ml of 1% Triton X-100 and followed by 2 ml of PBS and 2ml of water passed through the flow chamber.

2.2.19 Immuno-FISH

Immuno-FISH is a technique of fluorescence *in situ* hybridisation (FISH) coupled with an immuno-fluorescence staining. In our experiment, the detection of DNA damage (γH2A.x) was combined with the detection of telomeres (FISH) using a telomere

specific peptide nucleic acid probe. Fluorescence *in situ* hybridisation (FISH) is a method of molecular cytogenetics to use fluorescent probes to detect specific sequences of DNA on chromosomes. FISH was carried out using a Cy-3-labelled telomere specific (C3TA3) 3 peptide nucleic acid (PNA) probe (Panagene, Korea). To detect the colocalisation between γH2A.x foci with telomeres, cells were grown on 19 mm circular cover slips in 12-well plates. After experimental treatment procedures, all cover slips were washed twice with PBS and fixed with 1 ml 4 % PFA in PBS for 10 min. PFA was removed and cells were immediately stained.

Before starting the staining step, cells were washed twice with PBS and then permeablised using 1 ml PBG-Triton for 45 minutes. The plate was slightly shaken at room temperature. 400 µl of the diluted γH2A.x antibody in PBG was applied to the cover slip. The plate was slightly shaken for one hour at room temperature. After washing three times with PBG for five minutes cells were incubated with the second antibody (Alexa Fluor®, 1:2000 in PBG) for one hour at room temperature. After aspiration of the second antibody cells were washed 10 minutes three times with PBS and incubated with 1.3ml of fixative solution (methanol: acetic acid 3:1) for 1 hour. Cells were dehydrated for 2 minutes with cold ethanol solution from 70% followed with 90% and 100% ,respectivey. Then the cover slip was left to dry. The cover slip was immersed into PBS at 37^{o}C for 5 minutes then denature the chromosome inside the cells by incubate coverslip under 4%paraformaldehyde in PBS at 37 ^{o}C for 2 minutes. Cells were dehydrated again with cold ethanol solution from 70% follow with 90% and 100%, respectively. Then all cells was left to dry again.

To start the hybridisation, 10µl of hybridisation mix (described in 2.1.3) was applied onto a clean glass slide. The cover slip was flipped onto the hybridisation solution. Air bubbles were pressed out to make sure that all cells were immersed into the solution. Following this step, cells were protected from light.

Cells were denatured at 80°C by place the slide on the hot stainless plate leaving in the hot air incubator for 3 minutes, then incubated the slide in the humid chamber for 2 hours. Cells were washed 10 miuntes three times in wash buffer (70ml Formamide (70%), 1ml 1M Tris pH7.2 (10mM Tris), 1ml BSA 10% (0,1% BSA) and 28ml water) and followed with washes for 5 minutes three times in TBS-Tween 0.05%. Cells were dehydrated again with cold ethanol solution from 70% follow with 90% and 100%, as previously. After the cover slips were air dried, cells were washed with PBS for three times and nuclear staining was carried out with 400 µl of DAPI solution for 10 minutes. Afterwards, the washing step was repeated three times before mounting the

cover slips on slides using an anti-fade mounting medium (vecta-shield). Slides were sealed with nail polish and examined using a fluorescence microscope.

2.2.20 Co-localisation analysis

After performing the immuno-FISH staining, Z-stack pictures of the stained cell were taken using a Leica DM5500B microscope. Co-localisation between γH2A.X and PNA probe was analysed using Image J 1.46. Pictures in channel of the PNA probe (red colour as shown in 5.14B, Chapter 5) and γH2A.X (green colour as shown in 5.14C, Chapter 5) were adjusted for the best contrast and the two channels were merged. The co-localisation between PNA probe and γH2A.X (appeared as yellow colour as shown in 5.14D, Chapter 5) were counted manually in each z-stack. Every stack in the whole cell was analysed. At least 10 cells per group were analysed and summarised as an average of the number of foci per population and %TAF (percentage of γH2A.X foci colocalising with telomere) per cell.

2.2.21 Statistical Analysis

Statistical analysis was performed to elucidate the significance between different values. Anova-single factor analysis was performed using Microsoft Excel, 2007, Microsoft Excel, 2010 and One-way ANOVA was performed using SIGMA Plot 11 (Systat Software Inc, USA).

Chapter 3

Mitochondrial localisation of telomerase protect against nuclear DNA damage after exogenous stress

3.1 Introduction

In recent years, evidence suggests that telomerase, and particularly its catalytic subunit TERT, has additional physiological functions. TERT has been shown to play a role in chromatin remodelling and DNA damage response (Sharma et al., 2003, Masutomi et al, 2005, Park et al., 2009a). In mammals, cellular responses to DNA damage are mediated by various protein kinases including ATM (ataxia telangiectasia mutated) and ATR (ATM and Rad3-related) (Ljungman, 2010). Masutomi and colleagues reported that transient expression of hTERT in normal fibroblast modulates DNA damage response (DDR). Moreover, fibroblasts with stably suppressed hTERT function by RNA interference or catalytic inhibition exhibited a lack of induction of ATM and H2A.X phosphorylation after irradiation, irionotecan or etoposide treatment (Masutomi et al, 2005). Nitta and colleagues confirmed an interaction between TERT and ATM in mouse hematopoietic stem cells (Nitta et al., 2011). ATM and TERT double deficient mice expressed an increase in ageing progression and had shorter lifespan compared to ATM-null or TERT-null mice alone.

Reactive Oxygen Species (ROS, also called free radicals or oxygen radicals) are known to be one of the factors responsible for nuclear DNA damage (Passos et al., 2010). ROS are highly reactive small molecules containing unpaired electrons. These molecules can react with several organic molecules and can cause considerable damage and impair normal cellular function (Finkel and Holbrook 2000; Kirkinezos and Moraes 2001). ROS can damage nucleotides by generating adduct bases and sugar groups, single- and double-strand breaks in the nucleotide backbone, or cross-linking to other molecules. These altered nucleotides can eventually lead to mutation, DNA rearrangements or problems during transcription (Beckman and Ames 1998). Moreover, it is also important to point out that telomere dependent replicative senescence is also influenced by cellular stress since telomere attrition is also affected by the level of oxidative stress in the cell (von Zglinicki et al., 1995). Thus, reduction of ROS production might help to prevent DNA damage.

Previous experiments of our group have shown that mitochondria, a major source of intracellular ROS generation, in hTERT over-expressing fibroblasts seem to be better

protected. hTERT is excluded from the nucleus and protects mitochondria under oxidative stress conditions (Ahmed et al., 2008). These hTERT over-expressing fibroblasts show lower production of oxidative stress, less mitochondrial DNA damage, less mitochondrial mass, less mtDNA copy number and high mitochondrial membrane potential. This lower ROS production might be a major reason for the protection of mitochondria.

Specific aim of this chapter: To analyse whether mitochondrial localisation of TERT reduces DNA damage in the nucleus. First we investigate the effect of different subcellular shuttling of endogenous hTERT to the nuclear DNA damage under oxidative stress condition. Then we investigate different kinetic exclusion of endogenous hTERT compared between three different cell lines. To distinguish the exact effect of hTERT in a specific subcellular location with nuclear DNA damage, we used specific shooter vectors that deliver proteins specifically to various cellular locations. Cells were transfected with hTERT-containing shooter vectors as described in Chapter 2. These hTERT-containing shooter vectors include the localisation signals specific for the mitochondria or nucleus (further on called mito-hTERT and nucl-hTERT). Different cell lines were double stained with γH2A.X and myc-tag fused to TERT protein. γH2A.X was used because it is a sensitive target for detecting DNA double-strand breaks (DSBs) in cells and myc-tag was used to identify our exogenous hTERT expression. DNA damage foci were compared under normal condition and two exogenous stress treatments (hydrogen peroxide and irradiation). This experiment should show whether the reduction of mitochondrial superoxide by hTERT localisation in mitochondria has an indirect effect on the nuclear DNA protection by reducing the number of nuclear DNA damage foci.

3.2 Experimental procedure

3.2.1 Correlation between cellular TERT localisation and DNA damage level

Hela, MCF7, MRC5-hTERT and MRC5/SV40 cells have been used in this experiment. Subcellular shuttling of endogenous hTERT and DNA damage level of Hela, MCF7 and MRC5-hTERT has been investigated after treatment with 400μM hydrogen peroxide for 3 hours. The experiments on Hela and MCF-7 were performed by a master's student (Deepali Pal) while the second experiment on MCF7 and 3 independent experiments on MRC-hTERT cell line have been done by me. The localisation of hTERT in subcellular compartments has been quantified. We have classified the localisation of hTERT into 3 categories: nuclear TERT, cytoplasmic TERT and intermediate localisation. Nuclear TERT was the group which showed 75%-100% of TERT signal resides within the nucleus, cytoplasmic TERT was the group which showed 75%-100% of TERT signal resides outside the nucleus and all other percentages for the class of intermediate localisation. For each of the 3 classes we determined the number of γH2A.X foci from at least 30 cells per cell line per experiment.

3.2.2 hTERT specific shooter vector and cellular transfection

Hela, MCF7, MRC5, U87 and MRC5/SV40 have been used in to investigate the effect of specifically localised exogenous hTERT. To evaluate the transfection efficiency, Hela, MCF7, MRC5/SV40 and MRC5 have been transfected with specific nuclear and mitochondrial pShooter plasmids. The plasmid structure was described in Chapter 2. Initially, we intended to use MRC5 fibroblast as a model to avoid the effect of endogenous telomerase interfering with the result. pShooter were transfected to Hela, MCF7 and MRC5/SV40 by lipofectamine^{TM} 2000 and transfection attempted with Fugene^{R} HD and lipofectamine^{TM} 2000 in MRC5. Transfection efficiency of Hela was about 25% for mitochondrial transfection and 31% for nuclear transfection. The transfection efficiency of MCF7 was 20% for mitochondrial transfection and 18% for nuclear transfection. Transfection efficiency for MRC5/SV40 cells was about 30%. However, very rare transfected MRC5 cells were detected although the experiment had been repeated and although we modified the transfection protocol. MRC5 transfection still showed a very low transfection rate. Consequently, we continued to use only Hela, MCF7 and U87 and use MRC5/SV40 for a model without endogenous telomerase.

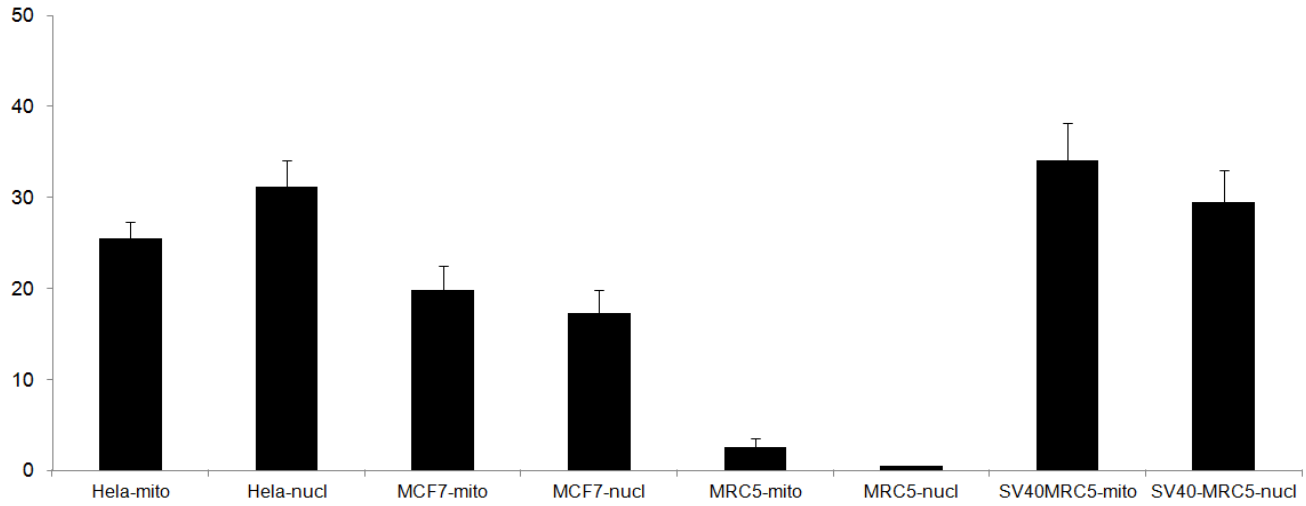

Figure 3.1 Transfection efficiencies of mito-hTERT and nucl-hTERT into Hela, MCF7, MRC5 and MRC5/SV40. pShooter were transfected to Hela, MCF7 and MRC5/SV40 by lipofectamine^{TM} 2000 and tested with Fugene^{R} HD and lipofectamine^{TM} 2000 in MRC5. 2 days after transfection, all cells were fixed and the transfection efficiency was determined using Immuno-fluorescence. Cells were stained with primary antibody against the myc-tag (1:500) and visualised using a fluorescence labelled secondary antibody alexa® fluor (Invitrogen).

3.3 Results

3.3.1 Different localisation of endogenous telomerase after stress treatment (H_2O_2) affects nuclear DNA damage

To investigate whether the localisation of hTERT affects nuclear DNA damage, first we investigated the sub-cellular shuttling of hTERT protein as shown in figure 3.2-3.4. These experiments on Hela and MCF-7 were performed by a master's student (Deepali Pal) while I repeated the MCF7 experiment and 3 independent experiments on the MRC5-hTERT cell line. Figure 3.2 shows the comparison between fractions of cells which represent different hTERT localisations after 3 hours of H_2O_2 treatment. Hela and MCF7 were combined as a group of cancer cells. There was a clear heterogeneity for nuclear TERT exclusion between cells in each cell type. In cancer cells, there seems to be no difference in frequency between the nucleus, intermediate and cytoplasm groups; each of those contained around 30% of cells. However, MRC5-hTERT showed a significant higher amount of the localisation of hTERT in cytoplasm and seems lower in the intermediate group compared to the cancer cells after 3 hours of treatment. Thus, it seems that endogenous hTERT was excluded from nucleus to cytoplasm faster in MRC5-hTERT under oxidative stress treatment compared to the cancer cells. Intriguingly, when we correlated the localisation of hTERT with the number of DNA

damage foci, the cytoplasmic localisation of hTERT correlated to no or a very low nuclear DNA damage while nuclear TERT localisation results in high nuclear damage as shown in figure 3.3-3.4.

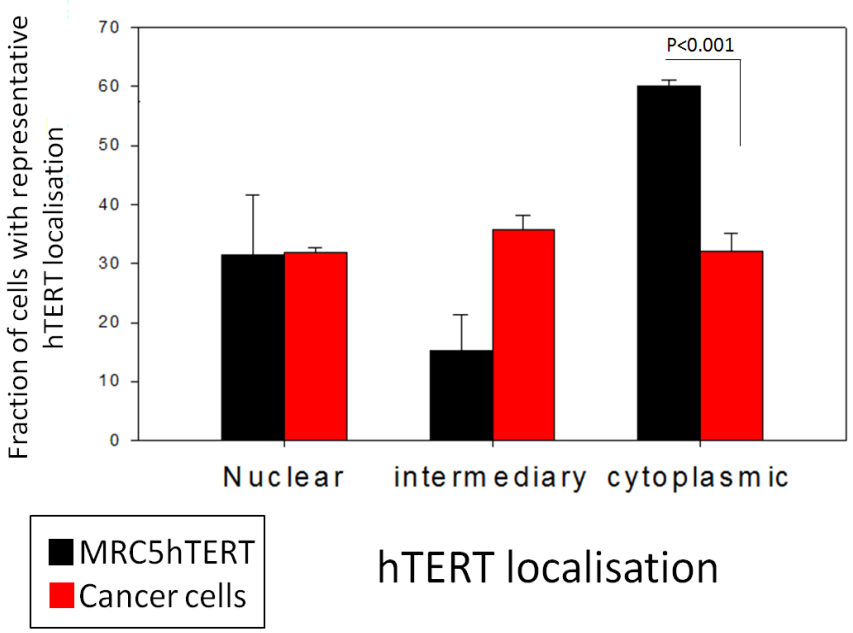

Figure 3.2 Comparison between fractions of cells which represent different hTERT localisations after 3 h of H_2O_2 treatment of cells. Hela and MCF7 were combined as a group of cancer cells since they were very similar to each other and compared to MRC5-hTERT which is hTERT over-expressing fibroblasts. Bars indicate means and standard error from 30 independent cells from each cell type. ANOVA single factor was used to analyse the significance between groups.

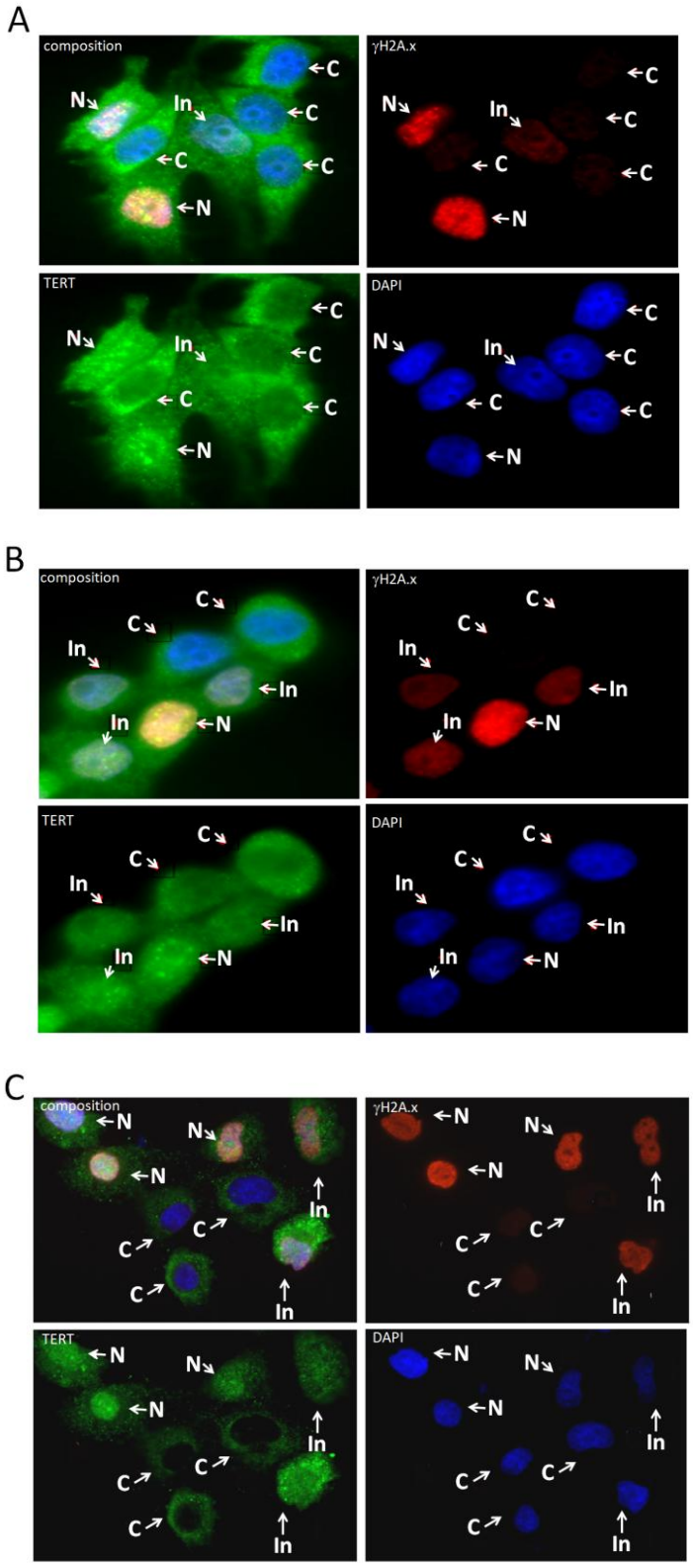

Figure 3.3 Representative images for the correlation between localisation of hTERT and DNA damage levels. Cells were treated with 400μM H_2O_2 for 3 hours. Cells were classified into three classes: nuclear TERT (N), cytoplasmic TERT (C) and intermediate localisation (In). Endogenous hTERT was stained and displayed as green colour. Red colour represents γH2A.X. The nucleus was stained with DAPI and displayed in blue. **A:** Hela **B:** MCF7and **C:** MRC5-hTERT.

Figure 3.3 shows representative images of Hela, MCF7 and MRC5-hTERT after 3 hours of 400μM H_2O_2 treatment. We found that the localisation of endogenous hTERT correlated to the level of γH2A.X foci which were used to identify nuclear DNA damage. It is interesting that when endogenous hTERT was excluded from nucleus to cytoplasm, all Hela, MCF7 and MRC5-hTERT displayed low amounts of γH2A.X foci (arrow with C). However, when hTERT was localised in the nucleus (arrow with N), cells displayed a high number of γH2A.X foci. All cells which showed intermediate hTERT exclusion (In) seemed to display an intermediate level of DNA damage foci. Thus, we quantified the amount of DNA damage foci correlated to the localisation of endogenous hTERT as shown in figure 3.4.

Figure 3.4 was summarised from at least 30 individual cells of Hela, 2 independent experiments of MCF7 and 3 independent experiments of MRC5-hTERT. We found a correlation between the average amounts of nuclear DNA damage per nucleus with the different localisation of endogenous hTERT. When hTERT is excluded from nucleus and localised in the cellular cytoplasmic area, the three cell types showed significant lower amounts of DNA damage foci compared to the group where hTERT localised in the nucleus. A similar significantly lower amount of DNA damage was found between the cytoplasmic group and the group where hTERT was still inbetween nucleus and cytoplasm. Thus, localisation of endogenous telomerase in different cellular compartments relates to the different amount of nuclear DNA damage. From our three cell lines, cells where hTERT remains in the nucleus displayed high DNA damage while cells which excluded hTERT from the nucleus displayed no or very low DNA damage. In addition, Hela showed the highest nuclear DNA damage compared to MCF7 and MRC5-hTERT in all categories. This might be because Hela contains an inactive p53. The role of the p53 status has been investigated to clarify the effect of p53 in Chapter 5.

3.3.2 Analysis of TERT exclusion kinetics

Next we investigated the kinetic exclusion of endogenous hTERT in all three cell lines after treatment with 400 μM H_2O_2. We have followed the exclusion of hTERT every 15 minutes for 1 hour, then for 2 more hours until 3 hours, and then investigated it at 24 hours (day1), 72 hours (day3) and 120 hours (day5) as shown in figure 3.5 and 3.6.

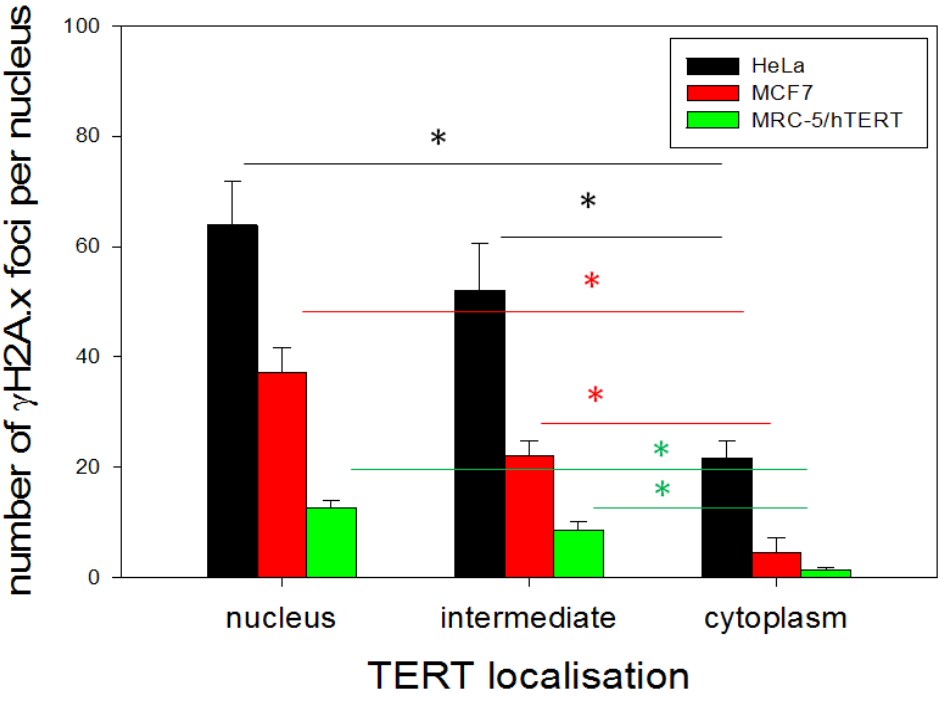

Figure 3.4 Correlation between subcellular TERT localisation and DNA damage levels in 3 cell lines. Cytoplasmic TERT localisation correlates with low nuclear DNA damage in all 3 cell lines while nuclear TERT localisation results in high nuclear damage after 3 hour of 400μM H_2O_2 treatment. One way ANOVA was used to analysed the significance of differences between groups. *$p<0.05$.

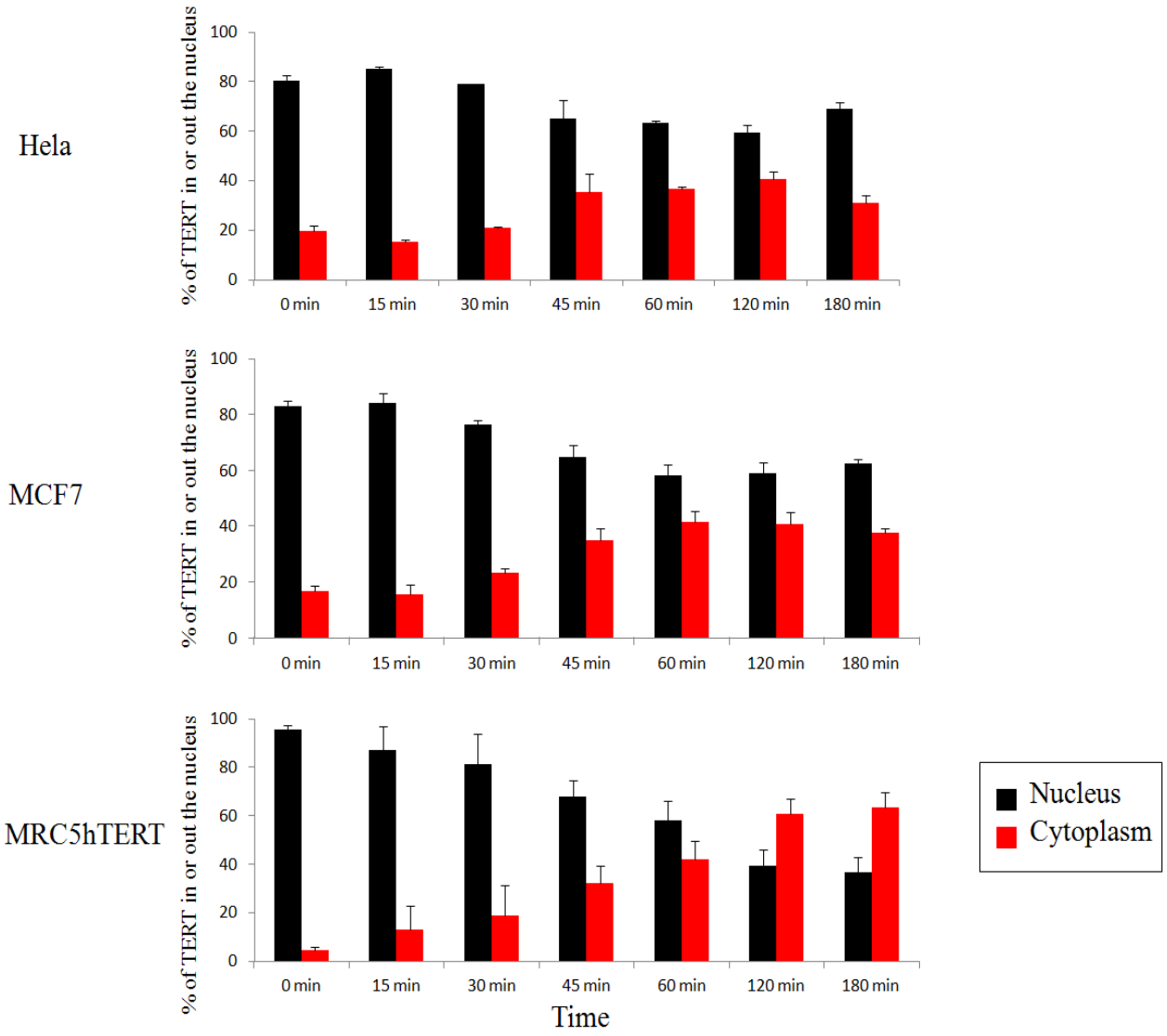

Figure 3.5 Short-term exclusion kinetics of endogenous hTERT in Hela, MCF7 and MRC5hTERT. All cells were treated with 400µM H_2O_2 and hTERT localisation was determined for nucleus and cytoplasm at 0 minute (untreated), every 15 minutes until one hour then every hour until 3 hours. Cells were fixed and analysed as described in Materials and Methods. Bars indicate means and standard error from at least 30 individual cells.

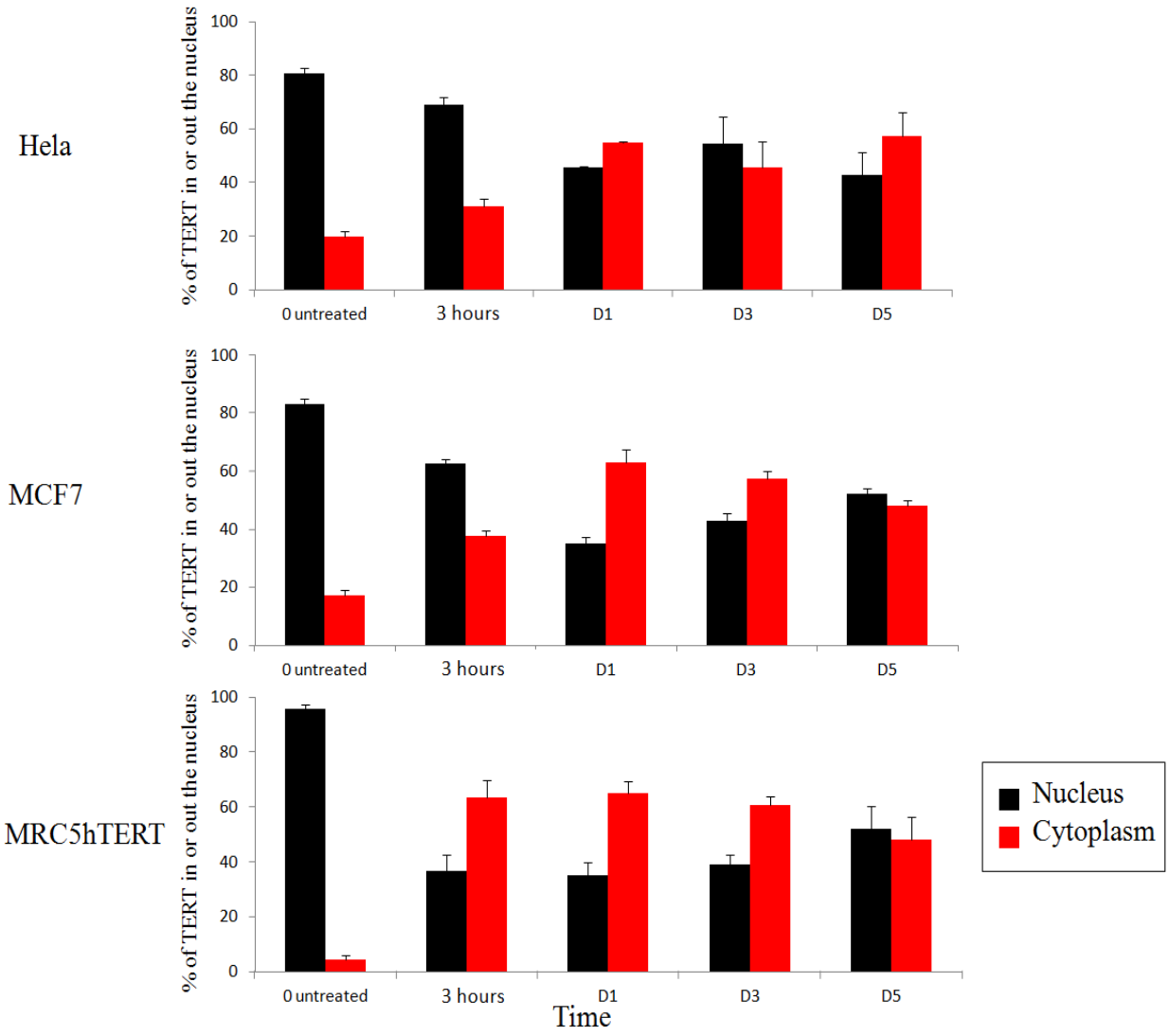

Figure 3.6 Long-term exclusion kinetics of endogenous hTERT in Hela, MCF7 and MRC5/hTERT cells. All cells were treated with 400µM H_2O_2 and then continued to culture under regular medium. hTERT localisation was investigated within the nucleus and cytoplasm before treatment, at 3 hours, 24 hours (day1), 72 hours (day3) and 120 hours (day5) after treatment. Cells were fixed, stained and analysed as described in materials and methods. Bars indicate means and standard error from at least 30 individual cells.

Results in figure 3.5 represent the short-term kinetic exclusion of endogenous hTERT after 400μM H_2O_2 treatment. Before treatment (at 0 min) most of endogenous hTERT of MRC5-hTERT was localised in the nucleus. However, we found that about 20% of hTERT in Hela and MCF7 was already localised outside the nucleus. Then all three cell lines were treated with 400μM H_2O_2 and fixed (see materials and methods) every 15 minutes until 1 hour, then every hour until 3 hours. Endogenous hTERT starts exclusion from the nucleus after 45-60 minutes post treatment start. At 3 hours (180 min) after treatment, only 30-40% of hTERT was excluded from nucleus to cytoplasm in both Hela and MCF7 but about 70% has been excluded in MRC5hTERT. Thus, hTERT seems to exclude faster in hTERT over-expressing fibroblasts.

Results of the long-term kinetic exclusion of endogenous hTERT are shown in figure 3.6. At 24 hours after treatment the exclusion level of hTERT in MRC5-hTERT was quite steady compared to the exclusion level at 3 hours after H_2O_2 treatment. This result is different from Hela and MCF7. Both cancer cells showed continuation of the exclusion of endogenous hTERT and reached the maximum exclusion level at 24 hours after treatment. Thus it seems that the exclusion of endogenous hTERT is slower in both cancer cell lines compared to MRC5-hTERT. This corresponds well with the higher fraction of cells with cytoplasmic TERT shown in figure 3.2. After 24 hours, cytoplasmic localisation of hTERT seems to gradually reduce in both MRC5-hTERT and MCF7. However, Hela showed a less obvious reduction of the cytoplasmic hTERT and constant until 120 hours (day5) post treatment. We hypothesise that the p53 status could be responsible for this difference. An experiment with an isogenic pair of glioblastoma cells which harbours active and inactive p53 related to the kinetic exclusion will been shown in chapter 5.

3.3.3 Modelling telomerase locations using shooter plasmids (over-expressed TERT)

In order to model the correlation found between physical location of hTERT in the mitochondria or nucleus with the amount of nuclear DNA damage, in the next experiment we used specific hTERT shooter vectors as described in Chapter 2 to deliver proteins specifically to various cellular locations in three cancer cell lines (Hela, MCF7 and U87). Cells were transfected with hTERT-containing shooter vectors (vector structure has been shown in 2.2.3 in chapter 2) which included localisation signals specific for mitochondria or the nucleus (further on called mito-hTERT and nucl-hTERT).

After transfection of various cell types with these hTERT expressing vectors, cells were treated with 2 different exogenous stresses (200 μM H_2O_2 or 20 Gy Irradiation). The reason for the lower H_2O_2 concentration was that the transfected cells were more sensitive than the untransfected cells. Transfected cells showed very high DNA damage which might be because the cells were additionally stressed by the transfection procedure in addition to stress treatment. We found apoptotic cells (about 40%) after lipofectamine transfection. Thus, we tested the sensitivity of cells under 100 and 200 μM H_2O_2 treatment and finally reduced H_2O_2 concentration to 200 μM. We also reduced time of treatment to be 1 hours. After stress treatment, transfected cells were double stained with γH2A.X for DNA damage foci and myc-tag fused to the TERT gene/protein in the shooter plasmids which was used to identify the localisation of exogenous (over-expressed) hTERT. The number of DNA damage foci was compared in the transfected cells under normal and stress conditions between mitochondria and nuclear shooter vector as well as with the un-transfected/not expressing cells. The aim of this experiment was to analyse whether the physical localisation of hTERT in mitochondria or nucleus has an effect on the nuclear DNA damage.

3.3.3.1 Localisation of exogenous hTERT affects nuclear DNA damage in Hela cells after H_2O_2 treatment

In order to model the localisation of hTERT, specific localised shooter vector were used to investigate the direct effect of hTERT in specific cell locations. Hela cells were transfected with mito-hTERT or nucl-hTERT and double stained with γH2A.X and myc-tag to investigate the effect of different physical location of hTERT in the mitochondria or nucleus with the amount of nuclear DNA damage. Representative images of Hela transfected with mito-hTERT and nucl-hTERT under basal conditions and H_2O_2 stress treatment are shown in figures 3.7 and 3.8. The level of DNA damage in Hela cells without transfection and transfected with mito-hTERT or nucl-hTERT is shown in figure 3.9 and the conclusion has been showed in figure 3.10.

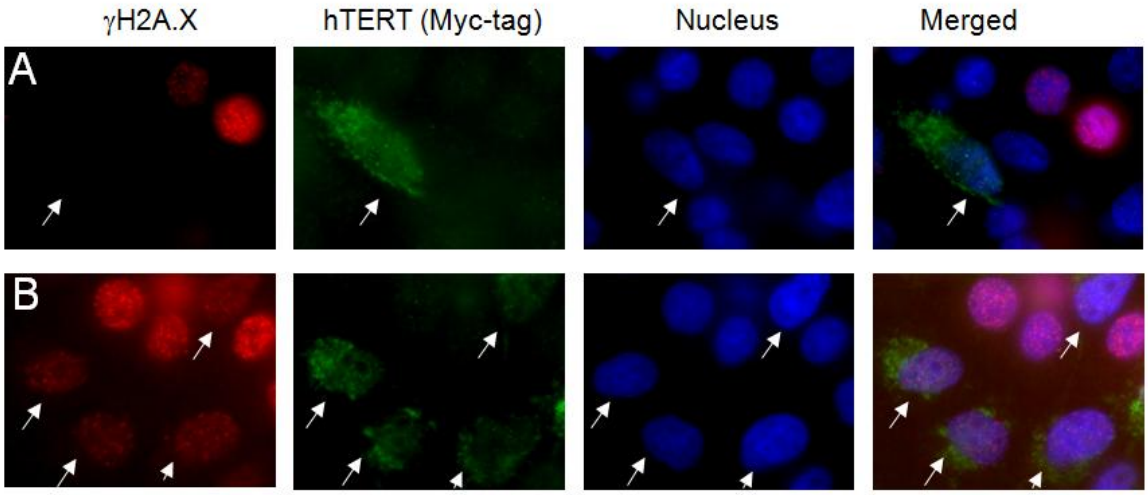

Figure 3.7 Double staining of Hela cells transfected with mito-hTERT shooter.
Cells were double stained with γH2A.X and myc-tag. Red colour represents DNA damage foci and green colour represents hTERT localisation. Nuclei were stained with DAPI (blue). White arrows indicate transfected cells. **A** is a representative image of cells transfected with mito-hTERT under basal condition and **B** is a representative image of cells transfected with mito-hTERT after 1 hr treatment with 200 μM H_2O_2.

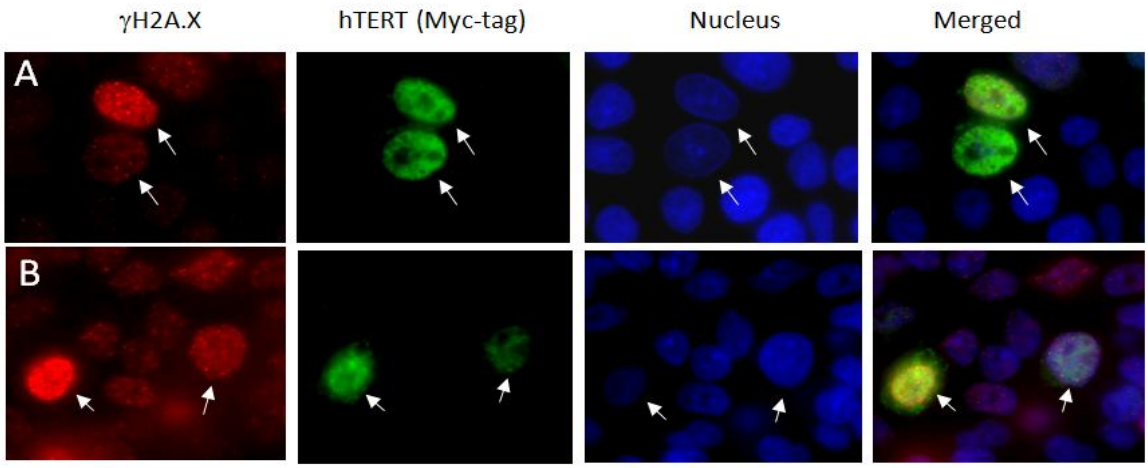

Figure 3.8 Double staining of Hela cells transfected with nucl-hTERT shooter.
Cells were double stained with γH2A.X and myc-tag. Red colour represents DNA damage foci and green colour represents hTERT localisation. Nuclei were stained with DAPI (blue). White arrows indicate transfected cells. **A** is a representative image of nucl-hTERT under basal condition and **B** is a representative image of cells transfected with nucl-hTERT after 1 hr treatment with200 μM H_2O_2.

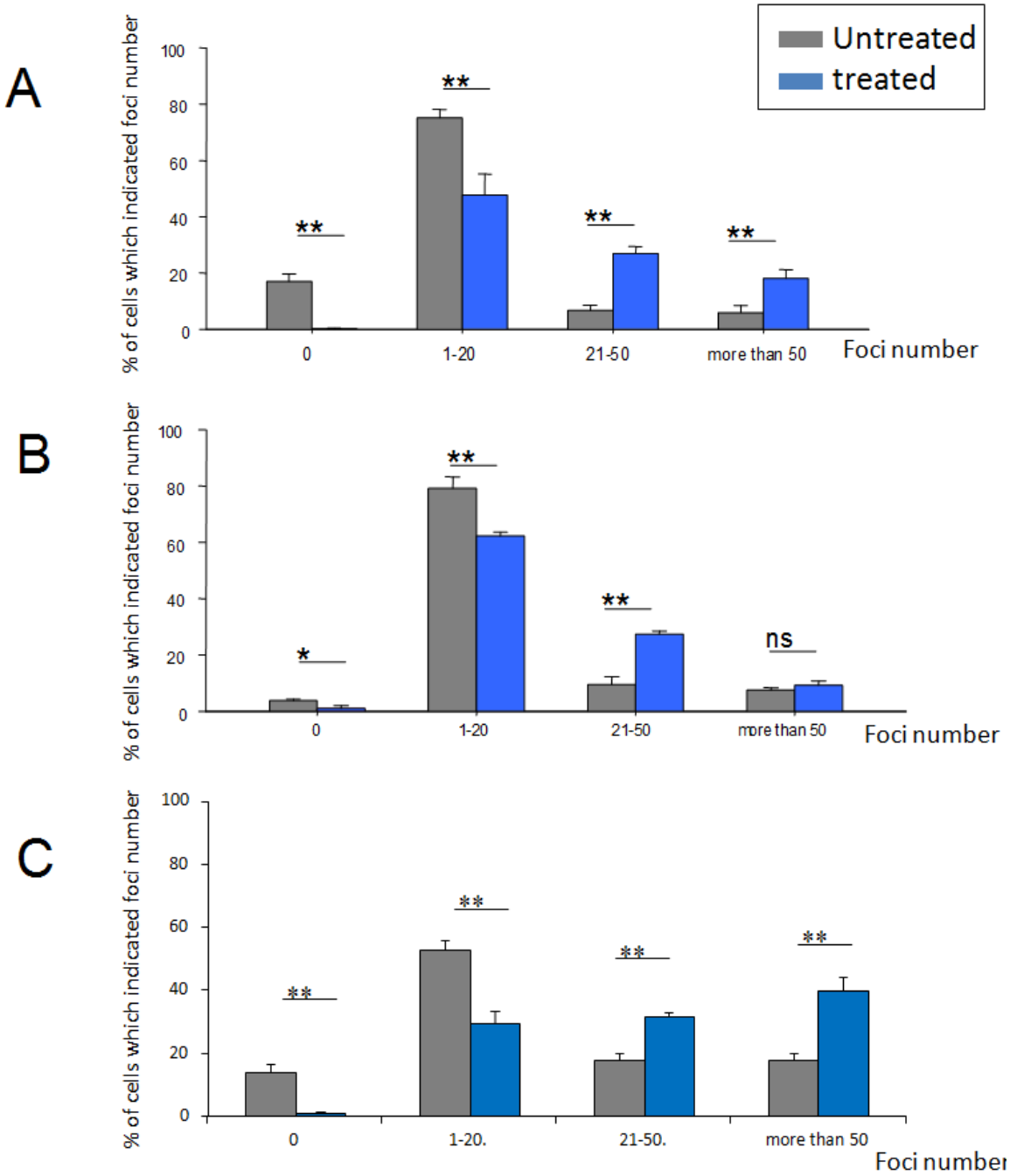

Figure 3.9 DNA damage foci in Hela cells transfected with mito-hTERT, nucl-hTERT and non transfected under normal and stress conditions. Cells were treated with 200 µM H_2O_2 for 1 h, then fixed and double stained with γH2A.X and myc-tag (for TERT identification) and damage foci number counted. **A:** non-transfected Hela. **B:** Hela transfected with mito-hTERT. **C:** Hela transfected with nucl-hTERT. Bars indicate mean and standard error from three independent experiments. Results have been compared using ANOVA-single factor * $P<0.05$, ** $P<0.01$, ns = non-significant difference.

As shown in figure 3.9, the number of DNA damage foci under normal and stress condition are different. DNA damage amounts were separated into 4 categories: first group: no-damage containing cells which did not show any DNA damage foci. This group was indicated as '0'. The second: a group with low damage which contained cells that showed between 1 to 20 damage foci. The third group: medium-high damage, this group consisted of cells which showed between 21 to 50 damage foci. The last group represents very high damage which means cells which showed more than 50 damage foci. In this category fell in particular cells with so many foci that it was not possible to count them separately.

In non-transfected and transfected Hela, there was a significant difference between the treated and untreated groups. This demonstrates that the treatment induced indeed DNA damage. In addition, even under basal conditions, Hela cells had already presented a number of damage foci in the nucleus (figure 3.9 A). Moreover, it is interesting that Hela transfected with nucl-hTERT showed more nuclear DNA damage foci than the non-transfected and mito-hTERT transfected groups even under basal condition. (figure 3.9 C). The quantitative comparison between groups is shown in figure 3.10.

After Hela was treated with 200 μM H_2O_2 for 1 hour the number of cells falling within the high and medium high damage group was significantly increased while the low and no damage groups were significantly decreased. It is interesting that the amount of high damage cells did not show a significant difference between treated and untreated cells in Hela transfected with mito-hTERT (figure 3.9 B). Importantly, Hela cells transfected with nucl-hTERT showed an even more pronounced increase of the high damage group compared to untreated and mito-hTERT transfected Hela. This experiment was repeated three times and nucl-hTERT Hela consistently showed the same pattern.

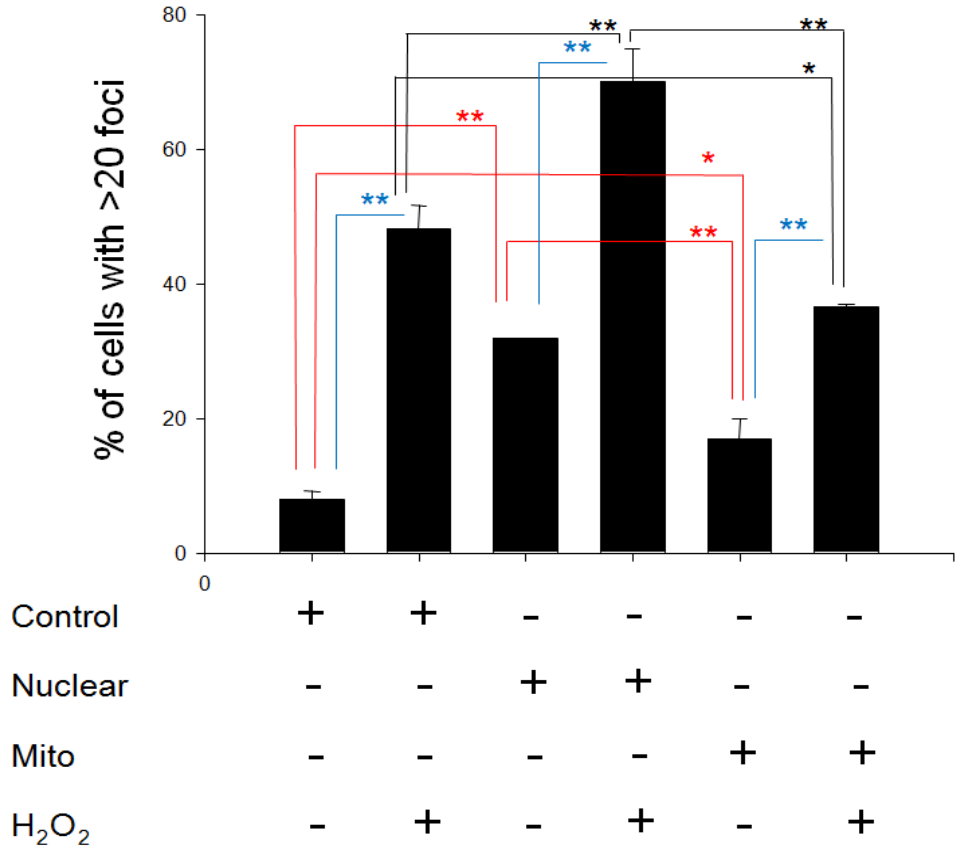

Figure 3.10 Comparison of damage foci in Hela cells transfected with both TERT shooter vectors under different conditions. The graph represents the percentage of cells which showed more than 20 damage foci. In the H_2O_2 positive groups, cells were treated with 200 μM H_2O_2 for 1 hour. Bars indicate mean and standard error from the same 3 independent experiments shown in fig. 3.9. Results have been compared using One way ANOVA: * P<0.05, ** P<0.01.

In order to subtract the background level of DNA damage that was present in Hela cells independent of the inflicted DNA damage, all results from Hela cells were summarised by considering only cells that contained more than 20 damage foci as shown in figure 3.10.

In comparison between mito-hTERT, nucl-hTERT and non-transfected cells, the results demonstrate a significant lower amount of high damage cells (>20 foci) in mito-hTERT shooter compared to the nuclear shooter and non transfected cells.

Under basal condition, mito-hTERT transfected Hela showed significantly lower damage compared to nucl-hTERT shooter. However, both shooter transfected cells contained a significant higher amount of damage foci compared to the non transfected cells. The reason for that is not clear and it occurred exclusively in Hela cells.

After H_2O_2 treatment, Hela cells with mito-hTERT shooter showed a significantly lower percentage of damage cells compared to both nucl-hTERT and non transfected cells

(P<0.01). As shown before in the whole damage analysis in nucl-hTERT Hela (see fig 3.9 C), we saw a significantly higher number of damage before and after H_2O_2 treatment. This data suggests that Hela cells transfected with nuclear hTERT shooter did already contain damage foci in untreated cells when hTERT localised in the nucleus and the damage increased significantly after stress conditions.

This result was summarised from 3 independent experiments which confirmed each other well. Thus, in conclusion, mitochondrial localisation of hTERT in Hela showed significant decrease in the percentage of highly damaged cells after H_2O_2 treatment while nuclear hTERT localisation showed a high DNA damage and even significantly increase after H_2O_2 treatment. This result shows an indirect effect of the protection capacity of mitochondrial hTERT localisation to nuclear DNA.

3.3.3.2 Localisation of exogenous hTERT affects nuclear DNA damage in MCF7 after H_2O_2 treatment

Because of the background problem of DNA damage in Hela, we decided to repeat the analysis with MCF7 cells since these have a functional p53 status in contrast to Hela cells. We were also interested whether this experiment could suggest any potential influence of the p53 status to mitochondrial protective function of hTERT and nuclear DNA damage. MCF7 cells were transfected with both shooters as described for Hela above under 3.3.2. Transfected MCF7 were double stained with γH2A.X and myc-tag in order to determine whether there are differences in nuclear DNA damage due to a different TERT localisation of the exogenous TERT from the two shooter vectors. MCF7 damage foci were determined under normal and stress condition as in Hela and cells were separated into the same 4 categories as in Hela. Representative images for shooter transfection are shown in figure 3.11 and 3.12 while quantitative results are summarised in fig. 3.13 and 3.14

Unlike Hela cells, only few MCF7 cells showed damage foci before treatment (figure 3.13 A). Thus, this cell line seems more suitable than Hela for the analysis of DNA after H_2O_2 treatment.

.

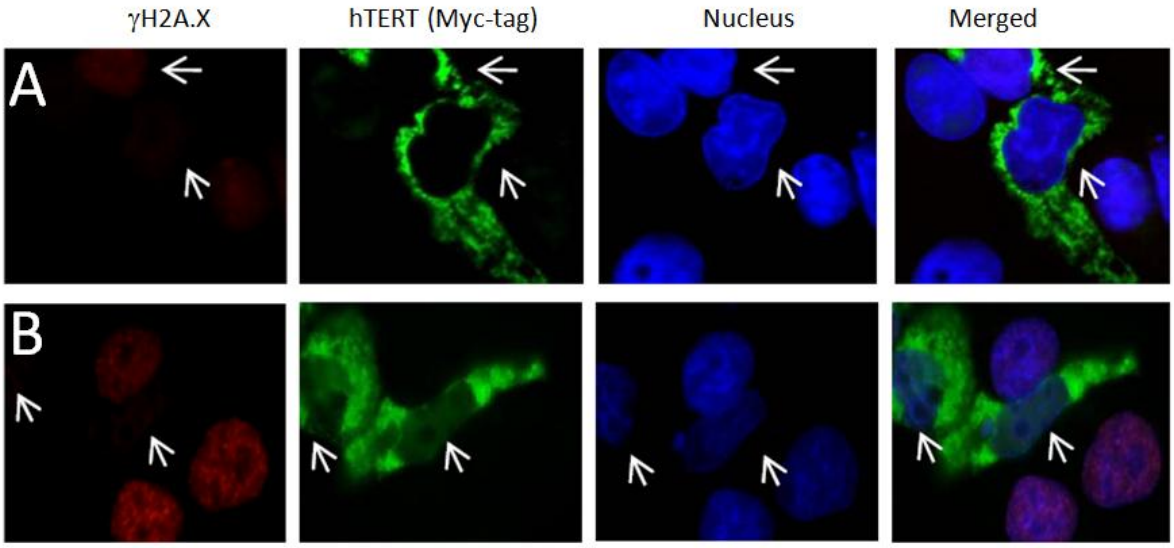

Figure 3.11 Double staining of MCF7 transfected with mito-hTERT shooter. Cells were double stained with γH2A.X and myc-tag. Red colour represents DNA damage foci and green colour represents hTERT localisation. Nuclei were stained with DAPI (blue). White arrows indicate transfected cells. **A** is a representative image of MCF7 cells transfected with mito-hTERT under basal condition and **B** is a representative image of MCF7 cells transfected with mito-hTERT after treatment with 200 μM H_2O_2 for1 hr.

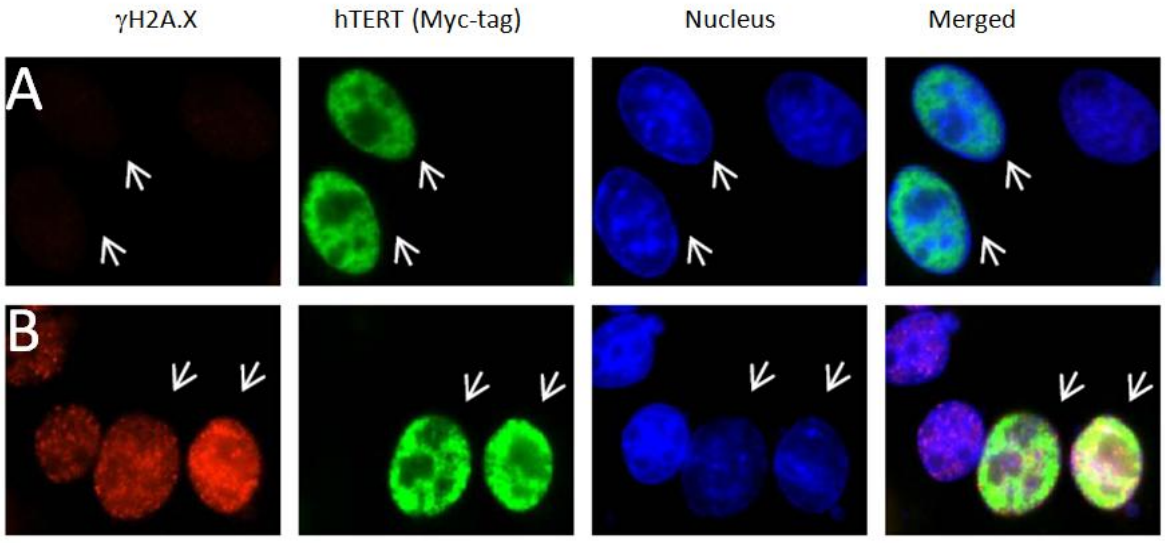

Figure 3.12 Double staining of MCF7 transfected with nucl-hTERT shooter. Cells were double staining with γH2A.X and myc-tag. Red colour represents DNA damage foci and green colour represents hTERT localisation. Nuclei were stained with DAPI (blue). White arrows indicate transfected cells. **A** is a representative image of MCF7 cells transfected with nuclTERT under basal condition and **B** is a representative image of MCF7 cells transfected with nuclTERT after treatment with 200 μM H_2O_2 for1 hr.

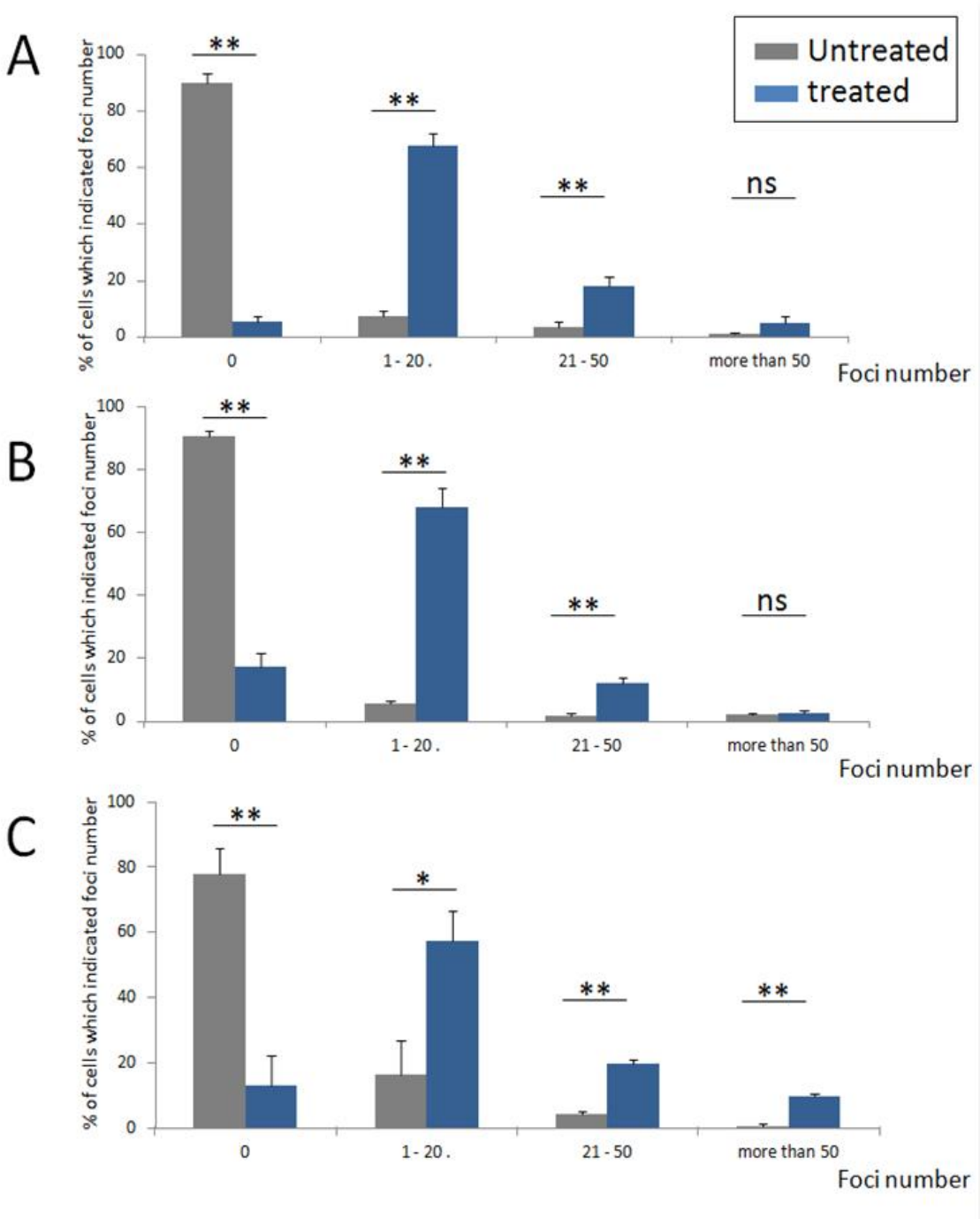

Figure 3.13 DNA damage foci of MCF7 transfected with mito-hTERT, nucl-hTERT and non-transfected under normal and stress conditions. Cells were treated with 200 μM H_2O_2 for 1 hr, then fixed and double stained with γH2A.X and myc-tag (for TERT identification) and damage foci number counted. **A:** non-transfected MCF7. **B:** MCF7 transfected with mito-hTERT. **C:** MCF7 transfected with nucl-hTERT. Bars indicate mean and standard error from three independent experiments. Results have been compared using ANOVA-single factor: ***** P<0.05, ****** P<0.01, ns = non-significant difference.

In non-transfected cells, there is a significant difference between treated and untreated cells in the group of zero, low (1 to 20), low to medium (21 to 50) and high damage (more than50 foci). However, no significant difference was found in the group of higher than 50 damage foci before and after treatment. However, this group only contained a very low cell fraction suggesting that the whole extend of DNA damage is slightly lower in MCF7 cells compared to Hela cells (figure 3.13A). A similar result was found in mito-hTERT MCF7 under basal and treated conditions. Cells which contained more than 50 damage foci did not show a significant difference before and after treatment (figure 3.13B). However, we found a significant difference between treated and non-treated cells in the group of higher than 50 damage foci in nucl-hTERT transfected MCF7 (figure 3.13C). However, comparison between nucl-hTERT and the non-transfected did not show a significant difference (figure 3.14). The comparison between mito-hTERT, nucl-hTERT and the non-transfected group before and after H_2O_2 treatment is summarised in figure 3.14. The result from MCF7 was also summarised from 3 independent experiments.

Under basal condition, no significant difference has been observed between mito-hTERT, nucl-hTERT and non-transfected MCF7. This result is different from Hela which showed a significantly higher damage when hTERT localised in the nucleus compared to mito-hTERT and the non-transfected group and increased pronouncedly after H_2O_2 treatment.

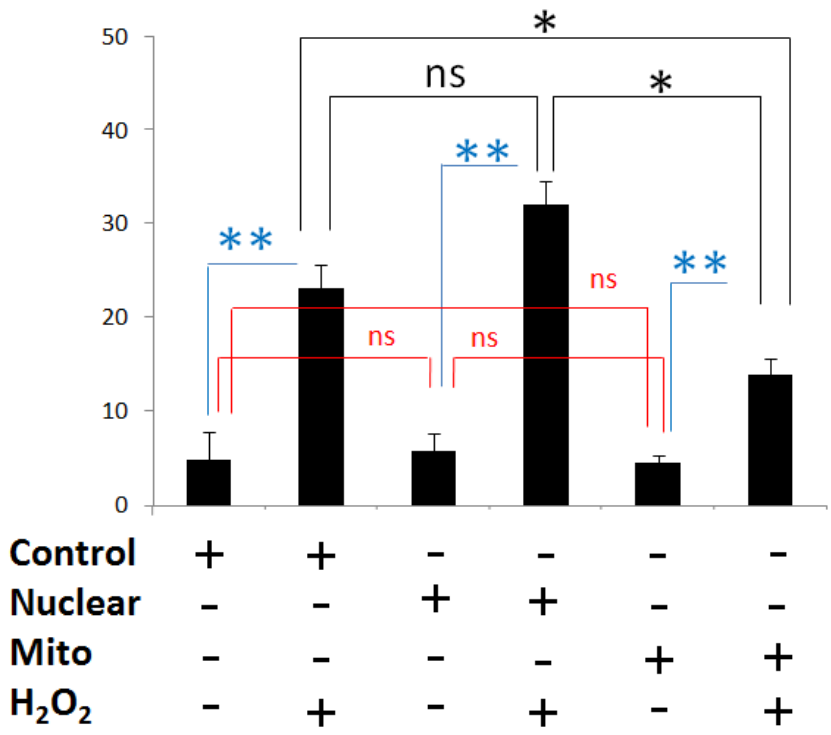

Figure 3.14 Comparison of damage foci number in MCF7 transfected with both TERT shooter vectors under different conditions. The graph represents the percentage of cells which showed more than 20 damage foci. Bars indicate mean and standard error from 3 independent experiments. Results have been compared using One way ANOVA ***** P<0.05, ****** P<0.01, ns = non-significant difference.

After H_2O_2 treatment, MCF7 showed a tendency for more resistance to the nuclear DNA damage in the mito-hTERT transfected group compared with nucl-hTERT and non transfected cells. This result might suggest a protective capacity of mitochondrial hTERT to nuclear DNA. Mitochondrial localisation of hTERT might help to prevent nuclear DNA damage after oxidative stress. However, there was no significant difference between nucl-hTERT and non-transfected MCF7 cells as found in Hela. We hypothesise that the different p53 status might be the reason of the higher of DNA damage of Hela when hTERT is localised in the nucleus compared to MCF7. An experiment to assess a possible correlation between p53 status and nuclear localisation of hTERT will be shown in Chapter 5.

3.3.3.3 Localisation of exogenous hTERT affects nuclear DNA damage in U87 after H_2O_2 treatment

We have used U87 as a third cancer cell line to investigate the effect of exogenous hTERT to nuclear DNA damage. U87 contains a functional p53 as in MCF7, hence, we can investigate the influence of the p53 status to mitochondrial protective function of hTERT and nuclear DNA damage. U87 cells were transfected with both shooters as described for Hela and MCF7. Transfected U87 was double stained with γH2A.X and myc-tag as described in materials and methods. U87 damage foci were determined under normal and stress condition and separated into 3 categories as: non damage (non foci damage detected), medium damage (contains 1-10 damage foci) and high damage (>10 damage foci). DNA damage quantitative results of U87 are summarised in fig. 3.15 and 3.16.

However, the results in U87 were different from those in MCF7. U87 showed high background damage as in Hela before treatment. 70-80% of U87 contained at least 1 damage foci before treatment (figure 3.15). This is similar to results from another group which found background DNA damage in U87 (Short et al., 2007) and might suggest that background DNA damage is dependent on cell types. In non-transfected U87, there is a significant difference between treated and untreated cells in the group of medium (1 to 10) and high damage (more than 10 foci) similar to U87 transfected with nucl-hTERT. However, in U87 transfected with mito-hTERT, no significant difference was found in the group of medium damage (1 to 10 damage foci before) between before and after treatment. The comparison between U87 transfected with mito-hTERT, nucl-hTERT and non-transfected U87 after H_2O_2 treatment is summarised in figure 3.16. The result of U87 is summarised from 3 independent experiments.

Under basal condition, no significant difference has been observed between mito-hTERT, nucl-hTERT and non-transfected U87 as in MCF7 suggest that high nuclear DNA damage in nucl-hTERT Hela under basal condition compared to mito-hTERT and the non-transfected group might be because the correlation between nuclear localisation of hTERT and inactive p53.

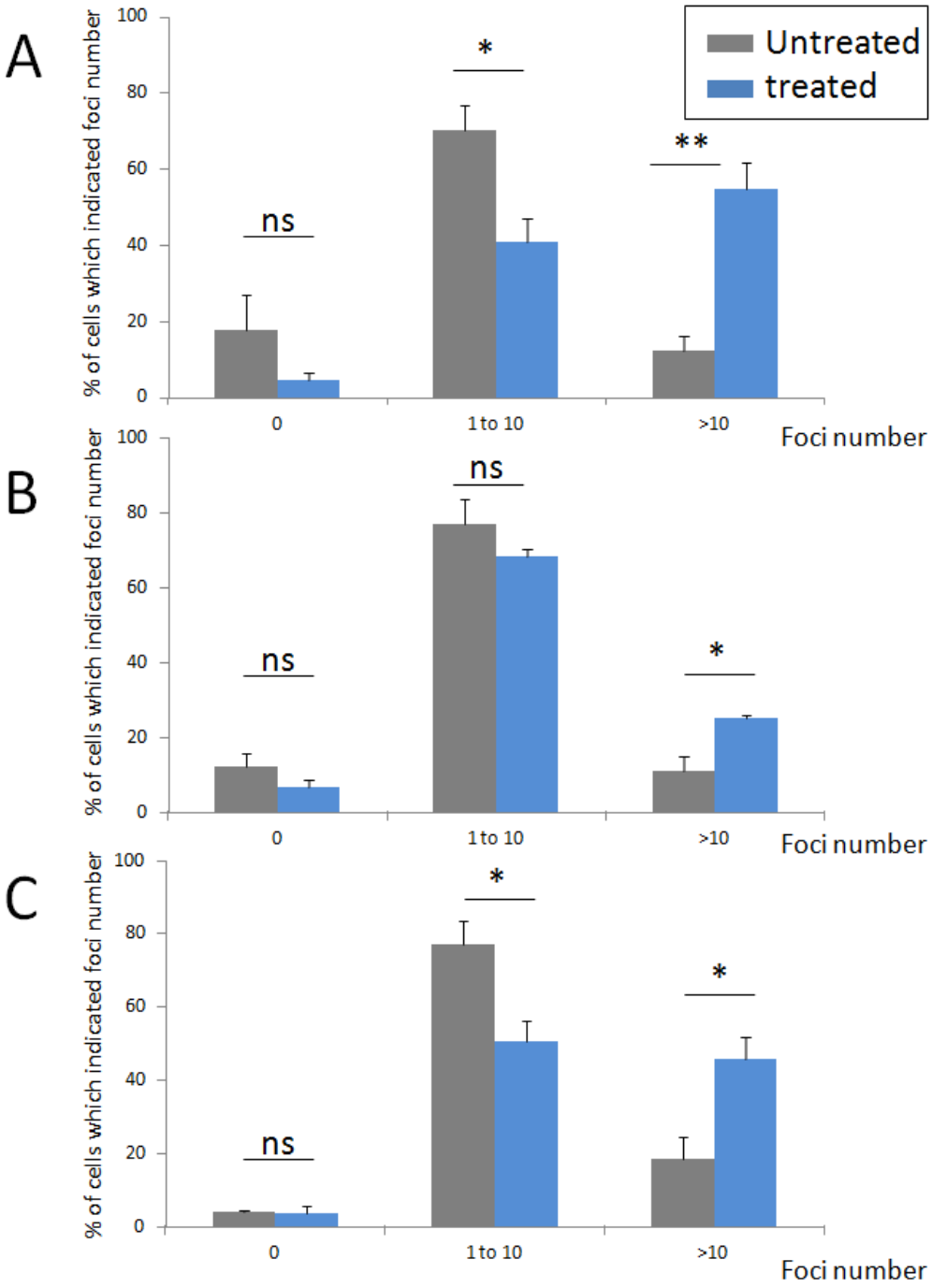

Figure 3.15 DNA damage foci of U87 transfected with mito-hTERT, nucl-hTERT and non-transfected under normal and stress conditions. Cells were treated with 200 μM H_2O_2 for 1 hr, then fixed and double stained with γH2A.X and myc-tag (for TERT identification) and damage foci number counted. **A:** non-transfected U87. **B:** U87 transfected with mito-hTERT. **C:** U87 transfected with nucl-hTERT. Bars indicate mean and standard error from three independent experiments. Results have been compared using ANOVA-single factor ***** P<0.05, ****** P<0.01, ns = non-significant difference.

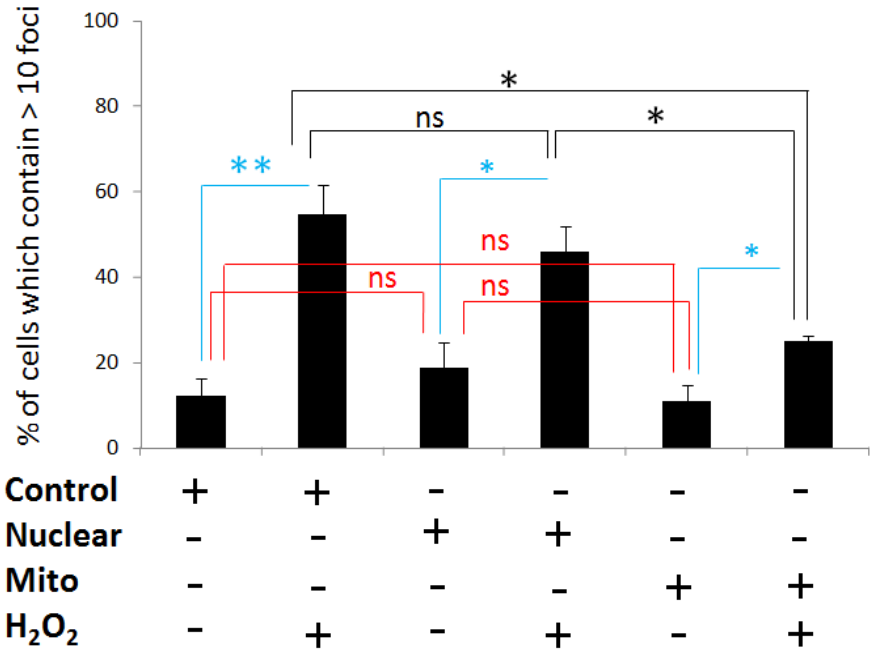

Figure 3.16 Comparison of DNA damage foci number in U87 transfected with both TERT shooter vectors under different conditions. The graph represents the percentage of cells which showed more than 10 damage foci. Bars indicate mean and standard error from 3 independent experiments. Results have been compared using One way ANOVA ***** P<0.05, ****** P<0.01, ns = non-significant difference.

After H_2O_2 treatment, U87 showed a tendency for more resistance to nuclear DNA damage in the mito-hTERT transfected group as found in Hela and MCF7. U87 cells transfected with mito-hTERT showed significantly lower damage compared to nucl-hTERT and non-transfected cells. This result confirms a protective capacity of mitochondrial hTERT to nuclear DNA. U87 transfected nucl-hTERT showed no significant difference compared to non-transfected U87 as in MCF7. This result is different from Hela which support our hypothesis that a different p53 status might be the reason for the higher DNA damage of Hela cells when hTERT is localised in the nucleus.

3.3.3.4 Control experiments

In order to confirm that the damage in the nucleus of nucl-hTERT shooter transfected in Hela was not the result of the shooter vector transfection itself, a control experiment using GFP shooter vectors was performed. pCMV-GFP mito and nuclear shooter vectors were transfected into Hela cells. Cells were treated with 200 μM H_2O_2 for 1hour, then fixed and stained with a γH2A.X antibody. A representative image of the mito/nucl GFP shooter transfection is shown in figure 3.17 and the quantitative comparison between mito/nucl GFP shooter and the non transfected cells is shown in figure 3.18. The result did not show any significant difference between any of the GFP vectors and non-transfected cells. Thus the damage in the nuclear hTERT transfected cells was not a direct result from transfection of the shooter or the ectopic protein expression.

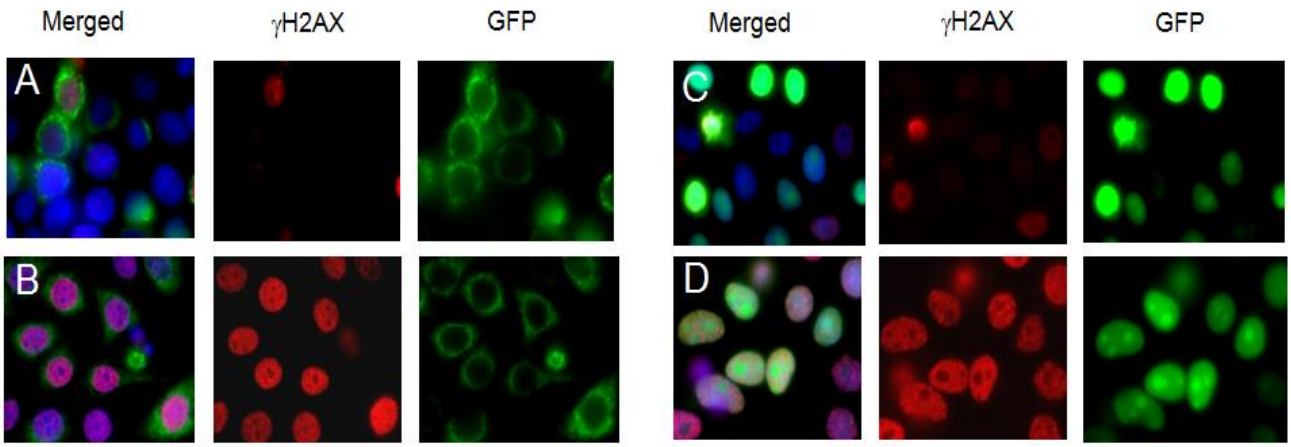

Figure 3.17 Control experiment using GFP shooter vectors for DNA damage analysis. Hela cells were transfected with pCMV-myc-mito/nucl-GFP and compared between untreated and treated conditions. **A** is Hela transfected with mito-GFP under basal condition. **B** is Hela transfected with mito-GFP and treated with 200 μM H_2O_2 for 1h, **C** is Hela transfected with nucl-GFP under basal condition and **D** is Hela transfected with nucl-GFP and treated with 200 μM H_2O_2 for 1h .

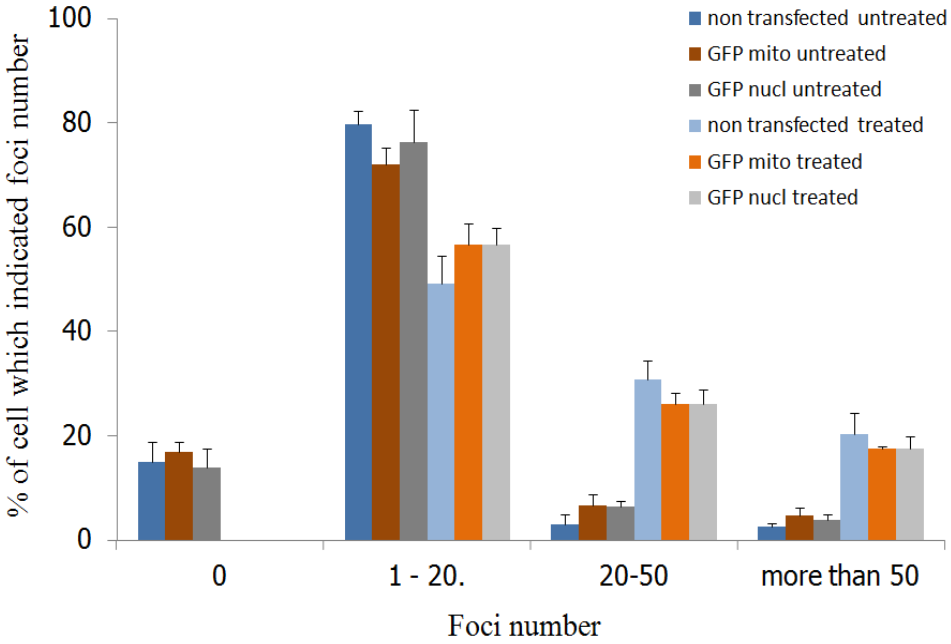

Figure 3.18 Comparison between mito-GFP, nucl-GFP and non-transfected Hela cells under basal and stress conditions. Bars indicated means and standard deviation from at least 50 individual cells.

3.3.4. Mitochondrial localisation of hTERT prevents DNA damage after x-irradiation

Hela, MCF7 and U87 were treated with irradiation in order to confirm the protective capacity of mitochondrial hTERT localisation onto DNA damage. However, we found that under 20Gy radiation that in Hela cells the over-expressed nucl-hTERT protein seemed to be rapidly excluded from the nucleus and performed similar to mito-hTERT (data shown in chapter 4). Thus, we were able to investigate the effect of mito-hTERT and nucl-hTERT only in MCF7 and U87 cells after irradiation.

3.3.4.1 Localisation of exogenous hTERT affects nuclear DNA damage in MCF7 after irradiation

MCF7 was transfected with mito-hTERT or nucl-hTERT shooter and was treated with 20 Gy irradiation, then double stained with γH2A.X and myc-tag as described before. The representative images of MCF7 transfected with mito-hTERT of nucl-hTERT and irradiated with 20 Gy irradiation are shown in figure 3.19 and 3.20.

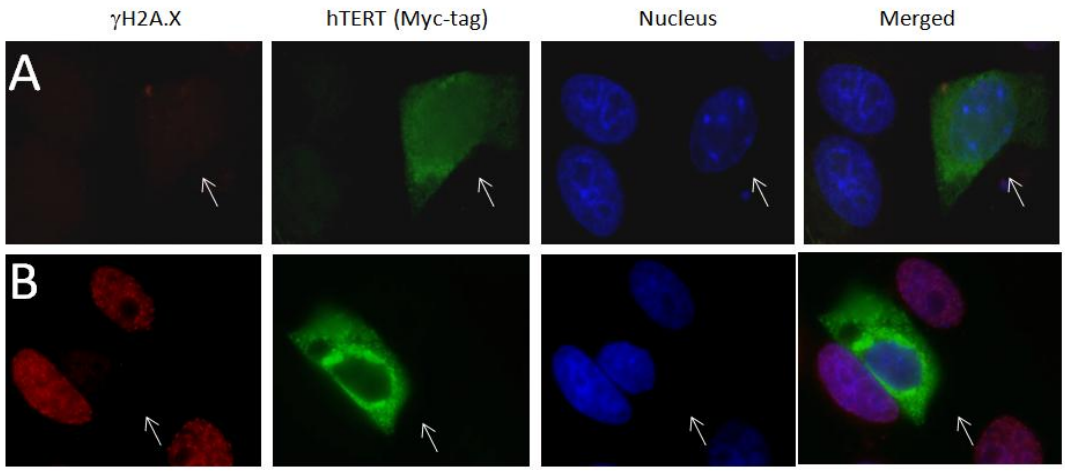

Figure 3.19 Double staining of MCF7 cells transfected with mito-hTERT shooter under untreated condition and x-irradiation. Cells were double stained with γH2A.X and myc-tag. Red colour represents DNA damage foci and green colour represents hTERT localisation. Blue is DAPI for nuclear stain. White arrows indicate transfected cells. **A** is a representative image of MCF7 cells transfected with mito-hTERT under basal condition and **B** is a representative image of MCF7 cells transfected with mito-hTERT after 20 Gy irradiation treatment.

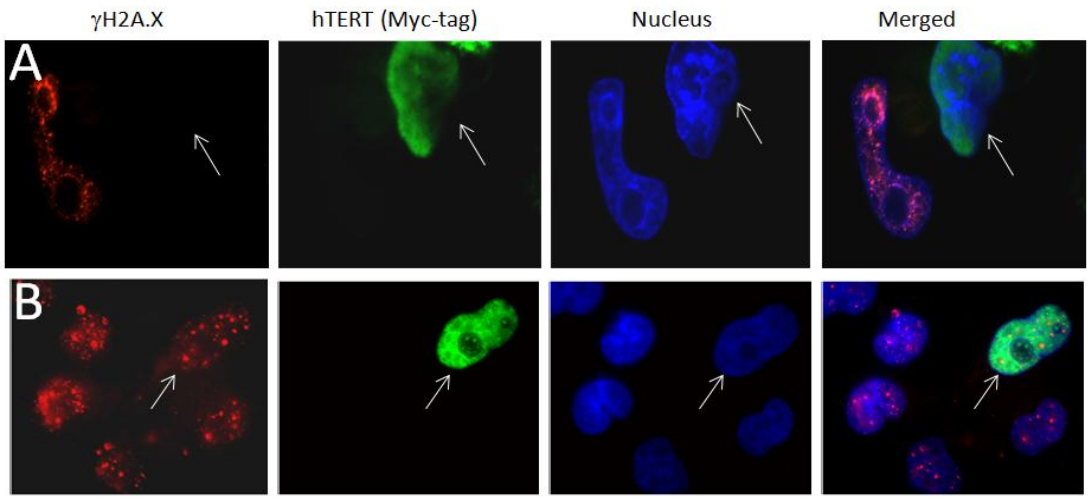

Figure 3.20 Double staining of MCF7 cells transfected with nucl-hTERT shooter under untreated condition and x-irradiation. Cells were double stained with γH2A.X and myc-tag. Red colour represents DNA damage foci and green colour represents hTERT localisation. Blue is DAPI for nuclear stain. White arrows indicate transfected cells. **A** is a representative image of cells transfected with nucl-hTERT under basal condition and **B** is a representative image of cells transfected with nucl-hTERT after 20 Gy irradiation treatment.

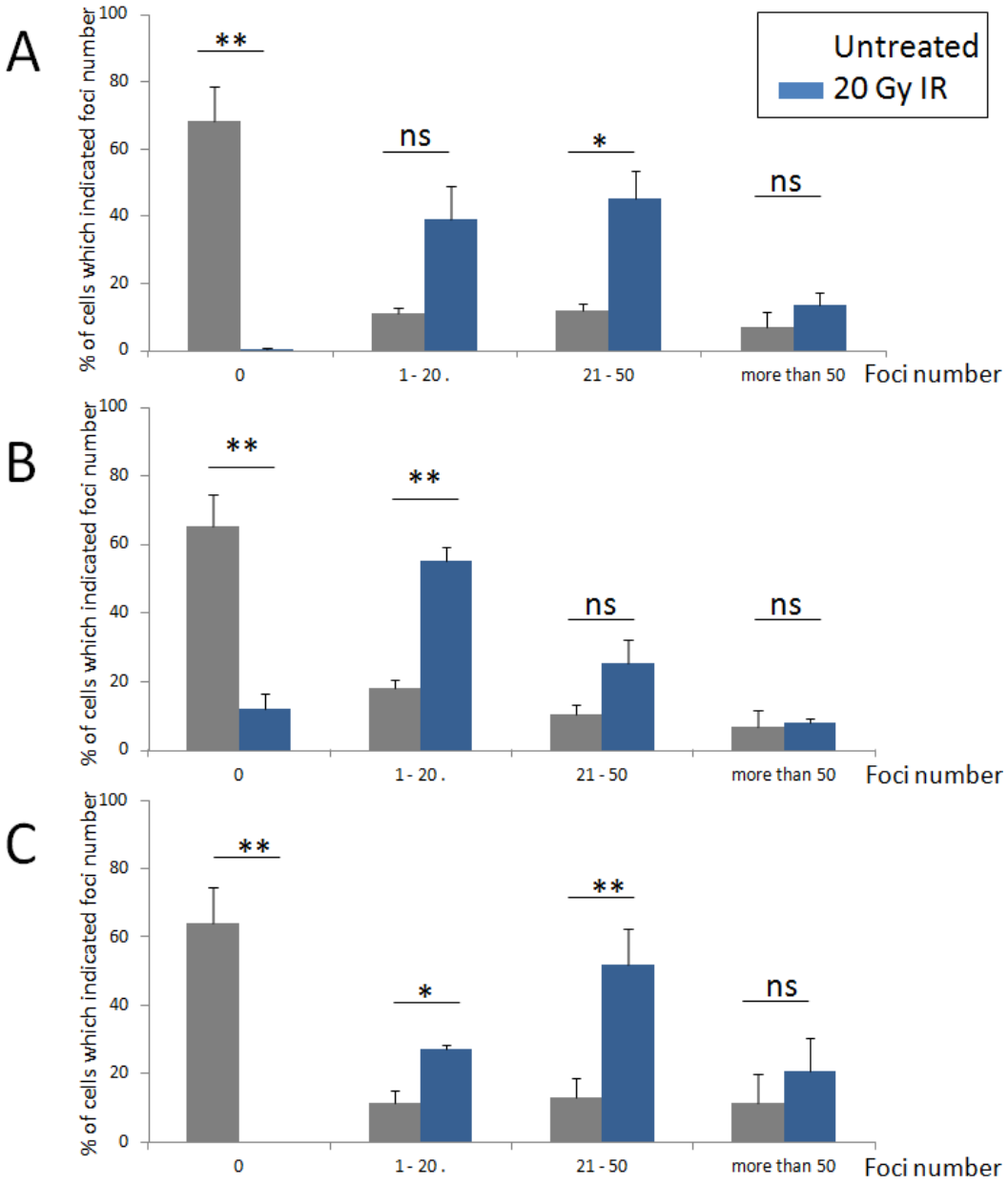

Figure 3.21 Damage foci of MCF7 transfected with mito-hTERT, nucl-hTERT and non- transfected under untreated condition and after X-irradiation. Cells were double stained with γH2A.X and myc-tag and damage foci number counted. Bars indicate means and standard error from three independent experiments. **A:** non-transfected MCF7. **B:** MCF7 transfected with mito-hTERT. **C:** MCF7 transfected with nucl-hTERT. Results have been compared using ANOVA-single factor * $P<0.05$, ** $P<0.01$, ns = non-significant difference.

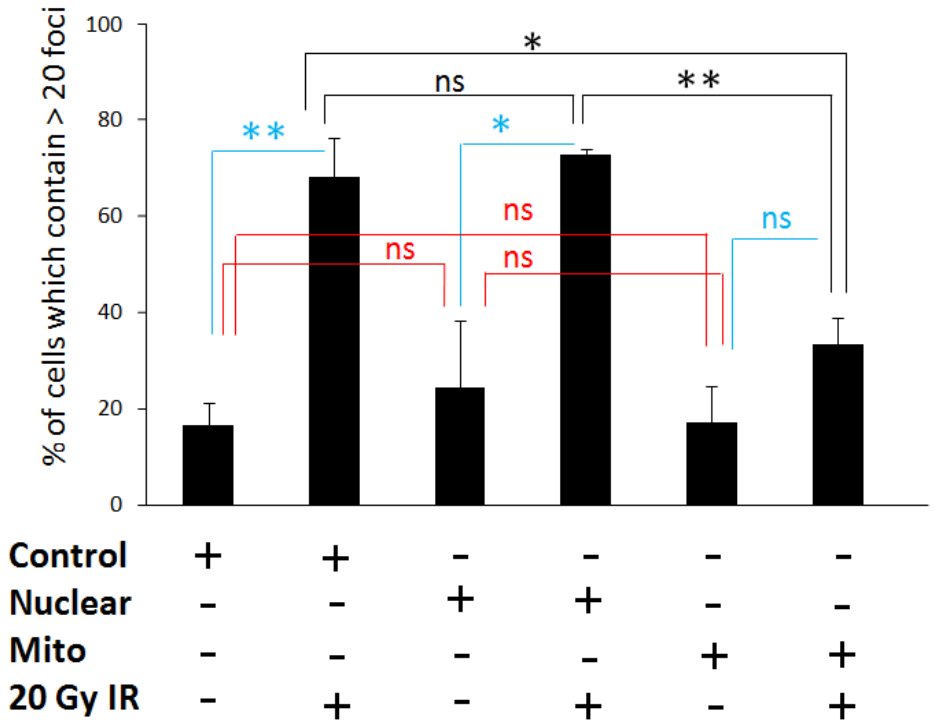

Figure 3.22 Comparison of damage foci number in MCF7 under untreated condition and after x-irradiation. The graph represents the percentage of cells which showed more than 20 damage foci. For irradiation cells were treated with 20 Gy X-ray and fixed within 15 minutes after treatment. Bars indicate means and standard error. Results have been compared using One way ANOVA ***** P<0.05, ****** P<0.01, ns = non-significant difference.

Figure 3.21 shows a number of DNA damage foci in untreated MCF7 and after 20 Gy irradiation. Cells were separated into 4 categories which were, zero (0), 1 to 20, 21 to 50 and more than 50 damage foci.

We found a significant increase of DNA damage in MCF7 after irradiation compared to the non-irradiated cells. However, this increasing of DNA damage was different in MCF7 transfected with mito-hTERT compared to nucl-hTERT and non-transfected MCF7. There was no significant difference between untreated and 20 Gy irradiated cells in the group of more than 50 damage foci in all non-transfected, mito-hTERT and nucl-hTERT transfected cells. We found no significant difference between untreated and irradiation in the group of 21 to 50 in mito-hTERT while nucl-hTERT and non-transfected cells showed a significantly higher amount of DNA damage after irradiation. Thus, in figure 3.22 we grouped the higher DNA damage groups together and compared only the group of more than 20 foci in MCF7 transfected with mito-hTERT, nucl-hTERT and non-transfected cells as we did before in MCF7 after H_2O_2 treatment. We

found no significant difference between the 3 transfection groups before treatment. However, after 20 Gy irradiation, there was a significantly lower number of cells with more than 20 DNA damage foci in cells transfected with mito-hTERT compared to non-transfected or cells transfected with nucl-hTERT. We found no difference between nucl-hTERT and the non-transfected group after 20 Gy irradiation. Thus, this result from irradiation confirms our previous H_2O_2 experiment regarding the ability of mitochondrial localisation of hTERT to prevent DNA damage under an independent stress condition.

3.3.4.2 Localisation of exogenous hTERT affects nuclear DNA damage in U87 after irradiation

U87 was transfected with mito-hTERT or nucl-hTERT shooter and was treated with 20 Gy irradiation and then double stained with γH2A.X and myc-tag as described before. U87 damage foci were determined under normal and stress condition and separated into 3 categories as described for the H_2O_2 experiment. The quantitative results of DNA damage of U87 after irradiation are summarised in fig. 3.23 and 3.24.

As shown in figure 3.23, we found no significant difference between untreated and 20 Gy irradiated cells in the group of more than 10 damage foci in U87 transfected with mito-hTERT while U87 transfected with nucl-hTERT and non-transfected cells showed significant difference. This result indicates no increase of DNA damage after 20 Gy irradiation in U87 transfected with mito-hTERT while U87 transfected with nucl-hTERT and non-transfected cell showed significant increased of nuclear DNA damage after 20 Gy irradiation. In figure 3.24 we grouped the high DNA damage groups (>10 damage foci) together as we did before in U87 after H_2O_2 treatment. We found no significant difference between the 3 transfection groups before treatment which is similar to MCF7. After 20 Gy irradiation, there was a significantly lower number of cells with more than 10 damage foci in U87 transfected with mito-hTERT compared to non-transfected or U87 transfected with nucl-hTERT. We found no difference between nucl-hTERT and the non-transfected group after 20 Gy irradiation as in MCF7. This result in U87 transfected with mito-hTERT confirms the lower DNA damage when hTERT is localized in mitochondria as MCF7 transfected with mito-hTERT after irradiation and the previous results in H_2O_2 experiment.

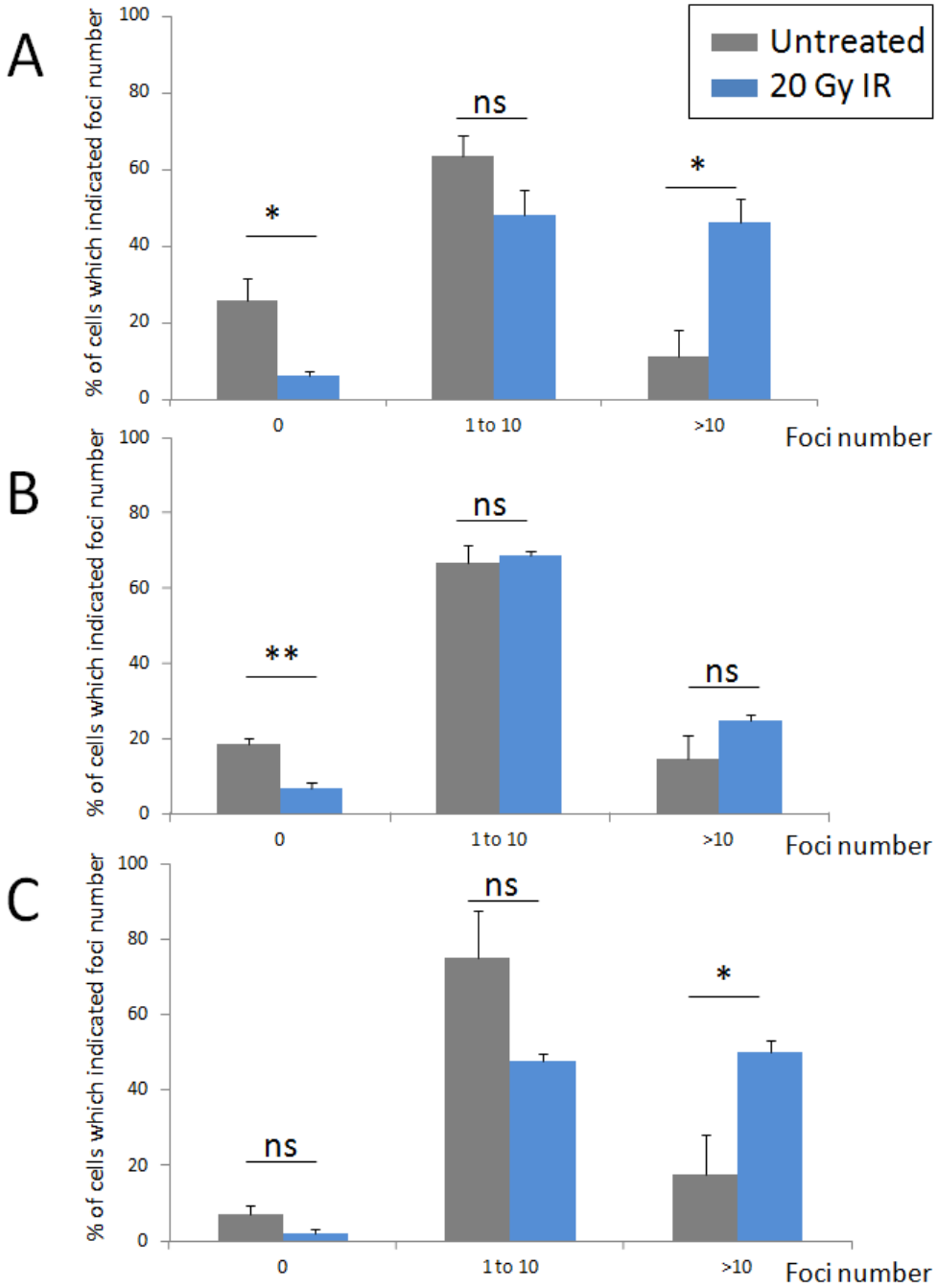

Figure 3.23 DNA damage foci of U87 transfected with mito-hTERT, nucl-hTERT and non transfected under normal and stress condition. Cells were treated with 20 Gy irradiation, then fixed and double stained with γH2A.X and myc-tag (for TERT identification) and damage foci number counted. **A:** non-transfected U87. **B:** U87 transfected with mito-hTERT. **C:** U87 transfected with nucl-hTERT. Bars indicate mean and standard error from three independent experiments. Results have been compared using ANOVA-single factor ***** P<0.05, ****** P<0.01, ns = non-significant difference.

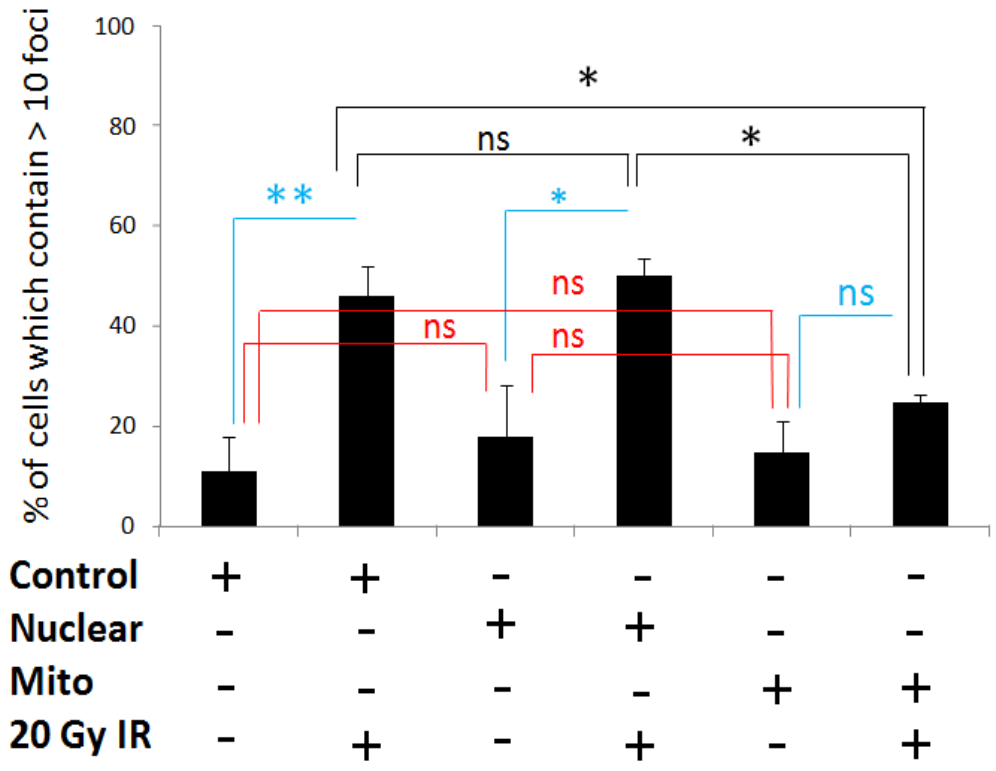

Figure 3.24 Comparison of DNA damage foci number in U87 transfected with both TERT shooter vectors under different conditions after x-irradiation. The graph represents the percentage of cells which showed more than 10 damage foci. Bars indicate mean and standard error from 3 independent experiments. Results have been compared using One way ANOVA * $P<0.05$, ** $P<0.01$, ns = non-significant difference.

3.3.5 Effect of mitochondrial localisation of hTERT on nuclear DNA damage in MRC5/SV40

To confirm our results of hTERT shooter experiments which have been done in cancer cell lines we proceeded to use cells without endogenous telomerase expression and chose MRC5/SV40. We were trying to use normal MRC5 fibroblast before, however, we have not succeeded in the transfection of mito-hTERT or nucl-hTERT to MRC5 using lipofectamine™ 2000 (2.2.2 in Chapter 2). Although we have tried other transfection agents such as FuGENE for the transfection we still got very few transfected cells. Thus we decided to use MRC5/SV40 instead of normal MRC5. This cell line is derived from normal MRC-5 fibroblasts transfected with a replication origin-defective early region of SV40 containing the gene of large T antigen (Huschtscha and Holliday, 1983). This MRC5/SV40 does not express endogenous hTERT which might influence the effect of our exogenous shooter.

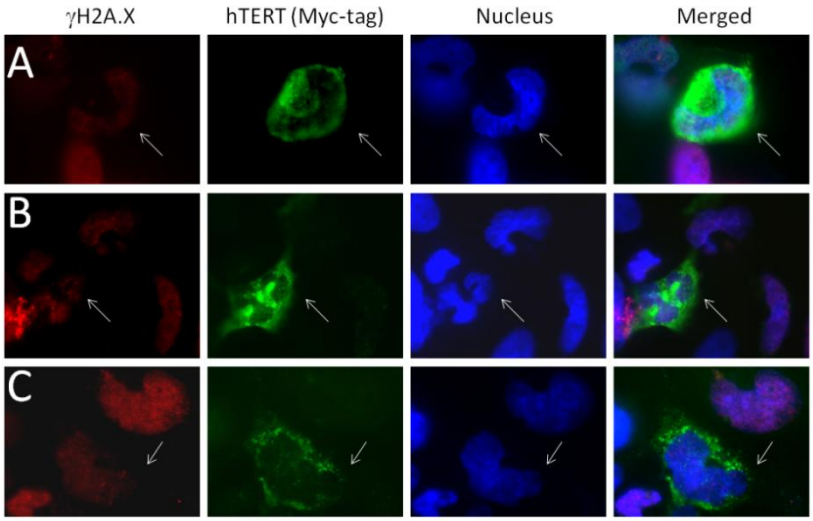

Figure 3.25 Double staining of MRC5/SV40 transfected with mito-hTERT shooter after 0, 5 and 10 Gy irradiation. Cells were double stained with γH2A.X and myc-tag. Red colour represents DNA damage foci and green colour represents hTERT localisation. Blue is DAPI staining for visualisation of nuclei. White arrows indicate transfected cells. **A** represents SV40MRC5 cells transfected with mito-hTERT under basal condition. **B** represents SV40MRC5 cells transfected with mito-hTERT after 5 Gy irradiation treatment and **C** represents SV40MRC5 cells transfected with mito-hTERT after 10 Gy irradiation.

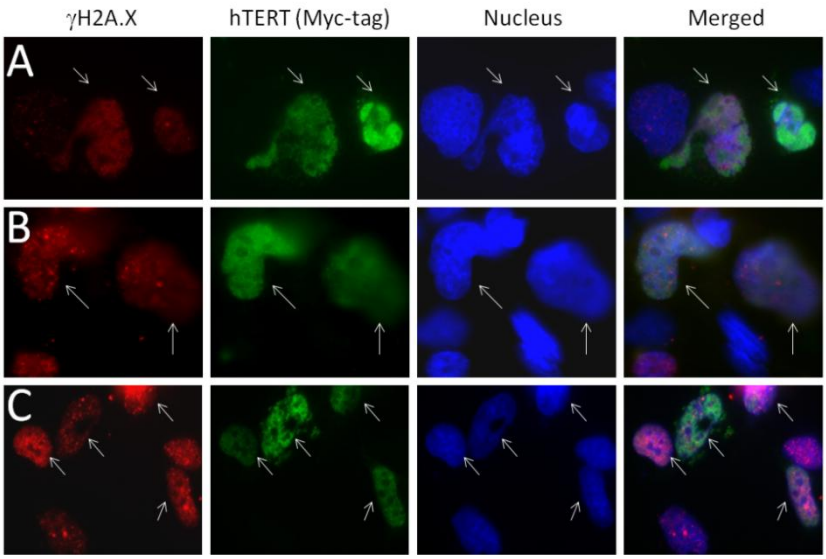

Figure 3.26 Double staining of MRC5/SV40 transfected with nuclTERT shooter after 0, 5 and 10 Gy irradiation. Cells were double stained with γH2A.X and myc-tag. Red colour represents DNA damage foci and green colour represents hTERT localisation. Blue is DAPI staining for visualisation of nuclei. White arrows indicate transfected cells. **A** represents MRC5/SV40 cells transfected with nucl-hTERT under basal condition**. B** represents MRC5/SV40 cells transfected with nucl-hTERT after 5 Gy irradiation treatment and **C** represents MRC5/SV40 cells transfected with nucl-hTERT after 10 Gy irradiation.

In MRC5/SV40, p53 is inactivated by SV40 large T-antigen (Lin and Simmons, 1991) similar to Hela cells where it is inactivated by HPV (papillomavirus). In this experiment, MRC5/SV40 was transfected with mito-hTERT or nucl-hTERT shooter vector as described in "Materials and Methods" and treated with different doses of x-irradiation.

Initially we irradiated MRC5/SV40 with a 20 Gy dose as in MCF7. However the cells displayed extremely high levels of DNA damage. Thus, we reduced the x-ray dose to 5 and 10 Gy. We categorised the number of damage foci into 3 groups in this experiment which were 0, 1 to 10 and more than 10 damage foci. Results of MRC5/SV40 before and after irradiation are shown in figure 3.25-3.28.

As shown in figure 3.27, there were no significant differences in the group of 0 damage foci in all MRC5/SV40 transfected with mito-hTERT, nucl-hTERT and non-transfected before and after irradiation. MRC5/SV40 already contained a large amount of damage in almost all of the cells before treatment which is similar to the situation in Hela. This suggests that acertain background damage in these two cell types might be due to a non-functional p53.

When we compared the group of 1 to 10 and more than 10 damage foci between untreated MRC5/SV40, 5 Gy and and 10 Gy irradiation in all mito-hTERT, nucl-hTERT and non-transfected cells, we found a significant increase of DNA damage foci of the 5 and 10 Gy irradiation group compared with non treated group in MRC5/SV40 transfected with nucl-hTERT and non-transfected. However, we have not found any significant difference between 5 Gy and 10 Gy irradiation when compared to the untreated group in MRC5/SV40 transfected with mito-hTERT. Moreover, we have not found a significant difference between DNA damage of MRC5/SV40 irradiated with 5 Gy and 10 Gy between non-transfected, mito-hTERT and nucl-hTERT. Thus, we summarised the results of MRC5/SV40 under basal condition compared with cells which were irradiated with 10 Gy. We subtracted the damage background by considering only cells which contained more than 10 damage foci.

Under basal condition, it seemed that nucl-hTERT promotes high amount of DNA damage foci. The nucl-hTERT group contained a significantly higher amount of DNA damage compared to non transfected group. However, we have not found a significant difference between mito-hTERT and nucl-hTERT before irradiation. There was also no significant difference between non-transfected and mito-hTERT before irradiation. This might be because of the high standard error in the mito-hTERT group.

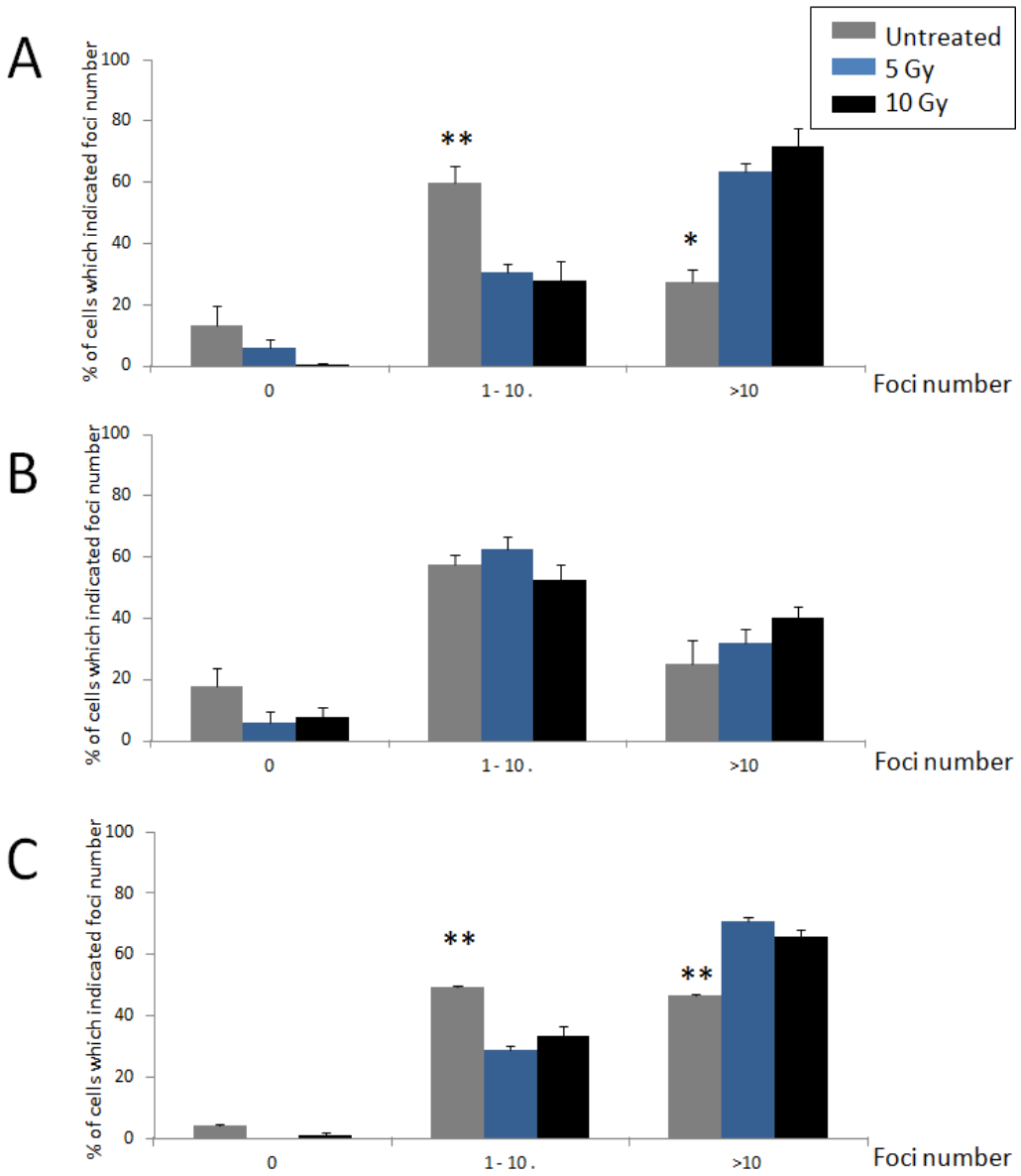

Figure 3.27 DNA damage foci of MRC5/SV40 transfected with mito-hTERT, nucl-hTERT and non-transfected cells untreated and after x-irradiation. Cells were double stained with γH2A.X and myc-tag and damage foci number counted. **A:** non-transfected MRC5/SV40. **B:** MRC5/SV40 transfected with mito-hTERT. **C:** MRC5/SV40 transfected with nucl-hTERT. Results have been compared using ANOVA-single factor ***** $P<0.05$, ****** $P<0.01$. Bars indicate mean and standard error from three independent experiments.

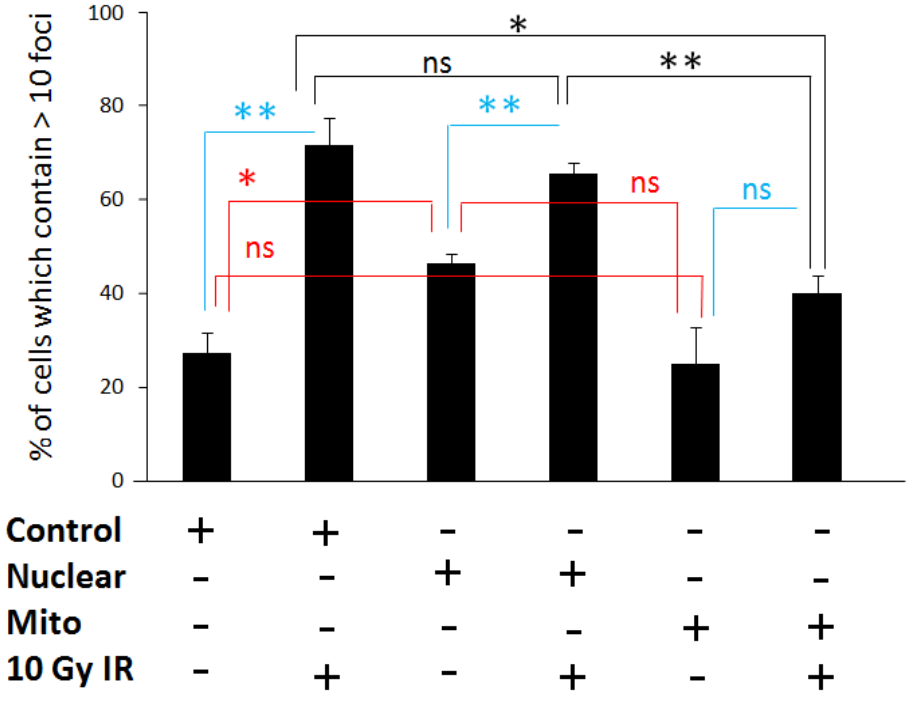

Figure 3.28 Comparison of damage foci number in MRC5/SV40 under basal conditions and after x-irradiation. The graph represents the percentage of cells which showed more than 10 damage foci. For irradiation cells were treated with 10 Gy X-ray and fixed within 15 minutes after treatment. ***** P<0.05, ****** P<0.01, ns = non-significant difference. Bars indicate means and standard error from 3 independent experiments.

After 10 Gy irradiation, MRC5/SV40 transfected with mito-hTERT shooter showed a significantly lower percentage of damage cells compared to both nucl-hTERT and non transfected cells. We have not found a significant difference between the non-transfected group and nucl-hTERT group after irradiation. Thus, this result clearly showed the protection of nuclear DNA was cause by the exogenous mitochondrially localised hTERT. Overall, the results in this chapter indicate a correlation between mitochondrial hTERT and nuclear DNA protection function.

3.3.6 Apoptosis induction in Hela, MRC5/SV40 and U87 transfected with mito-hTERT and nucl-hTERT

Since we found a significant decrease of DNA damage foci when hTERT is localised in the mitochondria we were interested whether this low DNA damage might related to lower apoptosis in cell transfected with mito-hTERT. Hela, MRC5/SV40 and U87 were transfected with nucl-hTERT and mito-hTERT and treated with 400 μM H2O2 or 20 Gy irradiation then washed with regular culture medium. MRC5/SV40 and U87 were

left one day for apoptosis induction while Hela was left 2 days before fixation due to a known delay in apoptosis induction of these cells. Cells were double stained for apoptosis (Activated Caspase 3) and exogenous hTERT localisation (c-myc staining). Results have been determined from 30-150 transfected cells per cell line and condition. A representative image and the analysis of apoptosis are shown in figures 3.29- 3.31.

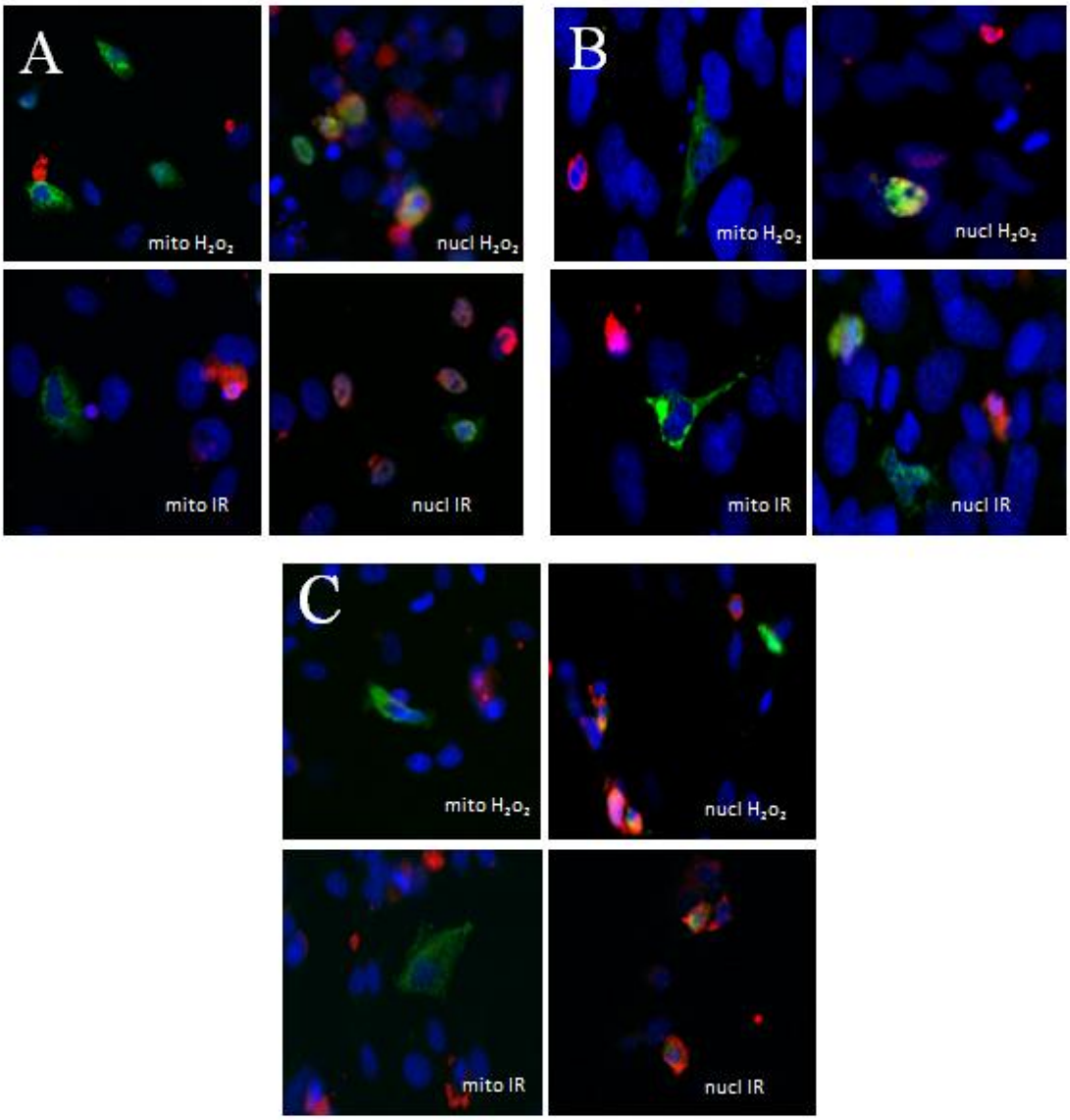

Figure 3.29 Mitochondrial TERT protects from apoptosis induction after H2O2 treatment and x-irradiation compared to cells transfected with nuclear TERT. Representative images of activated caspase 3 (red colour) in **A:** Hela, **B:** MRC5/SV40, **C:** U87 cells transfected with mito-hTERT and nuclear-hTERT (myc-tag staining as shown in green colour) after 400 H_2O_2 treatment for 3h and irradiation with 20Gy

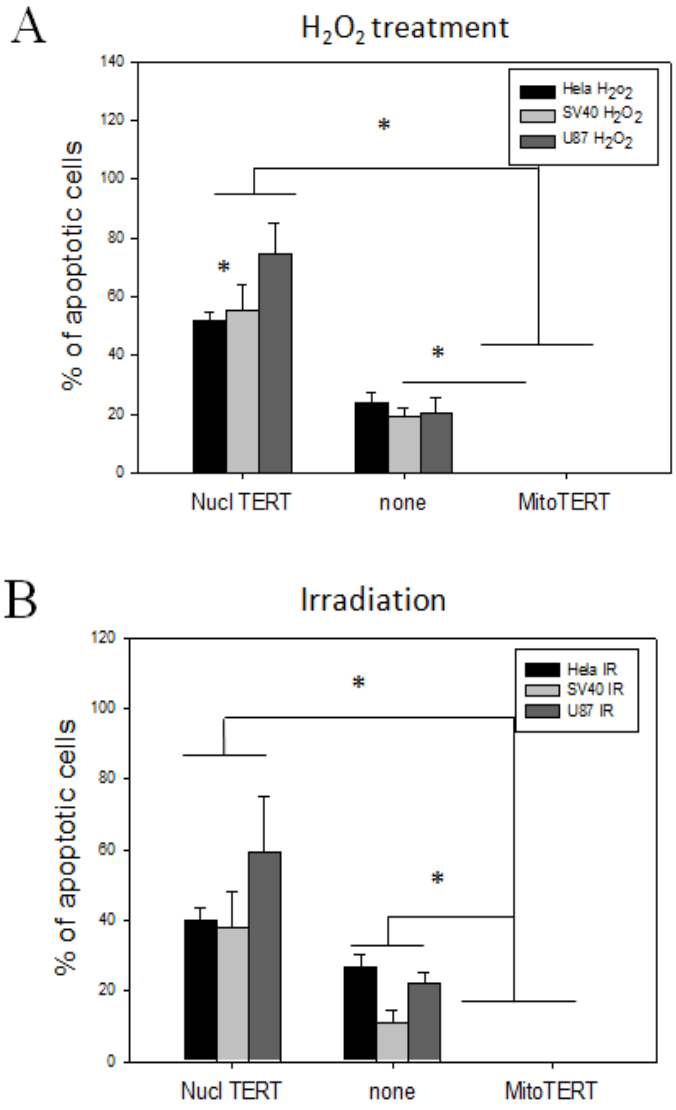

Figure 3.30 Quantification of the percentage of apoptotic cells of Hela, MRC5/SV40 and U87 transfected with mito-hTERT or nucl-hTERT after H_2O_2 or irradiation.
A: quantification of the percentage of apoptotic cells of the 3 cell lines after 400 mM H2O2 treatment. B: Quantification of the percentage of apoptotic cells of the 3 cell lines after x-irradiation (20Gy). Bars present mean and standard error from around 45 transfected cells per condition and cell line. * $p<0.05$

From figure 3.30, we have not found any single cell of Hela, U87 and MRC5/SV40 transfected with mito-hTERT showed any sign of apoptosis. The result was different in both 3 cell lines transfected with nucl-hTERT and untransfected cells. We found around 20% of untransfected cells and between 40-60% of cells transfected with nucl-hTERT were apoptotic. These results indicate a correlation between the localisation of hTERT, the induction of DNA damage and apoptosis. The damage found in cells with nucl-hTERT impacts directly on cell survival while mitochondrial TERT efficiently protects cells against apoptosis.

3.4 Discussion

In this chapter, we showed that endogenous hTERT shuttles from nucleus to mitochondria upon oxidative stress in a heterogeneous manner in three different cell lines. Two cancer cell lines in our experiments (Hela and MCF7) showed about 20% of hTERT already localised in the cytoplasm/mitochondria under basal conditions. This finding is consistent with published data from other groups (Sharma et al., 2011; Kovalenko et al., 2010; Ahmed et al., 2008; Haendeler et al., 2009). Under oxidative stress, the kinetic exclusion of hTERT is different between Hela, MCF7 and MRC5-hTERT. MRC5-hTERT cells showed a faster exclusion of endogenous hTERT to the cytoplasm with a maximum of hTERT exclusion at three hours post oxidative stress while it took longer time for Hela and MCF7 to exclude TERT from the nucleus. Both cancer cell lines took up to one day to reach the maximum hTERT exclusion. Interestingly, hTERT remained outside of the nucleus up to five days of follow-up in Hela and MCF7. Thus, nuclear TERT exclusion seems to be a persistent process which can last up to several days after a single treatment. The long persistence of hTERT protein outside the nucleus might be an important contributor to an increased resistance against DNA damage and decreased apoptosis of these cells.

However, cytoplasmic localisation of hTERT in MRC5-hTERT and MCF7 seems to gradually reduce after 24 hours after treatment while the cytoplasmic hTERT of Hela seems stable upon 5 days of our experiment. Both MRC5-hTERT and MCF7 habour an activated p53 while Hela contains an inactivated p53 because of the HPV subtype 18 (Human papillomaviruses) viral proteins E6 and E7 functionally inactivate the check point of p53 (Hopper-Seyler and Butz, 1993). Thus, we hypothesised that this different p53 status could play a role for the different kinetics of hTERT exclusion after oxidative stress.

Moreover, our result indicates a correlation between localisation of telomerase and the DNA damage pattern. We quantified the amount of DNA damage foci correlated with the localisation of endogenous hTERT and found that if endogenous hTERT was excluded from nucleus to cytoplasm/mitochondria under oxidative stress, all three cell lines in our experiment displayed no or very low amount of DNA damage. In contrast, if endogenous hTERT was localised in the nucleus and not exclude while cells were under oxidative stress, all three cell lines displayed high amount of DNA damage. Kovalenko and co-workers speculate in their paper that the high level of DNA damage when hTERT is localised in the nucleus might play a role in cell cycle delay in order to repair the damage site (Kovalenko et al., 2010a)After DNA damage, activated p53 will induce

p21 and Hzf, a human zinc-finger-containing p53 target gene to arrest the cell cycle. This process will allow time for DNA repair (Zhang et al., 2012). However, if the damage is beyond repair, Hzf will be degraded, and activates E2F1 will induce the process which triggers apoptosis. Therefore, the cellular outcome is closely associated with p53 levels. Thus lack of an active p53 in Hela might be a reason of higher DNA damage. Further experiments regarding the effect of p53 are described in Chapter 5.

To prove directly whether the different localisations of hTERT in the mitochondria or nucleus have indeed a direct influence to nuclear DNA damage, we used a model of specific hTERT shooter vectors to deliver TERT protein specifically to mitochondria or nucleus in Hela and MCF7. In addition, we used MRC5/SV40 which does not express an endogenous hTERT to confirm our model. We used two different exogenous stress treatments which were hydrogen peroxide and irradiation.

Un-transfected Hela cells under basal condition already presented a number of damage foci in the nucleus (figure 3.7). This suggests a certain background damage in this cancer cell type which is probably due to the functionally inactive p53 as found in other p53 negative cancer cells (Kovalenko et al., 2010a). In order to subtract the background level of DNA damage in Hela cells were summarised the damage data by considering only cells that contained more than 20 damage foci (figure 3.10). The results demonstrated a significant lower amount of DNA damage in mito-hTERT shooter compared to the nuclear shooter and non-transfected cells in both basal and treated condition. However, it was a surprising result to find a higher damage level before treatment in Hela cells transfected with nucl-hTERT when compared with both the mito-hTERT and the non-transfected group. After cells were treated with H_2O_2, the increase of the high damage group of nucl-hTERT was even more pronounced. This result supports the surprising suggestion that nuclear hTERT might even further increase the DNA damage foci in the nucleus. Kovalenko and colleagues found that over-expression of a hTERT with a mutation of the TERT nuclear export signal ($_{NES-}$hTERT) which prevents the translocation of hTERT from the nucleus can significantly decrease the proliferation rate and the ability to form colonies in soft agar in LNCaP, SQ20B and Hela cells. The cancer cells also showed an increase of DNA damage at telomeric and extra-telomeric sites (Kovalenko et al., 2010 b). This result is in excellent accordance to our finding that nuclear hTERT transfection in Hela cells showed also a high DNA damage before treatment.

To exclude that the high DNA damage of nucl-hTERT cells was the result of the shooter vector itself, a GFP experiment was performed. The results from mito-GFP and

nucl- GFP shooter did not show any difference between GFP vector transfected and non-transfected cells regarding with the DNA damage (figure 3.18). Thus the damage in the nucl-hTERT group was not a direct result from the shooter transfection or the ectopic protein expression, but rather specific for nuclearly localised TERT protein.

Next, we investigated the effect of specific hTERT localisation in MCF7 and U87 cells. As shown in figure 3.14 and 3.16, no significant difference had been observed between mito-hTERT, nucl-hTERT and non-transfected cells in MCF7 and U87 under basal conditions. One possibility which could explain this difference might be the fact that Hela has a different p53 activity from MCF7 and U87. After H_2O_2 treatment, MCF7 and U87 showed a tendency for more resistance to the nuclear DNA damage in the mito-hTERT transfected group. Both U87 and MCF7 transfected with mito-hTERT showed significantly lower damage compared to nucl-hTERT and non transfected cells. This result is similar to that in Hela and confirms the protective capacity of hTERT to nuclear DNA. Mitochondrial localisation of hTERT might help to prevent nuclear DNA damage after oxidative stress.

We confirmed results obtained by using H_2O_2 by using irradiation as a different stress treatment. We found that under 20Gy radiation, Hela nucl-hTERT seemed to be rapidly excluded from the nucleus and performed as mito-hTERT (data shown in chapter 4). Thus, we were able to investigate the effect of mito-hTERT and nucl-hTERT only in MCF7 and U87 cells. The results conclude in figure 3.22 and 3.24 showed similar results as in hydrogen peroxide experiment. After 20Gy irradiation, a significantly lower number of cells with more than 20 DNA damage foci in MCF7 and more than 10 damage foci in U87 have been found in cells transfected with mito-hTERT compared to non-transfected and nucl-hTERT. This result in both cancer cell types confirm that mitochondria localisation of hTERT could prevent DNA damage under an independent stress condition.

We confirmed our results from cancer cells by transfecting mito-hTERT and nucl-hTERT to a telomerase negative cell type. MRC5/SV40 which does not contain endogenous telomerase has been used to avoid the effect of endogenous telomerase which might influence the results in cancer cells. Under basal condition, nucl-hTERT transfected cells showed significant higher DNA damage compared to the non-transfected group. However, there was no significant difference between mito-hTERT and non transfected cells (figure 3.28). After irradiation, no significant difference has been found between nucl-hTERT and non transfected group. However, mitoTERT transfected MRC5/SV40 showed a significantly lower DNA damage level than both

nucl-hTERT and non transfected cell. This result confirms that localisation of an exogenous hTERT in mitochondria reduces nuclear DNA damage.

Finally, we analyse the apoptosis induction after exogenous stress (400 μM H_2O_2 treatment and 20Gy irradiation) in Hela, MRC5/SV40 and U87 in order to investigate the effect of hTERT localisation to cellular apoptosis. Intriguingly, we have not found any sign of apoptosis (active Caspase 3) in cell transfected with mitochondrial TERT. However, we found around 20% of untransfected cells and between 40-60% of cells expressing the nuclear shooter were apoptotic. This result confirms that indeed the induced DNA damage found in cells with nuclear TERT localisation impacts directly on cell survival while mitochondrial TERT efficiently protects against apoptosis.

Thus, from the overall results we can conclude that mitochondrial localisation of hTERT provides a novel mechanism of protection from nuclear DNA damage. The mechanism of this protection will be analysed in the next chapter.

Chapter 4

Mitochondrial localisation of hTERT protects against mitochondrial ROS generation after exogenous stress

4.1 Introduction

Telomerase plays an important role for the proliferative capacity of the cell and cell survival. As described in Chapter 1, the main function of telomerase is to maintain telomere length and protect linear chromosomes from end-to-end fusions. However, recent evidence shows additional functions of telomerase independently from telomere maintenance. It has previously been shown that telomerase catalytic subunit is excluded from the nucleus of various cell types upon oxidative stress (Haendeler et al., 2003, Santos et al., 2004, Ahmed et al., 2008, Indran et al., 2011) which is correlated to a protective effect of telomerase within mitochondria (Ahmed et al.,2008, Haendeler et al., 2009, Kovalenko et al., 2010a,b, Indran et al., 2011), including in cancer cells (Kovalenko et al., 2010b, Indran et al., 2011).

To analyse whether there exists a direct correlation between physical location of hTERT in the mitochondria and its protective function, we used specific shooter vectors that deliver proteins specifically to various cell locations. Cells were transfected with hTERT-expressing shooter vectors which included the localisation signals specific for mitochondria or the nucleus (further on called mito-hTERT and nucl-hTERT). We transfected cancer cells with these hTERT expressing vectors and compared their mitochondrial superoxide level under normal conditions (unstressed) and exogenous stress (H_2O_2 and x-irradiation) treatments. These experiments should uncover whether mitochondrial localisation of hTERT alone is sufficient and necessary to protect mitochondria effectively under normal and stress condition compared to the situation when only nuclear hTERT is present. Single cell staining experiments rather than FACS experiments for ROS measurement where used due to the relatively low (25-30%) transfection rate. We attempted to do FACS analysis but did not find any differences presumably due to the high background (around 70%) of un-transfected cells.

4.2 Results

4.2.1 Quantitative determination of mitochondrial superoxide level in Hela and MCF7 cells under exogenous stress (H_2O_2)

To prove whether there is a direct correlation between physical location of hTERT in the mitochondria and the level of mitochondrial ROS, Hela and MCF7 cells were transfected with mito-hTERT or nucl-hTERT and treated with 100 μM H_2O_2 for 1 hour, left for 24 hours before staining and comparing their mitochondrial superoxide levels with cells cultured under untreated conditions. The reason for this long incubation period was because H_2O_2 treatment itself produced high ROS levels at earlier time points while after 1 day the effect of exogenous H_2O_2 was gone and only mitochondrial ROS generated after H_2O_2 treatment is measured. We have also tested the concentration of H_2O_2 at 100, 200, 400 and 800 μM compared with untreated Hela cells and found that one day after treatment only 100 μM H_2O_2 concentration showed equal ROS production as the untreated cells. We found a little higher level of ROS in Hela treated with 200 μM H_2O_2 and even higher levels in 400 and 800 μM (data not shown) which indicated the effect of H_2O_2 treatment was not completely gone and might interfere with our result. Thus we chose 100 μM H_2O_2 concentration in our experiment. Results of the mitochondrial superoxide staining from both mito- and nucl-hTERT under basal and stress conditions are shown in figures 4.1-4.5.

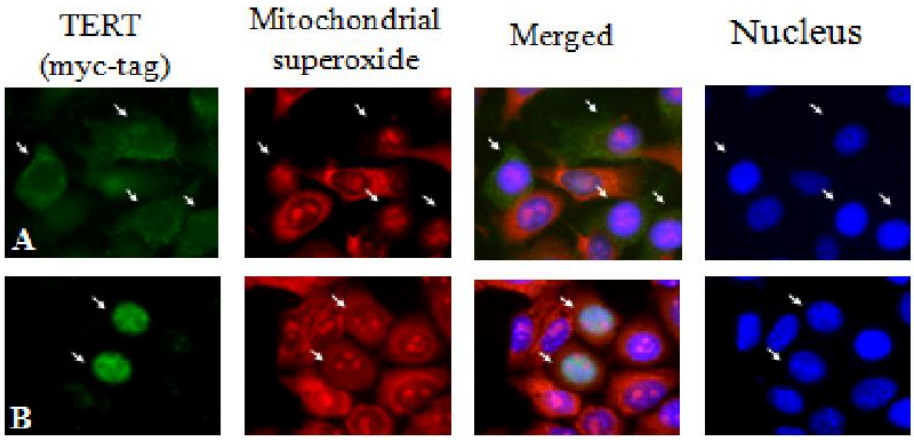

Figure 4.1 Hela cells: double staining of mitochondrial superoxide and TERT under normal (untreated) condition. Hela cells were transfected with mitochondrial-TERT (A) and nuclear TERT (B) shooter. Cells were double-stained with mitoSox for mitochondrial superoxide and myc-tag for TERT. White arrows indicate transfected cells.

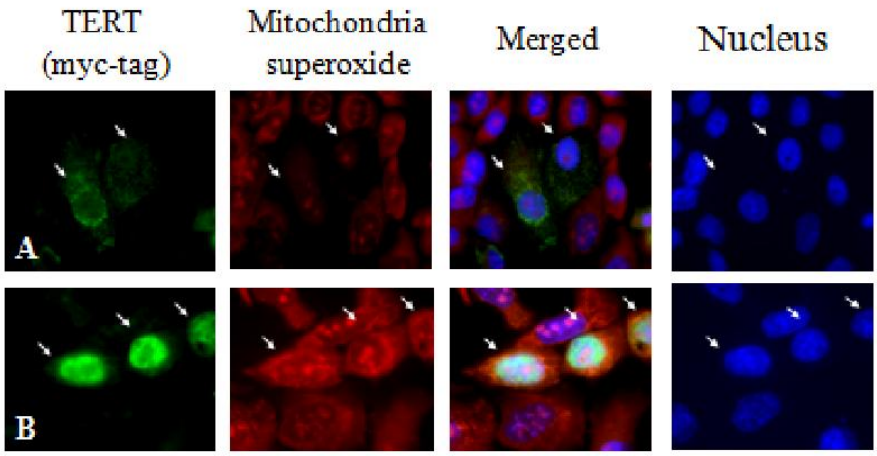

Figure 4.2 Hela cells: double staining of mitochondrial superoxide and TERT under stress condition. Hela cells were transfected with mitochondrial-TERT (A) and nuclear-TERT (B) shooter. Cells were treated with 100 μM H_2O_2 before staining with mitoSox for mitochondrial superoxide and myc-tag for TERT. White arrows indicate transfected cells.

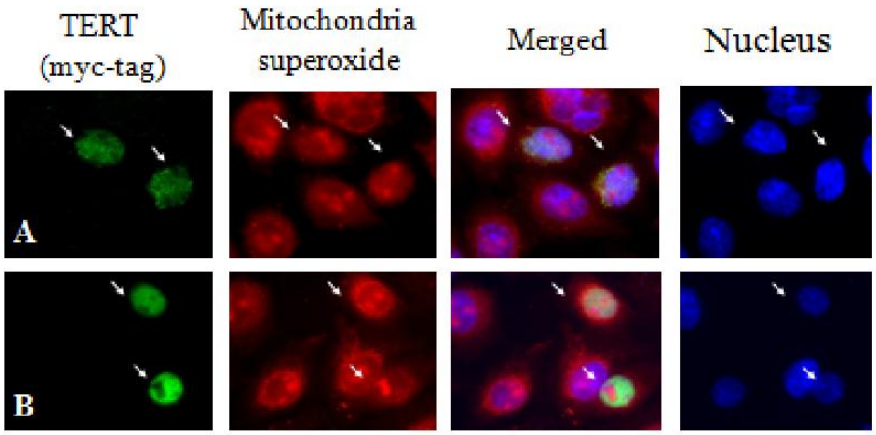

Figure 4.3 MCF7 cells: double staining of mitochondrial superoxide and TERT under normal condition. Cells were transfected with mitochondrial-TERT (A) and nuclear-TERT (B) shooter. Cells were double- stained with mitoSox for mitochondrial superoxide and Myc-tag for TERT. White arrows indicate transfected cells.

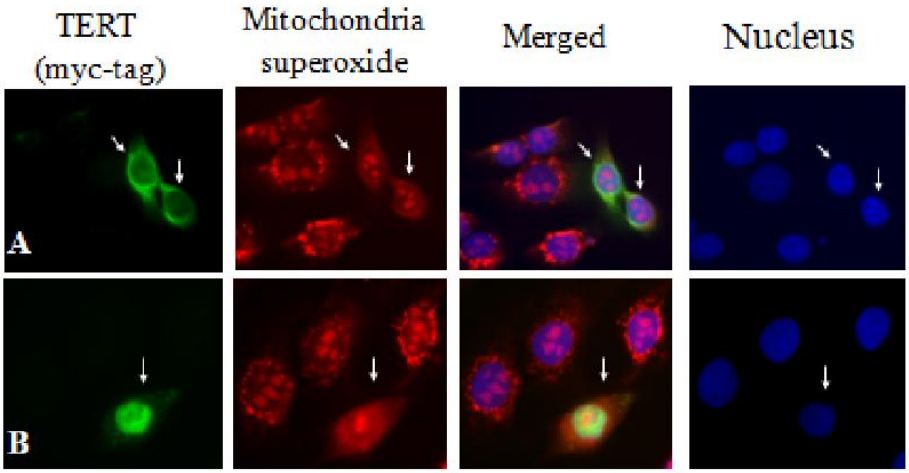

Figure 4.4 MCF7 cells: double staining of mitochondrial superoxide and TERT under stress condition. Cells were transfected with mitochondrial-TERT (A) and nuclear-TERT (B) shooter. Cells were treated with 100 mM H_2O_2 before staining with mitoSox for mitochondrial superoxide and myc-tag for TERT. White arrows indicate transfected cells.

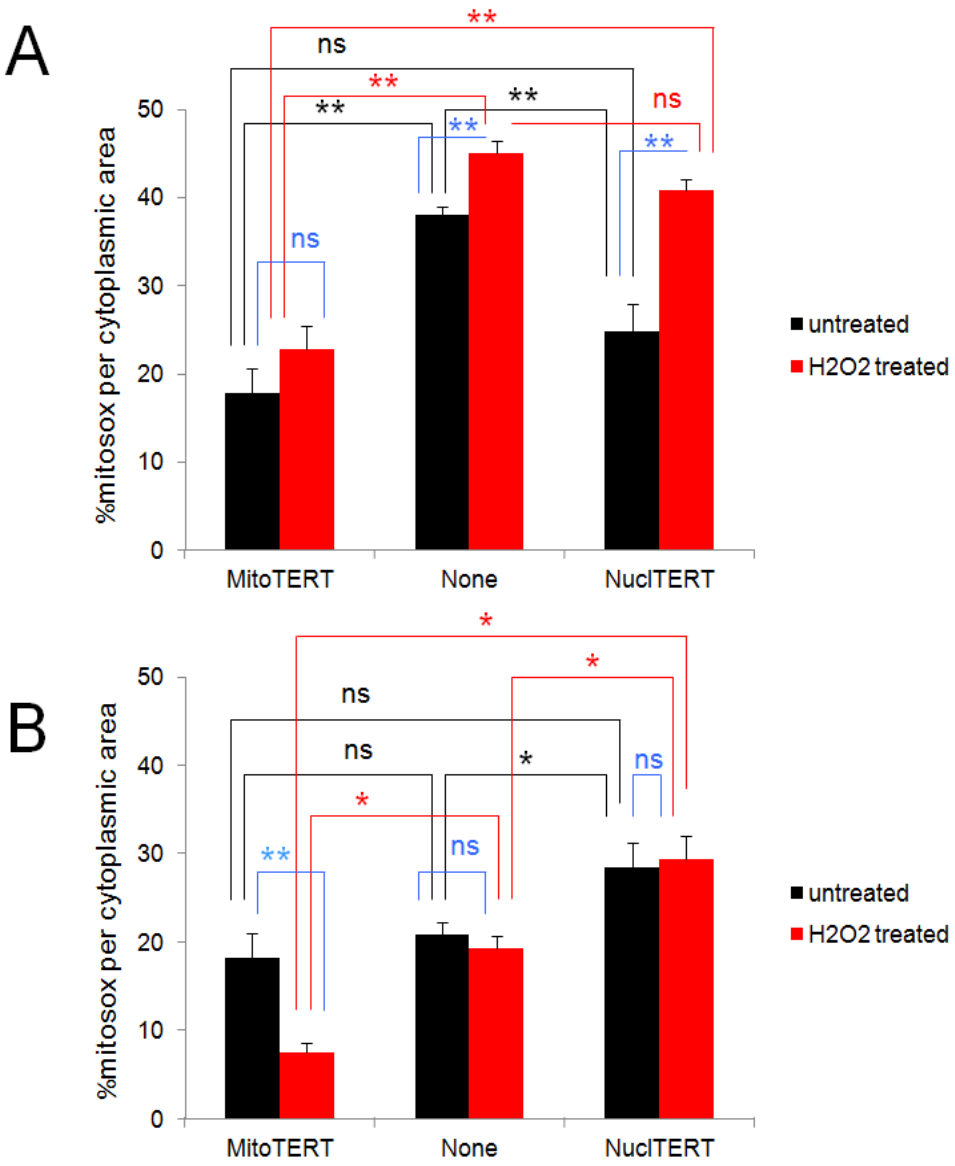

Figure 4.5 Comparison of mitochondrial superoxide levels in mito-hTERT and nucl-hTERT transfected as well as non-transfected cells in Hela and MCF7 under basal conditions and H_2O_2 stress treatment. A: Hela under basal condition and after H_2O_2 treated condition. **B:** MCF7 under basal condition and after H_2O_2 treated condition. Bars show mean and standard error from 3 independent experiments. One way Anova was used to test for significant differences between groups.

The results from figure 4.5 indicated lower levels of mitochondrial superoxide in cells transfected with mitochondrial hTERT after H_2O_2 treatment compared to nuclear hTERT. Under basal condition both Hela and MCF7 did not show a significant difference of ROS levels between mitochondrial hTERT expression and nuclear hTERT. Surprisingly, the level of ROS in nuclear-hTERT transfected MCF7 under basal condition was higher than in non-transfected cells ($P<0.05$). This result was different for Hela cells where both mito-hTERT and nuclear-hTERT showed statistically significant lower ROS levels under basal condition compared to non-

transfected cells (P<0.01) which might indicate a protective effect of hTERT before treatment. Under oxidative stress, Hela and MCF7 cells were treated with 100 μM H_2O_2 then left for 1 day before mitoSox staining and immuno-fluorescence staining. Mito-hTERT expression in both Hela and MCF7 showed significantly lower ROS level compared to nucl-hTERT (P<0.01). ROS levels in mito-hTERT Hela were lower than in non-transfected cells (P<0.01). However, the nuclear hTERT and non-transfected cells did not show significant differences. In MCF7, ROS level of mito-hTERT transfected cells was significantly lower than in cells transfected with nuclear hTERT (P<0.01) but it is interesting that the level of ROS in nuclear-hTERT transfected MCF7 was higher than in non-transfected cells (P<0.05). When compare between treated and non-treated condition of Hela and MCF7, the significant difference of non-transfected and nucl-hTERT transfected Hela between before and after treatment has been found. However, mito-hTERT transfected Hela did not show a significant increase of ROS level after H_2O_2 treatment compared with before treatment. In MCF7, no significant difference have been found when compare between before and after treatment in non-transfected and nucl-hTERT MCF7. It is interesting that mito-hTERT transfected MCF7 showed significant lower ROS level after H_2O_2 treatment. Thus these experiments showed that mitochondrial localisation of hTERT is necessary to protect mitochondria effectively under stress condition. This low level of ROS expression might be the reason for less nuclear DNA damage under exogenous stress under conditions when TERT is localised within mitochondria.

4.2.2 Control experiments (H_2O_2)

To confirm that the reduction of mitochondrial superoxide was indeed a specific effect of mitochondrial hTERT, three control experiments were performed to exclude the possibility that decreased mitoSox staining in cells harbouring mitochondrial TERT protein was due to a methodological artefact.

The first control is shown in figure 4.6. Hela and MCF7 were transfected with a control vector (pCDNA3.1), treated with 100 μM H_2O_2 and stained with mitoSox and myc-tag. Double staining with mitoSox and myc tag in pCDNA 3.1 transfected Hela and MCF7 did not show any change in mitosox due to the transfection per se. This data confirms that ROS expression does not influenced by the vector.

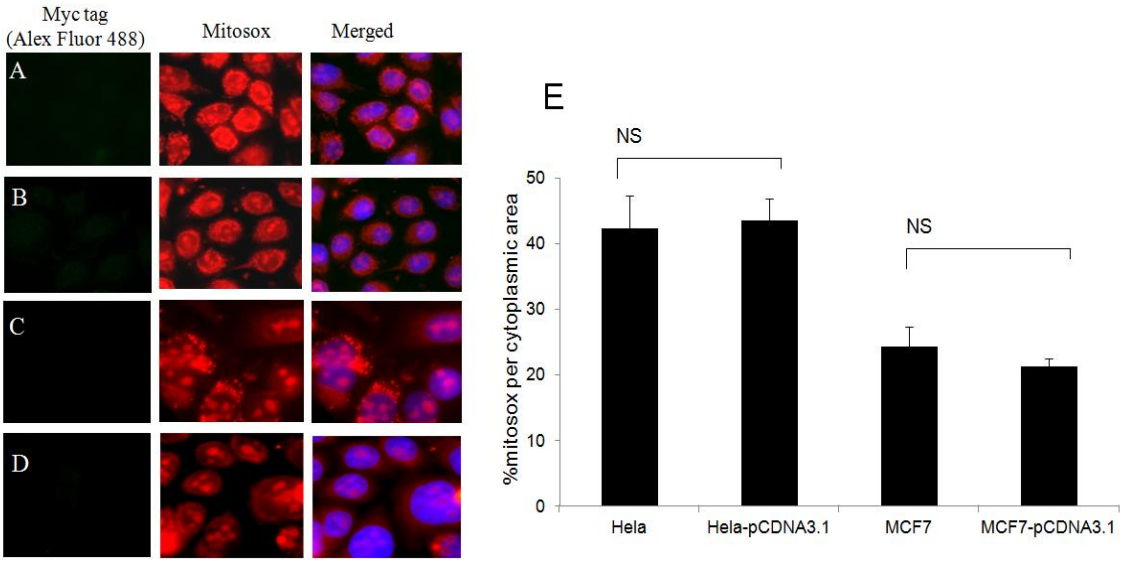

Figure 4.6 Hela and MCF7 transfected with pCDNA 3.1 (MOCK transfection) and stained with mitoSox and myc tag antibody. A-D: are respresentative images of **A:** Hela transfected with pCDNA3.1 and treated with 100 μM H_2O_2 for 1 hr. **B:** Hela non-transfected and treated with 100 μM H_2O_2 for 1 hr. **C:** MCF7 transfected with pCDNA3.1 and treated with 100 μM H_2O_2 for 1 hr. and **D:** MCF7 non transfected and treated with 100 μM H_2O_2 for 1 hr. **E:** The graph indicates the level of mitoSox measured by ImageJ. Bars indicate means and standard error from at least 50 cells for each group.

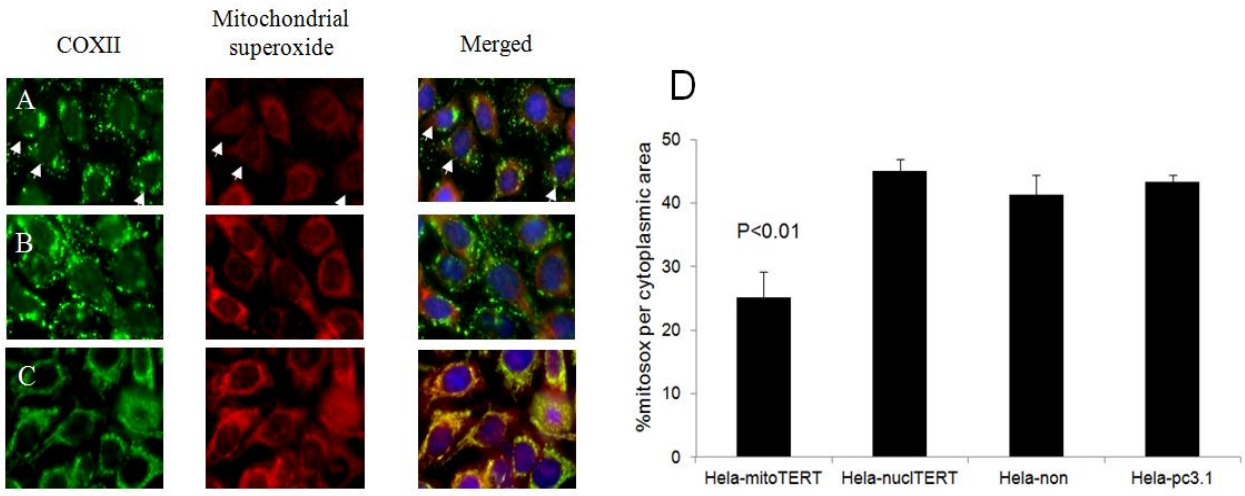

Figure 4.7 Hela transfected with mito-hTERT shooter and double staining with mitoSox and COX II. Hela was transfected with mito- and nucl-hTERT shooter plasmids, treated with 100 μM H_2O_2 for 1 hr and double stained with MitoSOX and COXII antibody. **A and B** are respresentative images of **A:** Hela transfected with mito-hTERT. Arrows indicate the speculated transfected cells which showed lower mitochondrial superoxide levels in A. **B:** Hela transfected with nucl-hTERT. **C:** is a respresentative image of Hela transfected with empty plasmid (pCDNA 3.1) used as a control. **D:** graph indicates the level of mitoSox in cells transfected with mito-hTERT and nucl-hTERT compared to non-transfected cells and cells transfected with

pCDNA3.1 vector. Bars indicate means and standard error from at least 50 cells for each group.

The second control is shown in figure 4.7. Hela and MCF7 cells were transfected with hTERT shooter (pCMV-myc-mito/nucl-hTERT) and then stained with mitoSox and COXII antibody in order to exclude that the myc antibody staining is responsible for a decrease in mitoSox. The COXII protein is a mitochondrial protein that is expressed in all mitochondria independent of a transfection event. If antibody staining would be responsible for the decrease in ROS it should be observed for all cells (transfected or not) in this experiment. Figure 4.7a shows the double staining of mitoSox and COXII which is a mitochondrial protein instead of the myc-tagged hTERT after mito-shooter transfection in Hela. We found that only 20-30% of all COXII stained cells showed low ROS level. This result indicated that the decreased of ROS level is not because of the antibody accumulated in mitochondria. We have not found a significant difference of ROS level between Hela non-transfected, Hela transfected with nucl-hTERT and Hela transfected with pCDNA3.1. This data suggests that the decreased mitochondrial superoxide levels in Hela and MCF7 transfected with mito-hTERT are not an artefact from the myc/TERT antibody staining.

In the third control, Hela and MCF7 were transfected with GFP shooter vectors (pCMV-myc-mito/nucl-GFP) in order to see whether it is the shooter transfection or an unspecific effect of the shooter expressed protein in the mitochondria that is responsible for the decrease in mito ROS. The images in figure 4.8 suggest a similar mitochondrial superoxide expression in cells with and without GFP expression. None of them showed any differences in mitoSox staining. This data suggests that the decreased mitochondrial superoxide levels in Hela and MCF7 are not an artefact from the shooter expressed protein. Thus the conclusion is that reduction of mitochondrial superoxide levels in Hela and MCF7 is a direct effect from the mitochondrial localisation of hTERT.

4.2.3 Quantitative determination of mitochondrial superoxide levels in U87 under exogenous stress (H_2O_2)

We used U87 as a third cancer cells to confirm the effect of hTERT in different subcellular locations. The results from figure 4.9 indicated lower levels of mitochondrial superoxide in cells transfected with mitochondrial hTERT after H_2O_2 treatment compared with nuclear hTERT and non-transfected cells. Under basal condition U87 showed a significantly lower

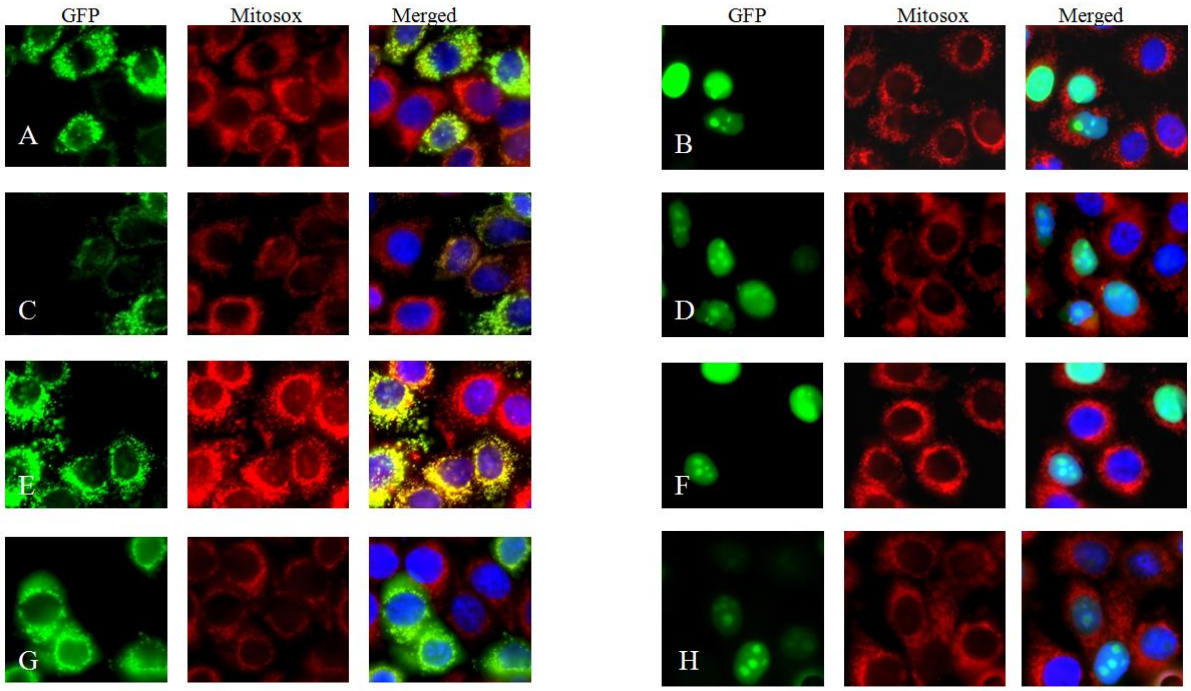

Figure 4.8 GFP control experiment, A-H are respresentative image of **A** Hela cells transfected with pCMV-myc-mito-GFP and treated with 100 μM H_2O_2, **B** Hela transfected with pCMV-myc-nucl-GFP and treated with 100 μM H_2O_2, **C** Hela transfected with pCMV-myc-mito-GFP and basal condition, **D** Hela transfected with pCMV-myc-nucl-GFP under basal condition, **E** MCF7 transfected with pCMV-myc-mito-GFP and treated with 100 μM H_2O_2, **F** MCF7 transfected with pCMV-myc-nucl-GFP and treated with 100 μM H_2O_2, **G** MCF7 transfected with pCMV-myc-mito-GFP under basal condition and **H** MCF7 transfected with pCMV-myc-nucl-GFP under basal condition.

ROS levels in mitochondrial hTERT expression compared with nuclear hTERT and non-transfected cells ($P<0.01$). Under oxidative stress, U87 was treated with 100 μM H_2O_2 as in Hela and MCF7 then left for 1 day before mitoSox and immuno-fluorescence staining. Mito-hTERT expression in U87 showed significantly lower ROS level compared to nucl-hTERT ($P<0.05$) and non-transfected cells ($P<0.01$). We found that after stress treatment, the ROS level in mito-hTERT, nucl-hTERT and non-transfected U87 were not significant increased compared with the untreated group. This low level of ROS expression under untreated and exogenous stress confirms the protective effect of hTERT to mitochondria. However, ROS measurement one day after 100 μM H_2O_2 treatment or only 100 μM H_2O_2 concentration might not suitable to showed the real increase of ROS level in U87.

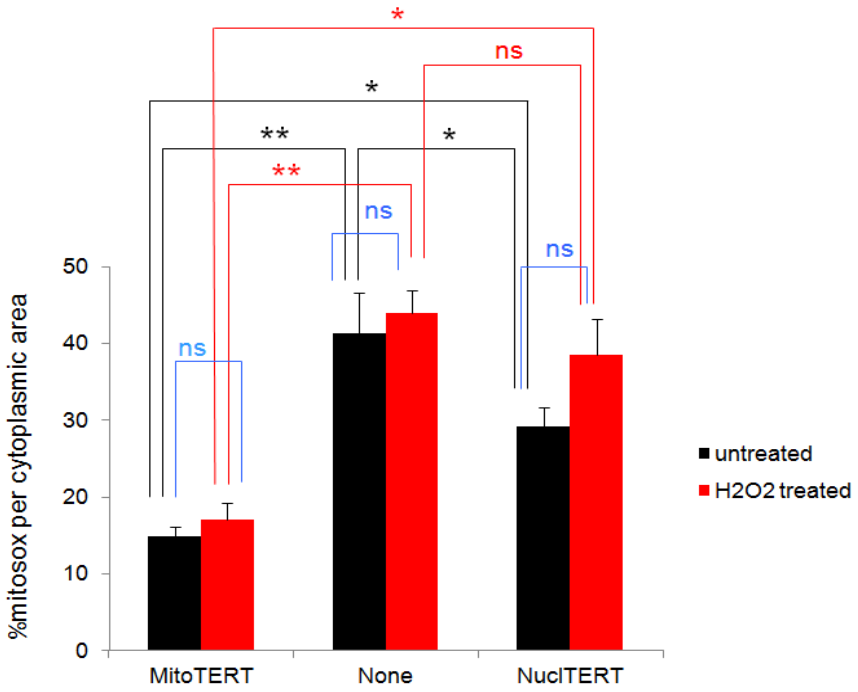

Figure 4.9 Comparison of mitochondrial superoxide levels in mito-hTERT and nucl-hTERT transfected as well as non-transfected cells in U87 under basal conditions and H_2O_2 stress treatment. Results were summarised from 3 independent experiments. Bars show mean and standard error. One way Anova was used to test for significant differences between groups.

4.2.4 Quantitative determination of mitochondrial superoxide levels in Hela and MCF7 after x-irradiation

Since the measurements of mitochondrial ROS in the H_2O_2 experiments was always done 1 day after treatment (since earlier time points showed a non-specific effect of the H_2O_2 treatment) we explored other DNA damage treatments and chose x-irradiation. Again, we tested whether there exists a direct correlation between physical location of hTERT in the mitochondria to the level of mitochondrial superoxide under a different stress condition. In addition, we performed a more kinetic approach in order to see whether there is any dynamics involved in the protection and to get an idea how long it lasts under our experimental conditions.

Mito-hTERT and nucl-hTERT were transfected into Hela and MCF7 cells which were then treated with x-rays at a dose of 20 Gy. All cells were double stained with mitoSox and myc-tag at day 0 (cells were fixed within 30 minute after irradiation), day 1 and day 2 compared with untreated cells. Results in Hela and MCF7 cells are shown in figures 4.10-4.15.

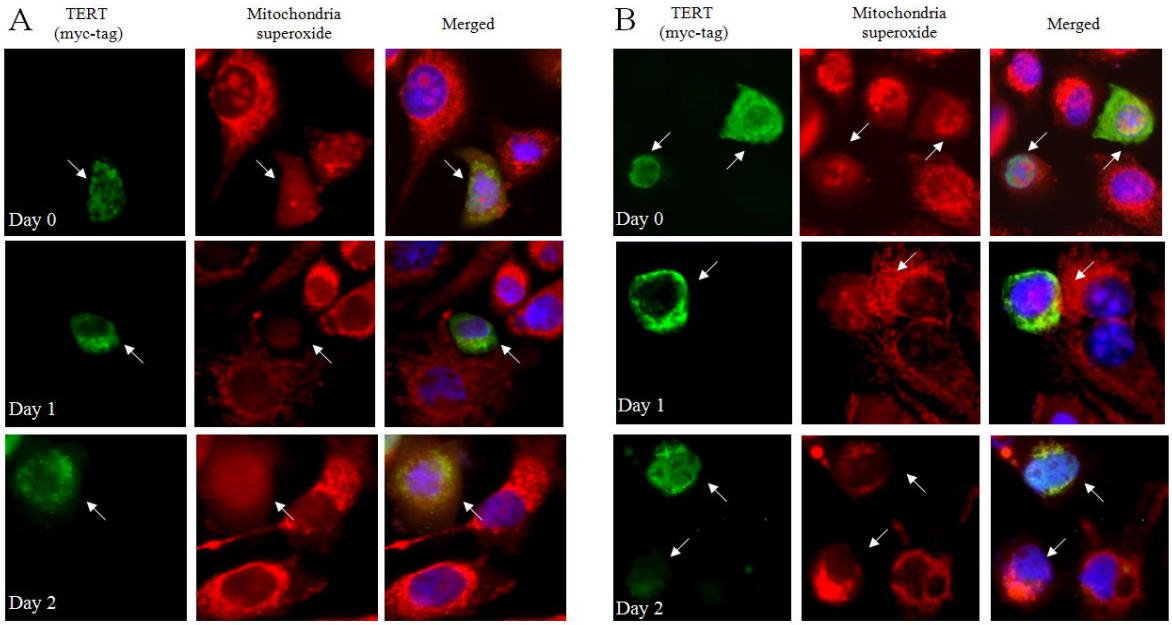

Figure 4.10 Kinetic levels of ROS after mito- and nucl-hTERT transfection in Hela (with irradiation). Cells were double stained with mitoSox (red) and myc-tag antibody (green) within 30 minute (day0), 1 day and 2 days after 20 Gy irradiation treatment. Arrows indicate transfected cells. **A** are respresentative images of Hela cells transfected with mito-hTERT shooter and **B** are respresentative images of Hela transfected with nucl-hTERT shooter.

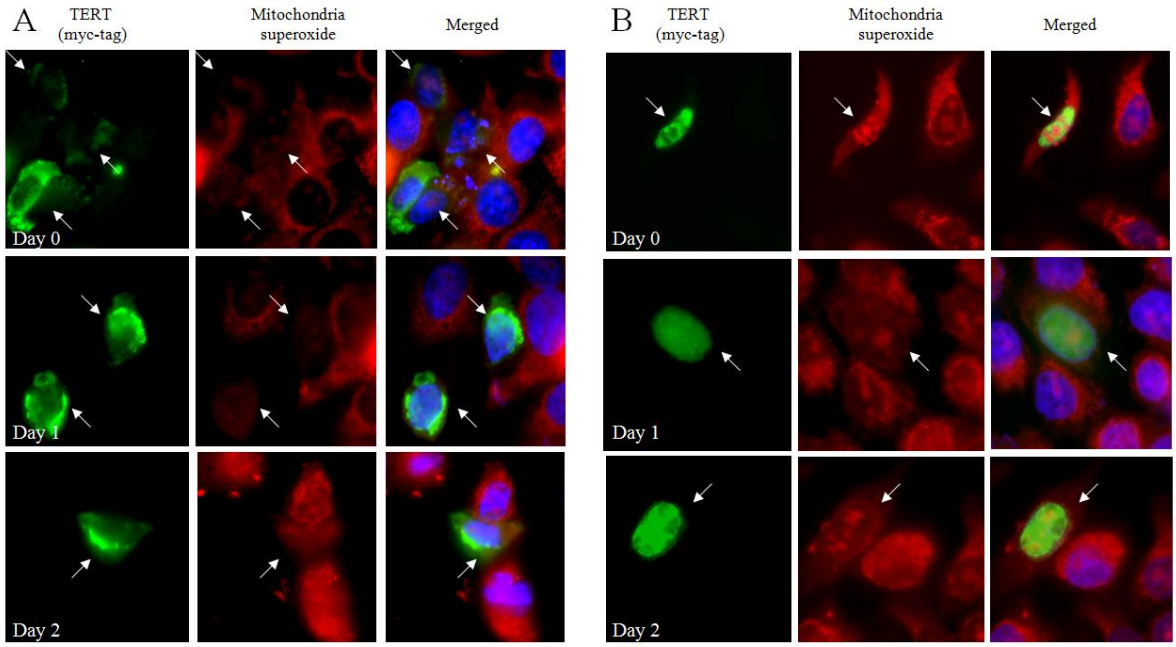

Figure 4.11 Kinetic levels of ROS after mito- and nucl-hTERT transfection in Hela (without irradiation). Cells were double stained with mitoSox (red) and myc-tag antibody (green) at day 0, 1 day and 2 days at the same time as cells after irradiation. Arrows indicate transfected cells. **A** are respresentative images of Hela cells transfected with mito-hTERT shooter and **B** are respresentative images of Hela transfected with nucl-hTERT shooter.

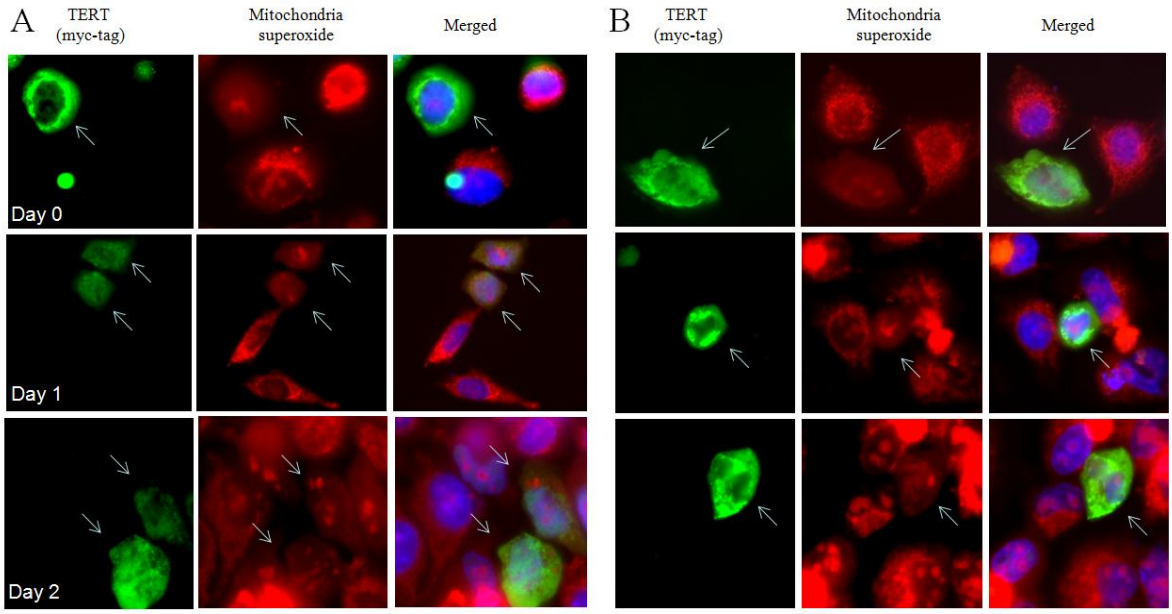

Figure 4.12 Kinetic levels of ROS after mito- and nucl-hTERT transfection in MCF7 (with irradiation). Cells were double stained with mitoSox (red) and myc-tag antibody (green) with in 30 minute (day 0), 1 day and 2 days after 20 Gy irradiation. Arrows indicate transfected cells. **A** are respresentative images of MCF7 transfected with mito-hTERT shooter and **B** are respresentative images of MCF7 transfected with nucl-hTERT shooter.

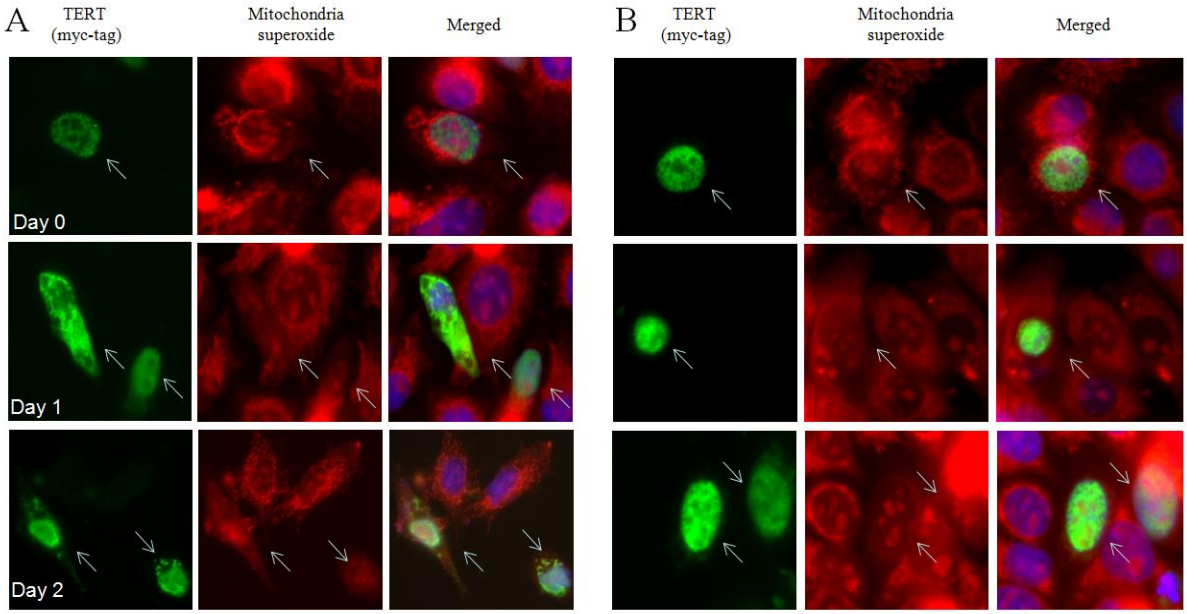

Figure 4.13 Kinetic levels of ROS after mito- and nucl-hTERT transfection in MCF7 (without irradiation). Cells were double stained with mitoSox (red) and myc-tag antibody (green) at day 0, 1 day and 2 days at the same time as cells after irradiation. Arrows indicate transfected cells. **A** are respresentative images of MCF7 cells transfected with mito-hTERT shooter and **B** are respresentive images of MCF7 transfected with nucl-hTERT shooter.

In figure 4.14 A, results indicated lower mitochondrial ROS level of Hela transfected with mito-hTERT shooter compared to the non-transfected cells before and after 20 Gy irradiation while no-significant difference between mito-hTERT Hela before and after treatment and nucl-hTERT Hela before and after treatment have been found (figure 4.14, blue line). This result indicates the protective effect of hTERT when it localised in mitochondria and nucleus in Hela before treatment. When compared untreated Hela group with Hela after 20 Gy irradiated group (figure 4.14 A), ROS level of all Hela showed no-significantly increased within 30 minute after irradiation compared with Hela before treatment. In the kinetic experiment, Hela transfected with mito-hTERT and nucl-hTERT shooter at day 0 and day 2 showed no significant differences in mitoSox levels (figure 4.15 A). Only the expression of mito-hTERT at day 1 correlated to significantly lower levels of mitoSox than nucl-hTERT ($P< 0.05$). The lack of significance at day 1 could be due to the large variation in mitoSox levels in the nuclear shooter transfected cells. Thus this result indicates a protective effect of both mito-hTERT and nucl-hTERT to ROS production in Hela after irradiation.

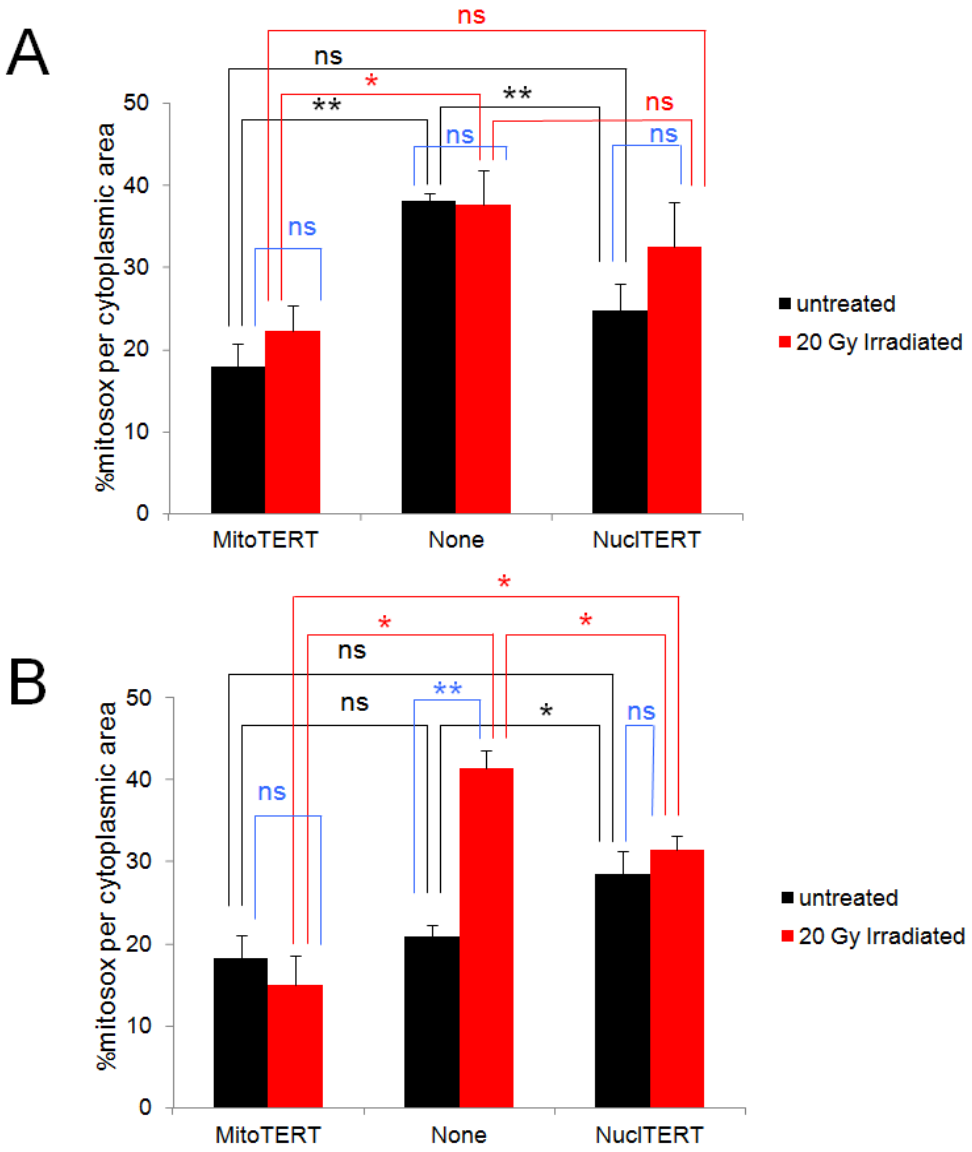

Figure 4.14 Comparison of mitochondrial superoxide levels in mito-hTERT, nucl-hTERT and non-transfected cells in Hela and MCF7 cells following X-irradiation. **A:** Hela under basal condition and treated with 20 Gy x-irradiation. **B:** MCF7 under basal condition and treated with 20 Gy x-irradiation. Both cell types were fixed within 30 minutes after irradiation. Results were summarised from 3 independent experiments for each cell line. One way Anova was used to test for significance between groups.

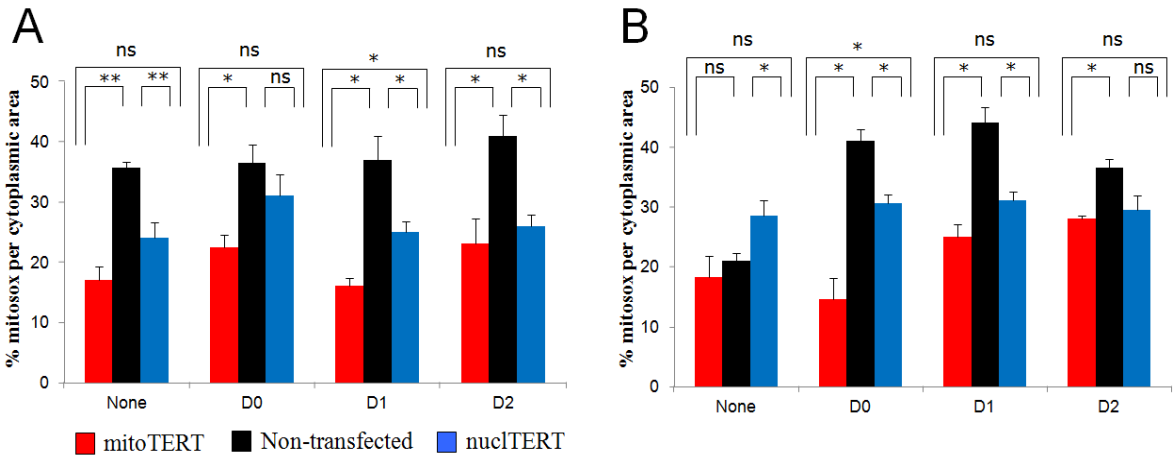

Figure 4.15 Kinetics of mitochondrial superoxide levels in mito-hTERT, nucl-hTERT and non-transfected cells in Hela and MCF7 after X-irradiation. A is ROS kinetics in Hela cells stained and measured within 30 minute after irradiation (day 0), 1 day and 2 days after 20 Gy irradiation treatment and **B** is ROS kinetics in MCF7 stained and measured within 30 minute after irradiation (day0), 1 day and 2 days after 20 Gy irradiation treatment. Results were summarised from 3 independent experiments for each cell line. Bars show mean and standard error. One way Anova was used to test for significance between groups.

The results of MCF7 under basal condition and irradiation are shown in figures 4.14 B. Within 30 minute after irradiation we saw a significant difference between the mitochondrial and the nuclear hTERT shooter transfected MCF7 ($P<0.05$) while there is no statistical difference in untreated and at day 1 and day 2 after irradiation as showed in figure 4.15 B. The comparison between MCF7 before and after 20 Gy irradiation indicates no significant difference of mito-hTERT MCF7 between before and after irradiation and nucl-hTERT MCF7 before and after irradiation while we found a significant increased of ROS level in non-transfected MCF7 after irradiation compared with non-transfected MCF7 before irradiation (figure 4.14 B). The latter results in figure 4.14 B and 4.15 B confirm the earlier results on MCF7 under untreated conditions from the H_2O_2 experiment. The kinetics of a disappearance of the difference between mito-hTERT and nucl-hTERT shooter regarding mitoSox levels at later time points is most likely the result of the nuclear TERT protein being excluded due to the applied DNA damage stress. Therefore these results might confirm our previous observations on endogenous and over-expressed general TERT that the exclusion of TERT takes time and is also dependent on the level of DNA damage inflicted by the irradiation.

4.2.5 Control experiments (x-irradiation)

Similar to those control experiments performed for H_2O_2 treatment, GFP control experiments have been done to confirm that the reduction of mitochondrial ROS was not an effect of the shooter vector transfection itself. Figures 4.16 and 4.17 show a GFP experiment performed under irradiation in order to confirm that the decrease of mitochondrial superoxide is due to the TERT protein and not the shooter transfection itself. Hela and MCF7 were transfected with GFP shooter (pCMV-myc-mito/nucl-GFP) and irradiated with 20 Gy dose. Results indicated similar mitochondrial superoxide levels in cells with or without GFP expression. All of the transfected and non-transfected cells did not show any differences in mitoSox staining. This data suggests that the decreased mitochondrial superoxide levels in Hela and MCF7 are not an artefact from the shooter vectors but indeed due to mitochondrially localised TERT protein.

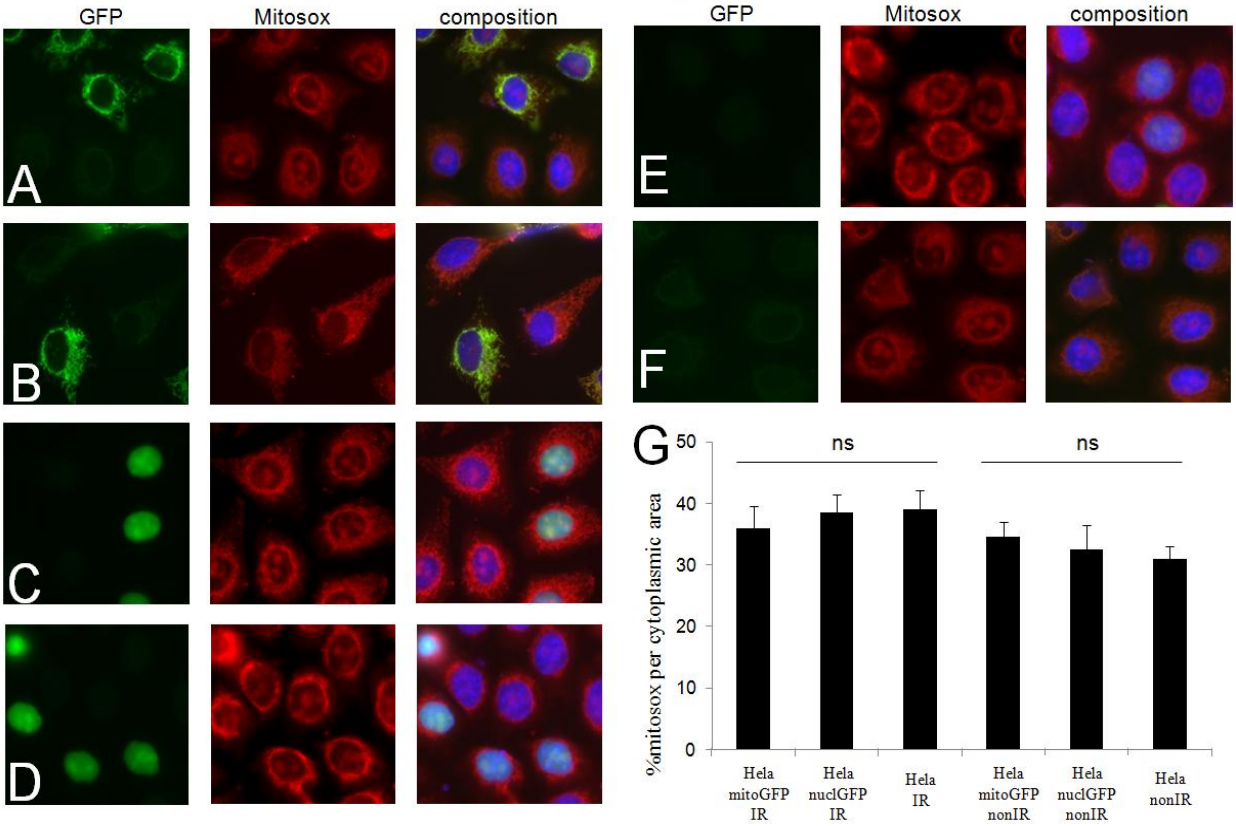

Figure 4.16 Control experiment: Hela transfected with GFP shooter.
A-D: respresentative images of Hela transfected with **A:** pCMV-myc-mito-GFP and irradiated with x-rays (20Gy), **B:** pCMV-myc-mito-GFP under normal condition, **C:** pCMV-myc-nucl-GFP and radiated with x-rays (20Gy) and **D:** pCMV-myc-nucl-GFP under normal condition. **E:** Hela non-transfected after 20 Gy irradiation. **F:** Hela non-transfected under normal condition. **G:** The graph demonstrates that the levels of mitoSox measured by ImageJ are similar for all cells transfected with either hTERT shooter vector. Bars indicate means and standard error from at least 50 cells for each group.

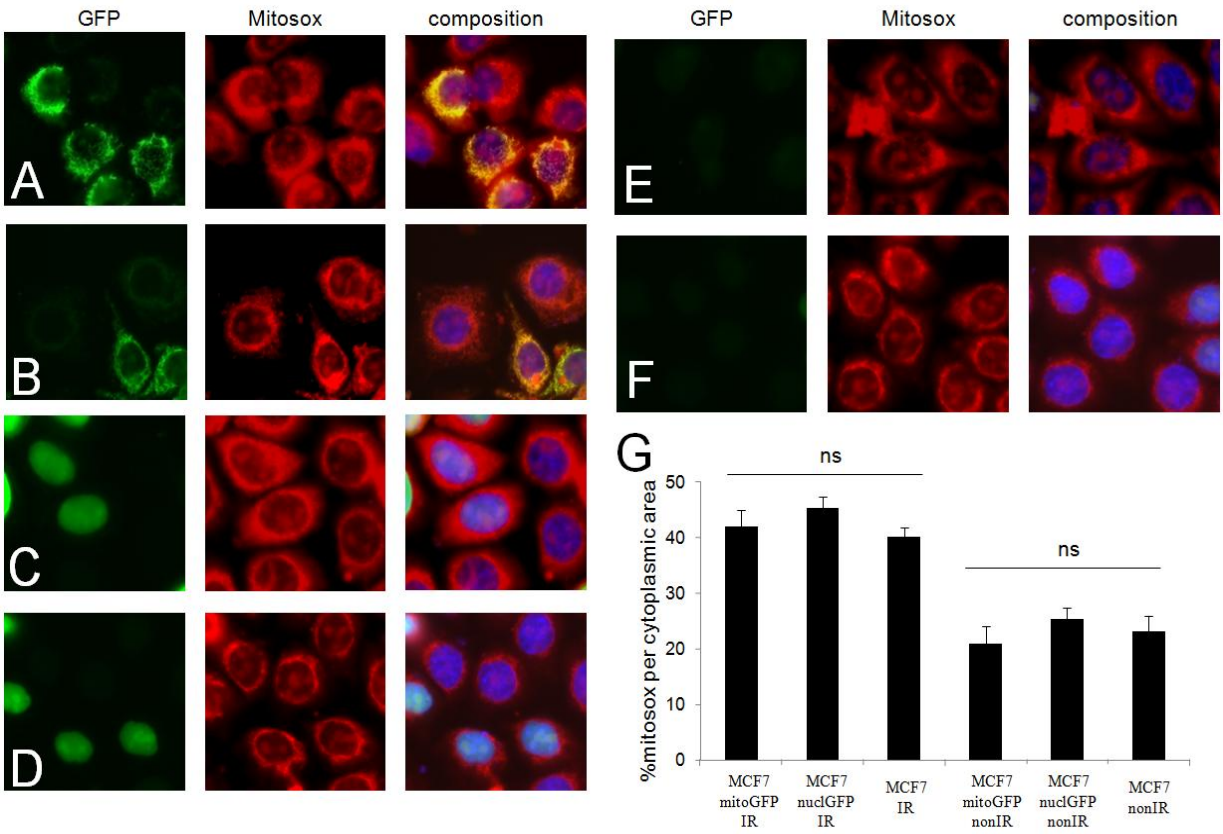

Figure 4.17 Control experiment: MCF7 transfected with GFP shooter.
A-D are respresentative images of MCF7 transfected with **A:** pCMV-myc-mito-GFP and irradiated with x-rays (20Gy), **B:** pCMV-myc-mito-GFP under normal condition, **C:**pCMV-myc-nucl-GFP and irradiated with x-rays (20Gy) and **D:** pCMV-myc-nucl-GFPunder normal condition (un-irradiated). **E:** Hela non-transfected after 20 Gy irradiation. **F:** Hela non-transfected under normal condition. **G:** the graph demonstrates that the level of mitoSox measured by ImageJ is similar for all cells transfected with either hTERT shooter vectors. Bars indicate means and standard error from at least 50 cells for each group.

4.2.6 Quantitative determination of mitochondrial superoxide levels in U87 after x-irradiation

Similar to the H_2O_2 experiment, we used U87 as a third cancer cell line to confirm the effect of hTERT in different subcellular locations after x-irradiation. Under basal condition U87 showed a significant lower of ROS levels in mitochondrial hTERT compared with nuclear hTERT and non-transfected cells ($P<0.01$ and $P<0.05$, respectively). U87 cells transfected with mito-hTERT and nucl-hTERT were treated with 20 Gy irradiation and stained for mitoSox and myc-tag antibody using immuno-fluorescence. After irradiation, mito-hTERT expression in U87 showed significantly lower ROS levels compared to nucl-hTERT and non-transfected cells ($P<0.01$ and $P<0.05$, respectively). No significant difference between nucl-hTERT U87 and non-

transfected cells has been found. When compare all U87 before and after treatment, similar results as in mito- and nucl- hTERT transfected U87 with H_2O_2 treatment have been found. No significant difference in mito-hTERT, nucl-hTERT and non-transfected U87 compare between before and after treatment has shown. It seems that mito-hTERT showed protective function even under basal condition in U87. Moreover, ROS level did not increased after irradiation. It is interesting that we haven't found a significant increase of ROS level in U87 in both after 100 μM H_2O_2 treatment (ROS measured 1 day after treatment) and 20 Gy irradiation (cells were fixed within 30 minute after irradiation) compared with the group of non-treated U87. However, the result of the lower level of ROS expression under untreated and exogenous stress still confirms the protective effect of hTERT to mitochondria as in a third independent cancer cell line.

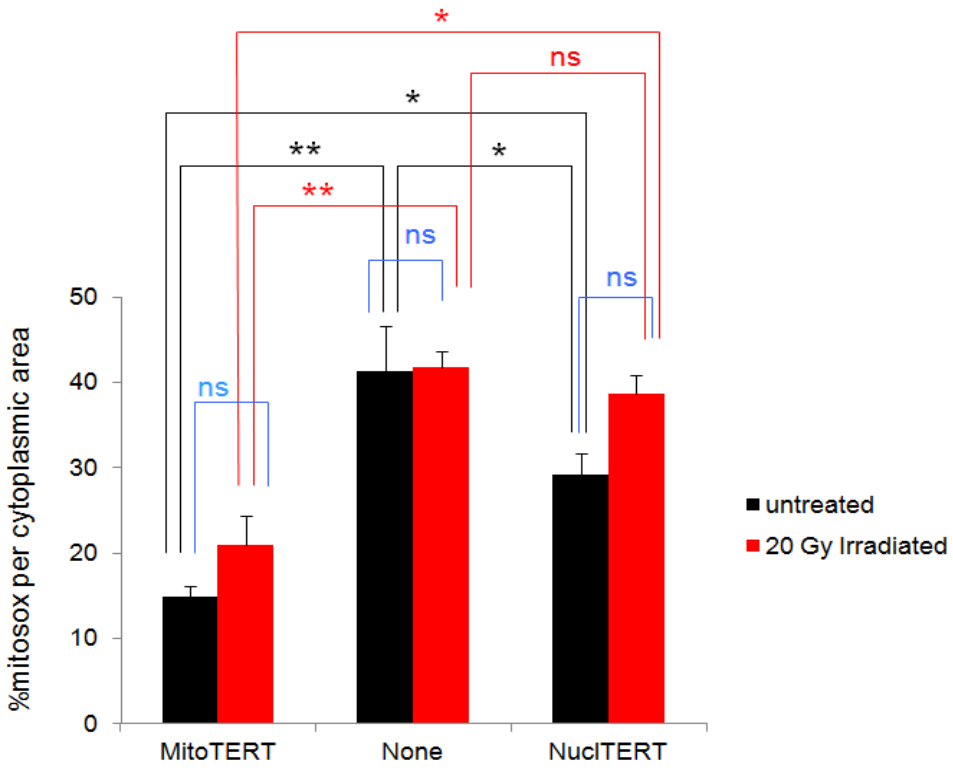

Figure 4.18 Comparison of mitochondrial superoxide levels in mito-hTERT and nucl-hTERT transfected as well as non-transfected cells in U87 under basal conditions and irradiation treatment. A: U87 under basal condition. **B:** U87 after 20 Gy irradiation. Results were summarised from 3 independent experiments. Bars show mean and standard error. One way Anova was used to test for significant differences between groups.

4.2.7 Quantitative determination of mitochondrial superoxide levels of cells without endogenous telomerase effect under basal condition (un-irradiated) and after irradiation.

As described in chapter 3 MRC5/SV40 is a cell line which contains an inactivated p53 due to expression of the T-antigen of the SV40 virus and does not express endogenous hTERT which potentially could interfere with the exogenous shooter. MRC5/SV40 cells were transfected with mito-hTERT or nucl-hTERT shooter vectors as described before and treated with different oxidative stress treatments.

And as mentioned in Chapter 3, we have not found a different effect between 5 Gy and 10 Gy irradiation. Thus in this experiment we have treated cells only with 10 Gy.

Mito-hTERT or nucl-hTERT were transfected into MRC5/SV40 and then treated with X-irradiation as described previously in chapter 3. All cells were fixed within 30 minutes after irradiation and double stained with mitoSox (live cell staining) and myc-tag (immunofluorescent). Representative images are shown in fig. 4.19 and quantification of the results is shown in figure 4.20.

Under basal conditions, there is no significant difference between mito-hTERT or nucl-hTERT transfected cells and the non-transfected group. In the comparison between untreated and after 10 Gy irradiation, ROS level of mito-hTERT, nucl-hTERT and non-transfected MRC5/SV40 did not showed any significant increase after irradiation compared with the untreated group. However, after irradiation, ROS in mito-hTERT transfected cells showed significant lower ROS level compared with nucl-hTERT and non-transfected MRC5/SV ($P<0.01$). Moreover, ROS in nucl-hTERT transfected cells after irradiation also showed significant lower level ($P<0.01$) than non-transfected cells after irradiation which might indicate a protection of nucl-hTERT to the ROS production.

This result after irradiation suggests the effect of exogenous hTERT onto the decrease of ROS production. Interestingly, variations between the 3 different experiments were much larger in untreated cells than after irradiation.

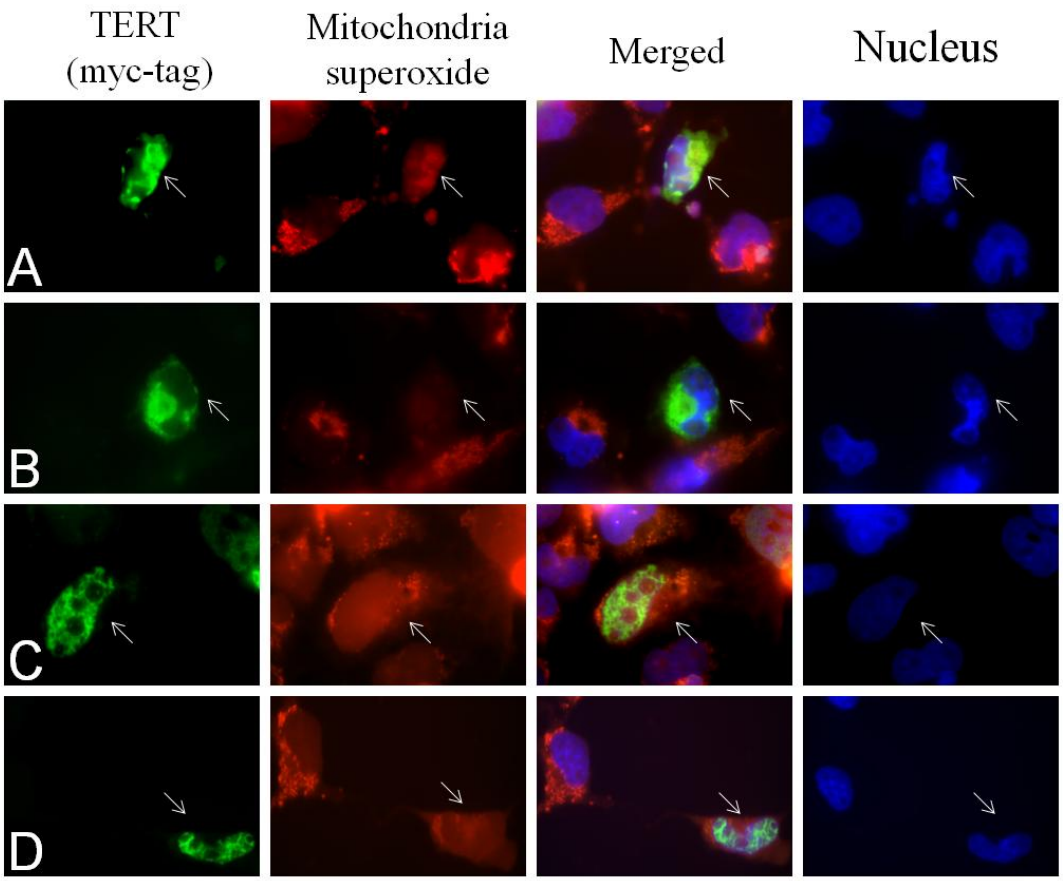

Figure 4.19 Double staining of ROS and TERT in MRC5/ SV40 cells transfected with mito-hTERT and nucl-hTERT shooter under basal (un-irradiated) condition and after 10 Gy irradiation. Cells were double stained with mitoSox and myc-tag. Red colour represents mitochondrial superoxide and green colour represents hTERT localisation. Arrows indicate transfected cells. **A** shows MRC5/ SV40 cells with mito-hTERT under basal condition. **B** shows MRC5/SV40 with mito-hTERT after 10 Gy irradiation. **C** shows MRC5/ SV40 with nucl-hTERT under basal condition **D** shows MRC5/ SV40 cells with nucl-hTERT after 10 Gy irradiation.

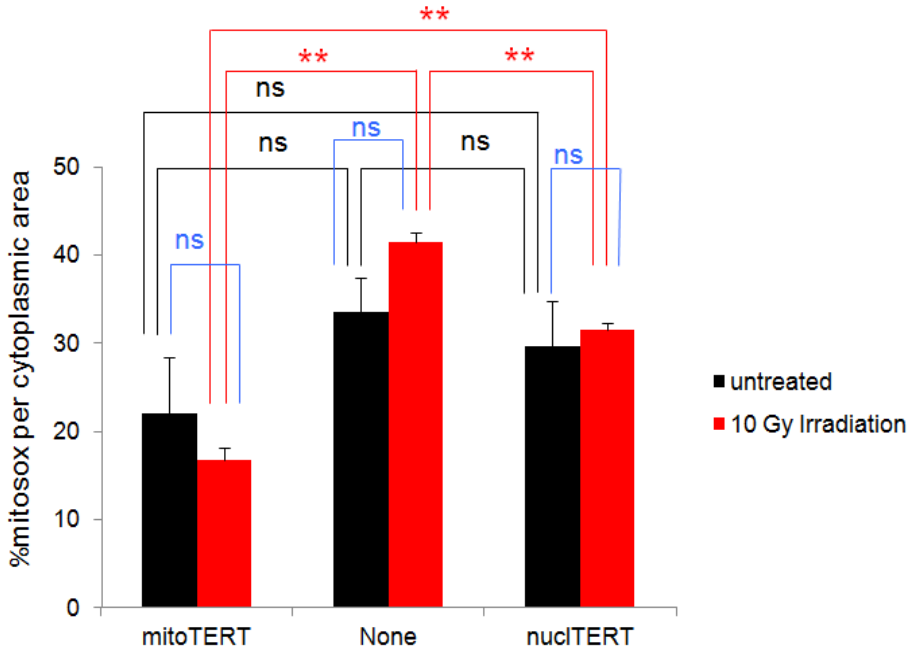

Figure 4.20 Comparison of mitochondrial superoxide levels in mito-hTERT, nucl-hTERT and non-transfected cells in MRC5/SV40 after X-irradiation. Cells were treated with 10 Gy doses and fixed immediately after irradiation. Bars show mean and standard error from 3 independent experiments. One way Anova was used to test for significance between groups.

4.2.8 Control experiment (MRC5/SV40 after x-irradiation)

To confirm that the reduction of ROS in MRC5/ SV40 is because of the localisation of the exogenous hTERT protein and not the shooter transfection itself MRC5/ SV40 had also been transfected with GFP shooter (pCMV-myc-mito/nucl-GFP) and irradiated with the same 10 Gy doses. Results from figure 4.21 indicate a similar mitochondrial superoxide expression in cells with or without GFP expression. None of the transfected cells under any condition showed any significant differences in mitoSox staining. Thus this data confirms that the decrease of mitochondrial superoxide levels in MRC5/ SV40 is not an artefact from the shooter vectors but indeed due to mitochondrially localised TERT protein.

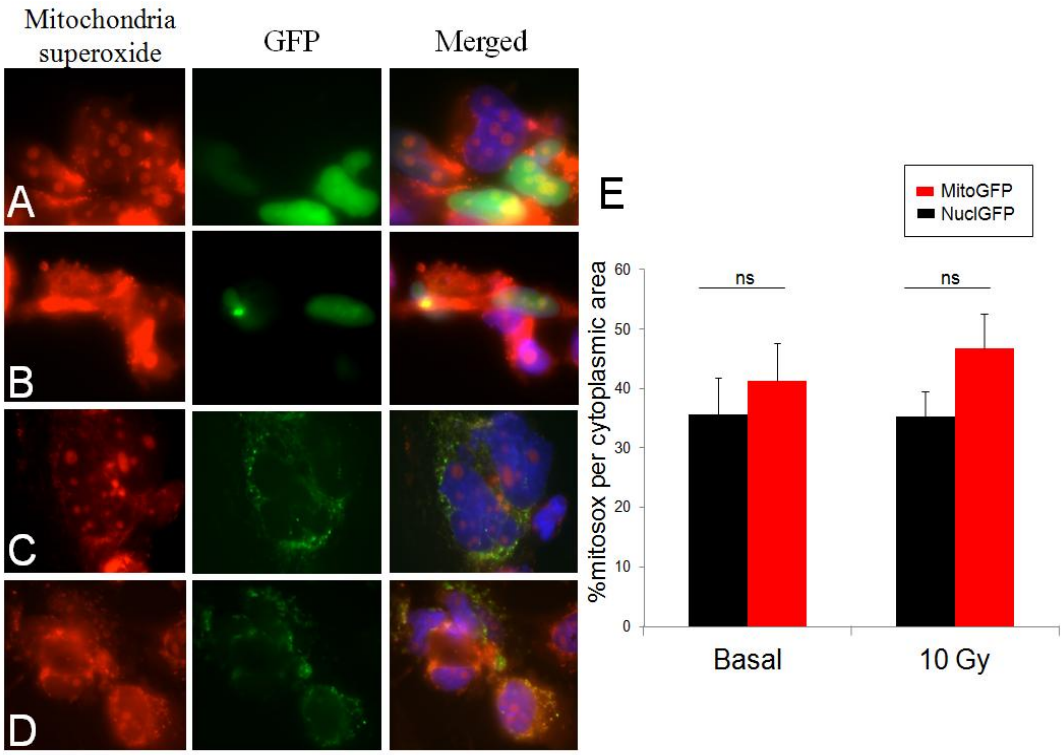

Figure 4.21 Control experiment: MRC5/SV40 transfected with GFP shooter. A-D are representative images of MRC5/SV40 cells transfected with **A:** pCMV-myc-mito-GFP under basal condition. **B:** pCMV-myc-mito-GFP and irradiated with X-rays (10Gy). **C:** pCMV-myc-nucl-GFP under basal condition. **D:** pCMV-myc-nucl-GFP and irradiated with X-rays (10Gy). **E:** The graph shows levels of mitoSox measured by ImageJ. Bars indicate means and standard error from at least 50 cells for each group.

4.3 Discussion

Previously published results of our group have shown that under oxidative stress hTERT is excluded from the nucleus and protects mitochondria in hTERT over-expressing fibroblasts (Ahmed et al., 2008). These cells show a lower production of oxidative stress, less mitochondrial DNA damage, lower mitochondrial mass and mtDNA copy number as well as higher mitochondrial membrane potential compared to telomerase negative parental fibroblasts. However, in the generally over-expressed system, it was hard to say whether it was rather the nuclear TERT which protected telomeres or the fraction of mitochondrial TERT that was responsible for the decrease in ROS. In order to separate both localisations properly we used organelle-specific TERT shooter vectors. Here we show that the specific location of hTERT in mitochondria protects cells against oxidative stress. Hela, MCF7, U87 and MRC5/SV40 were transfected using mitochondrial (mito-hTERT) and nuclear (nucl-hTERT) specific hTERT shooter vectors. In hydrogen peroxide treatment experiment, Hela, MCF7 and

U87 cells were transfected using mito-hTERT or nucl-hTERT shooter vectors and the mitochondrial ROS level measured one day after the treatment. The reason for this delay was to avoid the direct interference of the exogenous H_2O_2 which we used to treat cells onto the ROS measurement. One day delay after treatment was determined as the optimal time point for ROS measurement after H_2O_2 stress treatment.

Under basal condition, both Hela and MCF7 did not show a significant difference of ROS levels in mito-hTERT expression and nucl-hTERT (figure 4.5). However, the level of ROS in nucl-hTERT transfected MCF7 under basal condition was higher than in non-transfected cells ($P<0.05$). Both mito-hTERT and nucl-hTERT transfected Hela cells under basal condition showed statistically lower ROS levels compared to non-transfected cells ($P<0.01$). However, mito-hTERT and nucl-hTERT transfected Hela did not show a statistical difference between mitochondrial hTERT expression and nuclear hTERT. This result suggests a difference between the Hela and MCF7 cellular models and might indicate a protective effect of nucl-hTERT to ROS production. After H_2O_2 stress treatment, mito-hTERT expression in both Hela and MCF7 showed significantly lower ROS levels compared to nucl-hTERT ($P<0.01$) (figure 4.5). The control experiment also suggests that this reduction of mitochondrial superoxide levels was a direct effect from the mitochondrial localisation of hTERT. However, when both mito-hTERT and nucl-hTERT transfected cells were compared with the non-transfected groups, a slight difference in mitochondrial superoxide expression between Hela and MCF7 were detected. Nucl-hTERT Hela showed significant lower ROS level than non-transfected cells while nucl-hTERT MCF7 showed significant higher ROS level than non-transfected cells.

We used U87 as a third cancer cell line to investigate the effect hTERT in different sub-cellular location. U87 showed significant lower ROS level when transfected with mito-hTERT compared with nucl-hTERT and un-transfected cells in both before and after H_2O_2 stress treatment. The significant lower ROS production in U87 cells transfected with mito-hTERT compared with nucl-hTERT and non-transfected cells after H_2O_2 stress treatment confirms the results in Hela and MCF7 after stress treatment. However, the ROS level in nucl-hTERT U87 before treatment is similar with nucl-hTERT Hela before treatment which showed a significant lower ROS level than non-transfected cells. Both results might indicate a protective effect of nucl-hTERT in U87 before treatment. The reason for this protection is still unclear.

Since the measurement of mitochondrial ROS in the H_2O_2 experiments was done 1 day after treatment we explored other treatments and chose x-irradiation. This experiment

should confirm whether there exists a direct correlation between physical location of hTERT in the mitochondria and the level of mitochondrial superoxide under a different stress condition. Hela and MCF7 were transfected with mito-hTERT or nucl-hTERT and underwent irradiation (X-Rays at a dose of 20 Gy). In addition, we performed a kinetic approach at day 0 (cells were fixed within 30 minutes after irradiation) compared to non-irradiated and one day and two day post irradiation in order to see whether there is any dynamics involved in the protection.

Hela cells transfected with mito-hTERT and nucl-hTERT after 20 Gy irradiation showed slightly different results in ROS levels compared to Hela transfected with mito-hTERT and nucl-hTERT after H_2O_2 treatment (figure 4.5 to figure 4.14). After 20Gy radiation Hela transfected with mito-hTERT and nucl-hTERT showed no significant differences in mitoSox levels immediately after irradiation. For the kinetic approach (figure 4.15), Hela transfected with mito-hTERT and nucl-hTERT showed no significant differences at day 2 post treatment. However, only a slightly significant difference between mito-hTERT and nucl-hTERT has been found at day 1 ($P< 0.05$). The reason for this result could be due to the large variation in mitoSox levels in the nuclear shooter transfected cells or the protective effect of nucl-hTERT to mitochondrial ROS production. In irradiated MCF7, ROS levels of mito-hTERT and nucl-hTERT transfected cells has shown a slightly significant difference only immediately after irradiation ($P<0.05$). No statistical difference was detected at day1 and day 2 post irradiation. This low level of ROS in nucl-hTERT transfected in both Hela and MCF7 might be due to the nuclear shooter being excluded over time due to the applied stress (irradiation) and acts as a mito-hTERT.

Again, we used U87 as a third cancer cell line after x-irradiation. Under basal condition, U87 showed a significant lower ROS level in the mito-hTERT group compared with nucl-hTERT and un-transfected cells while no significant difference was found between nucl-hTERT U87 and non-transfected cells. After irradiation, mito-hTERT U87 showed significant lower ROS production compared with nucl-hTERT and non-transfected cells. In general, these results with irradiation confirm our previous observations on endogenous and over-expressed general TERT that the exclusion of TERT takes time and is also dependent on the level of DNA damage inflicted by the irradiation as shown in Chapter 3.

To confirm that the mitochondrial protection was due to the mitochondrial shooter vector and not because of endogenous telomerase, we tested the correlation between physical localisation of hTERT in the mitochondria or nucleus to the expression of ROS

in MRC5/SV40. This cell line does not express endogenous hTERT which might influence the effect of the transfected exogenous mito-hTERT shooter. Thus the protective function in this cell type could be atributed exclusively to the transfected hTERT. Under basal conditions, there was no significant difference between mito-hTERT, nucl-hTERT and the non-transfected group. However, after irradiation, ROS in the mito-hTERT transfected group was significantly lower than both nucl-hTERT and non transfected cells (figure 4.19). This result confirms the effect of exogenous hTERT to the lower ROS production when it was localised in mitochondria. However, ROS levels of nucl-hTERT in MRC5/SV40 after irradiation were also significantly lower than the non-transfected group which confirm the previous result of the protective capacity of nucl-hTERT to mitochondrial ROS production. Although MRC5/SV40 also contains an inactive p53 similar to Hela cells they did not show a similar result after irradiation. Thus the influence of p53 on the protective capacity of hTERT and the protective effect of nucl-hTERT to mitochondrial ROS production is unclear. Further experiments to investigate whether p53 status affects the protective function of telomerase will be described in chapter 5. To exclude the possibility that the reduction of ROS due to hTERT localised in mitochondria was the result of the shooter vector transfection itself, experiments using GFP containing shooter vectors were performed in all cell lines: Hela, MCF7 and MRC5/SV40 (figure 4.9, 4.16-17 and 4.20). The experiments using mito/nucl-GFP shooter vectors did not show any difference among GFP transfected and non-transfected cells. Thus this reduction of ROS expression was not a direct result from the shooter transfection or general ectopic protein expression. Taken together, all results confirm that mitochondrial localisation of telomerase protects against mitochondrial ROS generation after exogenous stress treatment.

It has to be concern that in some cells such as U87 and MRC5/SV40 and some condition such as Hela after 20 Gy irradiation, ROS level did not increased after stress treatment compared with the same cell types under basal condition. The reason for this probably be that the stress treatment condition might not high or suitable enough to show a real H_2O_2 effect. Thus the treatment condition should vary depend on cell type.

ROS is known to be responsible for nuclear DNA damage (Passos et al., 2010) the reduction of ROS when hTERT is localised in mitochondria cause the protection of DNA which we have found in Chapter 3. Passos and colleagues reported a feedback loop of ROS production through CDKN1A (p21), MAPK14 (p38MAPK) and TGFβ linked to DNA damage response in senescent fibroblasts (Passos et al., 2010). Nitta and colleagues reported that although p21 does not influence the protection of TERT in

ATM-deficient hematopoietic stem cells in aged mice (37 weeks old) however, TERT can partially protect the hematopoietic stem cells from ROS-induced apoptosis via inactivation of p38MAPK in mice (Nitta et al., 2011). Therefore this mechanism might be partially involved in the protective mechanism of mitochondrial localised telomerase. Further experiments correlating apoptosis induction and mitochondrial localisation of hTERT could explain the influence of mitochondrial telomerase to the cellular ageing process in telomerase positive cells.

Chapter 5

The influence of p53 status on the protective function of telomerase

5.1 Introduction

We have found some differences in mitochondrial superoxide expression and nuclear DNA damage between Hela and MCF7 as described in Chapters 3 and 4. One possible explanation for this difference could be that Hela and MCF7 display a different p53 status . Hela harbours an inactivation of p53 because of the HPV (Human papillomaviruses) subtype 18 viral proteins E6 and E7 that functionally inactivate the check point of p53 and p16 protein, respectively. Therefore p53 is compromised and non-functional in these cells (Hopper-Seyler and Butz, 1993). This is different from MCF7 which expresses a strange cytoplasmic localization of p53 and is also p16 negative (Valenzuela et a., 1997). Thus, we hypothesised that this different p53 status could play a role for the differences in mitochondrial superoxide and DNA damage between Hela and MCF7.

The tumour suppressor gene known as p53 is a DNA-binding protein which acts as a transcription factor to control the expression of proteins involved in the cell cycle. In response to DNA damage, p53 accumulates in the cell nucleus, which causes cells to undergo cell cycle arrest and DNA repair or apoptosis. It is believed that cancer cells defective in p53 have lost the ability to undergo cell cycle arrest. P53 is mutated in around 60% of all tumours and might contribute to better cancer cell survival because the cells don‘t arrest even with a high load of DNA damage.

The p53 gene is located on human chromosome 17p13.1. This gene is 20 kb long (Pei et al., 2012). Transcription of this gene produces a pre mRNA with eleven exons, which can then be spliced to an mRNA between 2 and 2.5 kb in length and containing two promoters (Roemer and Friedmann, 1994). Subsequent to translation and tetramerization, the p53 tumour suppressor goes on to regulate cell growth by controlling cell cycle progression at the G1/S and G2/M transitions, or by inducing apoptosis.

The p53 protein is activated upon DNA damage in the cell, which can be caused by ionising radiation, UV radiation, genotoxic stress, or extreme hypoxia (<1%). The up regulation of p53 occurs at the post-translational level (phosphorylation, tetramerisation), and is achieved through stabilisation of the protein (Choisy-Rossi et al., 1999). Upon induction, the main outcome of p53 activation is growth suppression, growth arrest at the G1, G2, and M checkpoints. The p53 protein also plays an

important role in cell death through the apoptotic pathway. Bax, a pro-apoptotic protein, is up-regulated by p53, while Bcl-2, an antiapoptotic protein, is down regulated by p53 (Zeimet et al., 2000). In addition to these transactivation pathways toward apoptosis, it has also been suggested that p53 may regulate apoptosis through a transcription-independent pathway p53 that can be induced by ROS. The cellular response to oxidative stress can embrace changes in nucleus, mitochondria and other cellular organelles.

Many groups have implicated ROS generation in the post translational modifications of p53. During cisplatin-induced apoptosis, ROS are involved in phosphorylation of p53 that leads to p53-mediated MAPK activation (Bragado et al. 2007). ROS are also implicated in the phosphorylation and activation of p53 via oxidative-stress-induced activity of platelet-derived growth-factor-β and ATM kinase which phosphorylates p53 in response to DNA damage under H_2O_2 stress condition in Human umbilical vein endothelial cells (Chen et al. 2003(b)).

P53 is a key effector in response to oxidative injury and DNA damage to a cell fate decisions. P53 has also been reported to translocate to the outer mitochondrial membrane to interact with both pro- and anti-apoptotic proteins and influence the induction of both apoptosis and autophagy. However, the physiological relevance of these non-transcriptional mechanisms are not clear (Chipuk & Green 2003).

Various mutations at hot spots have been described to inactivate it in many cancer types (Liu et al., 2009; Ye et al., 2009; Campitelli et al., 2012). The physiological expression of point-mutated p53 can strongly limit overall cellular p53 function (de Vries et al., 2002). The presence of a heterozygous point-mutated p53 allele resulted in delayed transcriptional activation of several p53 downstream target genes after irradiation in mouse embryonic stem cells (de Vries et al., 2002). Presence of mutated p53 reduced the ability of wild-type p53 in inducing p21, MDM2 and PIG3 (Willis et al., 2004). Thus mutant p53 exerts its dominant negative activity by abrogating functional wile-type p53.

In order to address our research question about the influence of p53 status on the protective function of telomerase we used an isogenic cell pair of the glioblastoma cell line U87 to analyse whether the p53 status might play any role for the correlation between mitochondrial protection of hTERT and nuclear DNA damage.

5.2 Experimental procedure

5.2.1 Cell lines and transfection efficiency

An isogenic pair of glioblastoma cells was used in this experiment. U87 and its isogenic clone which will be described as UP96 (U87 transfected with a mutant p53 vector that contained point mutation p53 at codon 143 were generated previously in our group, Saretzki et al., 1999). UP96 cells were maintained in the p53 mutated status by selection with G-418 sulfate. This method ensured that only cells which contained the vector pC53-SCX3 which expresses a p53 cDNA point-mutated at codon 143 were maintained. The phosphorylation of p53 in U87 and UP96 were analysed before and after 400 μM H_2O_2 treatment for 3 hours. For that a phospho-specific antibody, Phospho- p53 against Ser 15 (Cell Signalling) was used. The westernblot of U87 and UP96 after 400 μM H_2O_2 treatment were stripped with Western blot stripping buffer and then re-blotted with total p53 antibody and tubulin. Western blot analysis of U87 and UP96 is shown in figure 5.1. We found a positive band of phosphorylated p53 in U87, U87 mito-hTERT and U87 nucl-hTERT after H_2O_2 treatment while no phosphorylated p53 in UP96, UP96-mito-hTERT and UP96 nucl-hTERT have been found after H_2O_2 treatment. This result indicated an active p53 in U87 while no p53 activated in UP96.

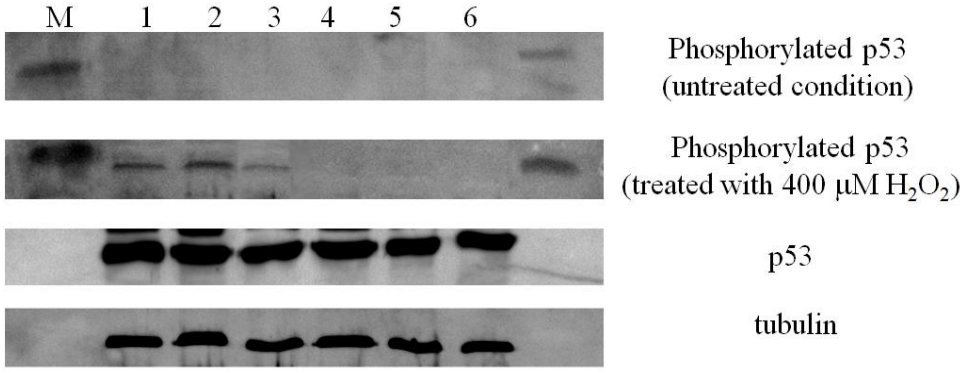

Figure 5.1 Westernblot of p53 and phosphorylated p53 in U87 and its isogenic form. Lane M is a western blot marker lane 1: U87, lane 2: U87 transfected with mito-hTERT shooter, lane 3: U87 transfected with nucl-hTERT, lane 4: UP96, lane 5: UP96 transfected with mito-hTERT shooter, lane 3: UP96 transfected with nucl-hTERT shooter

U87 and UP96 cells were transfected with hTERT shooter vector as described in Chapter 2. Figure 5.2 represents the transfection efficiencies for U87 and UP96 with lipofectamine 2000.

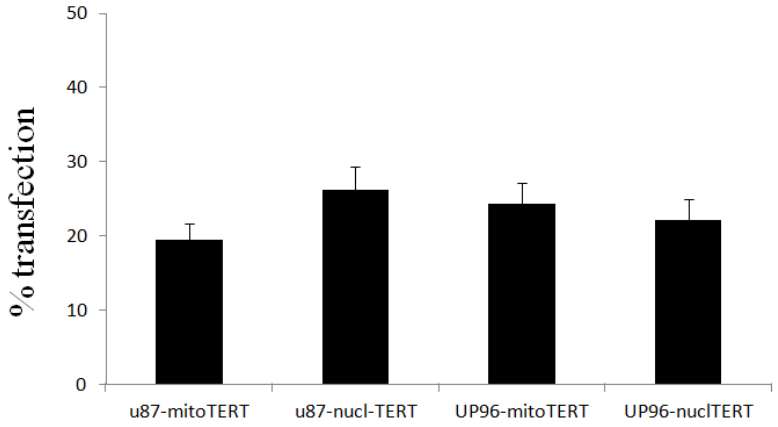

Figure 5.2 Transfection efficiencies of mito-hTERT and nucl-hTERT into U87 and UP96 cells. pShooter vectors were transfected to U87 and UP96 by lipofectamine™ 2000. 2 days after transfection, cells were fixed and the transfection efficiency was determined using immuno-fluorescence against the myc-tag.

5.3 Results

5.3.1 The effect of p53 expression onto the kinetic exclusion of TERT

We started this experiment with the comparison of the kinetic exclusion of endogenous hTERT after oxidative stress. U87 and UP96 were treated with 400μM H_2O_2 for 3 hours. Cells were fixed every 15 minutes until 1 hour and then at 2 and 3 hours. Representative images and results are shown in figures 5.3-5.5.

As shown in figure 5.5, there was no major difference found between U87 and UP96 cells in the short-term kinetic exclusion of endogenous hTERT after 400μM H_2O_2 treatment. The only difference was a slightly faster exclusion in U87 at 45 min compared to UP96 cells where the exclusion started only at 1 hour. However, there were some differences when compared to the previously analysed exclusion kinetics in other cancer cell lines. Firstly, before treatment (under basal condition) both U87 and UP96 already showed about 30% of hTERT localised in the cytoplasm. This is higher than Hela and MCF7 where we had found only 20% of hTERT already localised in the cytoplasm under untreated condition. Secondly, the maximum exclusion was reached after 2 hours with around 60% hTERT in the cytoplasm in both U87 and UP96. Thirdly, the nuclear hTERT exclusion reverted already back after 2 hours and was reduced to 40% while both Hela and MCF7 maintained a stable exclusion for several days (figure 3.6 in chapter 3). Therefore, considering the already high initial exclusion rate of 30% in U87 and its derivative the general exclusion levels seems small (not more that 20% (30-50%) additional) and it did not last for much longer than an hour. In general, except

a slight delay in the start of hTERT exclusion from the nucleus, p53 activity does not seem to play any major role in telomerase exclusion from nucleus to cytoplasm in this experimental system.

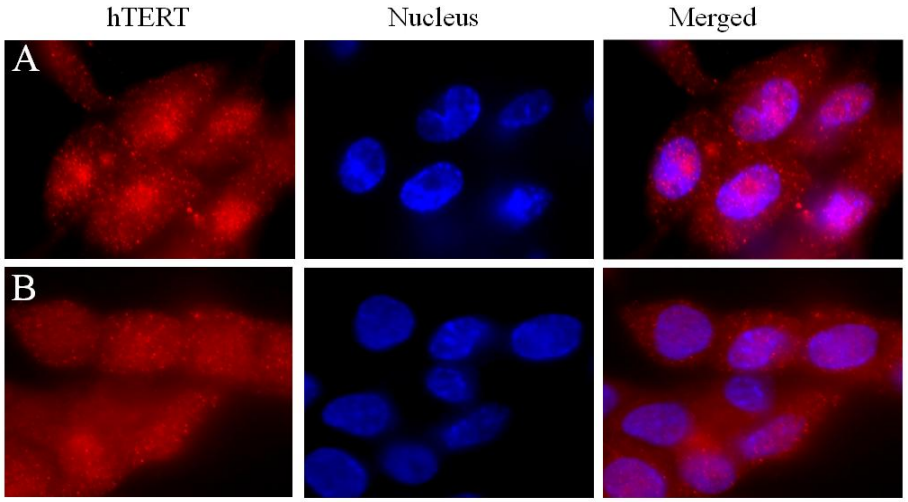

Figure 5.3 Endogenous hTERT localisation before and after H_2O_2 treatment in U87 cells. U87 cells were treated with 400 μM H_2O_2 for 3 hours and hTERT localisation within or outside the nucleus evaluated as described under 2.2.11 in Chapter 2. **A** is a representative image of U87 under basal condition. **B** is a representative image of U87 after 3 hours of 400 μM H_2O_2 treatment.

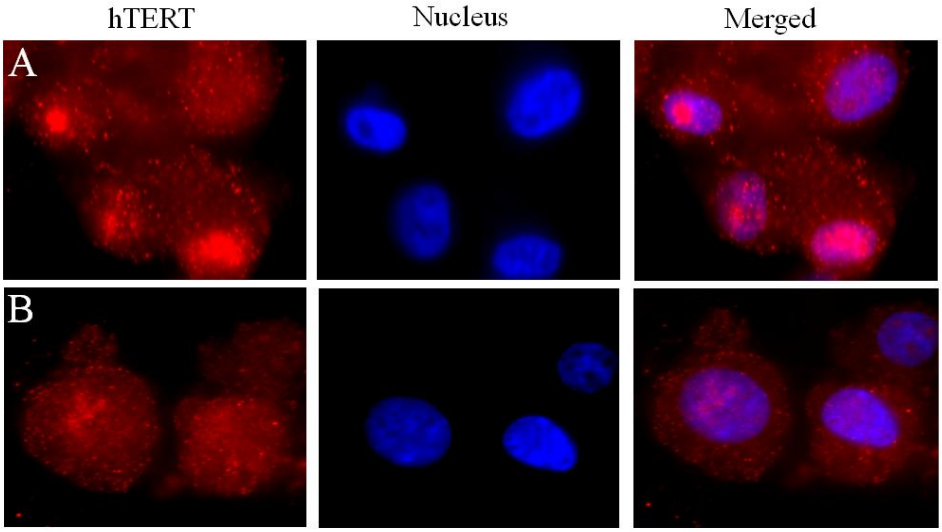

Figure 5.4 Endogenous hTERT localisation before and after H_2O_2 treatment in UP96 cells. UP96 cells were treated with 400 μM H_2O_2 for 3 hours and hTERT localisation evaluated within or outside the nucleus as described under 2.2.11in Chapter 2 . **A** is a representative image of UP96 under basal condition. **B** is a representative image of UP96 after 3 hours of 400 μM H_2O_2 treatment.

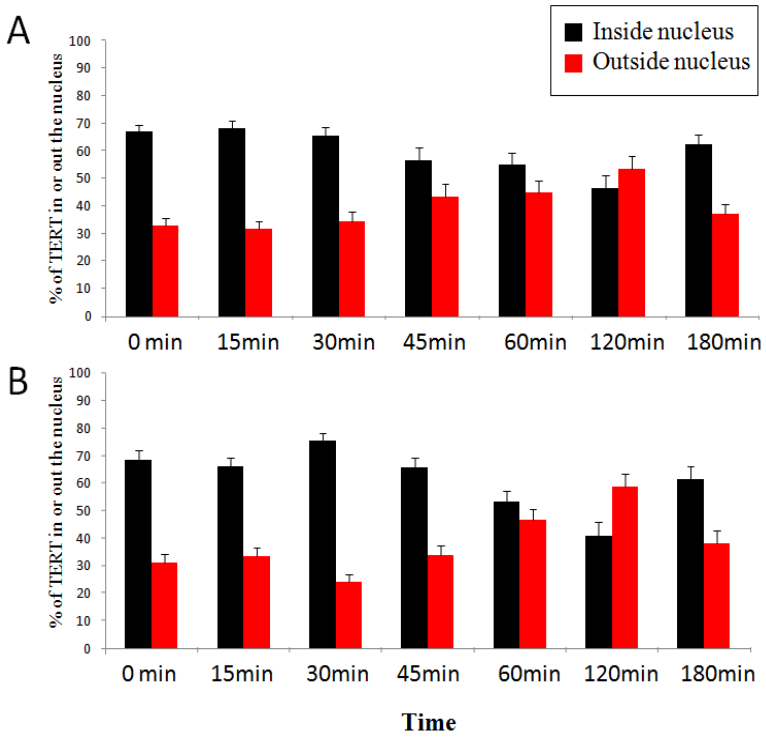

Figure 5.5 Short-term kinetic exclusion of endogenous hTERT in U87 and UP96. All cells were treated with 400µM H_2O_2 for 3 hours. **A:** U87 treated with H_2O_2. **B:** UP96 treated with H_2O_2. Cells were fixed at the indicated time points. The localisation of hTERT was measured in each individual cell using ImageJ. At least 30 cells per time point have been evaluated in each experiment. Bars indicate means and standard error from 3 independent experiments.

5.3.2 The effect of p53 status on nuclear DNA damage when hTERT is localised in different cell compartments

Since we found a difference in DNA damage and ROS levels when hTERT was localised in different cellular compartments in Hela and MCF7 we now used an isogenic cell pair in order to avoid any additional genetic differences between unrelated cancer cell lines. U87 and UP96 were transfected with mito-hTERT or nucl-hTERT, treated with 2, 5 10 and 20 Gy irradiation and then double stained with myc-tag and γH2A.X for DNA damage determination. Representative images of U87 and UP96 after different irradiation dosages are shown in figures 5.6 and 5.7. DNA damage foci of U87 and UP96 after different irradiation dosages are shown in figure 5.8 and summarised in figure 5.9.

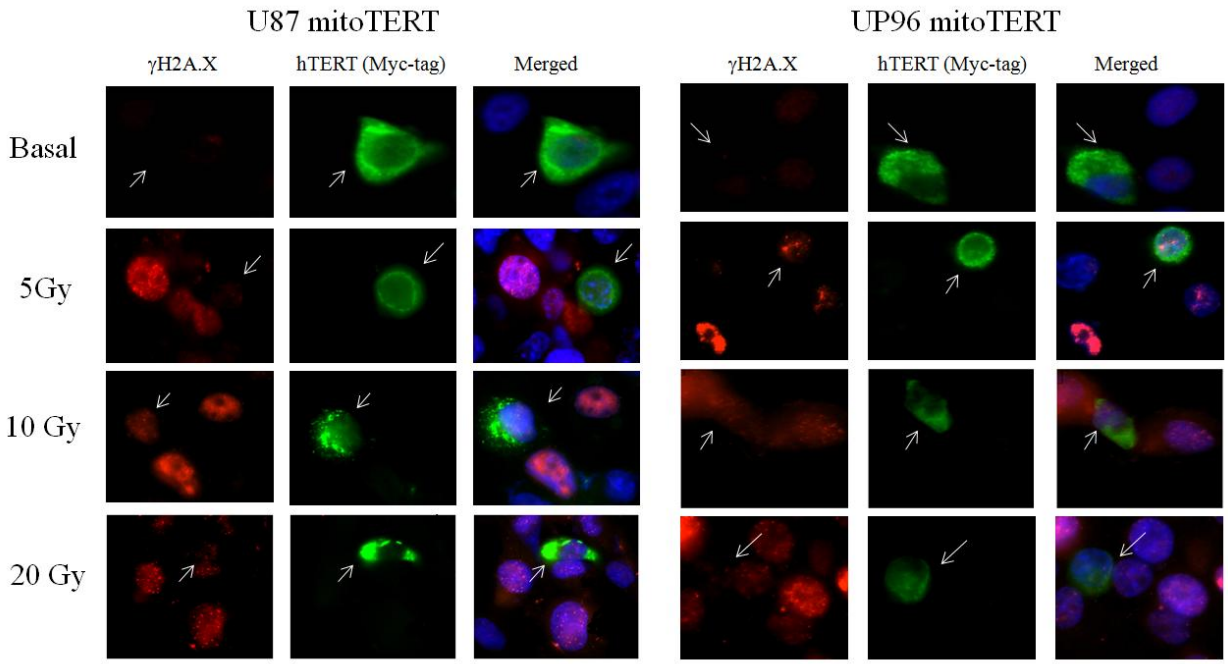

Figure 5.6 Double staining of U87 and UP96 cells transfected with mito-hTERT shooter under different dosages of x-irradiation. Cells were double stained with γH2A.X and myc-tag. Red colour represents DNA damage foci and green colour represents hTERT localisation. Blue is DAPI for nuclear staining. White arrows indicate transfected cells.

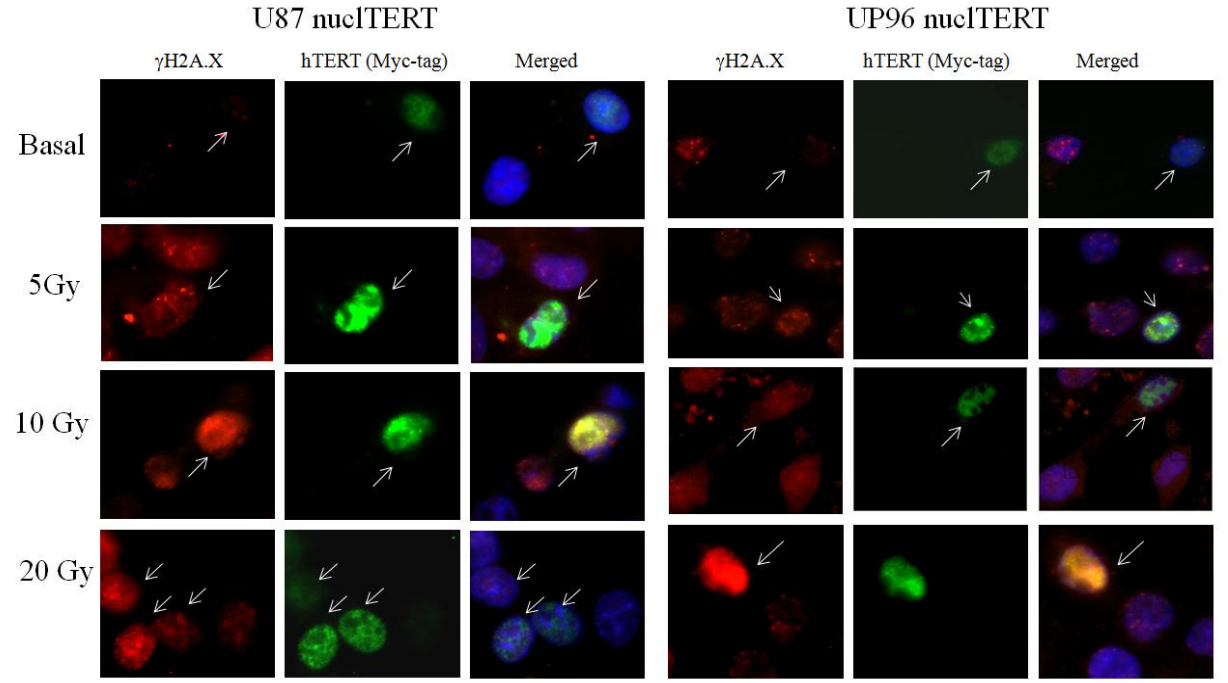

Figure 5.7 Double staining of U87 and UP96 cells transfected with nucl-hTERT shooter under different dosages of x-irradiation. Cells were double stained with γH2A.X and myc-tag. Red colour represents DNA damage foci and green colour represents hTERT localisation. Blue is DAPI for nuclear staining. White arrows indicate transfected cells.

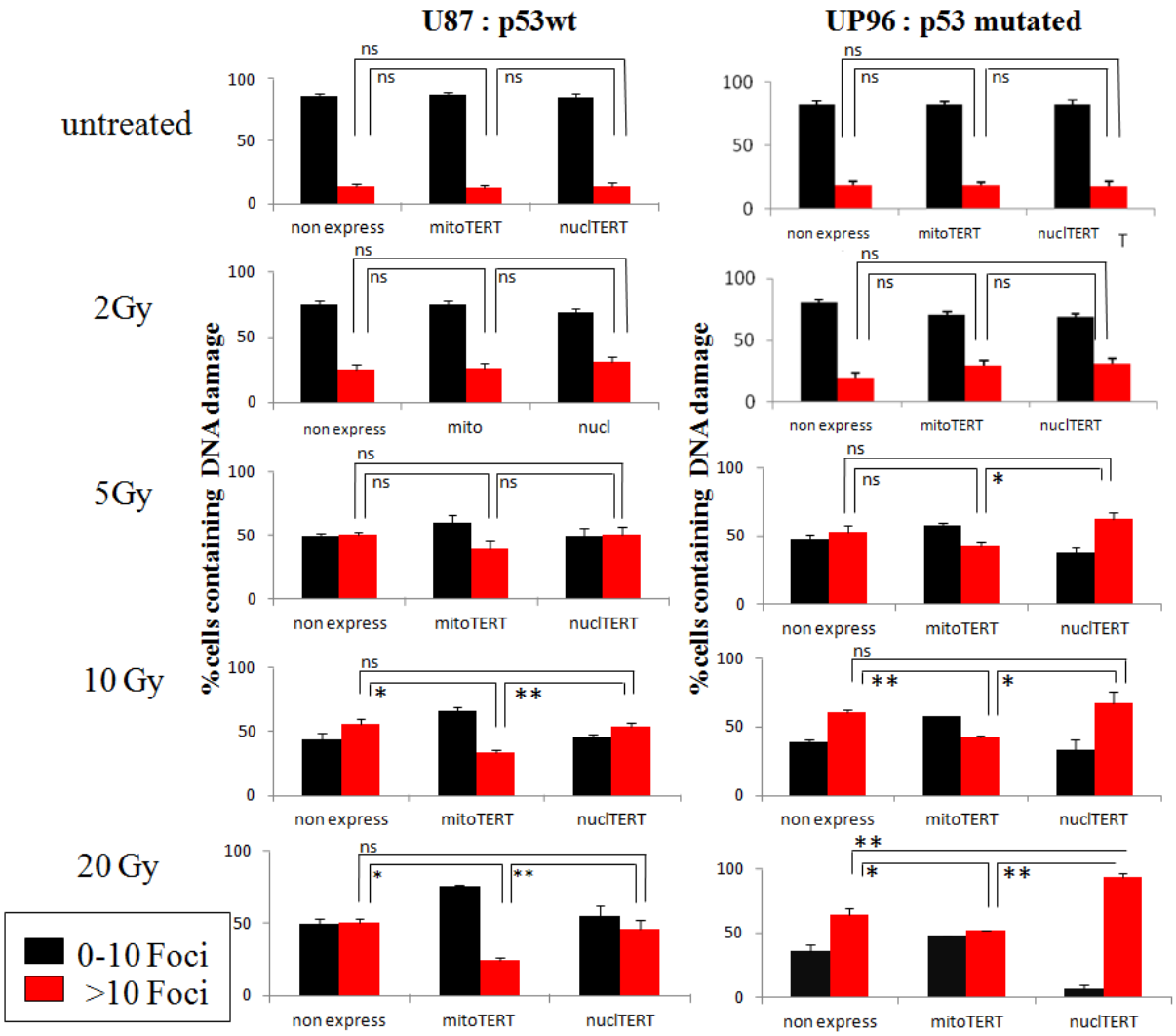

Figure 5.8 DNA damage foci in U87 and UP96 cells transfected with mito-hTERT, nucl-hTERT and non transfected after different dosages of x-irradiation. Cells were double stained with γH2A.X and myc-tag and DNA damage foci number were counted from each cell. At least 20 cells were analysed per experiment. Bars indicate means and standard error from 2-3 independent experiments. ***** P<0.05, ****** P<0.01, ns = non-significant difference.

As shown in figure 5.8 cells which contained DNA damage foci were categorised into 2 groups: the group which contained none or less than 10 damage foci and the group which contained more than 10 damage foci inside the nucleus. We found some background damage in both cell lines and chose the categories accordingly.

Under untreated condition, U87 and UP96 showed no significant difference for cells which contained more than 10 damage foci. Likewise, there were no differences between mito-hTERT, nucl-hTERT and non-transfected cells in U87 or any UP96.

Initially, we used low dose irradiation to treat the cells. After 2 Gy and 5 Gy irradiation treatments, no significant differences had been found between mito-hTERT, nucl-

hTERT and non transfected cells in U87. However, at 5 Gy irradiation UP96 cells transfected with nucl-hTERT were starting to show a significantly higher damage than mito-hTERT and non transfected group, while no significant difference has been found between non-transfected cells and cell with nucl-hTERT (see fig. 5.7).

Therefore, we increased the dosis of irradiation to 10 and 20 Gy. Under 10 Gy, mitochondrial localisation of hTERT started to express its protective function. Both U87 and UP96 transfected with mito-hTERT showed significantly lower damage in the group of more than 10 foci compared to both nucl-hTERT and non-transfected cells while no significant difference was found between nucl-hTERT and non-transfected U87. For UP96, on the other hand, a difference between non transfected and nucl-hTERT transfected cells appeared in the group of 10 Gy irradiation ($p<0.05$), but nucl-hTERT UP96 became significantly different ($p<0.01$) when we increased the irradiation dosage to 20 Gy. Here, we found a significant higher DNA damage in UP96 transfected with nucl-hTERT transfected cells compared to non transfected and mito-hTERT transfected cells while no significant difference was found between non transfected cells and nucl-hTERT transfected cells in U87 after 20 Gy irradiation. Thus, it seems that the specific increase of DNA damage in UP96 cells transfected with nucl-hTERT could be caused by the different p53 status of these cells compared to U87. Although for cells transfected with mito-hTERT under 20 Gy, both U87 and UP96 showed significant lower DNA damage compared to nucl-hTERT and non transfected cells, the decrease in DNA damage was much more pronounced in U87 cells. Thus, although p53 status does not influence the protective function of telomerase when it is localised in mitochondria *per se*, it seems to be more efficient when cells have a functioning p53 checkpoint.

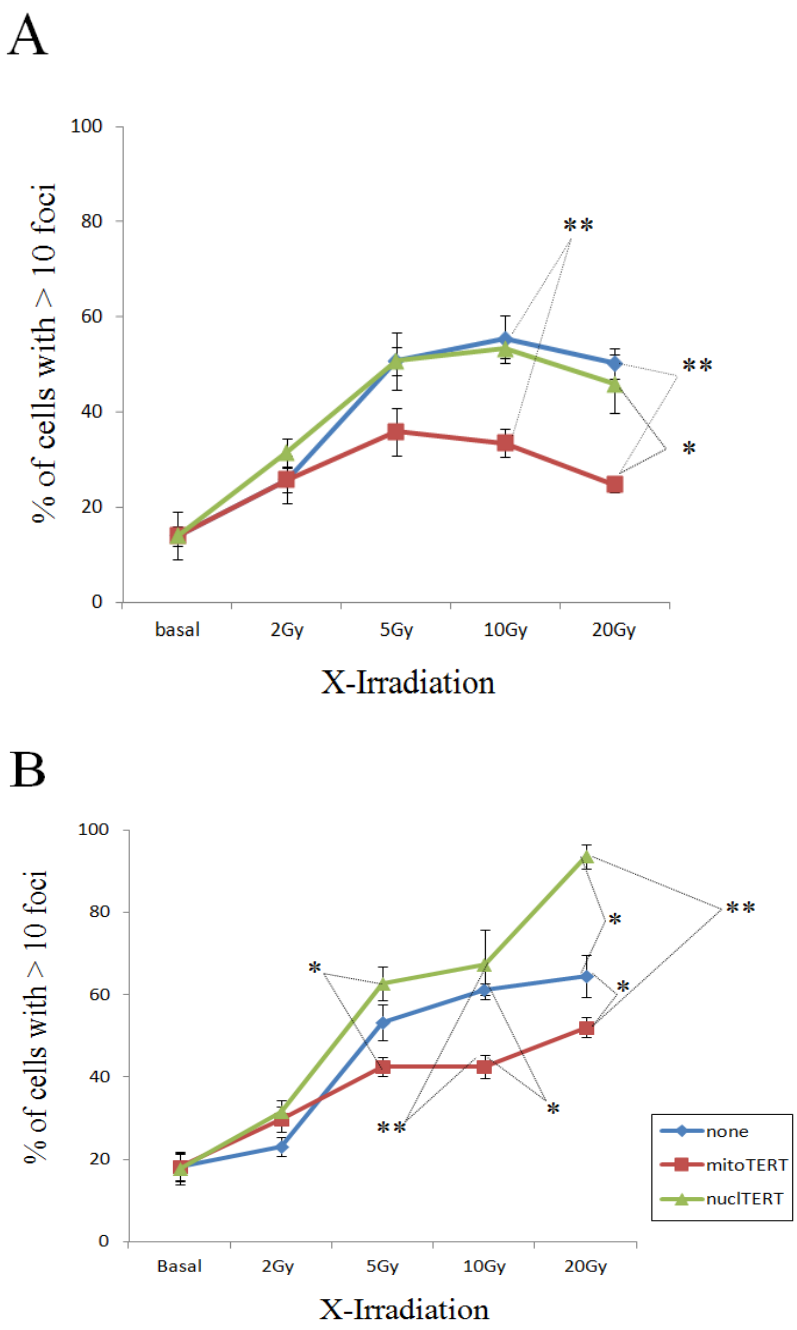

Figure 5.9 Comparison of damage foci number in U87 and UP97 transfected with mito-hTERT, nucl-hTERT and non transfected under basal conditions and after x-irradaition. The graph represents the percentage of cells with more than 10 damage foci. Cells were treated with different x-ray doses and fixed within 15 minutes after treatment. **A:** U87 after x-irradiation. **B:** UP96 after x-irradiation. ***** P<0.05, ****** P<0.01, ns = non-significant difference. The graph is the summary of 2-3 independent experiments per condition and cell type.

In figure 5.9, the results presented in figure 5.8 are shown as a kinetic expression with increasing irradiation doses and contains only cells with more than 10 foci. U87 and UP96 showed a different kinetics of DNA damage under increasing irradiation dosage.

When hTERT was localised in mitochondria, the damage of U87 which contains p53 wild type was reduced and significant lower when the dosage of irradiation increased. However, no significant difference has been found between the DNA damage level of nucl-hTERT and non-transfected U87 when we increased the irradiation dosage upto 20 Gy.

Interestingly, in nucl-hTERT transfected UP96, the DNA damage was increasing when irradiation dosage has increased. We found pronounced increase of the DNA damage after nucl-hTERT UP96 was irradiated at 20 Gy. However, mitochondrial hTERT localisation in UP96 was still expressing their protective capacity and helps to reduce nuclear DNA damage. Significantly lower DNA damage has been found in mito-hTERT UP96 compared with nucl-hTERT and non–transfected UP96. This experiment confirms the previous results in Hela and MCF7 regarding to the DNA damage after hydrogen peroxide treatment (figure 3.9 and 3.10). Thus, p53 status does influence the amount of protection of telomerase when it is localised in the mitochondria and exacerbates nuclear DNA damage when it is localised in the nucleus.

The comparison between U87 and UP96 after 20 Gy irradiation is shown in figure 5.10. Two results are striking: Firstly, although mitochondrial localisation of hTERT showed a protective capacity to DNA damage in both U87 and UP96 the protective effect was significantly ($P<0.01$) larger in U87 than in UP96 cells. Secondly, the level of DNA damage in UP96 transfected with nuclear shooter was significantly higher than U87 transfected with the same vector. Both mito-hTERT and nucl-hTERT transfected UP96 showed significant higher DNA damage than U87 after a high irradiation doses. There was no difference between U87 and UP96 in non-transfected cells. Therefore, the localisation of hTERT to the different cell compartments: nucleus or mitochondria, has a pivotal influence on the sensitivity of the respective cell against DNA damaging genotoxic stress. Thus, there might be a possible interaction between telomerase and mutated/inactive p53 of UP96 when a cell is under stress condition.

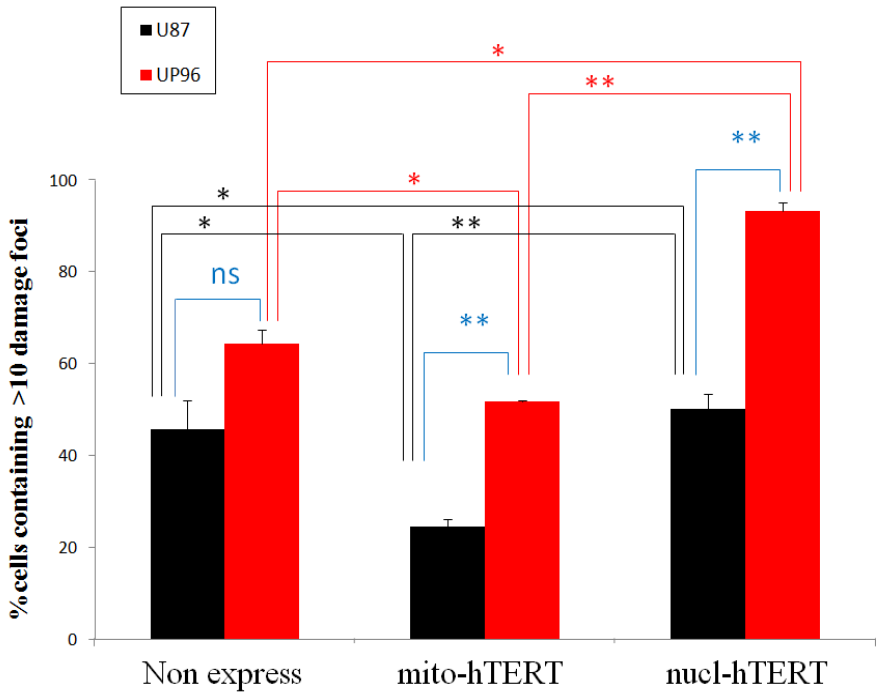

Figure 5.10 Comparison of DNA damage foci number in U87 and UP96 cells transfected with mito-hTERT, nucl-hTERT and non-transfected after 20Gy irradiation. The graph represents the percentage of cells which showed more than 10 damage foci. ***** P<0.05, ****** P<0.01, ns = non-significant difference. Bars indicate means and standard error from three independent experiments.

5.3.3 Quantitative determination of mitochondrial superoxide levels in U87 and UP96 after irradiation

As our previous experiment in Chapter 4 showed a correlation between mitochondrial ROS generation with different hTERT localisation. In order to characterise the effect of p53 to this protective function of telomerase, we compared the levels of mitochondrial superoxide in mito-hTERT, nucl-hTERT and non-transfected cells in U87 and UP96 under basal and stress conditions (irradiation treatment). Transfected and non–transfected U87 and UP96 were treated with X-irradiation at a dose of 2 Gy and 20Gy and compared with non-irradiated cells. All cells were double stained with mitoSox immediately within 15 minutes after irradiation, then fixed and stained with an antibody against myc-tag.

Figure 5.11 represent a comparison of mitochondrial superoxide levels in mito-hTERT, nucl-hTERT and non-transfected cells in U87 and UP96 between basal conditions and cells after 2 Gy irradiation. Interestingly, both cell lines transfected with mito-hTERT shooter demonstrated already a protective effect of lower ROS levels compared to nucl-hTERT and non-transfected cells before treatment. We found a significant difference between non-transfected U87 and nucl-hTERT transfected U87 which might indicate

the protective effect of nucl-hTERT to ROS production before treatment. However, no significant difference was found between non-transfected UP96 and UP96 transfected with nucl-hTERT.

After 2 Gy irradiation we found lower mitochondrial ROS levels in both U87 and UP96 cells transfected with mito-hTERT shooter compared to those transfected and nucl-hTERTshooter. We have not found a significant difference between U87 transfected with nucl-hTERT and the non-transfected group after 2 Gy irradiation. However, a significant difference has been found between non-transfected UP96 and nucl-hTERT UP96 after 2 Gy irradiation. Both mito-hTERT and nucl-hTERT transfected UP96 showed a significant lower ($P<0.01$and $P<0.05$, respectively) ROS level than non-transfected cells which indicate the protective effect of hTERT to ROS production.

Comparison of mitochondrial superoxide levels in mito-hTERT, nucl-hTERT and non-transfected U87 and UP96 between basal condition and 20 Gy irradiation is shown in figure 5.12. We found a similar significant lower mitochondrial ROS levels in both U87 and UP96 cells transfected with mito-hTERT shooter after 20Gy irradiation compared to those non-transfected and nucl-hTERT transfected cells. It is interesting that there are no significant difference between ROS level of mito-hTERT transfected group before and after 20Gy irradiation which indicated a protective function of hTERT in mitochondria. However, we found non-significant difference between both U87 and UP96 transfected with nucl-hTERT compared with the non-transfected group after 20 Gy irradiation. Both of them also showed significant higher of ROS level compared with the similar cells under basal condition.

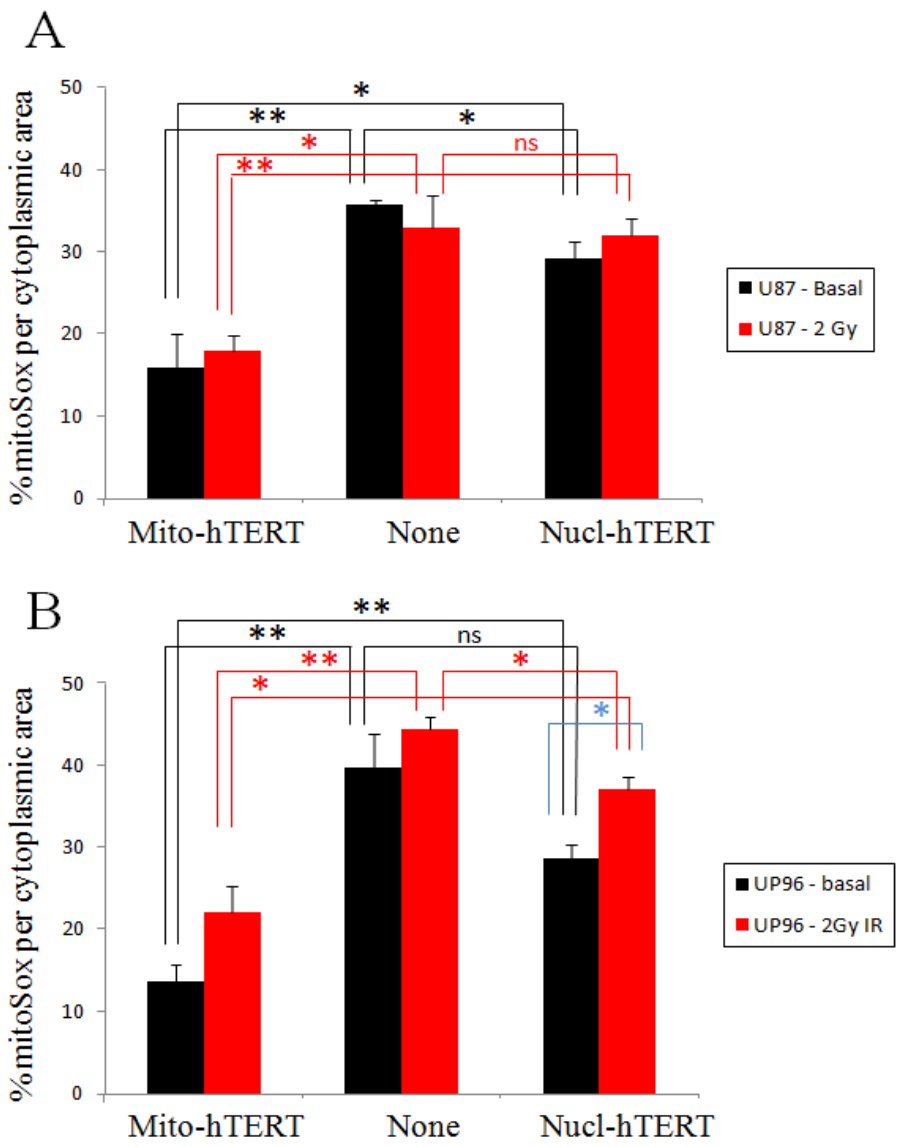

Figure 5.11 Comparison of mitochondrial superoxide levels in mito-hTERT, nucl-hTERT and non- transfected cells in U87 and UP96 under basal conditions and 2 Gy x-irradiation. A: U87 before (black) and after 2 Gy irradiation (red). **B:** UP96 before (black) and after 2 Gy irradiation (red). Bars show mean and standard error from 3 independent experiments. ***** P<0.05 ****** P<0.01, ns = non-significant difference. One way Anova was used to test for significant differences between groups.

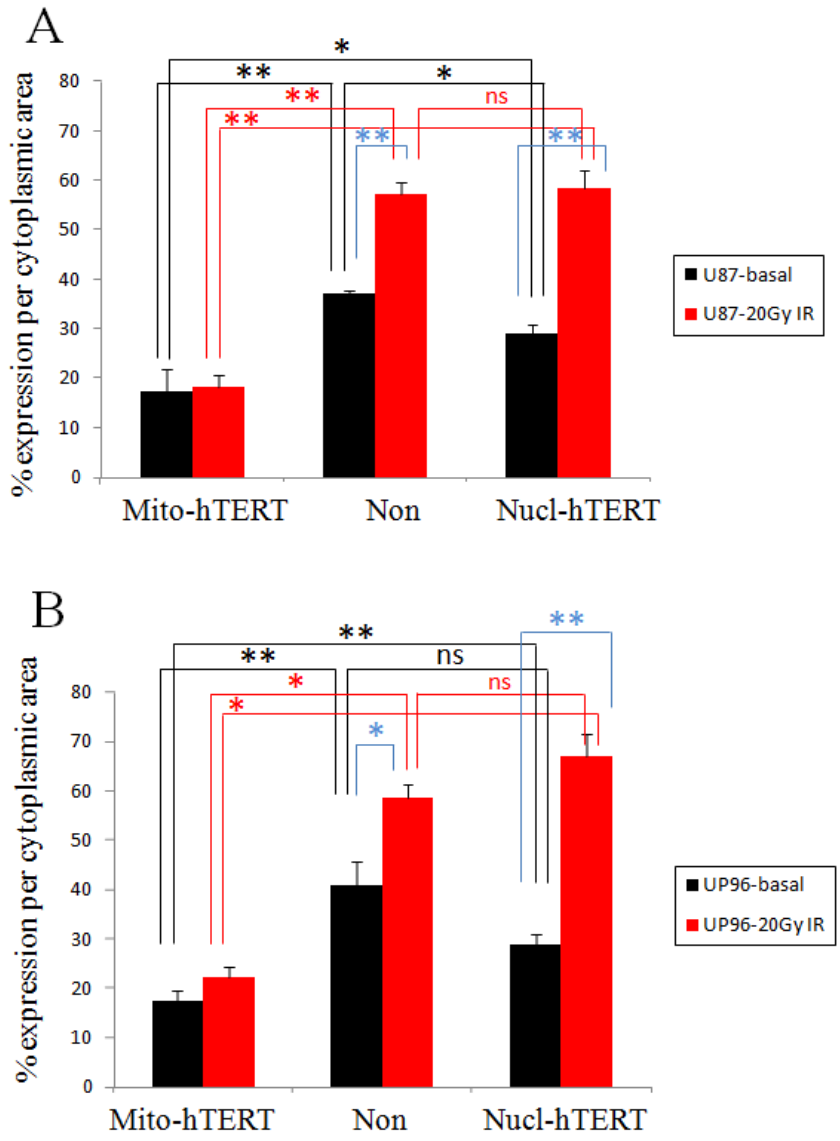

Figure 5.12 Comparison of mitochondrial superoxide levels in mito-hTERT, nucl-hTERT and non- transfected cells in U87 and UP96 under basal conditions and 20 Gy x-irradiation. A: U87 before (black) and after 20 Gy irradiation (red). **B:** UP96 before (black) and after 20 Gy irradiation (red). Bars show mean and standard error. ***** P<0.05 ****** P<0.01, ns = non-significant difference. One way Anova was used to test for significant differences between groups.

5.3.4 Where is the nuclear DNA damage generated due to nuclear TERT shooter localised in U87 and UP96?

Since we found a significant increase of DNA damage when hTERT is localised in the nucleus and nuclear telomerase is closely related to telomere maintenance we were interested whether the DNA damage is located on or outside the telomere. U87 and UP96 were transfected with nucl-hTERT and treated with 20 Gy irradiation. Cells were fixed within 15 minutes after irradiation and then triple stained for combined immuno-fluorescence staining and telomere –FISH. The protocol for Telo-Fish and co-localisation analysis was described in 2.2.17 in Chapter 2. A representative image and the analysis of the co-localisation are shown in figures 5.13- 5.14.

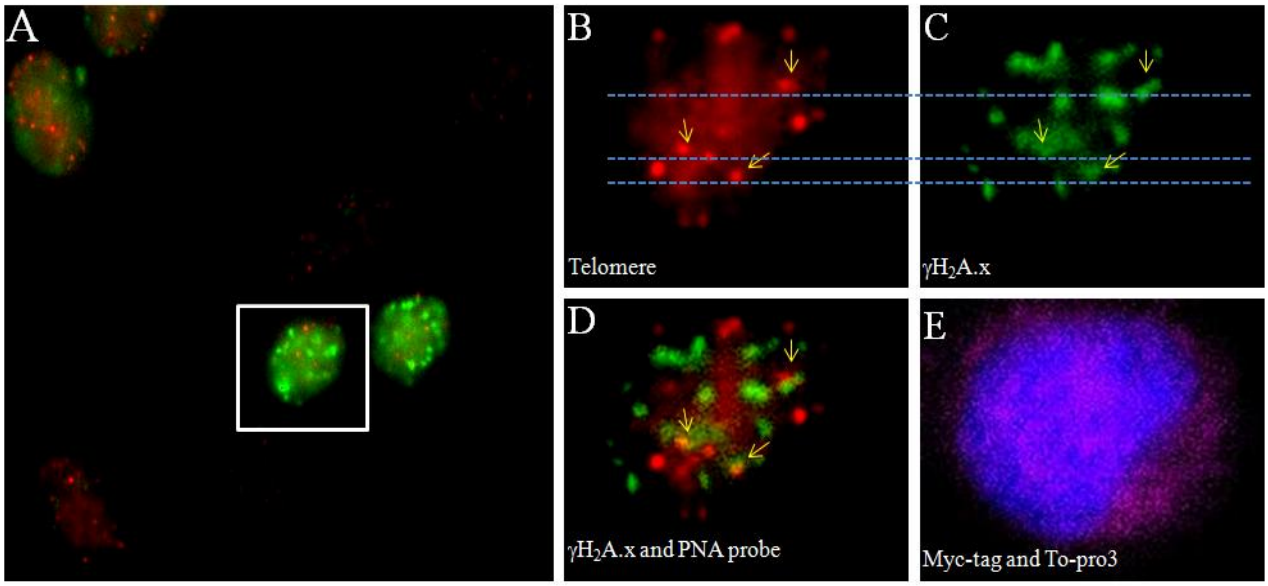

Figure 5.13 Representative image of telo-FISH in UP96 cells transfected with nucl-hTERT shooter. UP 96 was transfected with nuclTERT shooter and irradiated with 20 Gy. Cells were triple labelled with Alexa® Fluor 488 (green) for γH2A.X and Alexa® Fluor 633 (far red) for myc-tag staining and PNA probe (Cy3, red) for telomere hybridisation. Cells were stained with To-pro3 to show the nucleus. **A:** Merged image of 3 colour channels. The white square indicates the cell which was enlarged as shown in B- E. **B:** telomere signals from hybridisation with PNA probe (Cy3, red). **C:** DNA damage foci stained with gamma H2A.X. **D:** Merged picture between telomere signal and DNA damage foci. Yellow arrows indicate the colocalisation between PNA probe and DNA damage which appeared in yellow. **E:** Merged picture between Myc-tag and To-pro3.

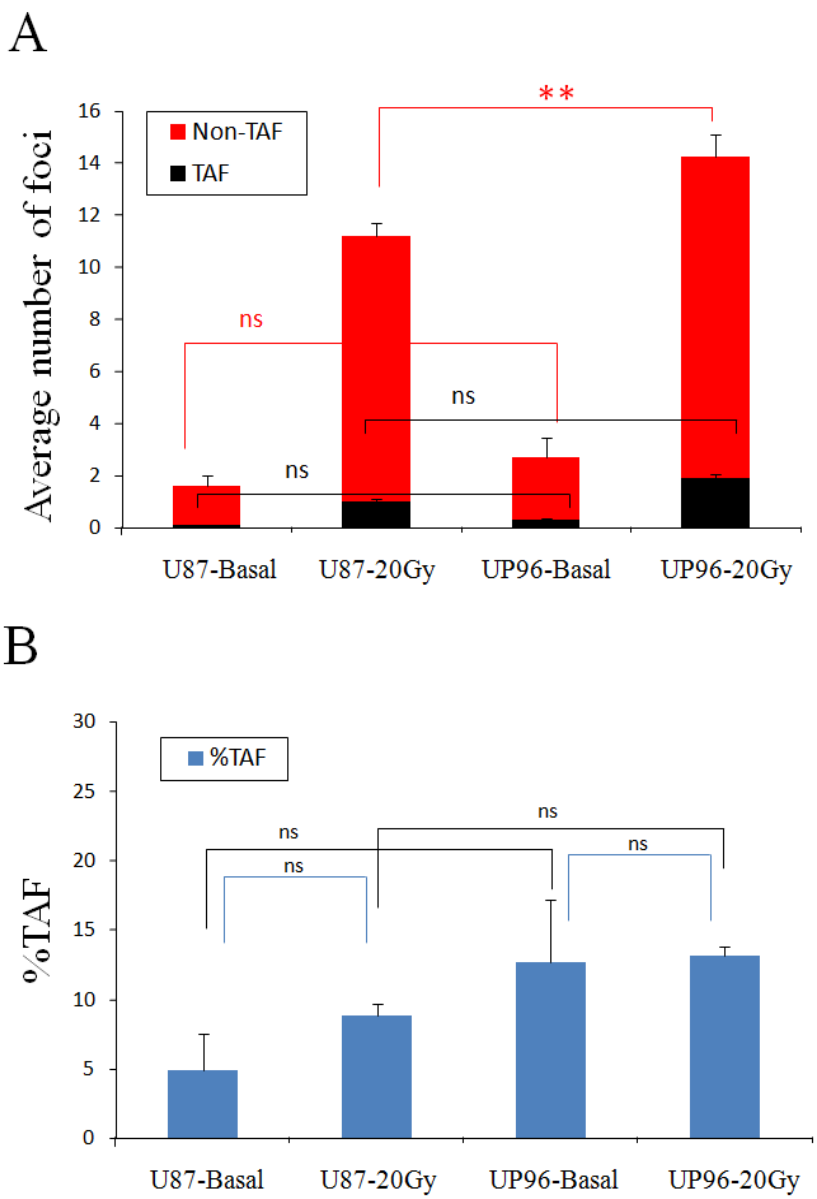

Figure 5.14 Levels of γH2A.X foci in U87 and UP96 under basal and 20 Gy irradiation. A: average number of γH2A.X foci in U87 and UP96 cells (all transfected with nuclear TERT shooter vector) under basal (untreated) condition and 20 Gy irradiation. Black bars represent an average of total number of γH2A.X foci colocalisation with telomeres (TAF). Red bars represent the average number of γH2A.X foci not colocalised with telomere. Data was averaged from 3 independent cell groups. **B:** percentage of γH2A.X foci colocalising with telomere (%TAF per cell) in U87 and UP96 under basal condition and after 20 Gy irradiation.

We found before that transfected of nucl-hTERT to UP96 showed significantly higher amount of DNA damage compared to non-transfected cells after 20 Gy irradiation. Thus, we analysed here only cells which contained high DNA damage (>10 foci per nucleus) in both U87 and UP96 to analyse the co-localisation between γH2A.X and telomere after 20 Gy irradiation.

The average amount of DNA damage in U87 and UP96 under basal and 20 Gy irradiation is shown in figure 5.15. We found a significant increase of non-telomeric DNA damage in UP96 after 20 Gy irradiation compared to U87 after irradiation. (red bar in figure 5.15A). However, we did not find any difference between telomeric γH2A.X foci (TAF, black bar in figure 5.15A) compared between U87 and UP96 under basal condition and U87 and UP96 after 20 Gy irradiation. The co-localisation percentage of γH2A.X to telomere ranged between 4 to 10% before irradiation and increased to about 12 to 15% after irradiation in both U87 and UP96. We have analysed at least 10 cells per group by using Z-stack images.

5.4 Discussion

We hypothesised from our previous results in chapter 3 that the difference in DNA damage between Hela and MCF7 transfected with nucl-hTERT shooter vectors could be due to their different p53 status. P53 in Hela is non-functional while MCF7 contains active p53. In order to clarify the role of p53 for mitochondrial protection of hTERT and DNA damage we used an isogenic cell pair of glioblastoma cells: U87 which contains wild type p53 and UP96 which contains a dominant negative mutated p53. Unfortunately, we have not compared the apoptosis data between U87 and UP96 which should be done in order to compare the effect of hTERT localisation after stress treatment to the apoptosis induction. Thus this experiment should be performed in order to investigate the effect of different p53 status to apoptosis induction in our cell system. For the influence of p53 status on the protective function of telomerase, first, we tested the localisation of hTERT in both cell lines. We found that U87 and UP96 have already about 30% of hTERT localised in the cytoplasm under basal condition. The cytoplasmic accumulation of hTERT in U87 and UP96 under untreated condition is slightly higher than in Hela and MCF7 which show only 20%. This high initial exclusion rate could possibly be a result from high stress experienced already under basal conditions which might be due to inadequate culture conditions. In addition, it is also possible that the high initial exclusion rate could be connected to the low additional hTERT exclusion under increased stress. Since we are the first to have analysed the hTERT exclusion systematically the reasons for this different kinetics in the 3 cancer cell lines remain elusive. We would speculate that additional genetic changes in each of the cancer cell lines might influence the hTERT exclusion behaviour.

In general, we have not found a major difference in the exclusion kinetics between un-transfected U87 and UP96 cells. However, U87 cells excluded hTERT slightly faster

(45 minutes) while the exclusion only started at 1h for UP96. In general, the exclusion reached a maximum after 2 hours and already decreased at 3 hours. This is in striking contrast to the other analysed cell lines. Thus, we could not detect any major influence of p53 activity on telomerase exclusion from nucleus to cytoplasm. However, a more careful analysis of different stress types and more time points could probably help to address that question in more detail.

For DNA damage, we found that under basal conditions U87 and UP96 showed no significant difference between mito-hTERT, nucl-hTERT and non-transfected cells. It is also interesting to note that UP96 cells which contain a mutated p53 similar to the functionally inactivated one in Hela cells did not show a significantly higher damage under basal conditions when transfected with nucl-hTERT. U87 and UP96 also did not show a significant difference between mito-hTERT, nucl-hTERT and non-transfected cells under low dose of irradiation. Thus, p53 activity does not correlate to the DNA damage level directly in this manner.

However, at 5 Gy irradiation UP96 cells transfected with nucl-hTERT were starting to show a significantly higher DNA damage. When we increased irradiation dosages even further the protective capacity of mitochondrial hTERT became increasingly pronounced. Both U87 and UP96 cells transfected with mito-hTERT showed significantly lower DNA damage compared to those containing nuclear hTERT and non –transfected cells. However, at 20 Gy there was a very clear effect of much better protection of mito-hTERT in U87 than in UP96 cells (figure 5.8).

Most importantly, when hTERT was localised in the nucleus, we discovered differences in the level of DNA damage in U87 and UP96 cells. The level of DNA damage in UP96 cells was significantly higher than in U87 cells transfected with mito-hTERT. We have not found a similar effect in non-transfected cells. This result means that the p53 status is clearly important for the outcome of irradiation or other stress treatments in cancer cells. In the context of p53 and apoptosis, cells which contain active p53 might apoptose easier than that cells contain mutated p53 but this process takes time to induce. In our experimental which we fixed cells within 15 minutes after irradiation, apoptosis induction is not relevant to our experimental system and effect our results. However, the fact that apoptosis is induced in non-transfected or transfected with nucl-hTERT cells corresponds to those having high ROS as well as high DNA damage levels. The mechanism which related to the higher DNA damage after irradiation when active hTERT is localised in nucleus in p53- cell is still unclear. We hypothesis that

telomerase localisation might possibly interact with p53 when a cancer cell is under stress condition.

Kovalenko and co-workers suggested that the high level of DNA damage when hTERT is localised in the nucleus might play a role in cell cycle delay in order to repair the damage site (Kovalenko et al., 2010b). Activated p53 will arrest the cell cycle to allow time for DNA repair (Zhang et al., 2012). My results demonstrate that nuclear localisation of hTERT could not reduce ROS generation under stress conditions compared to mitochondrial localisation of hTERT resulting in higher nuclear DNA damage. One could speculate that this higher level of ROS generation might activate p53 to arrest the cell cycle to allow time for DNA repair. Nuclear hTERT might help to delay cell cycle progression in cells which contains functional p53 but could not display this function when cell contains inactive p53. More detailed analysis of the relationship between hTERT and p53 along with other p53 related genes might help to explain the discovered correlation between nuclear localisation of telomerase and induction of DNA damage.

Regarding the influence of p53 on ROS levels described in chapter 4, we found that U87 and UP96 have lower mitochondrial ROS levels when transfected with mito-hTERT shooter compared with nucl-hTERT and non-transfected cells. This result confirms our previous findings on Hela and MCF7. It is interesting that we have found a significant induction of ROS generation in both U87 and UP96 transfected with nuclear hTERT and non-transfected cells after 20 Gy irradiation while no-significant increase of ROS production in both U89 and UP96 transfected with mito-hTERT. These results indicate that p53 protein does not influence the mitochondrial protective function of hTERT when it localised in mitochondria.

In co-localisation analysis between telomeric and non-telomeric DNA damage, we found a significant higher non-telomeric nuclear DNA damage level in UP96 transfected with nucl-hTERT shooter after 20 Gy irradiation compared to U87 transfected with nuclear hTERT after 20 Gy irradiation as we have found before. Unfortunately, due to technical difficulties we could not confirm that all analysed cells contained the nuclear hTERT shooter vector. In order to address the question whether there was a change in the amount of TAFs due to different 53 status we analysed the percentage of colocalisation of γH2A.X foci telomeres (%TAF). We have not found a significant difference in the localisation of the DNA damage between U87 and UP96 transfected with nucl-hTERT before and after 20 Gy irradiation. Thus the higher number of nuclear DNA damage when hTERT was localised in nucleus in cells

containing inactive p53 did not increase the percentage of co-localisation between DNA damage and telomere. Our experiment has found about 12-15% of TAFs in U87 and UP96 which is different from experiments of another group which reported about 40-50% co-localised between DNA damage and telomere in SQ20B and LNCaP transfected with hTERT harbouring a mutated the nuclear exclusion signal (Kovalenko et al., 2010b). Moreover, we have not found a significant increase of the percentage of co-localisation between DNA damage and telomere as reported in Kovalenko's experiment. So far, we are the second group which confirms that the localisation of hTERT in the nucleus correlates to nuclear DNA damage. However, our experiment used a different method which over-expressed the fully functional wild type hTERT in the nucleus and showed a correlation between nuclear localisation of hTERT and DNA damage in cells which contain different p53 activity under stress condition. The expression of telomerase is related to the activation of many genes (Baross et al, 2004; Ahmed et al., 2008; Daniels et al., 2010). Thus more detailed experiments on the correlation between hTERT and gene expression while p53 is inactive might help to better understand the pathway responsible for this DNA damage induction.

In conclusion, results in this chapter confirmed the protective function of mitochondrial telomerase regarding the reduction of ROS production after exogenous stress treatment while the influence of the p53 status was variable. The most dramatic influence has mutated p53 on DNA damage induction on cells with nuclear TERT localisation. It seems possible that telomerase interacts functionally with p53 in the nucleus. This experiment might open a novel link between telomerase and p53 activity while a cell is under stress condition.

Chapter 6

Mitochondrial localisation of telomerase reduces mitochondrial ROS and nuclear DNA damage after endogenous stress

6.1 Introduction

In previous chapters we have used hydrogen peroxide and irradiation to activate cellular oxidative stress. However, both of them are an exogenous stress inducers. In a further experiment we o used an endogenous stress inducer to investigate the protective function of telomerase when it is localised in the mitochondria. Thus we used paraquat which is a chemical which can directly activate mitochondrial ROS production (Ali et al., 1996; Castello et. al., 2007; Shibata et. al., 2010).

Paraquat (PQ^{2+}) is a bipyridyl compound (1,1‘ –dimethyl-4,4‘ –bipyridylium), the prototype toxin know to exert injurious effect through oxidative stress and bears a structural similarity to the Parkinson’s disease toxicant, 1-methyl-4-pheynlpyridinium (Mohammadi-Bardbori and Ghazi-Khansari, 2008). Paraquat has been originally developed as a herbicide. However, it is also widely used as a source of oxidative stress to cells. Paraquat-induced cytotoxicity is preceded by the increase in ROS production and mitochondria are a major source of paraquat-induced oxidative stress (McCarthy et al., 2004; Castello et al., 2007; Mohammadi-Bardbori and Ghazi-Khansari, 2008). Paraquat can penetrate the outer mitochondrial membrane and enter inter-membrane space and matrix (Castello et al., 2007). Cocheme and Murphy reported that paraquat causes mitochondrial oxidative damage in mammalian systems following its inner mitochondrial transmembrane potential ($\Delta\psi m$) dependent. Paraquat can entry and accumulate into the mitochondrial matrix and the mitochondrial complex I (NADH-ubiquinone oxidoreductase) is a major mitochondrial site for paraquat interference (Cocheme and Murphy, 2008). However, Castello and her team reported that the major site of paraquat interference is complex III (ubiquinol-cytochrome-c reductase) in the respiratory chain. Electrons from Complex II and complex III in the electron transport chain can be transfered to the PQ^{2+} molecule and are proposed to participate in mechanisms of superoxide production by PQ^{2+}(Castello et. al., 2007). Moreover, Yang and Tiffani-Castiglioni reported that paraquat might decrease the activity of mitochondrial complex V by abducting an electron (Yang and Tiffani-Castiglioni, 2007). Thus, impairment of mitochondrial complexes by paraquat results in inhibition of electron transport with subsequent increased production of superoxide anion (Boelsterli and Lim, 2007).

Based on these findings we decided to use paraquat as a mitochondrial ROS inducer to investigate the protective function of telomerase when localised in the mitochondria. This chapter should clarify whether the protective capacity of telomerase works not only from the exogenous stress but also protects a cell from endogenous, directly mitochondrially derived stress.

6.2 Results

6.2.1 Endogenous telomerase exclusion after paraquat treatment

We have previously shown that the exclusion level and localisation of telomerase is correlated to mitochondrial ROS generation as well as to nuclear DNA damage. However, we had used H_2O_2 and irradiation treatment in the previous experiments which are an exogenous stress induction. We were now interested in addressing the question whether telomerase is also protective when mitochondrial ROS are induced endogenously. Therefore, in this chapter we investigated the protective function of telomerase when cellular stress is induced by endogenous stress treatment by using paraquat. MRC5 and MRC5/hTERT cells were used in this experiment in order to investigate the protective effect to telomerase compared with cells without endogenous telomerase expression.

First, we investigated the kinetic hTERT exclusion after paraquat treatment. MRC5/hTERT cells were treated with 400 μM paraquat and the sub-cellular shuttling of hTERT protein at 1, 3, 6 and 24 hours after treatment were investigated. Representative images of MRC5/hTERT after paraquat treatment are shown in figure 6.1. The kinetic exclusion of hTERT in MRC5/hTERT after paraquat treatment is shown in figure 6.2. In figure 6.2 we do not show the exclusion results at early time points as for the exogenous stress treatment (H_2O_2) because we have not found a significant hTERT exclusion in the first 3 hours. Moreover, we have treated the cells for longer than 24 hours. However, no cells survived after 24 hours of paraquat treatment. We found that most cells were apoptotic at 48 hours paraquat treatment (data not shown).

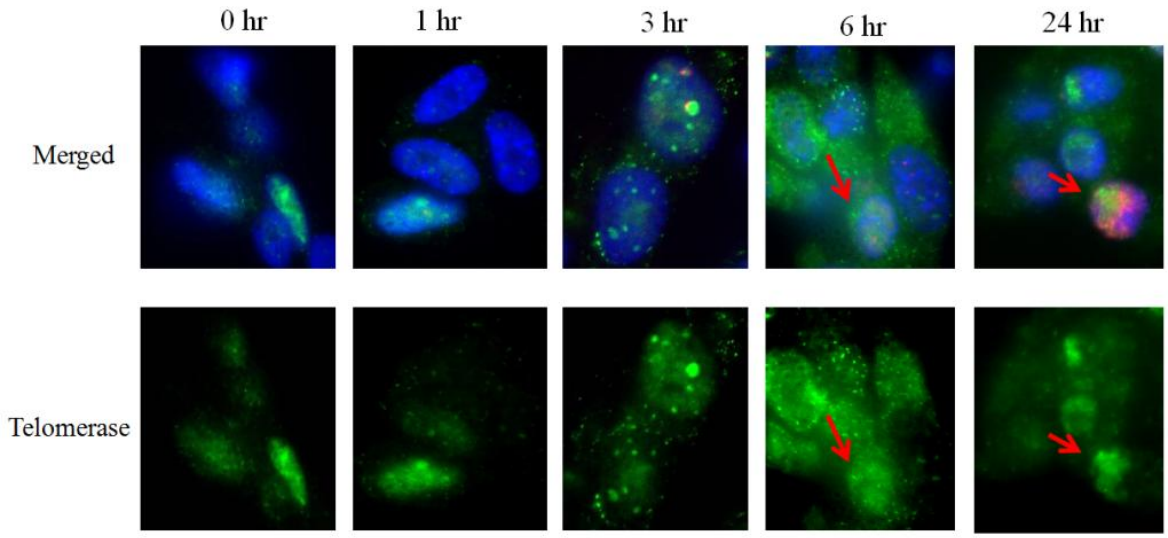

Figure 6.1 Representative images of the kinetic exclusion of endogenous hTERT in MRC5/hTERT cells after paraquat treatment. All cells were treated with 400μM paraquat. Green colour represents hTERT localisation. Nuclei were stained with DAPI (blue). Red signal indicates γH2A.X. Red arrow indicates cells which showed nuclear localisation of hTERT correlated to DNA damage. Cells were treated for the indicated time points up to 24 hours, then fixed immediately. The localisation of hTERT was measured in each individual cell by ImageJ.

Results in figure 6.2 represent a kinetic exclusion of endogenous hTERT in MRC5/hTERT cells after 400μM paraquat treatment (figure 6.2A) in parallel with 400μM H_2O_2 treatment (figure 6.2B). We have found that after paraquat treatment, hTERT starts to exclude slower than after H_2O_2 treatment where the exclusion started around 1 hour post treatment and reached a maximum of 50% exclusion already after 3 hours. At 1 and 3 hours (180 min) only 20% of hTERT was excluded from the nucleus to the cytoplasm after paraquat treatment while about 50-60% had been already excluded in MRC5/hTERT treated with H_2O_2 at 3 hours. The level of telomerase exclusion reached a maximum of around 50% in paraquat treatment at 6 hours post treatment. Thus, TERT seems to exclude slower in an endogenous stress treatment. No cells survived beyond 48 hours of paraquat treatment and telomerase exclusion already reversed back into the nucleus at 24 hours of treatment. A similar phenomenon has been found in MRC5/hTERT cells treated with H_2O_2, however, TERT predominantly locating in the nucleus was much slower (figure 6.2B). This experiment suggests a different exclusion behaviour of endogenous hTERT after paraquat treatment compared to H_2O_2 treatment.

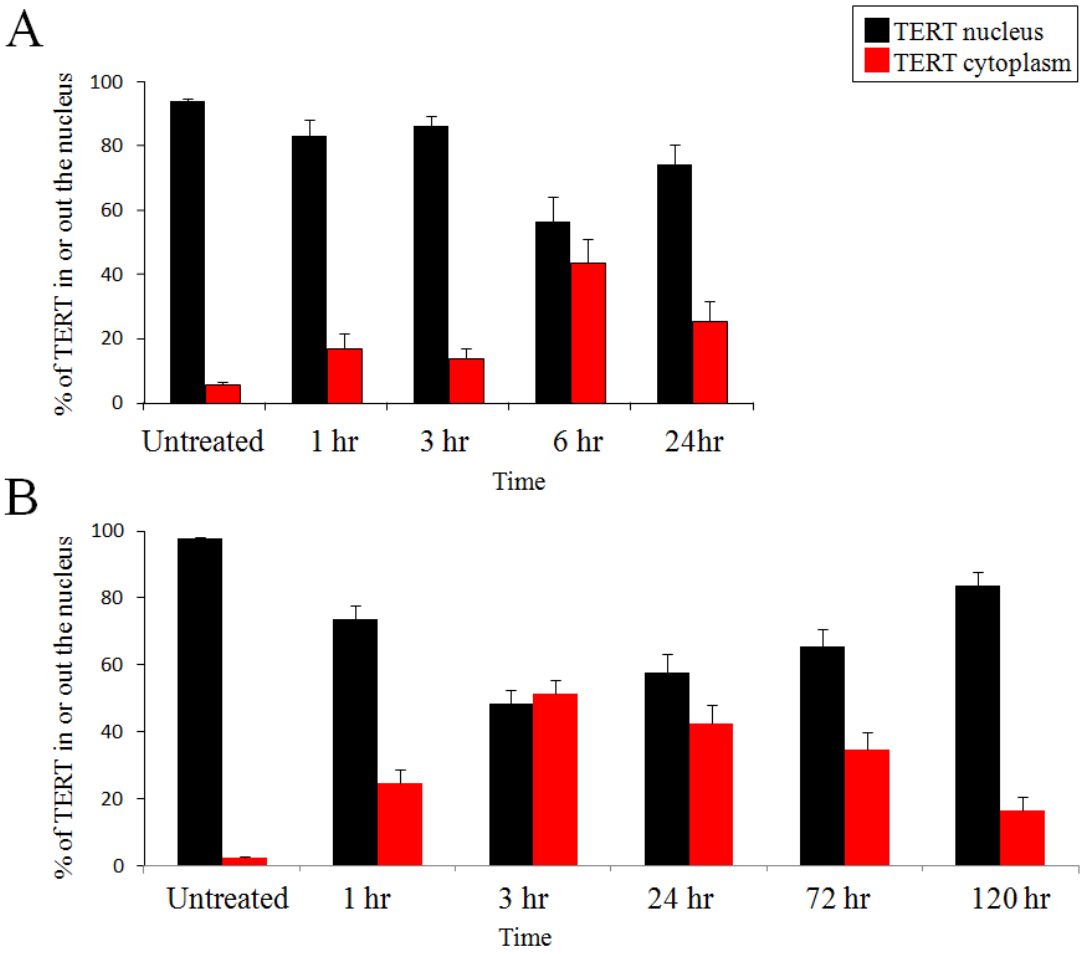

Figure 6.2 Comparison between paraquat and H_2O_2 treatment for the kinetic exclusion of endogenous hTERT in MRC5/hTERT cells. A: Kinetic exclusion of endogenous hTERT after 400μM paraquat treatment. **B:** Kinetic exclusion of endogenous hTERT after 400μM H_2O_2 treatment. Bars indicate means and standard error from at least 30 individual cells for every timepoint.

6.2.2 DNA damage in MRC5 and MRC5/hTERT cells after 400 μM paraquat treatment

To analyse whether the physical location of hTERT after paraquat treatment correlates to ROS generation and DNA damage, MRC5 and MRC5/hTERT cells were treated with 400μM paraquat and DNA damage examined at 1, 3, 6 and 24 hours after treatment. Representative images of MRC5 and MRC5/hTERT are shown in figure 6.3 and 6.4. A summary of DNA damage foci numbesr in MRC5 and MRC5/hTERT is shown in 6.5.

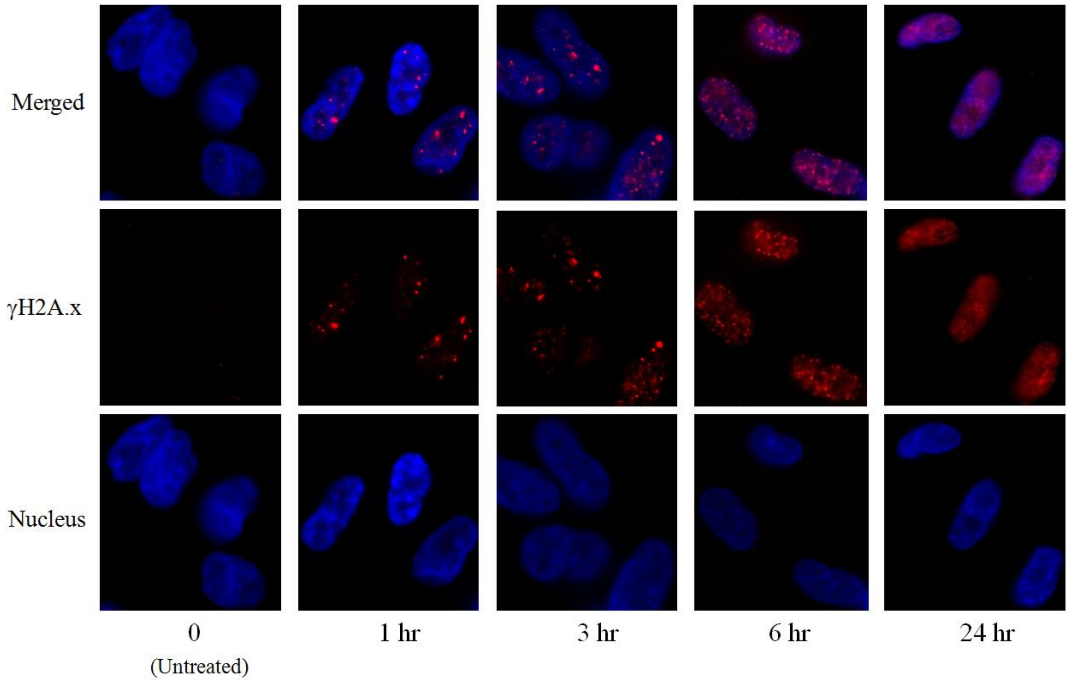

Figure 6.3 Formation of DNA damage under 400μM paraquat treatment in MRC5. Cells were treated with 400μM paraquat up to 24 hours and stained for γH2A.X. Red colour represents γH2A.X and blue colour represents nuclei.

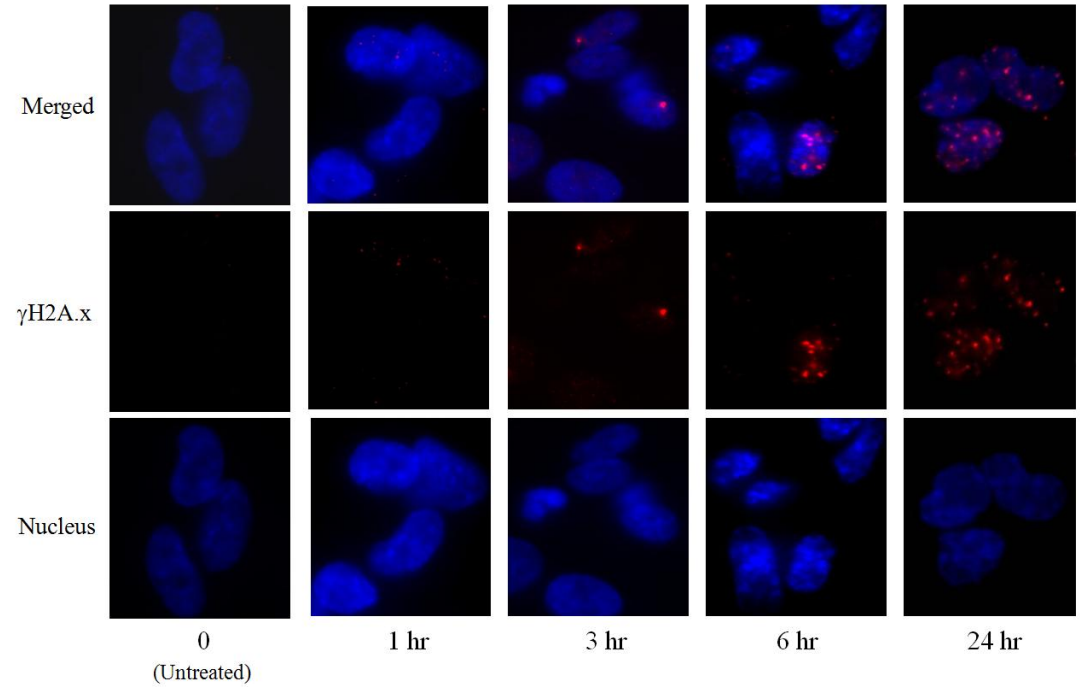

Figure 6.4 Formation of DNA damage after 400μM paraquat treatment in MRC5/hTERT. MRC5/hTERT were treated with 400μM paraquat up to 24 hours and stained for γH2A.X. Red colour represents γH2A.X and blue colour represents nuclei.

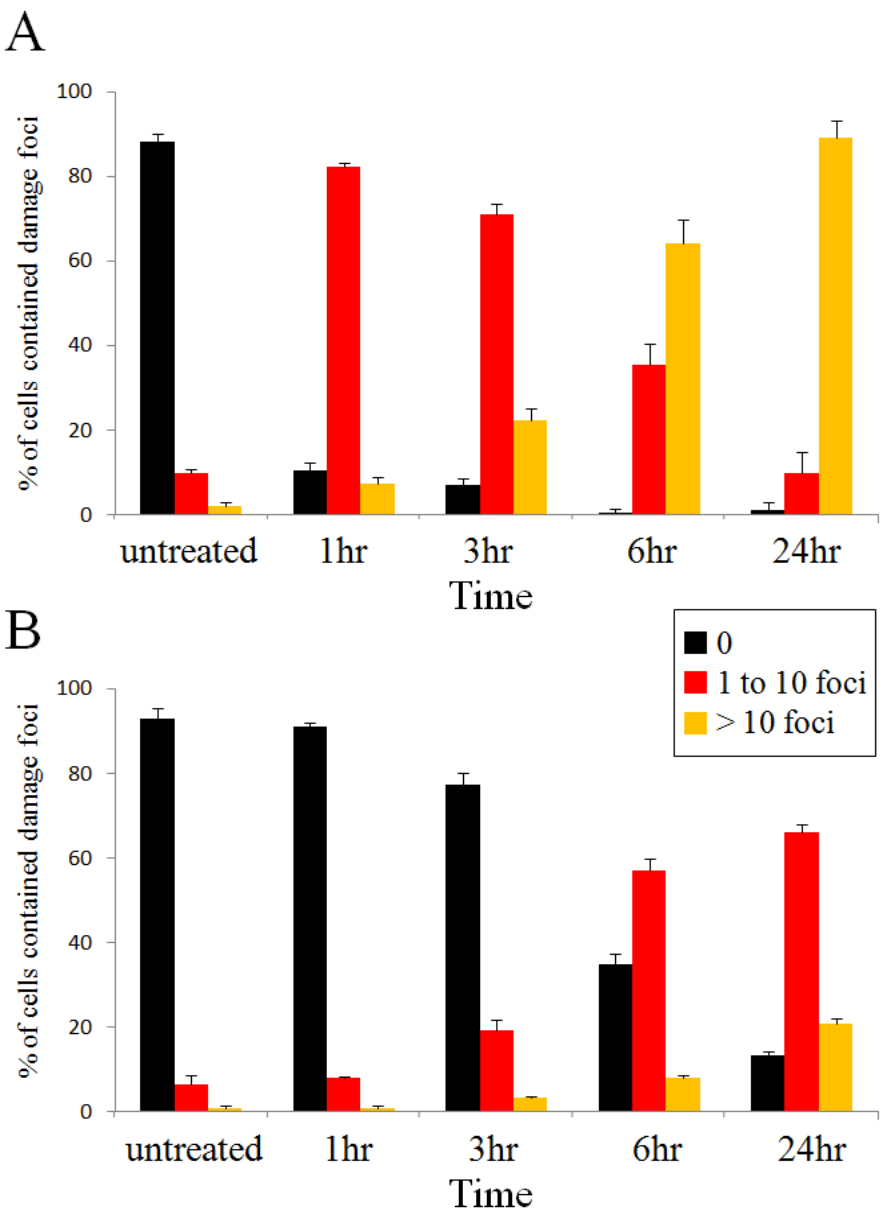

Figure 6.5 DNA damage foci in MRC and MRC5/hTERT under 400 μM paraquat treatment for the indicated time points. Cells were stained with γH2A.X and damage foci number counted. **A:** MRC5 under 400 μM paraquat treatment. **B:** MRC5/hTERT under 400 μM paraquat treatment. The bars represent means and standard error from three independent experiments.

Figure 6.5 shows the percentage of cells that contain DNA damage foci. The damage foci number of MRC5 and MRC5/hTERT were categorised into three groups which were: no DNA damage, 1-10 DNA damage foci and more than 10 DNA damage foci. Before paraquat treatment both cell types showed the same very low amount of damaged cells while around 90% had no damage at all. After paraquat treatment we found a different kinetics of increase in DNA damage between MRC5 and MRC5/hTERT. DNA damage response occurs much faster in MRC5 while it is significantly slower and there is also less DNA damage in MRC5/hTERT cells. After 1

hour of treatment, almost all MRC5 cells already showed a low amount of DNA damage (more than 80% of cells had 1-10 damage foci) while no difference to untreated cells was found in MRC5/hTERT cells.

With increasing treatment time, the amount of highly damaged cells (with more than 10 foci) increased continuously in MRC5 cells while MRC5/ hTERT cells accumulated significantly lower damage, mainly in the category of 1-10 damage foci. After 24 hours more than 90% of cells in MRC5 showed more than 10 damage foci while only 20-25% of cells in MRC5/hTERT had more than 10 damage foci. This result was summarised from three independent experiments which confirmed each other.

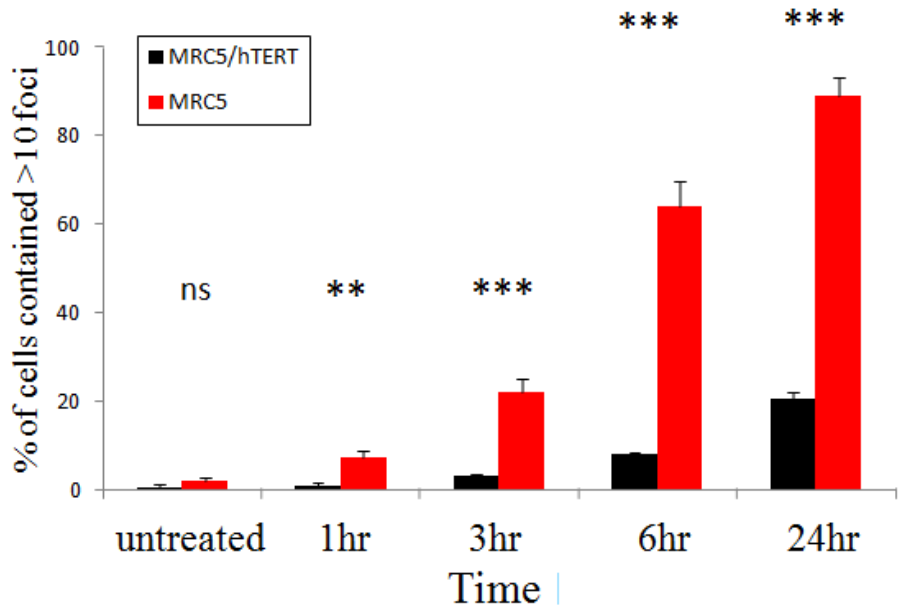

Figure 6.6 Comparison of DNA damage foci between MRC and MRC5hTERT after 400 μM paraquat treatment for the indicated time points. % of cells contained damage foci were summarised from the group of high damage (more than 10 foci) for each indicated time point. The bars represent means and standard error from three independent experiments. Ns = non-significant difference, ** $p<0.01$, ***$p<0.001$.

Figure 6.6 represents a comparison between percentages of cells that contained more than 10 damage foci of MRC5 and MRC5 at each indicated time point. We found a significant increased of DNA damage in MRC5 compared with MRC5/hTERT starting at 1 hour of paraquat treatment. Moreover, we found a highly significant difference between MRC5 and MRC5/hTERT at 3, 6 and 24 hours of paraquat treatment.

Thus, this experiment indicates that cells which contain endogenous telomerase show a protective capacity not only regarding mitochondrial DNA as had been demonstrated earlier (Ahmed et al., 2008) but, rather surprisingly, also regarding nuclear DNA damage. This result of a protective capacity of nuclearly excluded telomerase to protect from nuclear DNA damage confirms our previous experiments with exogenous stress treatments.

6.2.3 Quantitative determination of mitochondrial superoxide and peroxide levels after 400 μM paraquat treatment

To confirm the protective capacity of telomerase after endogenous stress we investigated whether expression of telomerase can reduce mitochondrial ROS generation by flow-cytometer (FACS) analysis. MRC5 and MRC5/hTERT were treated with 400 μM paraquat for 6 and 24 hours and the mitochondrial superoxide levels were investigated by mitosox staining and peroxide levels by dihydrorhodamine 123 (DHR) staining. The experiments were repeated more than 4 times for each staining at each time point. Results of mitosox at 6 hours after paraquat treatment and DHR at 6 and 24 hours after paraquat treatment were represented by absolute (arbitrary) units. However, since there was high variation of the level of mitosox of each single analysis at 24 hours after paraquat treatment, we summarised the data in percentage by adjust MRC5 and MRC5/hTERT before treatment as 100% and summarised the data of mitosox of MRC5 and MRC5/hTERT after paraquat treatment as an increase in percentage of mitosox compared with cells before paraquat treatment. All results are shown in figure 6.7.

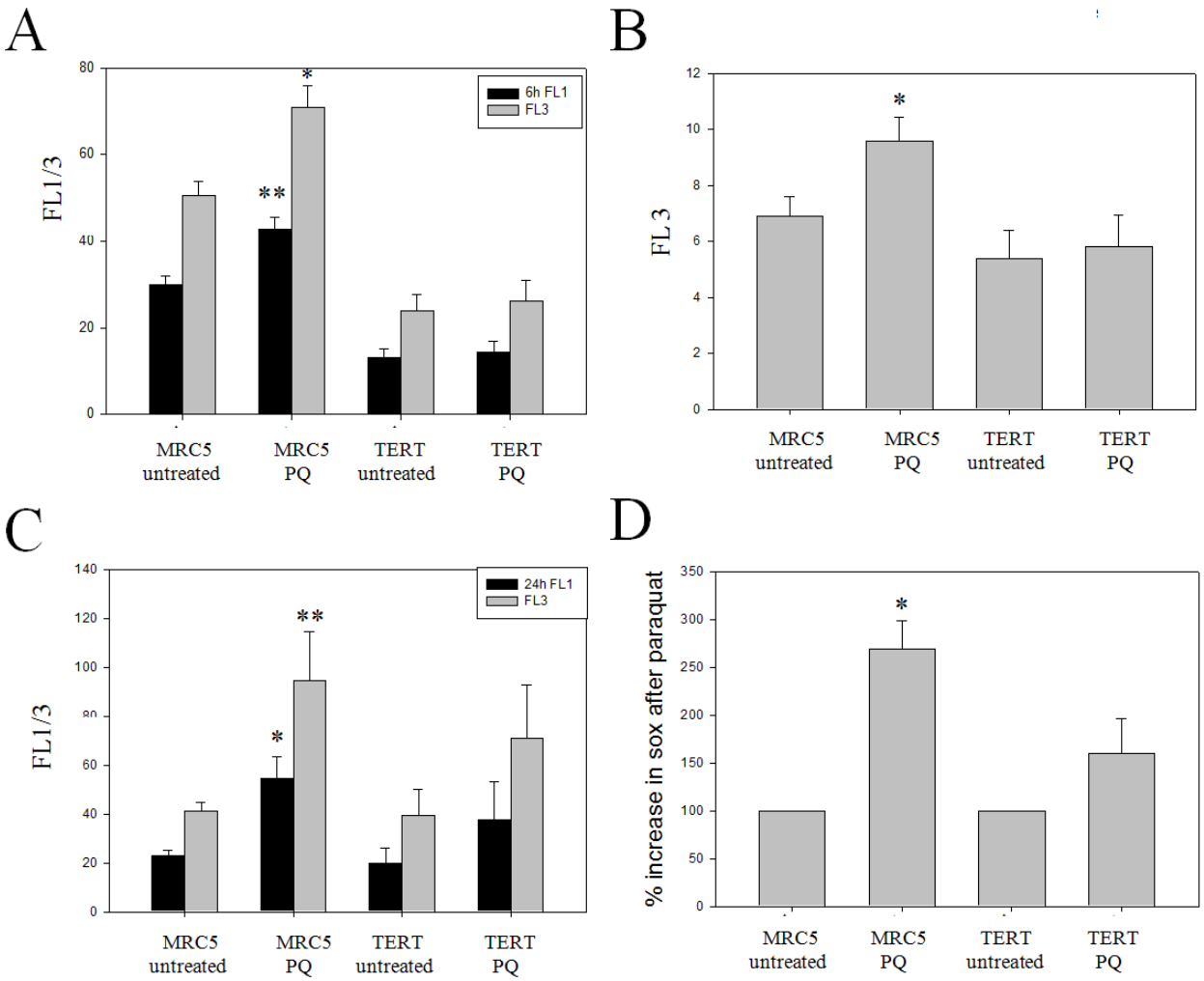

Figure 6.7 Mitochondrial superoxide and dihydrorhodamine 123 in MRC-5 and MRC5/hTERT after 6 and 24 hours paraquat treatment. A: represents FL1/FL3 from DHR staining after 6 hours of paraquat treatment. **B:** represents FL3 from mitosox staining after 6 hours of paraquat treatment. **C:** represents represent FL1/FL3 from DHR staining after 24 hour paraquat treatment.. **D:** represents FL3 from mitosox staining after 24 hour paraquat treatment. The graph represents percentage of untreated cells. Bars indicates means and standard error from at least 4 independent experiments. * $p<0.05$, ** $p<0.01$.

As shown in figure 6.7 MRC5 showed a significant difference for cells before and after paraquat treatment in both 6 and 24 hours time periods. We found a significant increase of FL1 and FL3 on MRC5 treated with paraquat (6 and 24 hours, figure 6.7 A and C) compared with MRC 5 before paraquat treatment which indicated a significant increased of peroxide level in MRC5. However, we have not found a significant difference between FL1 and FL3 in MRC5/hTERT before and after paraquat treatment (6 and 24 hours, figure 6.7 A and C). Similar results have been found in the mitochondrial superoxide level. Mitosox of MRC5 was significantly increased after paraquat treatment (6 and 24 hour, figure 6.7 B and C) compared with untreated cells. However, no significant difference was found in MRC5/hTERT before and after

paraquat treatment (6 and 24 hours) indicating a lower level of mitochondrial superoxide in MRC5/hTERT compared to MRC5 at 6 and 24 hours paraquat treatment. These results confirm our previous experiment which had shown that when telomerase is localised within mitochondria it expresses a protective capacity by reducing mitochondrial ROS production under cellular stress condition. Consequently, telomerase can protect mitochondria and reduce ROS generation under both endogenous and exogenous stress treatments. These results correspond well with the highest hTERT exclusion after 6 hours, while afterwards it already decreased again.

This reduction of ROS generation correlates to the DNA damage in MRC5 and MRC5/hTERT (see fig 6.5). MRC5 cells which do not have telomerase showed higher ROS generation and higher DNA damage after paraquat treatment while MRC5/hTERT which contains endogenous (over-expressed) telomerase showed lower ROS generation and lower DNA damage. Thus, from all these results, we can conclude that telomerase can reduce ROS generation which seems to correlate to lower nuclear DNA damage.

6.2.4 Confirmation of the mitochondrial protective capacity and lower DNA damage after paraquat treatment by using hTERT shooter vectors

To prove whether the protective function of telomerase to ROS generation and DNA damage was indeed because of the localisation of telomerase in mitochondria, in the next experiment we used the hTERT shooter vectors to deliver hTERT protein specifically to the nucleus or mitochondria. Because of the connection to Parkinson's disease we decided to use again the brain derived glioblastoma cell line U87. U87 was transfected with mito-hTERT or nucl-hTERT as described before. Transfected cells were then treated with 400μM paraquat for 1, 3, 6 and 24 hours similar to the fibroblasts used before. The results are shown in figures 6.8-6.9.

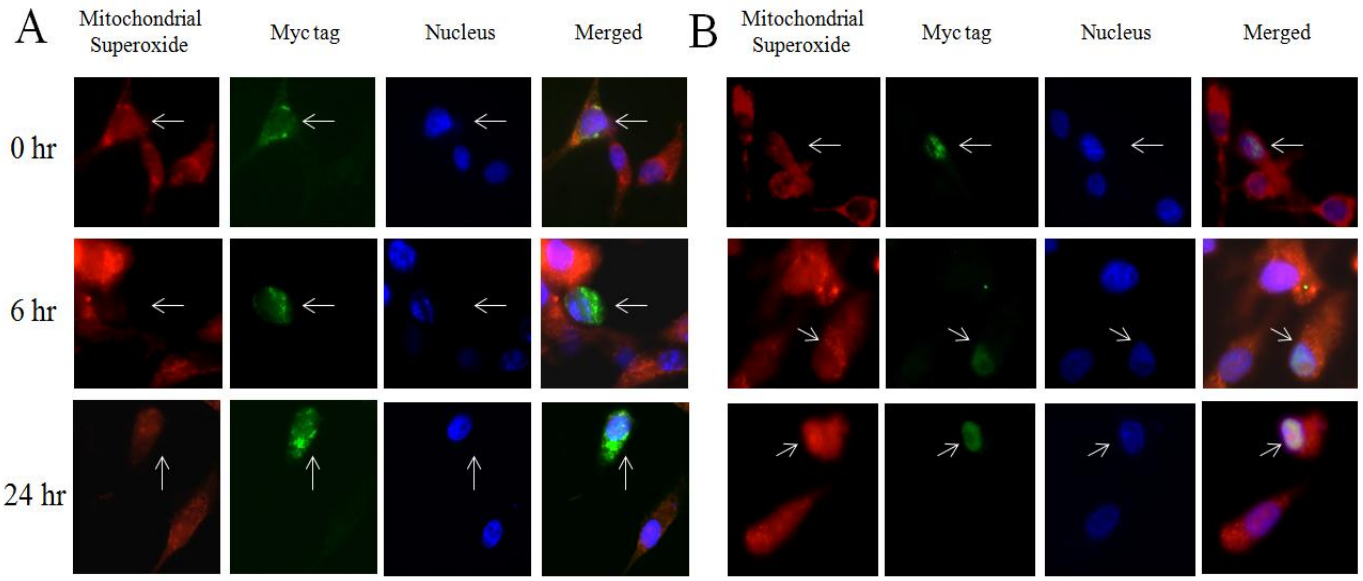

Figure 6.8 Determination of mitochondrial superoxide levels in U87 cells transfected with hTERT shooter vectors after paraquat treatment. Red colour represents mitochondrial superoxide. Myc-tag is represented in green colour. Nuclei were stained with DAPI (blue). White arrows indicate transfected cells. **A:** U87 cells were transfected with mito-hTERT shooter and treated with 400 μM paraquat for the indicated time. **B:** U87 cells were transfected with nucl-hTERT shooter and treated with 400 μM paraquat for the indicated time.

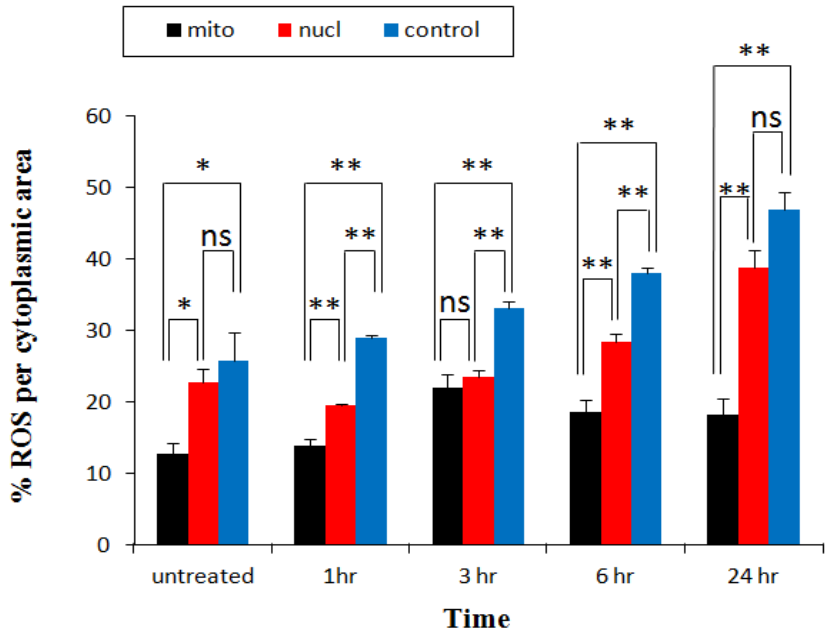

Figure 6.9 Kinetics of ROS levels in U87 for different time points after 400 μM paraquat treatment. All cells were treated with 400μM paraquat up to 24 hours. ROS level in each individual cell was measured using ImageJ. At least 30 cells per group have been evaluated. The graphs represent the average from 3 independent experiments. Bars indicate means and standard error. Ns = non-significant difference, * $p<0.05$, ** $p<0.01$.

As shown in figure 6.9, we have found a significantly lower ROS level in U87 transfected with mito-hTERT already before treatment demonstrated compared with nucl-hTERT and non-transfected U87. After treatment with 400μM paraquat, ROS level seems to increase vigorously until 24 hours under paraquat treatment in cells transfected with nucl-hTERT as well as in non-transfected cells. However, ROS levels in mito-hTERT and nucl-hTERT were not significantly different at 3 hours under paraquat treatment and no significant difference of ROS level have been found between nucl-hTERT and non-transfected cells at 24 hours. The reason for this is unclear , however, this result indicates the protective function of both mitochondria and nuclear hTERT to ROS production after paraquat treatment. But in all other time points, we found a significant lower ROS level when hTERT was localised in mitochondria under paraquat treatment. This result confirms our findings of previous experiments demonstrating the protective function of mitochondrial telomerase. ROS production was suppressed in cells transfected with mito-hTERT while increased in cells transfected with nucl-hTERT and the non transfected controls.

Thus, these results confirm again that mitochondrial localisation of hTERT can reduce mitochondrial ROS production from both exogenous and endogenous stress.

To prove whether this reduction of ROS generation due to mitochondrial localisation of hTERT can reduce nuclear DNA damage, U87 has been transfected with mito-hTERT or nucl-hTERT, treated with 400μM paraquat and then the DNA damage was examined at 1, 3, 6 and 24 hours after treatment. The results of this experiment are shown in figures 6.10-6.13.

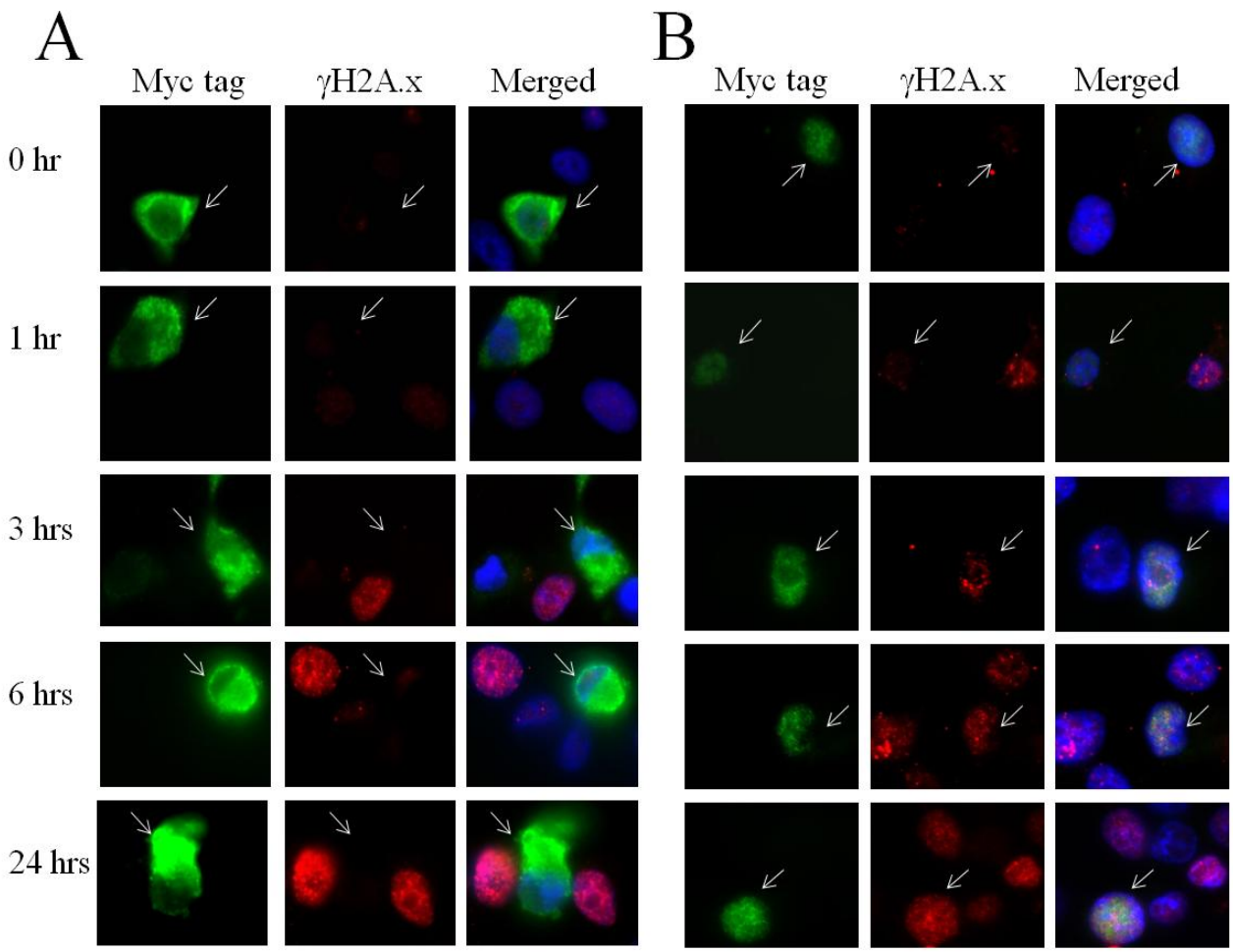

Figure 6.10 Representative images of the accumulation of DNA damage foci in U87 cells transfected with mito-hTERT and nucl-hTERT after paraquat treatment. Cells were treated with 400 μM paraquat up to 24 hours and stained for γH2A.X. Red colour represents DNA damage foci and green colour represents hTERT localisation. Blue is nuclear DAPI stain. White arrows indicate transfected cells. **A:** U87 transfected with mito-hTERT. **B:** U87 transfected with nucl-hTERT.

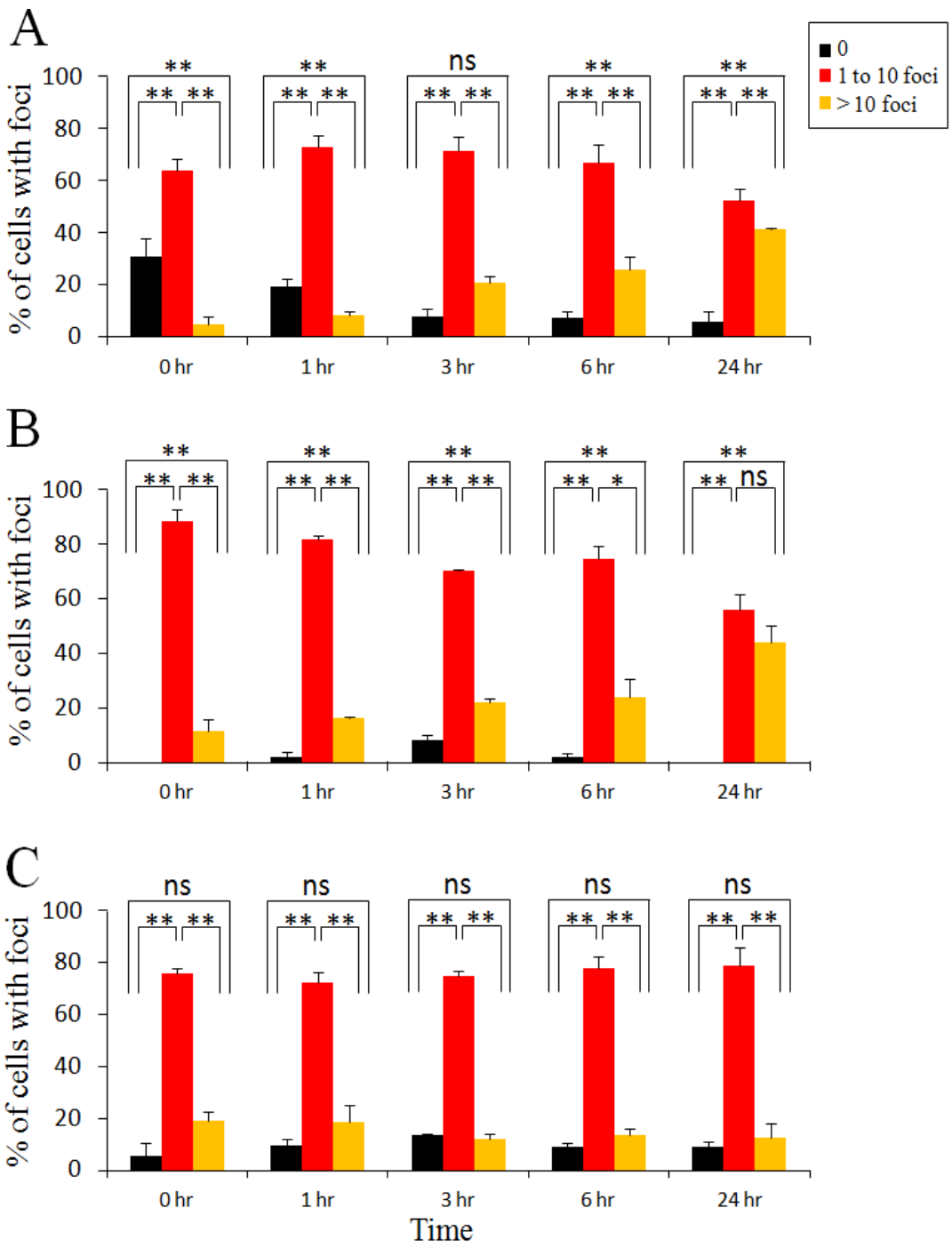

Figure 6.11 Kinetics of accumulation of DNA damage foci in U87 cells transfected with mito-hTERT and nucl-hTERT. A: non-transfected U87. **B:** nucl-hTERT transfected U87. **C:** mito-hTERT transfected U87. Cells were treated with 400 μM paraquat up to 24 hours. Cells were stained with γH2A.X and DNA damage foci numbers counted. Bars represent means and S.E. from three independent experiments. Ns = non-significant difference,* $p<0.05$, **$p<0.01$.

Figure 6.11 shows the percentage of cells containing DNA damage foci. U87 was treated with 400μM paraquat as in the previous experiments and then stained with γH2A.X to examine the DNA damage foci number. Cells were categorised into three groups which were: no damage, 1-10 damage foci and more than 10 damage foci as in the experiment using MRC5 and MRC5/hTERT cells.

Again, a different kinetic increase of DNA damage between cells transfected with mito-hTERT and nucl-hTERT has been found. DNA damage occurs faster in U87 cells transfected with nucl-hTERT while it stays low and there was no significant difference between the groups which showed no damage and more than 10 damage foci at all time points in mito-hTERT U87 after paraquat treatment. The DNA damage in non-transfected cells and those transfected with nucl-hTERT seemed to increases continuously until 24 hours of paraquat treatment. At 24 hours paraquat treatment, about 50% of U87 transfected with nucl-hTERT showed more than 10 damage foci while only 15-20% of U87 transfected with mito-hTERT have more than 10 damage foci. This result demonstrates that localisation of hTERT in mitochondria can prevent or reduce DNA damage under endogenous stress treatment. Thus mitochondrial localisation of hTERT can protect nuclear DNA from damage in both endogenous and exogenous stress inducers.

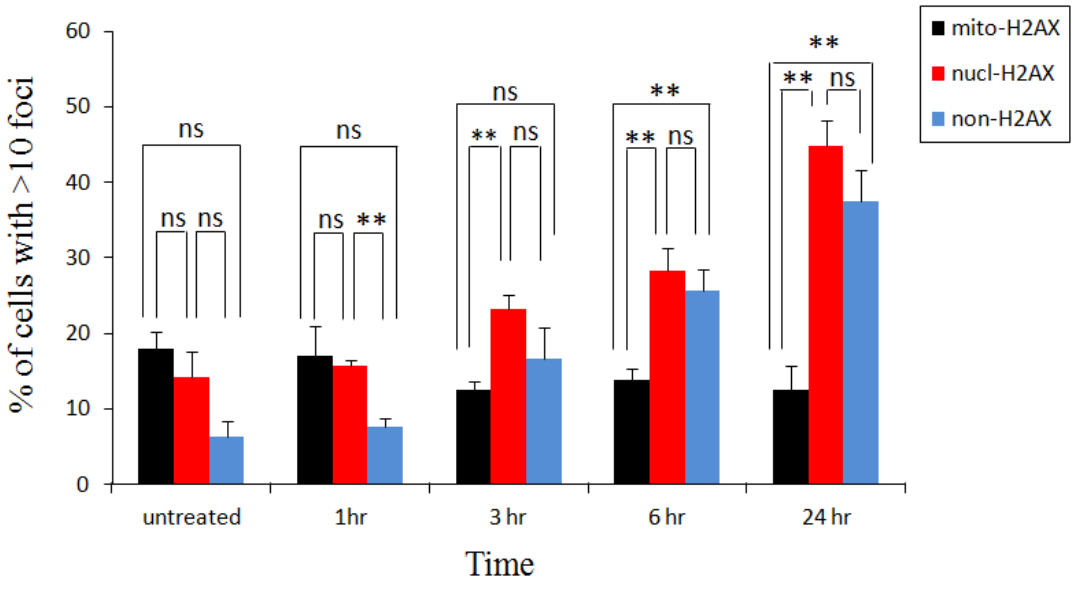

Figure 6.12 Kinetics of accumulation of DNA damage foci in the group of more than 10 damage foci in U87 cells transfected with mito-hTERT and nucl-hTERT. Cells were treated with 400 μM paraquat up to 24 hours. Cells which contained more than 10 damage foci were summarised for each time point. Bars represent means and S.E. from three independent experiments. Ns = non-significant difference, * $p<0.05$, ** $p<0.01$.

Next, we compared the group of high DNA damage (displaying more than 10 foci) of U87 transfected with mito-hTERT, nucl-hTERT or non-transfected cells. As the result in figure 6.12 shows, we have not found a significant difference between high DNA damage between mito-hTERT, nucl-hTERT and non-transfected U87 before 3-6 hours of paraquat treatment. However, after 3-6 hours of paraquat treatment, mito-hTERT U87 showed significant lower of high DNA damage compared with nucl-hTERT and the non- transfected group. We have not found a significant difference between U87 transfected with nucl-hTERT and the non-transfected group which correlated with the result of U87 after irradiation (figure 5.9 in Chapter 5).

Furthermore, results from Chapter 3 and 4 and previous results in this chapter showed that ROS levels positively correlated to the amount of nuclear DNA damage. Thus in this experiment we correlated ROS levels using mitosox staining to the occuring of DNA damage on parallel coverslips when U87 was transfected with different shooter vectors as shown in figure 6.13.

We found a very interesting correlation between ROS level and the amount of DNA damage foci. Under basal condition, although ROS level was already low in cells transfected with mito-hTERT we have not found a significantly lower level of DNA damage foci compared to U87 transfected with nucl-hTERT under basal condition. However, after the start of the treatment U87 with paraquat, ROS levels of U87 transfected with mito-hTERT did not increase with the time of treatment which correlates to a stably low DNA damage in the nucleus (figure 6.12 A, B, blue line). In contrast in U87 transfected with nucl-hTERT, the ROS level was increased continuously which could be the cause for the induction of nuclear DNA damage (figure 6.12 A, B, red line). Overall this experiment seems to suggest that localisation of hTERT within mitochondria could directly cause the reduction of ROS production which in turn could prevent nuclear DNA damage under endogenous stress treatment.

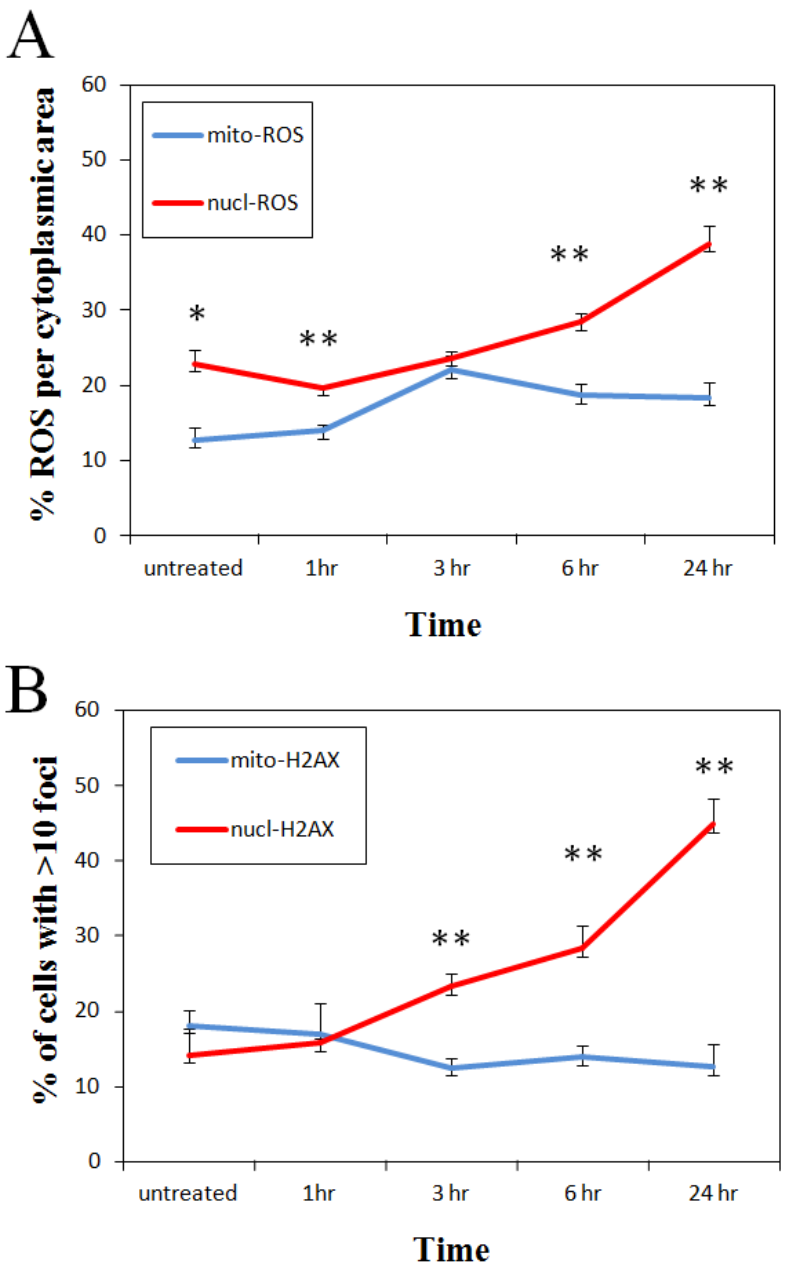

Figure 6.13 ROS levels and DNA damage foci in U87 cells transfected with mito-hTERT and nucl-hTERT after paraquat treatment. A: ROS level of U87 transfected with mito-hTERT or nucl-hTERT shooter. **B:** DNA damage foci in the group of more than 10 damage foci in U87 cells transfected with mito-hTERT or nucl-hTERT. Cells were treated with 400 μM paraquat up to 24 hours. Bars indicate means and standard error from three independent experiments. * $p<0.05$, ** $p<0.01$.

6.3 Discussion

In our initial experiments we have used hydrogen peroxide and irradiation to activate cellular oxidative stress. H_2O_2 can oxidise transition metals in many cellular components. H_2O_2 directly damages the iron-sulfur clusters of key enzymes and can inactivate enzymes that use single iron atoms to bind substrates, such as ribulose-5-phosphate epimerase. H_2O_2 also reacts with the intracellular pool of unincorporated ferrous iron and thereby generates hydroxyl radicals (Sawyer et. al., 1985). Ionising radiation can directly induce DNA double-strand breaks (DSBs) which are the most dangerous lesions (Firsanov et al., 2011). Irradiation of tumor tissues and the use of drugs that directly produce DSBs or induce replication stress are widely applied for cancer therapy (Redon et al., 2010). However, both of these are exogenous stress inducers. In our last experiment we sought to induce endogenous stress in order to investigate the protective function of telomerase when it is localised in the mitochondria. Thus we used paraquat which is a chemical which can directly activate mitochondrial ROS production.

We found that under 400μM paraquat treatment the maximum hTERT exclusion from the nucleus to the cytoplasm occurred at 6 hours and and reduced at 24 hours in MRC5/hTERT. This maximum exclusion point is slower than another treatment (H_2O_2). Cocheme and Murphy reported that paraquat caused mitochondrial oxidative damage in mammalian systems following its $\Delta\psi m$-dependent accumulation into the mitochondrial matrix (Cocheme et al., 2008). Castello and her colleagues found that mitochondria can uptake paraquat in different ways. In their experiment, the level of paraquat uptake into extracted mitochondria was different depending on the respiration substrates (Castello et al., 2007). Thus, the uptake level of paraquat even into whole cells might be affected by the culture medium or culture condition which might relate to the time required for paraquat uptake to reach the effective level. Moreover, we have not found MRC5/hTERT (and also other cells treated with paraquat) that survived after 48 hours paraquat treatment. The continuous treatment of paraquat in our experiment might cause continuously uptake paraquat into mitochondria that might have detrimental effects for cellular survival at such high concentrations.

We found a different kinetics increase in DNA damage after paraquat treatment between MRC5 and MRC5/hTERT cells. The occurence of DNA damage was faster in MRC5 cells while significantly slower in MRC5/hTERT. After 24 hours treatment, 80% of cells in MRC5 had a high amount (>10) of DNA damage foci while only 20-25% of cells in MRC5/hTERT displayed high amount of damage DNA foci.

MRC5/hTERT cells also showed lower ROS production and peroxide levels than MRC5 after paraquat treatment which confirm previous results from our group that MRC5/hTERT showed lower mitochondrial superoxide generation compared with MRC5 after hyperoxic (40% oxygen in the incubator) treatment (Ahmed et al., 2008). We found a significant difference between ROS levels and peroxide levels of MRC5 cells compared between untreated and 6 hours paraquat treatment and untreated with 24 hours paraquat treatment. In contrast, MRC5/hTERT cells indicated no-significant difference between before treatment and after 6 and 24 hour paraquat treatment in both ROS and peroxide.

These results confirm the protective function of telomerase under both endogenous and exogenous stress treatment in cells with over-expressed hTERT (MRC5/hTERT) compared with the same background cell type (MRC5) without hTERT. MRC5 does not express telomerase which indicated that the reduction of ROS production and protection of nuclear DNA damage under stress condition was the effect of overexpression of telomerase in MRC5/hTERT. Moreover, we have found only 20% of hTERT excluded from nucleus to cytoplasm at 1 and 3 hours after paraquat treatment in MRC5/hTERT. And the exclusion has reached the highest exclusion level (40-50%) at 6 hours of paraquat treatment. This exclusion level of hTERT is different from the exclusion of hTERT in MRC5/hTERT after H_2O_2 treatment. It is interesting that even the small amount of hTERT which was excluded from the nucleus under stress condition could be enough for the mitochondrial protection compared to cells without endogenous hTERT (MRC5). However, our group has also shown that a stable hTERT over-expression in MRC-5 fibroblasts can lead to changes in gene expression (Daniels et al., 2010). Therefore it is not clear whether hTERT shuttling is the only parameters that influences a decrease in mitochondrial ROS. Indran et al., (2011) have demonstrated a higher level of MnSOD as well as more cellular glutathione in Hela cells overexpressing hTERT. Although we have not found a higher antioxidant expression in our system (data not shown) we cannot exclude the influence of additional factors.

Next, we aimed to analyse more directly whether localisation of hTERT in mitochondria could be the reason for mitochondrial protection after endogenously induced stress. We have used mito-hTERT and nucl-hTERT shooter vectors transfected into U87 as in the previous experiment. We found a decrease in ROS production in U87 transfected with mito-hTERT after paraquat treatment. We also found a lower amount of DNA damage in U87 transfected with mito-hTERT compared with nucl-hTERT and non-transfected U87 after paraquat treatment.

As concluded in figure 6.13, different localisations of hTERT display a differential effect on ROS generation as we have found before: mitochondrial localisation of hTERT promotes lower ROS production and lower nuclear DNA damage while nuclear localisation of hTERT does not show this protection.

Thus, mitochondrial localisation of hTERT is the reason for lower ROS production and indirectly protects nuclear DNA from damage induction after endogenous stress treatment. Haendeler and colleagues reported that TERT increased respiratory chain activity which is most pronounced at complex I (Haendeler et al., 2009). Interestingly, mitochondrial complex I (NADH-ubiquinone oxidoreductase) is a major mitochondrial site for superoxide production by paraquat (Cocheme and Murphy, 2008). Thus the protection of complex I of the respiratory chain might be a reason for lower ROS production after paraquat treatment in cells with either nuclear hTERT exclusion such as MRC5/hTERT cells or direct mitochondrial hTERT localisation using mito-hTERT shooter transfection.

Finally, overall results from this chapter definitely indicate that mitochondrial localisation of hTERT protects mitochondria by reducing ROS production from the respiratory chain which might be a reason for the lower nuclear DNA damage after endogenous stress treatment.

Chapter 7
General discussion

7.1 Has different localisation of telomerase an effect on nuclear DNA damage?

Various groups have reported the shuttling of telomerase catalytic subunit from the nucleus to mitochondria upon oxidative stress (Santos et al., 2004, 2006; Ahmed et al., 2008; Haendeler et al., 2009; Indran et al., 2011). We found that localisation of hTERT is directly correlated to the different levels of DNA damage foci after various oxidative stress treatments such as hydrogen peroxide, paraquat treatment and irradiation. Endogenous telomerase is excluded from the nucleus in a time and stress dependent manner. However, there seems to be heterogeneity in hTERT exclusion within various cell populations (analysed in Hela, MCF7, and MRC5/hTERT cells). Importantly, in cells where hTERT still remains in the nucleus, cells accumulate high DNA damage after stress treatment (hydrogen peroxide and irradiation). In contrast, when hTERT is excluded from the nucleus and shuttles to mitochondria, cells show no or very low nuclear DNA damage. Cells which showed an intermediate exclusion pattern of hTERT exclusion (roughly 50% in the nucleus and cytoplasm) also showed an intermediate range of DNA damage (see fig 3.4 in Chapter 3).

It seems surprising that the localisation of hTERT in the nucleus did not protect DNA from nuclear DNA damage and, even more intriguingly, seemed even to promote DNA damage while localisation of hTERT in mitochondria has an indirect effect to protect nuclear DNA from damage. This finding leads to the speculation that, although telomerase exerts its canonical, telomere maintaining function in the nucleus when a cell gets under stress, nuclear hTERT has a negative effect on DNA damage response which we measured using γH2A.X. Consequently, in addition to lowering mitochondrial ROS when localised within the organelle there might be an additional biological function for hTERT exclusion from the nucleus. Both processes could be tightly connected. Moreover, this result also suggests that cells which contain endogenous telomerase show a protective capacity not only regarding mitochondrial DNA as had been demonstrated earlier (Ahmed et al., 2008) but, rather surprisingly, also regarding to nuclear DNA damage.

Passos and colleagues have shown recently that there exists a positive feed-back loop between nuclear DNA damage resulting in mitochondrial dysfunction which in turn induces more nuclear DNA damage (Passos et al., 2010). Although this loop was found

in senescent fibroblasts and might take much longer time to take effect one cannot exclude that a similar process takes place in our system (telomerase positive cells including various cancer cell lines) and occurs in a shorter time frame as well.

To prove our findings of the effect of endogenous telomerase on nuclear DNA damage, we used a model of specific hTERT shooter vectors to deliver the protein to specific cellular organelles - mitochondria and nucleus.

While in cells with endogenous telomerase the applied stress triggered nuclear exclusion, in our shooter vector system hTERT is already located in the respective compartment-nucleus or mitochondria- when the stress occurs. The TERT shooter plasmids carry a targeting protein sequences which leads hTERT into a specific location of a cell. Thus, cells containing exogenous hTERT shooters which stayed in there resemble those cancer cells where endogenous hTERT was not excluded within 3 hours, while in a longer time frame exogenous hTERT could still be excluded since for longer time points (up to 5 days) at least 40% of telomerase per cell were excluded from the nucleus (figure 3.6).

From the hTERT shooter model, we have found that different localisations of exogenous hTERT showed a different protective effect to nuclear DNA after induced DNA damage in three cancer cell lines (Hela, MCF7 and U87). Mitochondrial localisation of hTERT after shuttling was correlated to much lower DNA damage while nuclear localisation of hTERT did not show this protection and in cells without an active p53 it seemed and even increase the level of nuclear DNA damage significantly.

This result is in accordance with previous findings from another group that confinement to the nucleus of hTERT that is unable to shuttle due to a mutated nuclear exclusion signal might correlates to an increase of nuclear and mitochondrial DNA damage (Kovalenko et al., 2010 a,b). Kovalenko and co-workers explain their findings by an activation of DNA damage response genes ATM, Chk2 and p53 when hTERT is locked inside the nucleus that might increase the amount of DNA damage (Kovalenko et al., 2010b). We found that cells which harbour an activate p53 (MCF7, U87 and MRC5/hTERT) showed no significant difference of DNA damage level when hTERT is localised in the nucleus compared with the control group (non-transfected cells) while cells that harbour an inactivated p53 (Hela) showed a significantly higher DNA damage level even under basal condition when hTERT is localised in the nucleus compared with the control group (non-transfected cells). We hypothesise that p53 status might play a role with this higher DNA damage when hTERT is localised in the nucleus.

In addition, to confirm our results from cancer cells, we used MRC5/SV40 cells which do not contain endogenous telomerase as a model to avoid any potential interference of endogenous telomerase with the transfected TERT shooter vectors which might influence the results in cancer cells. We found a significantly lower DNA damage level in MRC5/SV40 which contained mitochondrial hTERT compared with MRC5/SV40 containing nuclear hTERT and the control group (non-transfected MRC5/SV40) after irradiation. This result confirms that localisation of an exogenous hTERT in mitochondria reduces nuclear DNA damage independent of any endogenous telomerase expression. Investigating the potential underlying mechanism for the lower DNA damage in mitochondrial TERT containing cells we were able to correlate it with a decrease of mitochondrial superoxide level.

7.2 Is physical localisation of hTERT in mitochondria necessary and sufficient for a decrease of mitochondrial superoxide after stress treatment?

Previous results from four groups, including ours, have shown that telomerase catalytic subunit is excluded from various cell types upon oxidative stress (Haendeler et al., 2003, Santos et al., 2004, Ahmed et al.,2008, Indran et al., 2011) which is correlated to a protective effect of telomerase within mitochondria (Ahmed et al.,2008, Haendeler et al., 2009, Kovalenko et al., 2010a,b, Indran et al., 2011), including in cancer cells (Kovalenko et al., 2010b, Indran et al., 2011). Our experiments in Chapter 4 have shown that the specific location of hTERT in mitochondria protects cells against oxidative stress in cancer cell lines (Hela, MCF7 and U87) and fibroblasts (MRC5/SV40). Modelling TERT localisation using specific hTERT shooter vectors in Hela, MCF7 and U87 showed a significant lower mitochondrial superoxide production when hTERT was localised in mitochondria compared with nuclear localisation under H_2O_2 stress treatment. However, the detection of ROS had been performed one day after treatment to avoid the interfering with the exogenous H_2O_2 which was used to treat the cells onto the ROS measurement. Therefore, we used X-irradiation to stress cells and detected ROS production within 30 minutes after treatment. We found a reduction of mitochondrial superoxide levels as a direct effect from the mitochondrial localisation of hTERT in MCF7 and U87. However, no significant difference in ROS levels was found between Hela harbouring mitochondrial hTERT shooter and nuclear hTERT shooter. Even Nuclear hTERT transfected cells, somehow, showed a significant higher ROS level than mitochondrial hTERT transfected cells, but in some condition such as in Hela under basal condition (figure 4.5 and 4.14) or MRC5/SV40 after irradiation (figure

4.20) the level of ROS production is significant lower than non transfected cells which might indicate a protective effect of nuclear hTERT to the ROS production. The reason for this is still unclear.

We have also performed a kinetics over time of ROS levels in Hela and MCF7 after irradiation with 20 Gy and followed it up to 2 days post irradiation. We found no significant difference between mitochondrial hTERT transfected cells compared with nuclear hTERT transfected cells in both Hela and MCF7 at day 2 after irradiation. This result could also confirm the protective effect of nuclear hTERT to cellular ROS production. One possibility to explain this phenomenon might be that nuclear hTERT might be excluded from the nucleus over the time after stress treatment.

Next, we have used MRC5/SV40 cells which do not contain endogenous telomerase to exclude any potential interference of endogenous telomerase in cancer cells with the exogenous hTERT shooter to ROS production, We found a significant difference in the amount of mitochondrial superoxide production in MRC5/SV40 transfected with mitochondrial hTERT shooter compared with nuclear hTERT transfected and the control group (non-transfected MRC5/SV40). These results confirm that mitochondrial localisation of hTERT protects against mitochondrial superoxide production after exogenous stress treatment and that there was no interfereing influence of endogenous telomerase in the 3 cancer cell lines.

Haendeler and coworkers reported that TERT is transported into the mitochondria via TIM/TOM complex, enters the mitochondrial matrix and binds to mitochondrial DNA coding regions for ND1 and ND2 and increases complex I respiratory efficiency (Haendeler et al., 2009). They also showed that binding of TERT to the mitochondrial DNA can protect the mitochondria against ethidium bromide and UV damage induction and increases overall respiratory chain activity which increases mitochondrial respiratory efficiency in HEK cells and mouse primary lung fibroblasts. Analysis of respiration in heart and liver mitochondria in TERT-/- mice indicated a particular importance of TERT in tissues with a high respiratory rate in vivo (Haendeler et al., 2009). Moreover, inhibition of endogenous hTERT expression using siRNA in endothelial cells (Ahmed et al., 2008) and shRNA in HEK293 (Haendelere et al., 2009) also shows increase of oxidative stress.

Indran and co-workers reported that siRNA-mediated gene silencing in transiently hTERT over-expressing Hela cells increased the level of ROS generation (Indran et al., 2011). Hela cells transfected with a vector containing hTERT displayed significantly lower mitochondrial ROS levels compared with wildtype Hela cells and Hela cells

transfected with the control vector after H_2O_2 treatment (Indran et al., 2011). However, they have not specified the exact hTERT localisation in their system since it is a general over-expression system in Hela-cells already highly expressing telomerase without transfection. Our experiments have shown here that mitochondrial localisation of telomerase protects against mitochondrial ROS generation and could indirectly protect nuclear DNA from damage under stress condition. As telomerase activity has been detected in 90% of all human malignancies (Shay and Bacchetti, 1997). It is possible that anti-cancer treatments such as chemotherapeutic drugs or irradiation could induce the mechanism of telomerase catalytic subunit shuttling to mitochondria, decreasing mitochondrial ROS generation and prevents nuclear DNA damage. Passos et al (2010) has demonstrated a positive feedback loop between mitochondrial ROS and nuclear DNA damage. The exogenous ROS generation by irradiation in fibroblasts damages mitochondria and accelerate nuclear DNA damage (Passos et al., 2010). We showed here an interaction between mitochondria and nucleus also exists in cancer cells. The results from our experiments might speculate that the exclusion of telomerase could contribute to mitochondria and nuclear DNA protection and might increased resistance of those cancer cells against various anti-cancer treatments.

7.3 Has endogenously induced stress the same effect as exogenous induction of ROS?

We have found that mitochondrial localisation of telomerase can protect mitochondria not only against exogenous stress activators (H_2O_2 and irradiation) but also against an endogenous stress inducer: paraquat. When we treated MRC5/hTERT with 400 μM paraquat we found that the exclusion of hTERT occurred slower than in the same cell type treated with H_2O_2. However, no fibroblast could survive beyond 48 hours of paraquat treatment which was different from MRC5/hTERT treated with exogenous stress (H_2O_2). The reason for this might be the continuous uptake of paraquat into mitochondria over the whole time (up to 24h).

We found significantly higher nuclear DNA damage in MRC5 compared with MRC5/hTERT after treatment with 400 μM paraquat. This result correlates well with a significant lower level of ROS production in MRC5/hTERT compared with MRC5 after 400 μM paraquat (figure 6.13). To confirm our findings that protective function of telomerase to ROS generation and DNA damage was indeed caused by the localisation of telomerase in mitochondria, we used a model of specific hTERT shooter vectors in

U87. We decided to use this brain derived glioblastoma cell line because we want to connect our results for the further investigation in Parkinson's disease. We found a decrease in ROS production and nuclear DNA damage in U87 cells transfected with mitochondrial hTERT compared with cells transfected with nuclear hTERT and the control group (non-transfected U87) after paraquat treatment. Thus, this result suggested that mitochondrial localisation of hTERT protects mitochondria by reducing ROS production which indirectly protected nuclear DNA under endogenous stress as we found in the exogenous stress condition.

Paraquat is known to induce cellular cytotoxicity by increasing in mitochondrial ROS production (McCarthy et al., 2004; Castello et al., 2007; Mohammadi-Bardbori and Ghazi-Khansari, 2008). Cocheme and murphy reported that mitochondrial complex I (NADH-ubiquinone oxidoreductase) is a major mitochondrial site for superoxide production by paraquat (Cocheme and Murphy, 2008). Haendeler and co-workers found that telomerase can increase respiratory efficiency, in particular at complex I (Haendeler et al., 2009). Thus, the protection of complex I of the respiratory chain might be a reason for lower ROS production after paraquat treatment in cells with either nuclear hTERT exclusion such as MRC5/hTERT cells or direct mitochondrial hTERT localisation using shooter vector transfection. The reduction of mitochondrial ROS producation by telomerase catalytic subunit in cells such as U87 could suggest a protective role of telomerase in neuronal cells. Mitochondrial localisation of hTERT might play a role in mitochondria protection against mitochondrial dysfunction which is thought to be one of the major pathological mechanisms responsible for Parkinson's disease.

7.4 Does p53 status influence the protective function of telomerase?

Our results in Chapter 3 showed that there seems to be a correlation between p53 activity and the effect of nuclear hTERT on the induction of nuclear DNA damage. We found that cancer cells which harbour an active p53 (MCF7, U87) showed no significant difference between DNA damage when hTERT is localised in the nucleus compared with the control group (non-transfected cells). However, cells that harbour an inactivated p53 (Hela) showed significantly higher DNA damage when hTERT was localised in the nucleus under basal and stress condition compared with the control group (non-transfected Hela). We hypothesised that the p53 status might play a role for this higher DNA damage while hTERT is localised in the nucleus. By using an isogenic

pair of glioblastoma cells (U87 and UP96) that only differed in their p53 status, we aimed to distinguish the effect of p53 on the protective function of telomerase.

Firstly, we have analysed the kinetic hTERT exclusion of U87 and UP96. We did not find a major difference in the kinetic exclusion of the endogenous telomerase of U87 and UP96 and most likely that there was no influenced by difference p53 activation.

Regarding DNA damage, U87 and UP96 cells transfected with mitochondrial hTERT showed significantly lower DNA damage compared to those containing nuclear hTERT and the control group (non-transfected cells) suggesting a protective function of mitochondrial telomerase to nuclear DNA in high dosages irradiation. Interestingly, UP96 which harbours mutated p53 showed a significantly higher DNA damage when transfected with nuclear hTERT shooter compared with mitochondrial hTERT shooter (figure 5.9).

High levels of DNA damage when hTERT is localised in the nucleus might play a role in cell cycle delay in order to repair the damage site (Kovalenko et al., 2010a). Activated p53 arrests the cell cycle to allow time for DNA repair (Zhang et al., 2012). However, if the damage is beyond repair, p53 can induce a permanent cell cycle arrest (senescence) or a process which triggers apoptosis. However it is not clear what is the molecular mechanism for a potential interaction between inactive p53 status, higher nuclear DNA damage and nuclear localisation of hTERT under stress condition. Experiments which examine the correlation between hTERT and gene expression while p53 is inactive might help to better understand the pathway responsible for this DNA damage induction.

We found significantly lower ROS levels in U87 and UP96 cells transfected with mitochondrial hTERT shooter compared with cells transfected with nuclear hTERT and the control group (non-transfected cells). This result confirms our previous result in Hela and MCF7 cells. Moreover, it is interesting that, in both U87 and UP96 treated with 20Gy irradiation, we have found a significant induction of ROS generation in both U87 and UP96 transfected with nuclear hTERT and non-transfected cells, however, no-significant increase of ROS production in both U89 and UP96 transfected with mito-hTERT. These results indicate that p53 protein does not influence the mitochondrial protective function of hTERT.

We found a significantly higher non-telomeric DNA damage in UP96 transfected with nuclear hTERT compared with U87 transfected with nuclear hTERT after 20 Gy irradiation (figure 5.15 in Chapter 5). However, we have not found a significant difference of the non-telomeric DNA damage between UP96 transfected with nuclear

hTERT compared with U87 transfected with nuclear hTERT under basal. Moreover, no-significant difference between telomeric DNA damage have been found between U87 and UP96 under basal and after 20 Gy irradiation. This result suggests that different p53 status does not increase the amount of telomeric DNA damage after stress treatment. This result is different from the result of another group (J Santos's group) which has demonstrated a significant increase of the percentage of telomeric DNA damage between cells without transfection and cells contained mutated nuclear exclusion signal hTERT which locks the hTERT inside nucleus which is comparable to our nuclear shooter in LNCaP and SQ20B cells under basal condition (Kovalenko et al., 2010b). Our experiment used a slightly different experiment model which transfected the fully-functional hTERT into the nucleus and evaluated the correlation between hTERT and DNA damage in cells which harbour different p53 under stress condition. It is interesting that SQ20B in Kovalenko's experiment harbours a mutated p53 while LNCaP contains aberrant methylation of p16 but still expresses wild type p53. Under basal condition both SQ20B and LNCaP showed a significant increase of the percentage of total DNA damage and the percentage of telomeric DNA damage in cells containing mutated nuclear hTERT compared with cell without nuclear hTERT. Our experiment found that under basal condition cells contained mutated inactive p53 which contained nuclear hTERT did not show significant difference in % of total DNA damage and % Telomeric DNA damage compared with cell contained wild type active p53 and contained nuclear hTERT suggests that the increase of nuclear DNA damage in Kovalenko's experiment was because of the effect of nuclear hTERT blocked inside the nucleus under basal condition. However, after the cells was stressed by irradiation (20 Gy) we found a pronounced increasing of non-telomeric DNA damage while there was no significant difference between telomeric DNA damage between cells contained inactive p53 compared with cell contain active p53. This result suggests that nuclear hTERT may play more roles on nuclear DNA damage in cells which lack active p53 under stress condition.

7.5 Summary

Our study has found different nuclear exclusion patterns of endogenous telomerase after hydrogen peroxide treatment in cancer cells and a telomerase over-expressing cell line and showed a significant correlation between localisation of telomerase catalytic subunit and DNA damage. Cells where hTERT remains in the nucleus displayed high DNA

damage while cells which excluded hTERT from the nucleus displayed no or very low DNA damage.

Thus, we used organelle specific hTERT localisation vectors to specify the effect of telomerase in nucleus and mitochondria after exogenous and endogenous stress treatment. We found that mitochondrial localisation of hTERT protects nucleus from DNA damage while nuclear localisation of hTERT correlated with higher amounts of DNA damage.

Since reactive oxygen species (ROS) are known to be responsible for nuclear DNA damage, we have tested the correlation between the localisation of hTERT and the expression of mitochondrial ROS. Our results indicated that mitochondrial localisation of hTERT decrease mitochondrial ROS generation level directly after both endogenous and exogenous stress which might be a reason of the prevention of nuclear DNA damage.

We hypothesised that p53 status might influence the protective function of telomerase. Our results in an isogenic cell pair of glioblastoma cells showed that p53 status does not prominently influence the protective function of mitochondrial hTERT. However, nuclear hTERT of cells which contained inactive p53 displayed a significantly higher DNA damage than cells which contained an active p53. This effect became more pronounced when stress levels where increased. We hypothesise that hTERT localisation might possibly interact with p53 when a cancer cell is under stress condition. However, the molecular mechanism for that is unknown.

In conclusion, our results demonstrate a novel link between mitochondrial localisation of hTERT, decrease of mitochondrial ROS and the protective capacity of telomerase to nuclear DNA from damage after stress treatments.

7.6 Future directions

The results and discussion presented in this thesis have improved the understanding that mitochondrial localisation of hTERT protects against nuclear DNA damage and mitochondrial ROS production after exogenous and exogenous stress. However, a number of questions remain outstanding:

- Why does nuclear localisation of hTERT promote nuclear DNA damage when p53 is inactive? More experiments about the connection between nuclear hTERT localisation and genes related with the activation of p53 might be beneficial to answer this question.

- What factors influence the different exclusion kinetic of endogenous hTERT under stress treatment? Since we found different kinetic exclusion in different cancer cell types, understanding of the factors which influence telomerase kinetic exclusion would be important in order to block the exclusion of telomerase which could be developed for a cancer therapy in the future.
- Why can a small amount of hTERT which is excluded from the nucleus be sufficient to reduce mitochondrial ROS production and protect the nucleus DNA from damage? It is intriguing that in paraquat treatment experiment, even the small amount of hTERT which was excluded from the nucleus before reaching highest exclusion rate at 6 hour in MRC5/hTERT was enough for the mitochondrial protection and protect nucleus DNA from damage compared with cells without endogenous hTERT (MRC5).
- Does hTR localisation or the expression level correlate with the induction of DNA damage when hTERT is localised in the nucleus under stress condition? hTR is necessary for the canonical function of telomerase. However, there is a report by Ting and co-workers that hTR can stimulates the kinase activity of DNA Dependent Protein Kinase (DNA-PK) which is required for the repair of DSBs via the non-homologous end-joining (NHEJ) pathway (Ting et al., 2009). As we found a link between nuclear localisation of hTERT, inactive p53 and increase of DNA damage under stress condition, does hTR corroborate on this correlation?
- Do cells such as cancer stem cells, adult stem cells or endothelial cells show a similar phenotype when hTERT is localised in different cellular compartments? It has been shown that cancer stem cells express high telomerase activity level (Joseph et al., 2010). However nothing is known about TERT shuttling or the effect of TERT when it is localised in different cellular compartments in these cell types. Thus experiments on other cell types would be interesting and enhance the understanding of telomerase in cellular ageing and longevity.

References

Ahmed S, Passos JF, Birket MJ, Beckmann T, Brings S, Peters H, Birch-Machin MA, von Zglinicki T, Saretzki G. 2008. Telomerase does not counteract telomere shortening but protects mitochondrial function under oxidative stress. J. Cell Sci. 17: 1046–1053.

Alexeyev MF. 2009. Is there more to aging than mitochondrial DNA and reactive oxygen species? FEBS J. 276(20):5768-87.

Ali S, Jain SK, Abdulla M, Athar M. 1996. Paraquat induced DNA damage by reactive oxygen species. Biochem Mol Biol Int. 39(1):63-7.

Aslan M, Cort A, Yucel I. 2008. Oxidative and nitrative stress markers in glaucoma. Free Radical Biology and Medicine. 45(4):367-376.

Atema A, Chène P. 2002. The gain of function of the p53 mutant Asp281Gly is dependent on its ability to form tetramers. Cancer Lett. 185(1):103-9.

Attardi LD, Reczek EE, Cosmas C, Demicco EG, McCurrach ME, Lowe SW, Jacks T. 2000. PERP, an apoptosis-associated target of p53, is a novel member of the PMP-22/gas3 family. Genes Dev. 14(6):704-18.

Avilion AA, Piatyszek MA, Gupta J, Shay JW, Bacchetti S, Greider CW. 1996. Human telomerase RNA and telomerase activity in immortal cell lines and tumor tissues. Cancer Res. 56(3):645-50.

Bachor C, Bachor OA, Boukamp P. 1999. Telomerase is active in normal gastrointestinal mucosa and not up-regulated in precancerous lesions. J Cancer Res Clin Oncol. 125(8-9):453-60.

Banin S, Moyal L, Shieh S, Taya Y, Anderson CW, Chessa L, Smorodinsky NI, Prives C, Reiss Y, Shiloh Y. 1998. Enhanced phosphorylation of p53 by ATM in response to DNA damage. Science. 281; 1674-1677.

Baross A, Schertzer M, Zuyderduyn SD, Jones SJ, Marra MA, Lansdorp PM. 2004. Effect of TERT and ATM on gene expression profiles in human fibroblasts. Genes Chromosomes Cancer. 39(4):298-310.

Bartkova J, Rezaei N, Liontos M, Karakaidos P, Kletsas D, Issaeva N, Vassiliou LV, Kolettas E, Niforou K, Zoumpourlis VC, Takaoka M, Nakagawa H, Tort F, Fugger K, Johansson F, Sehested M, Andersen CL, Dyrskjot L, Ørntoft T, Lukas J, Kittas C, Helleday T, Halazonetis TD, Bartek J, Gorgoulis VG. 2006. Oncogene-induced senescence is part of the tumorigenesis barrier imposed by DNA damage checkpoints. Nature. 444(7119):633-7.

Baumann P, Cech TR. 2001. Pot1, the putative telomere end-binding protein in fission yeast and humans. Science. 292(5519):1171-5.

Beckman KB, Ames BN. 1998. The free radical theory of aging matures. Physiol Rev. 78(2):547-81.

Ben-Porath I, Weinberg RA. 2005. The signals and pathways activating cellular senescence.
Int J Biochem Cell Biol. 37(5):961-76.

Blander G, de Oliveira RM, Conboy CM, Haigis M, Guarente L. 2003. Superoxide dismutase 1 knock-down induces senescence in human fibroblasts. J Biol Chem. 278(40):38966-9.

Blasco MA. 2005. Telomeres and human disease: ageing, cancer and beyond. Nat Rev Genet. (8):611-22.

Boelsterli UA, Lim PL. 2006. Mitochondrial abnormalities--a link to idiosyncratic drug hepatotoxicity? Toxicol Appl Pharmacol. 220(1):92-107.

Bodnar AG, Ouellette M, Frolkis M, Holt SE, Chiu CP, Morin GB, Harley CB,Shay JW, Lichtsteiner S, Wright WE. 1998. Extension of life-span byintroduction of telomerase into normal human cells. Science. 279 349–352.

Bouvard V, Zaitchouk T, Vacher M, Duthu A, Canivet M, Choisy-Rossi C, Nieruchalski M, and May E. 2000. Tissue and cell-specific expression of the p53-target genes: bax, fas, mdm2 and waf1/p21, before and following ionising irradiation in mice. Oncogene. 19; 649-660.

Brachmann RK. Vidal M. Boeke JD. 1996. Dominant-negative p53 mutants selected in yeast cancer hot spots. Proc. Natl Acad. Sci. USA, 93:4091- 4095.

Bragado P, Armesilla A, Silva A, Porras A. 2007. Apoptosis by cisplatin requires p53 mediated p38alpha MAPK activation through ROS generation. Apoptosis. 12(9):1733-42.

Bragado, P., Armesilla, A., Silva, A. & Porras, A. 2007. Apoptosis by cisplatin requires p53 mediated p38alpha MAPK activation through ROS generation. Apoptosis., 12, 1733-1742.

Brown JP, Wei W, Sedivy JM. 1997. Bypass of senescence after disruption of p21CIP1/WAF1 gene in normal diploid human fibroblast. Science. 277(5327): 831-4.

Broccoli D, Young JW, de Lange T. 1995. Telomerase activity in normal and malignant hematopoietic cells.Proc Natl Acad Sci U S A. 92(20):9082-6.

Campitelli M, Jeannot E, Peter M, Lappartient E, Saada S, de la Rochefordière A, Fourchotte V, Alran S, Petrow P, Cottu P, Pierga JY, Lantz O, Couturier J, Sastre-Garau X. 2012. Human papillomavirus mutational insertion: specific marker of circulating tumor DNA in cervicalcancer patients. PLoS One. ;7(8):e43393.

Castello PR, Drechsel DA, Patel M. 2007. Mitochondria are a major source of paraquat-induced reactive oxygen species production in the brain. J Biol Chem. 282(19):14186-93.

Chapman EJ, Hurst CD, Pitt E, Chambers P, Aveyard JS, Knowles MA. 2006. Expression of hTERT immortalises normal human urothelial cells without inactivation of the p16/Rb pathway. Oncogene. 25(36):5037-45.

Chehab NH, Malikzay A, Stavridi ES, and Halazonetis TD. 1999. Phosphorylation of Ser-20 mediates stabilization of human p53 in response to DNA damage. Proceedings of the National Academy of Sciences of the United States of America. 96; 13777-13782.

Chène P. 1998. In vitro analysis of the dominant negative effect of p53 mutants. Journal of Molecular Biology. 281(2): 205-209.

Chen, K., Albano, A., Ho, A. & Keaney, J. F., Jr. 2003(a). Activation of p53 by oxidative stress involves platelet-derived growth factor-beta receptor-mediated ataxia telangiectasia mutated (ATM) kinase activation. J.Biol.Chem., 278, 39527-39533.

Chen MH, Yang WK, Whang-Peng J, Lee LS, Huang TS. 1998(a). Differential inducibilities of GFAP expression, cytostasis and apoptosis in primary cultures of human astrocytic tumours. Apoptosis. 3(3):171-82.

Chen QM, Bartholomew JC, Campisi J, Acosta M, Reagan JD, Ames BN. 1998(b). Molecular analysis of H2O2-induced senescent-like growth arrest in normal human fibroblasts: p53 and Rb control G1 arrest but not cell replication. Biochem J. 332;43-50.

Chen X, Gao H, Wei P, Zhang Z, Liu Y. 2003(b). Expression of apoptosis-related genes Fas/FasL, Bax/Bcl-2 and Caspase-3 in rat corpus luteum during luteal regression. Sci China C Life Sci. 46(3):273-85.

Chipuk JE, Bouchier-Hayes L, Kuwana T, Newmeyer DD, Green DR. 2005. PUMA couples the nuclear and cytoplasmic proapoptotic function of p53. Science. 309(5741):1732-5.

Chipuk, J. E. & Green, D. R. 2003. p53's believe it or not: lessons on transcription-independent death. J.Clin.Immunol., 23, 355-361.

Choi J, Southworth LK, Sarin KY, Venteicher AS, Ma W, Chang W, Cheung P, Jun S, Artandi MK, Shah N, Kim SK, Artandi SE. 2008. TERT Promotes Epithelial Proliferation through Transcriptional Control of a Myc- and Wnt-Related Developmental Program. *PLoS Genet.* 4(1)**: e10.**

Choisy-Rossi C, Reisdorf P, Yonish-Rouach E. 1999. The p53 tumor suppressor gene: structure, function and mechanism of action. Results Probl Cell Differ. 23:145-72.

Cochemé HM and Murphy MP. 2008. Complex I is the major site of mitochondrial superoxide production by paraquat. J Biol Chem. 283(4):1786-98.

Cong YS, Shay JW. 2008. Actions of human telomerase beyond telomeres. Cell Research. 18:725-732.

Cong YS, Wen J, Bacchetti S. 1999. The human telomerase catalytic subunit hTERT: organization of the gene and characterization of the promoter. Hum. Mol. Genet. 8: 137–142.

Cong YS, Wright WE, Shay JW, 2002. Human telomerase and its regulation, Microbiol. Mol. Biol. Rev. 66: 407–425.

Cory S, Adams JM. 2002. The Bcl2 family: regulators of the cellular life-or-death switch. Nat Rev Cancer. 2(9):647-56.

d'Adda di Fagagna F, Reaper PM, Clay-Farrace L, Fiegler H, Carr P, Von Zglinicki T, Saretzki G, Carter NP, Jackson SP. 2003. A DNA damage checkpoint response in telomere-initiated senescence. Nature. 426(6963): 194-8.

Daniels DJ, Clothier C, Swan DC, Saretzki G. 2010. Immediate and gradual gene expression changes in telomerase over-expressing fibroblasts. Biochem Biophys Res Commun. 399(1):7-13.

De Bont R, van Larebeke N. 2004. Endogenous DNA damage in humans: a review of quantitative data. Mutagenesis. 19(3):169-85.

Deng Y, Chan SS, Chang S. 2008. Telomere dysfunction and tumour suppression: the senescence connection. Nat Rev Cancer. 8(6):450-8.

De Lange T. 2005. Telomere-related genome instability in cancer. Cold Spring Harb Symp Quant Biol. 70:197-204.

Del Bufalo D, Rizzo A, Trisciuoglio D, Cardinali G, Torrisi MR, Zangemeister-Wittke U, Zupi G, Biroccio A. 2005. Involvement of hTERT in apoptosis induced by interference with Bcl-2 expression and function. Cell Death Differ. 12(11):1429-38.

de Vries A, Flores ER, Miranda B, Hsieh HM, van Oostrom CT, Sage J, Jacks T. 2002. Targeted point mutations of p53 lead to dominant-negative inhibition of wild-type p53 function. Proc Natl Acad Sci U S A. 99(5):2948-53.

Dierick JF, Eliaers F, Remacle J, Raes M, Fey SJ, Larsen PM, Toussaint O. 2002. Stress-induced premature senescence and replicative senescence are different phenotypes, proteomic evidence. Biochem Pharmacol. 64(5-6):1011-7.

Di Micco R, Fumagalli M, Cicalese A, Piccinin S, Gasparini P, Luise C, Schurra C, Garre' M, Nuciforo PG, Bensimon A, Maestro R, Pelicci PG, d'Adda di Fagagna F. 2006. Oncogene-induced senescence is a DNA damage response triggered by DNA hyper-replication.
Nature. 444(7119):638-42.

Dimroth P, Kaim G. and Matthey U. 2000. Crucial role of the membrane potential for ATP synthesis by F(1)F(o) ATP synthases. J Exp Biol. 203(1): 51-59.

Evan GI, Lewis GK, Ramsay G, Bishop JM. 1985. Isolation of monoclonal antibodies specific for human c-myc proto-oncogene product. Mol Cell Biol. 5(12):3610-6.

Fan Y, Liu Z, Fang X, Ge Z, Ge N, Jia Y, Sun P, Lou F, Björkholm M, Gruber A, Ekman P, Xu D. 2005. Differential expression of full-length telomerase reverse transcriptase mRNA and telomeraseactivity between normal and malignant renal tissues. Clin Cancer Res. 11(12):4331-7.

Feng J, Funk WD, Wang SS, Weinrich SL, Avilion AA, Chiu CP, Adams RR, Chang E, Allsopp RC, Yu J, et al. 1995. The RNA component of human telomerase. Science. 269(5228):1236-41.

Finkel T, Holbrook NJ. 2000. Oxidants, oxidative stress and the biology of ageing. Nature. 408(6809):239-47.

Firsanov DV, Solovjeva LV, Svetlova MP. 2011. H2A.X phosphorylation at the sites of DNA double-strand breaks in cultivated mammalian cells and tissues. Clin Epigenetics. 2(2):283-97.

Fischer-Fantuzzi L, Vesco C. 1988. Cell-dependent efficiency of reiterated nuclear signals in a mutant simian virus 40 oncoprotein targeted to the nucleus. Mol Cell Biol. 8(12):5495-503.

Frazier MW, He X, Wang J, Gu Z, Cleveland JL, Zambetti GP. 1998. Activation of c-myc gene expression by tumor-derived p53 mutants requires a discrete C-terminal domain. Mol Cell Biol. 18(7):3735-43.

Fu W, Killen M, Culmsee C, Dhar S, Pandita TK, Mattson MP. 2000. The catalytic subunit of telomerase is expressed in developing brain neurons and serves a cell survival-promoting function. J Mol Neurosci. 14(1-2):3-15.

Fu W, Lu C, Mattson MP. 2002. Telomerase mediates the cell survival-promoting actions of brain-derived neurotrophic factor and secreted amyloid precursor protein in developing hippocampal neurons. J Neurosci. 22(24):10710-9.

Gao Q, Reynolds GE, Wilcox A, Miller D, Cheung P, Artandi SE, Murnane JP. 2008. Telomerase-dependent and -independent chromosome healing in mouse embryonic stem cells.DNA Repair (Amst). 7(8):1233-49. Epub 2008 May 23.

Geserick C, Blasco MA. 2006. Novel roles for telomerase in aging. Mech Ageing Dev. 127(6):579-83.

Ghosh U, Bhattacharyya NP. 2005. Benzamide and 4-amino 1,8 naphthalimide treatment inhibit telomerase activity by down-regulating the expression of telomerase associated protein and inhibiting the poly(ADP-ribosyl)ation of telomerase reverse transcriptase in cultured cells. FEBS J. 272(16):4237-48.

González-Suárez E, Samper E, Ramírez A, Flores JM, Martín-Caballero J, Jorcano JL, Blasco MA. 2001. Increased epidermal tumors and increased skin wound healing in transgenic mice overexpressing the catalytic subunit of telomerase, mTERT, in basal keratinocytes. EMBO J. 20(11):2619-30.

Greenberg RA, O'Hagan RC, Deng H, Xiao Q, Hann SR, Adams RR, Lichtsteiner S, Chin L, Morin GB, DePinho RA. 1999. Telomerase reverse transcriptase gene is a direct target of c-Myc but is not functionally equivalent in cellular transformation. Oncogene. 18(5):1219-26.

Greider CW, Blackburn EH. 1985. Identification of a specific telomere terminal transferase activity in Tetrahymena extracts. Cell. 43(2 Pt 1):405-13.

Greider CW, Blackburn EH. 1987. The telomere terminal transferase of Tetrahymena is a ribonucleoprotein enzyme with two kinds of primer specificity. Cell. 51(6):887-98.

Griffith JD, Comeau L, Rosenfield S, Stansel RM, Bianchi A, Moss H, de Lange T. 1999. Mammalian telomeres end in a large duplex loop. Cell. 97(4):503-14.

Hayflick L. 1965. Mycoplasmas and human leukemia. Wistar Inst Symp Monogr, 4: 157-65.

Haendeler J, Dröse S, Büchner N, Jakob S, Altschmied J, Goy C, Spyridopoulos I, Zeiher AM, Brandt U, Dimmeler S. 2009. Mitochondrial telomerase reverse transcriptase binds to and protects mitochondrial DNA and function from damage. Arterioscler. Thromb. Vasc. Biol. 29 (6): 929–935.

Haendeler J, Hoffmann J, Brandes RP, Zeiher AM, Dimmeler S. 2003. Hydrogen peroxide triggers nuclear export of telomerase reverse transcriptase via Src kinase family-dependent phosphorylation oftyrosine 707. Mol Cell Biol 23:4598–4610.

Haendeler J, Hoffmann J, Diehl JF, Vasa M, Spyridopoulos I, Zeiher AM, Dimmeler S. 2004. Antioxidants inhibit nuclear export of telomerase reverse transcriptase and delay replicative senescence of endothelial cells. Circ. Res. 94 (6): 768–775.

Halliwell B, Cross CE. 1994. Oxygen-derived species: their relation to human disease and environmental stress. Environ Health Perspect. 102 Suppl 10:5-12.

Hammond EM, Denko NC, Dorie MJ, Abraham RT, and Giaccia AJ. 2002. Hypoxia links ATR and p53 through replication arrest. Molecular and cellular biology. 22;1834-1843.

Hansford R. 2002. Oxidative Phosphorylation. Encyclopedia of Life Sciences DOI: 10.1038/npg.els.0001371.

Hayflick l, Moorhead PS. 1961. The serial cultivation of human diploid cell strains. Exp Cell Res. 25:585-621.

Herbert B, Pitts AE, Baker SI, Hamilton SE, Wright WE, Shay JW, Corey DR 1999. Inhibition of human telomerase in immortal human cells leads to progressive telomere shortening and cell death. Proc Natl Acad Sci U S A. 96(25):14276-81.

Hemann MT, Narita M. 2007. Oncogenes and senescence: breaking down in the fast lane. Genes Dev. 21(1):1-5.

Hoffmeyer K, Raggioli A, Rudloff S, Anton R, Hierholzer A, Del Valle I, Hein K, Vogt R, Kemler R. 2012. Wnt/β-catenin signaling regulates telomerase in stem cells and cancer cells. Science. 336(6088):1549-54.

Hollstein M, Rice K, Greenblatt MS, Soussi T, Fuchs R, Sørlie T, Hovig E, Smith-Sørensen B, Montesano R, Harris CC. 1994. Database of p53 gene somatic mutations in human tumors and cell lines. Nucleic Acids Res. 22(17):3551-5.

Hoppe-Seyler F, Butz K. 1993. Repression of endogenous p53 transactivation function in HeLa cervical carcinoma cells by human papillomavirus type 16 E6, human mdm-2, and mutant p53.J Virol. 67(6):3111-7.

Huschtscha LI, Holliday R. 1983. Limited and unlimited growth of SV40-transformed cells from human diploid MRC-5 fibroblasts. J Cell Sci. 63:77-99.

Huyen Y, Jeffrey PD, Derry WB, Rothman JH, Pavletich NP, Stavridi ES, Halazonetis TD. 2004. Structural differences in the DNA binding domains of human p53 and its C. elegans ortholog Cep-1. Structure. 12(7):1237-43.

Indran IR, Hande MP, Pervaiz S. 2011. hTERT overexpression alleviates intracellular ROS production, improves mitochondrial function, and inhibits ROS-mediated apoptosis in cancer cells. Cancer Res. 71(1):266-76.

Imlay JA, Fridovich I. 1991. Assay of metabolic superoxide production in Escherichia coli. J Biol Chem. 266(11):6957-65.

Itahana K, Campisi J, Dimri GP. 2004. Mechanisms of cellular senescence in human and mouse cells. Biogerontology. 5(1):1-10.

Itahana K, Zou Y, Itahana Y, Martinez JL, Beausejour C, Jacobs JJ, Van Lohuizen M, Band V, Campisi J, Dimri GP. 2003. Control of the replicative life span of human fibroblasts by p16 and the polycomb protein Bmi-1. Mol Cell Biol. 23(1):389-401.

Jagadeesh S, Banerjee PP. 2006. Telomerase reverse transcriptase regulates the expression of a key cell cycle regulator, cyclin D1. Biochem Biophys Res Commun. 347(3):774-80.

Jiang P, Du W, Heese K, and Wu M. 2006. The Bad guy cooperates with good cop p53: Bad is transcriptionally up-regulated by p53 and forms a Bad/p53 complex at the mitochondria to induce apoptosis. Molecular and cellular biology. 26;9071-9082.

Kakkar P, Singh BK. 2007. Mitochondria: a hub of redox activities and cellular distress control. Mol Cell Biochem. 305(1-2):235-53.

Kampinga HH, Van Waarde-Verhagen MA, Van Assen-Bolt AJ, Nieuwenhuis B, Rodemann HP, Prowse KR, Linskens MH. 2004. Reconstitution of active telomerase in primary human foreskin fibroblasts: effects on proliferative characteristics and response to ionizing radiation. Int J Radiat Biol. 80(5):377-88.

Kanaya T, Kyo S, Hamada K, Takakura M, Kitagawa Y, Harada H, Inoue M. 2000. Adenoviral expression of p53 represses telomerase activity through down-regulation of humantelomerase reverse transcriptase transcription. Clin Cancer Res. 6(4):1239-47.

Kang HT, Lee HI, Hwang ES.2006. Nicotinamide extends replicative lifespan of human cells.Aging Cell. 423-36. Epub 2006 Aug 25.

Karawajew L, Rhein P, Czerwony G, Ludwig WD. 2005. Stress-induced activation of the p53 tumor suppressor in leukemia cells and normal lymphocytes requires mitochondrial activity and reactive oxygen species. Blood. 105(12):4767-75.

Klapper W, Shin T, Mattson MP. 2001. Differential regulation of telomerase activity and TERT expression during brain development in mice. J Neurosci Res. 64(3):252-60.

Kharbanda S, Kumar V, Dhar S, Pandey P, Chen C, Majumder P, Yuan ZM, Whang Y, Strauss W, Pandita TK, Weaver D, Kufe D. 2000. Regulation of the hTERT telomerase catalytic subunit by the c-Abl tyrosine kinase. Curr Biol. 10(10):568-75.

Kilian A, Bowtell DD, Abud HE, Hime GR, Venter DJ, Keese PK, Duncan EL, Reddel RR, Jefferson RA. 1997. Isolation of a candidate human telomerase catalytic subunit gene, which reveals complex splicing patterns in different cell types. Hum Mol Genet. 6(12):2011-9.

Kirkinezos IG, Moraes CT. 2001. Reactive oxygen species and mitochondrial diseases. Semin Cell Dev Biol. 12(6):449-57.

Klingelhutz AJ, Foster SA, McDougall JK. 1996. *T*elomerase activation by the E6 gene product of human papillomavirus type 16. Nature. 380(6569):79-82.

Ko LJ, Prives C. 1996. p53: puzzle and paradigm. Genes Dev. 10(9):1054-72.

Kondo Y, Kondo S, Tanaka Y, Haqqi T, Barna BP, Cowell JK. 1998. Inhibition of telomerase increases the susceptibility of human malignant glioblastoma cells to cisplatin-induced apoptosis. Oncogene. 16(17):2243-8.

Kovalenko OA, Caron MJ, Ulema P, Medrano C, Thomas AP, Kimura M, Bonini MG, Herbig U,Santos JH. 2010a A mutant telomerase defective in nuclear-cytoplasmic shuttling fails to immortalize cells and is associated with mitochondrial dysfunction. Aging Cell. 2010 9(2):203-19.

Kovalenko OA, Kaplunov J, Herbig U, deToledo S, Azzam EI, et al. 2010b Expression of NES-hTERT in Cancer Cells Delays Cell Cycle Progression and Increases Sensitivity to Genotoxic Stress. PLoS ONE 5(5): e10812. doi:10.1371/journal.pone.0010812

Kyo S, Takakura M, Taira T, Kanaya T, Itoh H, Yutsudo M, Ariga H, Inoue M. 2000. Sp1 cooperates with c-Myc to activate transcription of the human telomerase reverse transcriptase gene (hTERT). Nucleic Acids Res. 2000. 28(3):669-77.

Lambert PF, Kashanchi F, Radonovich MF, Shiekhattar R, and Brady JN. 1998. Phosphorylation of p53 serine 15 increases interaction with CBP. The Journal of biological chemistry. 273; 33048-33053.

Lane DP. 1992. Cancer. p53, guardian of the genome. Nature. 358; 15-16.

Leem SH, Londoño-Vallejo JA, Kim JH, Bui H, Tubacher E, Solomon G, Park JE, Horikawa I, Kouprina N, Barrett JC, Larionov V. 2002. The human telomerase gene: complete genomic sequence and analysis of tandem repeat polymorphisms in intronic regions. Oncogene. 21(5):769-77.

Lenaz G. 2001. The mitochondrial production of reactive oxygen species: mechanisms and implications in human pathology. IUBMB Life. 2001 Sep-Nov;52(3-5):159-64.

Lendvay TS, Morris DK, Sah J, Balasubramanian B, Lundblad V. 1996. Senescence mutants of Saccharomyces cerevisiae with a defect in telomere replication identify three additional EST genes. Genetics. 144(4):1399-412.

Leu Q, Kaneko S, Yang L, Feldman RI, Nicosia SV, Chen J, and Cheng JQ. 2004(a). Aurora-A abrogation of p53 DNA binding and transactivation activity by phosphorylation of serine 215. The Journal of biological chemistry. 279;52175-52182.

Li H, Zhao L, Yang Z, Funder JW, Liu JP. 1998. Telomerase is controlled by protein kinase Calpha in human breast cancer cells. J Biol Chem. 273(50):33436-42.

Lin JY, Blackburn EH. 2004. Nucleolar protein PinX1p regulates telomerase by sequestering its protein catalytic subunit in an inactive complex lacking telomerase RNA. Genes Dev. 18(4):387-96.

Lin JY, Simmons DT, 1991, The ability of large T antigen to complex with p53 is necessary for the increased life span and partial transformation of human cells by simian virus 40. J Virol. 65(12)**:** 6447–6453.

Lincz LF, Mudge LM, Scorgie FE, Sakoff JA, Hamilton CS, Seldon M. 2008. Quantification of hTERT splice variants in melanoma by SYBR green real-time polymerase chain reaction indicates a negative regulatory role for the beta deletion variant. Neoplasia. 10(10):1131-7.

Lingner J, Cech TR. 1996. Purification of telomerase from Euplotes aediculatus: requirement of a primer 3' overhang. Proc Natl Acad Sci U S A. 93(20):10712-7.

Lingner J, Hughes TR, Shevchenko A, Mann M, Lundblad V, Cech TR. 1997. Reverse transcriptase motifs in the catalytic subunit of telomerase. Science. 276(5312):561-7.

Liu YC, Chen CJ, Wu HS, Chan DC, Yu JC, Yang AH, Cheng YL, Lee SC, Harn HJ. 2004. Telomerase and c-myc expression in hepatocellular carcinomas. Eur J Surg Oncol. 30(4):384-90.

Liu DP, Song H, Xu Y. 2010. A common gain of function of p53 cancer mutants in inducing genetic instability. Oncogene. 29(7):949-56.

Ljungman M. 2010. The DNA damage response--repair or despair? Environ Mol Mutagen. 51(8-9):879-89.

Lu T, Finkel T. 2008. Free radicals and senescence. Exp Cell Res. 314(9):1918-22.

Maeda T, Tashiro H, Katabuchi H, Begum M, Ohtake H, Kiyono T, Okamura H. 2005. Establishment of an immortalised human ovarian surface epithelial cell line without chromosomal instability. Br J Cancer.93(1):116-23.

Maida Y, Yasukawa M, Furuuchi M, Lassmann T, Possemato R, Okamoto N, Kasim V, Hayashizaki Y, Hahn WC, Masutomi K. 2009. An RNA-dependent RNA polymerase formed by TERT and the RMRP RNA. Nature. 461(7261):230-5.

Marchenko ND, Wolff S, Erster S, Becker K, Moll UM. 2007. Monoubiquitylation promotes mitochondrial p53 translocation. EMBO J. 26(4):923-34

Marchenko ND, Zaika A, Moll UM. 2000. Death signal-induced localization of p53 protein to mitochondria. A potential role in apoptotic signaling. J Biol Chem. 275(21):16202-12.

Martins CP, Brown-Swigart L, and Evan GI. 2006. Modeling the therapeutic efficacy of p53 restoration in tumors. Cell. 127; 1323-1334.

Massard C, Zermati Y, Pauleau AL, Larochette N, Métivier D, Sabatier L, Kroemer G, Soria JC. 2006. hTERT: a novel endogenous inhibitor of the mitochondrial cell death pathway. Oncogene. 25(33):4505-14

Masutomi K, Yu EY, Khurts S, Ben-Porath I, Currier JL, Metz GB, Brooks MW, Kaneko S, Murakami S, DeCaprio JA, Weinberg RA, Stewart SA, Hahn WC. 2003. Telomerase maintains telomere structure in normal human cells. Cell. 114(2):241-53.

Masutomi K, Possemato R, Wong JM, Currier JL, Tothova Z, et al. 2005. The telomerase reverse transcriptase regulates chromatin state and DNA damage responses. Proc Natl Acad Sci USA 102:8222–8227.

McCarthy S, Somayajulu M, Sikorska M, Borowy-Borowski H, Pandey S. 2004. Paraquat induces oxidative stress and neuronal cell death; neuroprotection by water-soluble Coenzyme Q10. Toxicol Appl Pharmacol. 201(1):21-31.

McSharry BP, Jones CJ, Skinner JW, Kipling D, Wilkinson GW. 2001. Human telomerase reverse transcriptase-immortalized MRC-5 and HCA2 human fibroblasts are fully permissive for human cytomegalovirus. J Gen Virol. *8*2(Pt 4):855-63.

Mihara M, Erster S, Zaika A, Petrenko O, Chittenden T, Pancoska P, Moll UM. 2003. p53 has a direct apoptogenic role at the mitochondria. Mol Cell. 11(3):577-90.

Milner J. Medcalf E A. Cook C A. 1991. Tumor suppressor p53: analysis of wild-type and mutant p53 complexes. Mol. Cell. Biol. 11:12 -19.

Miyashita T, Reed JC. 1995. Tumor suppressor p53 is a direct transcriptional activator of the human bax gene. Cell. 80(2):293-9.

Mohammadi-Bardbori A, Ghazi-Khansari M. 2008. Alternative electron acceptors: Proposed mechanism of paraquat mitochondrial toxicity. Environ Toxicol Pharmacol. 26(1):1-5.

Morin GB. 1989. The human telomere terminal transferase enzyme is a ribonucleoprotein that synthesizes TTAGGG repeats. Cell. 59(3):521-9.

Moyzis RK, Buckingham JM, Cram LS, Dani M, Deaven LL, Jones MD, Meyne J, Ratliff RL, Wu JR. 1988. A highly conserved repetitive DNA sequence, (TTAGGG)n, present at the telomeres of human chromosomes. Proc Natl Acad Sci U S A. 85(18):6622-6.

Nakano K, Vousden KH. 2001. PUMA, a novel proapoptotic gene, is induced by p53. Mol Cell. 7(3):683-94.

Nakamura TM, Morin GB, Chapman KB, Weinrich SL, Andrews WH, Lingner J, Harley CB, Cech TR. 1997. Telomerase catalytic subunit homologs from fission yeast and human. Science. 277(5328):955-9.

Nitta E, Yamashita M, Hosokawa K, Xian M, Takubo K, Arai F, Nakada S, Suda T. 2011. Telomerase reverse transcriptase protects ATM-deficient hematopoietic stem

cells from ROS-induced apoptosis through a telomere-independent mechanism. Blood. 117(16):4169-80.

Ohtani N, Mann DJ, Hara E. 2009. Cellular senescence: its role in tumor suppression and aging. Cancer Sci. 100(5):792-7.

Olovnikov AM. 1973. A theory of marginotomy. The incomplete copying of template margin in enzymic synthesis of polynucleotides and biological significance of the phenomenon. J Theor Biol. 41(1):181-90.

Pantoja C, Serrano M. 1999. Murine fibroblasts lacking p21 undergo senescence and are resistant to transformation by oncogenic Ras. Oncogene. 18(35):4974-82.

Park J, Andrew SV, Ji YH, Jinkuk C, Sohee J, Marina S, Woody C, Zhaojing M, Peggie C, Hong J. 2009a. Telomerase modulates Wnt signalling by association with target gene chromatin. Nature, 460*:* 66-72

Passos JF, Nelson G, Wang C, Richter T, Simillion C, Proctor CJ, Miwa S, Olijslagers S, Hallinan J, Wipat A, Saretzki G, Rudolph KL, Kirkwood TB, von Zglinicki T. 2010. Feedback between p21 and reactive oxygen production is necessary for cell senescence. Mol Syst Biol. 6:347.

Passos JF, Saretzki G, von Zglinicki T. 2007. DNA damage in telomeres and mitochondria during cellular senescence: is there a connection? Nucleic Acids Res. 35(22):7505-13.

Pei D, Zhang Y, Zheng J. 2012. Regulation of p53: a collaboration between Mdm2 and Mdmx. Oncotarget. 3(3):228-35.

Protti A. and Singer M. 2006. Bench-to-bedside review: Potential strategies to protect or reverse mitochondrial dysfunction in sepsis-induced organ failure. *Critical Care.* 10**:**228.

Pei D, Zhang Y, Zheng J. 2012. Regulation of p53: a collaboration between Mdm2 and Mdmx. Oncotarget. 3(3):228-35.

Reddel RR. 2005. Alternative lengthening of telomeres, telomerase, and cancer. Cancer Lett. 194(2):155-62.

Rahman R, Latonen L, Wiman KG. 2005. hTERT antagonizes p53-induced apoptosis independently of telomerase activity. Oncogene. 24(8):1320-7.

Redon CE, Dickey JS, Nakamura AJ, Kareva IG, Naf D, Nowsheen S, Kryston TB, Bonner WM, Georgakilas AG, Sedelnikova OA. 2010. Tumors induce complex DNA damage in distant proliferative tissues in vivo. Proc Natl Acad Sci USA 107 (42):17992–17997

Richter T, von Zglinicki T. 2007. A continuous correlation between oxidative stress and telomere shortening in fibroblasts. Exp Gerontol. 42(11):1039-42.

Rizzuto R, Sandonà D, Brini M, Capaldi RA, Bisson R. 1991. The most conserved nuclear-encoded polypeptide of cytochrome c oxidase is the putative zinc-binding subunit: primary structure of subunit V from the slime mold Dictyostelium discoideum. Biochim Biophys Acta. 1129(1):100-4.

Roemer K, Friedmann T. 1994. Mechanisms of action of the p53 tumor suppressor and prospects for cancer gene therapy by reconstitution of p53 function. Ann N Y Acad Sci. 716:265-80; discussion 280-2.

Rubio MA, Davalos AR, Campisi J. 2004. Telomere length mediates the effects of telomerase on the cellular response to genotoxic stress. Exp. Cell Res. 298 (1): 17–27.

Ryan M T. 2005. Mitochondria Protein Import: Methods. Encyclopedia of Lfe. Sciences: 1-3.

Saitoh M, Nishitoh H, Fujii M, Takeda K, Tobiume K, Sawada Y, Kawabata M, Miyazono K, Ichijo H. 1998. Mammalian thioredoxin is a direct inhibitor of apoptosis signal-regulating kinase (ASK) 1. EMBO J. 1;17(9):2596-606.

Santos JH, Meyer JN, Skorvaga M, Annab LA, Van Houten B. 2004. Mitochondrial hTERT exacerbates free-radical-mediated mtDNA damage. Aging Cell 3: 399–411.

Santos JH, Meyer JN, Van Houten B. 2006. Mitochondrial localization of telomerase as a determinant for hydrogen peroxide-induced mitochondrial DNA damage and apoptosis. Hum. Mol. Genet. 15 (11): 1757–1768.

Saretzki G. 2010. Cellular senescence in the development and treatment of cancer. Curr Pharm Des. 16(1):79-100.

Saretzki G. 2009. Telomerase, mitochondria and oxidative stress. Exp Gerontol. 44(8):485-92.

Saretzki G, Ludwig A, von Zglinicki T, Runnebaum IB. 2001. Ribozyme-mediated telomerase inhibition induces immediate cell loss but not telomere shortening in ovarian cancer cells. Cancer Gene Ther. 8(10):827-34

Saretzki G, Sitte N, Merkel U, Wurm RE, von Zglinicki T. 1999. Telomere shortening triggers a p53-dependent cell cycle arrest via accumulation of G-rich single stranded DNA fragments. Oncogene. 18(37):5148-58.

Saretzki G, Walter T, Atkinson S, Passos JF, Bareth B, Keith WN, Stewart R, Hoare S, Stojkovic M, Armstrong L, von Zglinicki T, Lako M. 2008. Downregulation of multiple stress defense mechanisms during differentiation of human embryonic stem cells. Stem Cells. 26(2):455-64.

Sarin KY, Cheung P, Gilison D, Lee E, Tennen RI, Wang E, Artandi MK, Oro AE, Artandi SE. 2005. Conditional telomerase induction causes proliferation of hair follicle stem cells. Nature. 436(7053):1048-52.

Sawyer DT, Roberts JL Jr, Calderwood TS, Sugimoto H, McDowell MS. 1985. Reactivity and activation of dioxygen-derived species in aprotic media (a model matrix for biomembranes). Philos Trans R Soc Lond B Biol Sci. 311(1152):483-503.

Schmitt CA, Fridman JS, Yang M, Baranov E, Hoffman RM, and Lowe SW. 2002. Dissecting p53 tumor suppressor functions in vivo. Cancer cell. 1;289-298.

Schultz BE. and Chan SI. 2001. Structures and proton-pumping strategies of mitochondrial respiratory enzymes. Annual Review of Biophysics and Biomolecular Structure 30(1): 23-65.

Seimiya, H., Sawada, H., Muramatsu, Y., Shimizu, M., Ohko, K., Yamane, K., Tsuruo, T., 2000. Involvement of 14-3-3 proteins in nuclear localization of telomerase. EMBO J. 19 (11), 2652–2661

Sharma GG, Gupta A, Wang H, et al. 2003. hTERT associates with human telomeres and enhances genomic stability and DNA repair. Oncogene. 22:131-146.

Sharma NK, Reyes A, Green P, Caron MJ, Bonini MG, Gordon DM, Holt IJ, Santos JH. 2012. Human telomerase acts as a hTR-independent reverse transcriptase in mitochondria. Nucleic Acids Res. 40(2):712-25.

Shay JW, Bacchetti S. 1997. A survey of telomerase activity in human cancer. Eur J Cancer. 33(5):787-91.

Shibata M, Hakuno F, Yamanaka D, Okajima H, Fukushima T, Hasegawa T, Ogata T, Toyoshima Y, Chida K, Kimura K, Sakoda H, Takenaka A, Asano T, Takahashi S. 2010. Paraquat-induced oxidative stress represses phosphatidylinositol 3-kinase activities leading to impaired glucose uptake in 3T3-L1 adipocytes. J Biol Chem. 285(27):20915-25.

Shibue T, Takeda K, Oda E, Tanaka H, Murasawa H, Takaoka A, Morishita Y, Akira S, Taniguchi T, Tanaka N. 2003. Integral role of Noxa in p53-mediated apoptotic response. Genes Dev. 17(18):2233-8.

Shin DS, Chahwan C, Huffman JL, Tainer JA. 2004. Structure and function of the double-strand break repair machinery. DNA Repair (Amst).(8-9):863-73.

Shippen-Lentz D, Blackburn EH. 1989. Telomere terminal transferase activity from Euplotes crassus adds large numbers of TTTTGGGG repeats onto telomeric primers. Mol Cell Biol. 9(6):2761-4.

Short SC, Martindale C, Bourne S, Brand G, Woodcock M, Johnston P. 2007. DNA repair after irradiation in glioma cells and normal human astrocytes. Neuro Oncol. 9(4):404-11.

Sitte N, Merker K, Von Zglinicki T, Grune T, Davies KJ. 2000. Protein oxidation and degradation during cellular senescence of human BJ fibroblasts: part I--effects of proliferative senescence.FASEB J. 14(15):2495-502.

Smith LL, Coller HA, Roberts JM. 2003. Telomerase modulates expression of growth-controlling genes and enhances cell proliferation. Nat Cell Biol, 5:474–479.

Smogorzewska A, de Lange T. 2002. Different telomere damage signaling pathways in human and mouse cells. EMBO J. 21(16):4338-48.

Smogorzewska A, de Lange T. 2004. Regulation of telomerase by telomeric proteins. Annu Rev Biochem. 73:177-208.

Smogorzewska A, van Steensel B, Bianchi A, Oelmann S, Schaefer MR, Schnapp G, de Lange T. 2000. Control of human telomere length by TRF1 and TRF2. Mol Cell Biol. 20(5):1659-68.

Takakura M, Kyo S, Sowa Y, Wang Z, Yatabe N, Maida Y, Tanaka M, Inoue M. 2001. Telomerase activation by histone deacetylase inhibitor in normal cells. Nucleic Acids Res. 29(14):3006-11.

Terrin L, Dolcetti R, Corradini I, Indraccolo S, Dal Col J, Bertorelle R, Bonaldi L, Esposito G, De Rossi A. 2007. TERT inhibits the Epstein-Barr virus lytic cycle and promotes the proliferation of primary B lymphocytes: implications for EBV-driven lymphomagenesis. Int J Cancer. 121(3):576-87.

Ting NS, Pohorelic B, Yu Y, Lees-Miller SP, Beattie TL. 2009. The human telomerase RNA component, hTR, activates the DNA-dependent protein kinase to phosphorylate heterogeneous nuclear ribonucleoprotein A1. Nucleic Acids Res. 37(18):6105-15.
Turrens JF. 1997. Superoxide production by the mitochondrial respiratory chain. Biosci Rep. 17(1):3-8.

Ulaner GA, Hu JF, Vu TH, Giudice LC, Hoffman AR. 1998. Telomerase activity in human development is regulated by human telomerase reverse transcriptase (hTERT) transcription and by alternate splicing of hTERT transcripts. Cancer Res. 58(18):4168-72.

Valenzuela MT, Núñez MI, Villalobos M, Siles E, McMillan TJ, Pedraza V, Ruiz de Almodóvar JM. 1997. A comparison of p53 and p16 expression in human tumor cells treated with hyperthermia or ionizing radiation. Int J Cancer. 72(2):307-12.

Vega LR, Mateyak MK, Zakian VA. 2003. Getting to the end: telomerase access in yeast and humans. Nat Rev Mol Cell Biol. 4(12):948-59.

Ventura A, Kirsch DG, McLaughlin ME, Tuveson DA, Grimm J, Lintault L, Newman J, Reczek EE, Weissleder R, and Jacks T. 2007. Restoration of p53 function leads to tumour regression in vivo. Nature. 445, 661-665.

Villunger A, Michalak EM, Coultas L, Müllauer F, Böck G, Ausserlechner MJ, Adams JM, Strasser A. 2003. p53- and drug-induced apoptotic responses mediated by BH3-only proteins puma and noxa. Science. 302(5647):1036-8.

Voet D and Voet JG. 2004. Biochemistry, Third Edition. U.S., Wiley International Edition.

von Zglinicki T, Pilger R, Sitte N. 2000. Accumulation of single-strand breaks is the major cause of telomere shortening in human fibroblasts. Free Radic Biol Med. 28(1):64-74.

von Zglinicki T, Saretzki G, Döcke W, Lotze C. 1995. Mild hyperoxia shortens telomeres and inhibits proliferation of fibroblasts: a model for senescence? Exp Cell Res. 220(1):186-93.

von Zglinicki T, Saretzki G, Ladhoff J, d'Adda di Fagagna F, Jackson SP. 2005. Human cell senescence as a DNA damage response. Mech Ageing Dev. 126(1):111-7.

Wallace DC. 2006. A mitochondrial paradigm of metabolic and degenerative diseases, aging, and cancer: A dawn for evolutionary medicine. Faseb Journal 20(5): A1474-A1474.

Wei CL, Wu Q, Vega VB, Chiu KP, Ng P, Zhang T, Shahab A, Yong HC, Fu Y, Weng Z. 2006. A global map of p53 transcription-factor binding sites in the human genome. Cell. 124; 207-219.

Wesbuer S, Lanvers-Kaminsky C, Duran-Seuberth I, Bölling T, Schäfer KL, Braun Y, Willich N, Greve B. 2010. Association of telomerase activity with radio- and chemosensitivity of neuroblastomas. Radiat Oncol. 5:66.

Willis Amy , Eun Joo Jung, Therese Wakefield and Xinbin Chen. 2004. Mutant p53 exerts a dominant negative effect by preventing wild-type p53 from binding to the promoter of its target genes. Oncogene 23, 2330–2338

Wong JM, Kusdra L, Collins K. 2002. Subnuclear shuttling of human telomerase induced by transformation and DNA damage. Nat. Cell Biol. 4 (9): 731–736

Wright WE, Shay JW. 2005. Telomere biology in aging and cancer. J Am Geriatr Soc. 53(9 Suppl):S292-4.

Wu YL, Dudognon C, Nguyen E, Hillion J, Pendino F, Tarkanyi I, Aradi J, Lanotte M, Tong JH, Chen GQ, Ségal-Bendirdjian E. 2006. Immunodetection of human telomerase reverse-transcriptase (hTERT) re-appraised: nucleolin and telomerase cross paths. J Cell Sci. 119(Pt 13):2797-806.

Xu D, Popov N, Hou M, Wang Q, Björkholm M, Gruber A, Menkel AR, Henriksson M. 2001. Switch from Myc/Max to Mad1/Max binding and decrease in histone acetylation at the telomerasereverse transcriptase promoter during differentiation of HL60 cells. Proc Natl Acad Sci U S A. 98(7):3826-31.

Xu JH, Wang YC, Geng X, Li YY, Zhang WM. 2009. Changes of the alternative splicing variants of human telomerase reverse transcriptase during gastric carcinogenesis. Pathobiology. 76(1):23-9.

Xue W, Zender L, Miething C, Dickins RA, Hernando E, Krizhanovsky V, Cordon-Cardo C, and Lowe SW. 2007. Senescence and tumour clearance is triggered by p53 restoration in murine liver carcinomas. Nature. 445;656-660.

Yan J, Jetten AM. 2008. RAP80 and RNF8, key players in the recruitment of repair proteins to DNA damage sites. Cancer Lett. 271(2):179-90.

Yang C, Przyborski S, Cooke MJ, Zhang X, Stewart R, Anyfantis G, Atkinson SP, Saretzki G, Armstrong L, Lako M. 2008. A key role for telomerase reverse transcriptase unit in modulating human embryonic stem cell proliferation, cell cycle dynamics, and in vitro differentiation. Stem Cells.26(4):850-63.

Yang Y, Chen Y, Zhang C, Huang H, Weissman SM. 2002. Nucleolar localization of hTERT protein is associated with telomerase function. Exp Cell Res. 277(2):201-9.

Yang W, Tiffany-Castiglioni E. 2007. The bipyridyl herbicide paraquat induces proteasome dysfunction in human neuroblastoma SH-SY5Y cells. J Toxicol Environ Health A. 70(21):1849-57.

Yasumoto S, Kunimura C, Kikuchi K, Tahara H, Ohji H, Yamamoto H, Ide T, Utakoji T. 1996. Telomerase activity in normal human epithelial cells. Oncogene. 13(2):433-9.

Ye Y, Wang D, Su C, Rong T, Guo A. 2009. Combined detection of p53, p16, Rb, and EGFR mutations in lung cancer by suspension microarray. Genet Mol Res. 8(4):1509-18.

Yu J, Wang Z, Kinzler KW, Vogelstein B, and Zhang L. 2003. PUMA mediates the apoptotic response to p53 in colorectal cancer cells. Proceedings of the National Academy of Sciences of the United States of America. 100;1931-1936.

Yu J, Zhang L, Hwang PM, Kinzler KW, and Vogelstein B. 2001. PUMA induces the rapid apoptosis of colorectal cancer cells. Molecular cell. 7;673-682.

Zeimet A, Riha K, Berger J, Widschwendter M, Hermann M, Daxenbichler G, Marth C. 2000. New insights into p53 regulation and gene therapy for cancer. Biochem Pharm. 8:1153-63.

Zhang J, Chan EK. 2002. Autoantibodies to IGF-II mRNA binding protein p62 and overexpression of p62 in human hepatocellular carcinoma. Autoimmun Rev. 1(3):146-53.

Zhang L, Yu J, Park BH, Kinzler KW, and Vogelstein B. 2000. Role of BAX in the apoptotic response to anticancer agents. Science. 290;989-992.

Zhang P, Chan SL, Fu W. 2003. Mendoza M, Mattson MP TERT suppresses apoptosis at a premitochondrial step by a mechanism requiring reverse transcriptase activity and 14-3-3 protein-binding ability. FASEB J. 17: 767–769

Zhang P, Liu F, Wang W. 2012. Regulation of the DNA Damage Response by p53 Cofactors. Biophys J. 102(10):2251-60.

Zhou L, Zheng D, Wang M, Cong YS. 2009. Telomerase reverse transcriptase activates the expression of vascular endothelial growth factor independent of telomerase activity. Biochem Biophys Res Commun. 386(4):739-43.